PITTING AND STRESS CORROSION CRACKING OF STAINLESS STEELS

Janardhan Rao Saithala

A thesis submitted in partial fulfillment of the requirements of
Sheffield Hallam University
for the degree of Doctor of Philosophy

October 2007

ABSTRACT

An investigation has been performed to determine the pitting resistance of stainless steels and stress corrosion cracking of super duplex stainless steels in water containing chloride ions from 25 - 170^{0}C. The steels studied are 12% Cr, FV520B, FV566, 304L, Uranus65, 2205, Ferallium Alloy 255, and Zeron100. All these commercial materials used in very significant industrial applications and suffer from pitting and stress corrosion failures. The design of a new experimental setup using an autoclave enabled potentiodynamic polarisation experiments and slow strain rate tests in dilute environments to be conducted at elevated temperatures. The corrosion potentials were controlled using a three electrode cell with computer controlled potentiostat.

The experimental programme to determine pitting potentials was designed to simulate the service conditions experienced in most industrial plants and develop mathematical model equations to help a design engineer in material selection decision. Stress corrosion resistance of recently developed Zeron100 was evaluated in dilute environments to propose a mechanism in chloride solutions at high temperatures useful for the nuclear and power generation industry.

Results have shown the significance of the composition of alloying elements across a wide range of stainless steels and its influence on pitting. Nitrogen and molybdenum added to modern duplex stainless steels was found to be unstable at higher temperatures. The fractographic results obtained using the scanning electron microscope (SEM) has given insight in the initiation of pitting in modern duplex and super duplex stainless steels. A mathematical model has been proposed to predict pitting in stainless steels based on the effect of environmental factors (temperature, chloride concentration, and chemical composition). An attempt has been made to identify the mechanism of SCC in Zeron100 super duplex stainless steel.

The proposed empirical models have shown good correlation between predicted pitting potential values with experimental results. It has been shown that the SCC mechanism in Zeron100 supports the slip assisted anodic dissolution model of SCC. The relationship between pitting and stress corrosion in dilute environments is established and empirical equations have been proposed to determine the damage region for wide range of stainless steels.

Acknowledgements

I would first like to thank my supervisor Professor John D Atkinson for his help in giving an opportunity to work in his laboratory and for his valuable guidance through out my PhD work. Also, I owe a great deal of thanks to the many technical staff I have been privileged to work with over the years, Including Tony Earshaw, Tim O' Hara, John Bickers, Steve Magowan, Roger, Brian, Bryan Palmer, BobGrant, Mac Jackson, and John Bradshaw. Many thanks as well to late Clive Brashaw for setting up the test machine, and colleagues Martin Corrigan, Andrew Higgins, and Shivaraj, in the research office.

I am grateful to Roger Francis of Weir Materials, Manchester for the generous supply of the material for this project.

Finally and most significantly, I am grateful to my parents S.S.Prasad, and S.Meenakumari, and my brother S.V.Ramesh and sister S.Radhika, and In-laws Srinivas and Swathi for putting up with me, not only whilst doing this PhD work but for their financial and moral support through out my career.

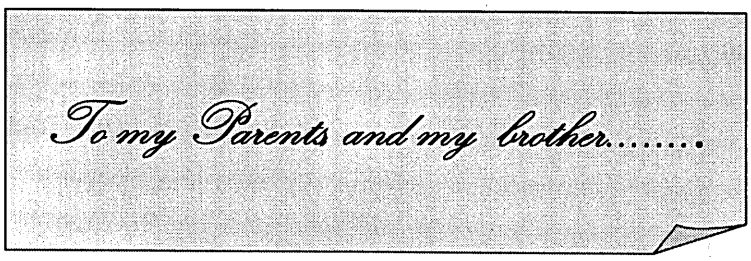
To my Parents and my brother.....

Statement of postgraduate study

This dissertation is submitted for the degree of Doctor of Philosophy at Sheffield Hallam University. The research work undertaken in the thesis was conducted under the supervision of Professor J.D.Atkinson in the Materials Engineering Research Institute, Sheffield Hallam University, between October 2003 and August 2007.

This work is original to the best of my knowledge, except where acknowledgements and references are made to previous work. Neither this nor any similar dissertation has been or is being submitted for any other degree or qualification at any other university.

Part of this work has been presented and published in the Public domain,

J.R.Saithala and J.D.Atkinson "*Pitting and Environmental assisted cracking of stainless steels*", Poster at MERI Research Day, July 2004.

J.R.Saithala and J.D.Atkinson *"Effect of chemical composition and chloride concentration on Pitting and Environmental assisted cracking of super duplex stainless steel"*, MERI Research away day, Oct 2004.

J.R.Saithala and J.D.Atkinson "*The effect of chloride on pitting in wide range of stainless steels, PREN (13-42) and stress corrosion cracking of super duplex stainless steel in 15ppm chloride at 130^{0}C*", Poster at CORROSION NACE 2005, New Orleans, Louisiana, USA

J.R.Saithala and J.D.Atkinson "*Pitting and Stress corrosion cracking of super duplex stainless steel at high temperature*", CORROSION NACE 2006, Sandiego, California, USA

J.R.Saithala and J.D.Atkinson "*Effect of Temperature and chloride concentration on the pitting behaviour of Zeron100, 2205 and Ferallium alloy255 duplex stainless steels"* DUPLEX 2007, Grado, Italy.

J.R.Saithala and J.D Atkinson *"Stress Corrosion behaviour of duplex stainless steels in dilute chloride solutions at 130^{0}C*" DUPLEX 2007, Grado, Italy.

The following award (NACE) was achieved through this work

"Harvey Herro Award & First prize winner for the best poster presentation in applied corrosion technology" CORROSION NACE 2006.

Nomenclature

d	depth
da/dt	Crack velocity
t	time
A, B	Constants
Ag/AgCl	Silver –Silver chloride electrode
Cl^-	Chloride ion
CPT	Critical pitting temperature
D_F	Final diameter
D_o	Original diameter
E_{corr}	Free corrosion potential
E_P	Pitting potential
E_{rp}	Repassivation potential
E_{scc}	Stress corrosion cracking potential
F	Faraday constant
I_a	anodic current density
I_{crit}	Critical current density
I_p	Passive current density
KOH	Potassium hydroxide
L_F	Final guage length
L_o	initial guage length
M	atomic weight
N	Number of cracks
O_2	oxygen
PREN	Pitting resistance equivalent number

RE	Reference electrode
SCC	Stress corrosion cracking
SCE	Saturated Calomel electrode
SEM	Scanning electron microscope
SSRT	Slow strain rate test
T	Temperature
UTS	Ultimate tensile strength
Z	Valency of solvated species
%RA	Percentage reduction in area
α	Ferrite
γ	Austenite
σ_{max}	Maximum stress
μ	Micro
ϵ_{CT}	Crack tip strain rate
ϵ_{app}	applied strain rate

List of figures

CHAPTER 1

1. Introduction

Selection of stainless steels for a particular application remains a specialised judgement as many different grades of stainless steels are available and used in various engineering applications for their excellent corrosion resistance. But unfortunately almost all stainless steels are susceptible to one or the other form of corrosion damage. Corrosion problems occurring in various forms are complex, to determine the conditions when it causes the failure of engineering equipment or to protect the geometry of a structure always remains as a challenge. For a design engineer it is difficult to select a stainless steel with corrosion allowance for its applicability.

It has been reported that almost 30% of cases of the corrosion failures in power stations is caused by localised corrosion including pitting and stress corrosion cracking (SCC) (Shibata, 2007). Once these damage processes initiate they will allow the material to deteriorate, leading to catastrophic structural failure, resulting in plant/rig (operations) shutdown and economic losses. Therefore, these failures are considered to be serious and important. It is not always easy to design a structure or piping system resistant to pitting or environment assisted corrosion as this is not always uniformly distributed and it occurs at areas difficult to access. The sensitivity to these corrosion processes alters with small changes in the environment, metallurgical variations making it difficult to study the exact mechanism involved.

Most of the pitting studies (Truman, 1977; 1987; Smialowska, 1987) on a wide range of stainless steels were investigated at room temperatures to estimate the pitting susceptibility in sea water. Elevated temperatures and pressures are common in the chemical processing or power generation industries in operations involving aqueous solutions. It is often misleading for a design engineer or material selector to base their decision on the data available at ambient temperature, to choose a suitable alloy for a variety of metal- environment systems.

It has long been appreciated that growth of corrosion pits on stainless steels is accelerated in the presence of higher temperatures compared to room temperature. All stainless steels are subjected to pitting under various electrochemical potentials generated basically from surrounding environment mainly temperature, oxygen and chloride concentration. It is important to know how stainless steels behave when they are operated at different temperatures and to link the performance of the individual grade to other grade allows a user to get clear picture, and will assist for better material selection. Up to now, no systematic studies of the combined effect of temperature, chloride and chemical composition on the intensity of pitting corrosion, has been performed across the full range of composition of stainless steels. As these parameters are closely interrelated and there has been no attempt to link these controlling parameters for a wide range of stainless steels to establish an empirical model that can assess pitting for design use.

On the other hand while it has been frequently stated that duplex and super duplex stainless steels (DSS & SDSS) have excellent corrosion resistance, such generalisations although supportable can often be misleading unless tested in specific

environments. The manufacturers of these materials create an impression of their immunity from corrosion failures. This does not concur with recent failures seen in North Sea (Leonard, 2003). The motivation for the current study was to better understand materials used in the oil and gas industry, and to extend the range of stainless steels used in the power generation industry. So far the studies related to DSS have been conducted in boiling chloride and H_2S environments (Jargelius et al, 1991; Kwon et al 1993; Ghoshal et al, 1993; Wen Ta Sai et al, 1993, 2000; Oltra et al, 1997; El-Yazgi, 1998) and no studies of DSS and SDSS have been reported in dilute chloride environments. It was highlighted in a recent HSE report that the need to establish operating limits and failure mechanisms of SDSS (Leonard, 2003).

This research is directed towards the extension of the studies of Truman (1977, 1987) considering independent materials which are used widely for significant applications in high temperature aqueous environments. The combined effects of environment, chemical composition as well as producing data for technically important systems at elevated temperatures is considered to be important. This kind of approach should lead to a better understanding of the environmental assisted attack on metal surfaces and can quantify to prejudge the service behaviour.

Therefore, the present work was carried out in two phases, one deal with pitting and other focussing on SCC in SDSS & DSS, and they are discussed in individual chapters. The first phase was to study pitting on wide range of materials and second phase was to study SCC of DSS & SDSS. Investigation involves study of the temperature, chloride dependence on pitting resistance of the commercially important alloys, which include FV520B (turbine blades), 304L (Reactor pipe work),

Uranus65 (nitric acid tanks), 2205 (Heat exchangers), Alloy 255 (Submarines), Zeron100 (Subsea flowlines, pumps).

The objectives of the present investigation were to

1. Design an experimental set up that enabled potentiodynamic polarisation tests to be carried out in an autoclave in a controlled environmental condition on various industrial representative steels.

2. To investigate the temperature dependence of three stages involved in PREN vs Pitting Potential curve in chloride solution and establish a relationship.

3. Develop and experimentally verify a mathematical/empirical model that allowed predicting pitting susceptibility for wide range of stainless steels in the combination of different temperatures and chloride solutions.

4. Compare the relative susceptibility of pitting corrosion in high temperature aqueous solutions under potentiodynamic polarisation scans, with those measured at room temperature.

5. To study the Stress Corrosion Cracking mechanism of Zeron100 SDSS in dilute chloride solutions under controlled potential conditions.

6. Independent investigation of polarisation behaviour of zeron100 in various chloride environments for different temperatures and oxygen levels.

7. Identify the critical SCC conditions that can impose damage on the most popular and expensive duplex stainless (2205, Alloy 255, Zeron100) by using the fractographic techniques available in the scanning electron microscope (SEM) to enable the understanding of the mechanisms involved in cracking to be improved.

8. To establish a relation ship between pitting potential and stress corrosion cracking potential in dilute chloride solutions, which is required for any design engineer to assess the life of a component with a minimum of testing.

CHAPTER 2
Literature Review

2. 1 Introduction

The aim of this chapter is to briefly review the recent and relevant information that is used to discuss the investigations carried out on pitting and stress corrosion cracking of stainless steels in the present study.

Pitting and stress corrosion cracking are among the major contributors for environment assisted failures in the field of corrosion. Studies are vital because of the difficulty involved in detecting the actual pits in real life which have potential to cause damage to any engineering equipment.

In the following sections the general mechanisms of pitting and stress corrosion cracking will be briefly reviewed. Since pitting and stress corrosion cracking occurs as the results of the interaction of metallurgical, environmental and mechanical factors, the significance of these three aspects on Pitting and SCC will be discussed individually in different sections.

2.2 Stainless Steels Overview and characteristics

Stainless steels are alloys containing a minimum of 11% chromium and they were discovered in 1910 in Sheffield when H. Brearly was trying to develop barrels for heavy guns, and in search of more resistant material to abrasive wear (Bela Leffler, 2000). Since then, a number of grades based on the composition, stainless steels were developed each year and have found applications in various forms for wide range of industries. These stainless steels are characterised in terms of their microstructure, chemical composition and mechanical properties as martensitic, ferritic, austenitic, martensitic - austenitic, duplex, super duplex and precipitation hardening steels. Stainless steels are in growing demand about 6% year at present, (Charles, 2007). The demand for these materials is due to their applicability in corrosion resistant equipment, and availability in various product forms. However the chemical composition of these materials play an important role. Since chromium alone cannot achieve all the properties the elements like nickel, nitrogen, and molybdenum were added to provide specific properties and corrosion resistance, whereas carbon, molybdenum, nitrogen, titanium, copper and aluminium are added to achieve strength (Sedricks,1996). Among these elements mentioned, nickel has become to be very expensive and the short supply of nickel recently has given the momentum to develop, duplex stainless steels that significantly improve the strength and corrosion properties.

2.2.1 Brief Review of Duplex stainless steels:

Duplex Stainless steels are defined as the alloys that consist of two phases (Austenite and Ferrite) approximately of equal proportion. The first kind of this type of alloy was referred by Bain and Griffith in the published notes on ferritic- austenitic structures (Gunn, 1996). The introduction of ferrite into austenitic stainless steel

increased the resistance to sensitisation as stainless steels used to have high carbon content which are developed in 1930s and the second reason for use of ferrite in austenitic was to improve the proof stress of castings (Roscoe & Gradwell, 1986). In the late 1960s and 1970s there are two main reasons that contributed to the rapid development of duplex stainless. Firstly it was a previous another nickel shortage that increased the price of austenitic stainless steels, and the increase in usage of these materials in the offshore oil industry which can handle aggressive environments, and secondly it was improved processes techniques allowing greater control in the chemical composition especially nitrogen (Roscoe & Gradwell, 1986).

The first generation duplex stainless steel was type 329 (UNS 32900) which showed good corrosion resistance because of high chromium and molybdenum contents and soon it was revealed that it was not showing resistance to welding or any heat treatments losing its toughness. Nitrogen was initially used as a substitute for austenite stabilizer nickel, but it was quickly found that it had some other benefits, which include improvement in tensile properties, pitting and crevice corrosion (Davison & Redmond, 1991).

However, the chemical composition of the duplex stainless steels needs more careful attention in order to balance the ferrite and austenite phase, as the solubility of certain elements like carbon and nitrogen is not the same in both the phases. Due to the formation of carbides and nitride as precipitates in the grain boundary region which creates a chromium depletion region also in turn reduces the corrosion resistance, to overcome this phenomenon nickel and nitrogen were added to the steel to achieve desired balance in both the phases.

2.2.2 Super Duplex stainless steel

During the modification of the existing 25%Cr duplex stainless steels in 1980s Zeron100 was invented as the first kind of super duplex stainless steel (SDSS) by Weir Materials Ltd in Manchester (Francis et al, 1997). It was initially used in major piping systems after its major success its applications spread across major industries. The advantage of Zeron100 to be supplied in various product forms made from single alloy allowed the usage of it across wide range of industrial applications.

Zeron100 has got good mechanical properties, along with high strength and hardness which gives resistance to corrosion and erosion. It has superior 0.2% proof stress compared to austenitic alloys. Warburton et al (1995) explained that high strength combined with high resistance to localised corrosion, and environmental assisted stress corrosion made it viable to use it in high temperature and pressure applications. The applications and advantages of Zeron100 and various duplex stainless steels in various industries was summarized and discussed by various authors(Coussement & Fruytier,1991; Davison & Redmond, 1991; Fruytier, 1991; Francis et al, 1997).

2.3 Corrosion in general

Corrosion is defined as the chemical or electrochemical reaction between material and the environment which causes deterioration of the material and its properties. Stainless steel relies on its passive film for its corrosion resistance, which passivates and protects the metal. To maintain the film it is essential to have oxygen in the environment, this condition is achieved at different condition which can be explained by electrochemical theory. Corrosion in general involves two reactions that can be occurred on metal surface, the oxidation or anodic reaction and reduction or cathodic reaction. An oxidation involves creation of metal ions and electrons which can represented by a general equation

$$M \rightarrow M^{+n} + ne^{-} \qquad (2.1)$$

The equation shows the removal of metal atom by oxidizing it to its ion. On the other side cathodic reaction that involves consumption of electrons occur frequently at cathodic sites on the metal surface. The most common cathodic reactions are

Evolution of hydrogen $2H^{+} + 2e \rightarrow H_2$ (2.2)

Oxygen reduction (acid solutions) $O_2 + 4H^{+} + 4e \rightarrow 2H_2O$ (2.3)

Metal ion reduction: $M^{n+} + e \rightarrow M^{(n-1)}$ (2.4)

The supply of oxygen to the metal is diminished under cathodic conditions where as passive film formation can take place under anodic conditions, since corrosion of metal involves simultaneous oxidation and reduction reactions. The type of reaction depends on the properties of the environment (e.g. Solution, temperature, pH etc) and the electrochemical potential of the metal. Each metal has a characteristic, inherent activity which can be described in terms of free energy, ΔG or electrochemical potential, E. The inherent activity is nothing but the magnitude of the free energy change on the metal going to metal corrosion product. The free energy change of a

reaction is equal to the negative of the product of the number of the electrons in the reaction times a constant value (Faradays constant) times the electrode potential, expressed as

$$\Delta G = -nFE \tag{2.5}$$

The change in free energy accompanying a corrosion reaction can be calculated from the electrode potential reaction, and the significance of the direction in which a reaction will proceed can be calculated using the Nernst equation,

$$E = E^0 + \frac{RT}{nF} \ln \frac{[ox]}{[red]} \tag{2.6}$$

Where E^0 is the standard half cell potential, R is the gas constant, T is the absolute temperature (in degree Kelvin), n is the number of electrons involved in the reaction , F is the Faraday, and (red) and (ox) is the concentration of the reduced and oxidised species, respectively.

For a metal in a corrosive environment, the oxidation (or anodic) and reduction (or cathodic) take place simultaneously at the metal surface. An electrode that is in contact with two or more oxidation – reduction systems is called a mixed electrode. The potential of a mixed electrode cannot be either a equilibrium potential for oxidation reactions or that for reduction reactions, but at an intermediate value where the total rates of oxidation and reduction are equal. This potential is called the corrosion potential (E_{corr}) and the corresponding current at the intersection is called I_{corr}.

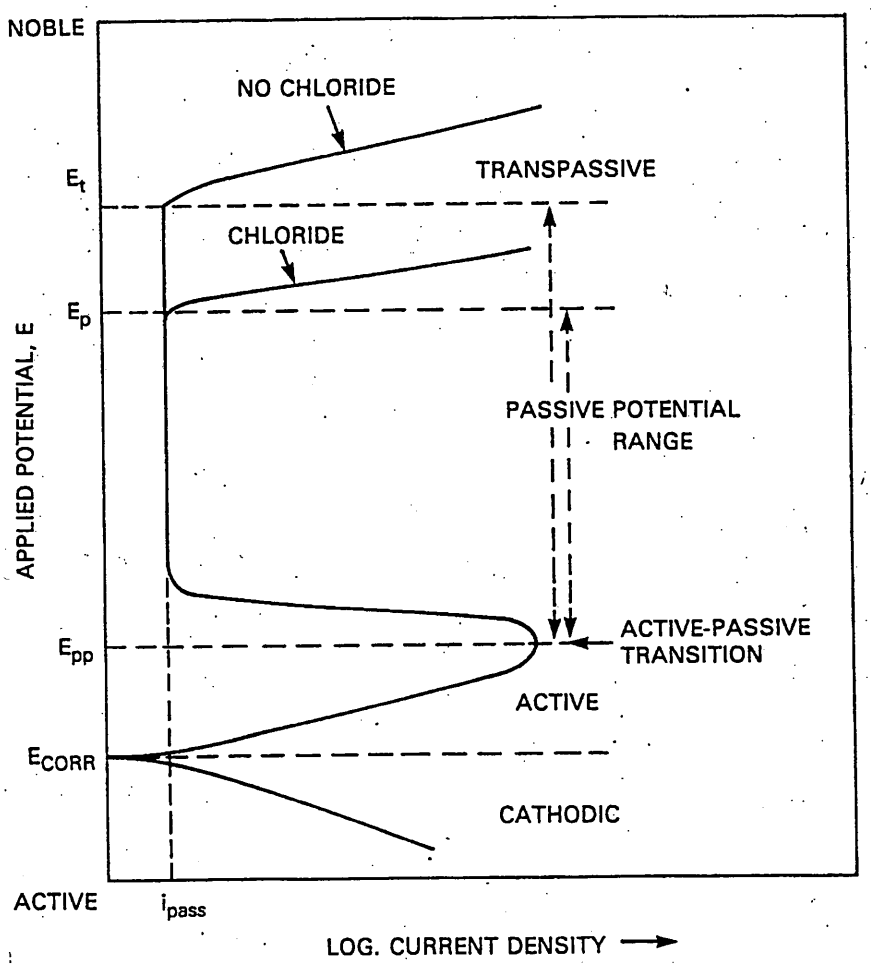

Figure: 2.1 Schematic polarisation curve for a stainless steel in a sulphuric acid solution (Sedricks ,1996)

In laboratory tests different anodic or cathodic potentials than the equilibrium corrosion potential can be achieved by using a potentiostat, which is a power supply unit with a feed back loop that provides current to the electrodes and maintains the potential required at constant value with respect to a reference electrode.

The deviation from equilibrium potential is called polarisation, which can be defined as the displacement of the electrode potential (anodic or cathodic) resulting from a net current. A polarisation curve of a material in a solution is the relation ship between the applied potential and the current density through the electrode as shown in Fig 2.1. The above figure explains a lot of terms related to the pitting behaviour of stainless steels. In the active anodic region, the measured current tends to increase

with the applied potential and then starts to decrease at a potential called the primary passivation potential E_{pp}. The occurrence of this is known as the active-passive transition. Above this potential the current usually drops to a low value and becomes nearly stable with increase in applied potential called as passive current, $i_{pass.}$ The potential range over which the current remains at low value is called the passive potential range and it is a range where stainless steels remains passive and the corrosion rate is low.

On increasing the applied potential towards positive direction, there exists a critical potential where the current tends to increase with the applied potential this potential is termed as pitting potential, E_p or breakdown potential, E_b. This particular potential value is defined by the combination of alloy and environment. In case of the above figure, in a chloride free aqueous sulphuric acid solution, the oxygen evolution occurs at a potential called E_t, the onset of transpassive behaviour. In case of chloride containing solution this occurs at less positive potentials, and the current tend to increase. This increase in the current allows the pits to form on the stainless steel surface, with further increase results in larger penetration depths, resulting in the damage of the industrial equipment.

2.3.1 Passive film

As already stated under certain electrochemical conditions, a surface film is formed on stainless steel, giving rise to a passive behaviour characterised by low corrosion rate. These films play an important role in defining the susceptibility of metals to different kinds of localised corrosion. The quality of the passive film formed on the metal surface play an important role in ranking of stainless steels. Study of the properties of passive films formed on the stainless steels is complicated as the films formed are very thin (Smialowska,1986). A film without defects acts as an insulator

and protects the metal from corrosion attack. But it is not always possible to maintain the stability of the film as it depends on the environments in the which the metal is present. Film breakdown is an important event that occurs before the attack on the metal takes place. An example of simple model of film breakdown in which substrate steel dissolution initiates at small defects in the initial oxide film was proposed by Townsend et al, (1981) as shown in Fig 2.2.

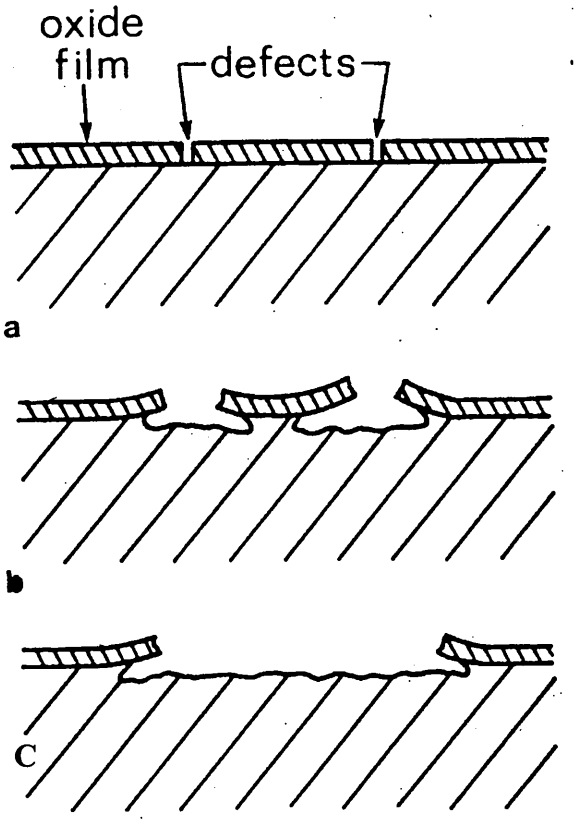

Figure:2.2 Model of film breakdown (a) Substrate covered with defect containing oxide film (b)under -cutting of oxide film by substrate dissolution at defects; and (c) extensive loss of film(Townsend et al, 1981).

The model explains that film breakdown proceeds by dissolution of the substrate containing defects and undercutting of the oxide film. The assumption of this model is that the properties of the initial oxide film are not critical factors in corrosion behaviour. According to Okamoto, 1973 the passive films on stainless steel contains water bound metal ions, containing three bridges on the metal surface namely, (1)H_2O -- M -- OH_2 (2)HO -- M -- OH and (3)O -- M -- O. In the situation in

which the passivity is maintained, the metal ions, which are produced by anodic dissolution through the undeveloped part of the film, form intermediates denoted as MOH^+. The MOH^+ ion is captured by the surroundings H_2O molecules and links into the gel-like film, as shown below with the release of hydrogen ions.

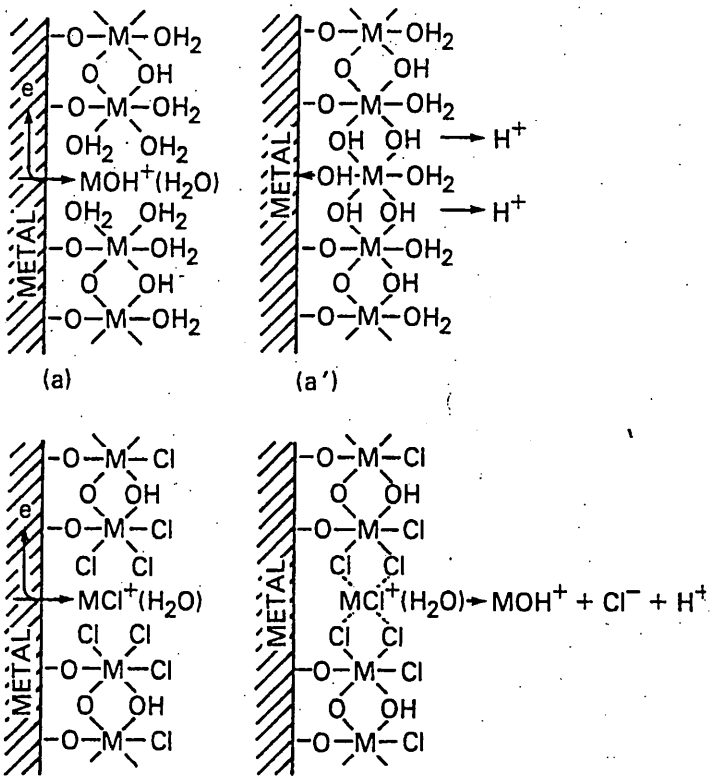

Figure: 2.3 Metal ions dissolved through an undeveloped part of the film (a)are captured to form a film (a) resulting from bridging with OH groups. Chloride ions replacing water molecules (b) prevent the bridging reaction (b)′ resulting in breakdown of the film (Okamoto, 1973).

When the chloride ions enter into the solution they replace the water molecules most easily in the undeveloped part of the film i.e. at H_2O -- M -- OH_2 bridge sites. The introduction of chloride ions at these bridge sites results in the formation of soluble metal chloride complexes and their removal from the film B′. This reaction constitutes the breakdown of passivity and the initiation of localised corrosion.

It has been reported (Smialowska, 1990) that the properties of the passive film plays a dominant role in defining the pitting resistance of an alloy. The factors effecting film resistance were summarised in a diagram as shown below.

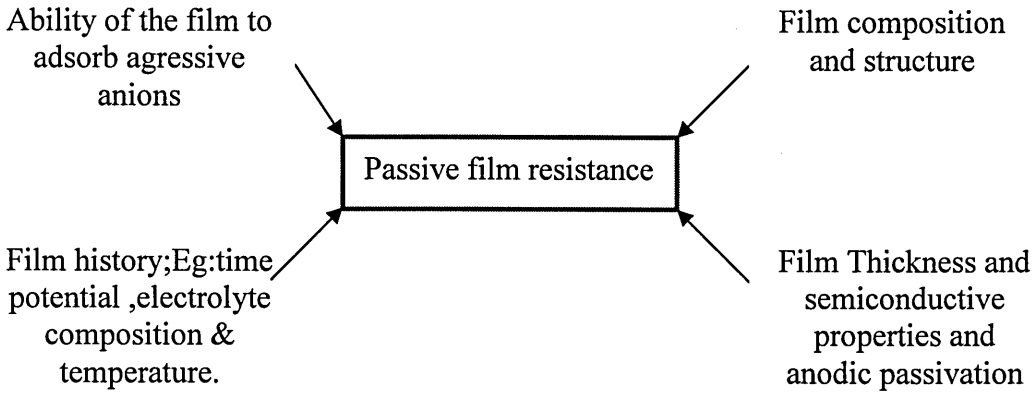

Figure:2.4 Schematic representation of factors effecting film resistance

Smialowksa divided the existing models for pitting into two groups one assuming that pits initiate at the oxide/electrolyte interface, and another assuming that pits initiate at the oxide/metal interface. Few valid reasons were quoted by the author that in first case that a)Imperfection of the passive film can be caused by the presence of pores, flaws, and gaps through which anions may enter and reach the bare metal surface, b) collapse of the film resulting in accumulation of vacancies at the oxide/metal interface, and finally c)mechanical breakdown of the film caused by stress in the film. In the second case it can be a) due to the replacement of oxygen ions in the oxide lattice by chloride ions, b)formation of chloride complexes with metal cations and finally c) formation of salt nuclei at the surface. In all these above cases as highlighted earlier in Fig 2.4 passive film properties play an important role in defining the pitting resistance of stainless steels. However this study is conducted at elevated temperatures and doesn't involve in measuring the properties of film and highlight the importance of the characteristics that could play a role.

2.4 Pitting

Pitting is a result of the breakdown of the passive film that covers a given metal or alloy (Smialowska, 1990). Smialowska highlighted the fact that factors influencing pit initiation such as adsorption of halogen ions, film composition and structure, passivation conditions, film thickness, and semiconductive properties. Currently models for pit initiation are developed based on the attack of halogen anions on passive films on stainless steels.

Corrosion can be localised or uniform depending on the type of attack. Of all the different types of corrosion, pitting is encountered most frequently in metallic materials in industrial applications. This study is more relevant towards this type of localised corrosion which is termed as "Pitting" and its influence on the stressed samples. It is an important parameter to be considered while selection of stainless steels for industrial applications. several factors like temperature, concentration of the species, pH, chemical composition of the parent material etc.

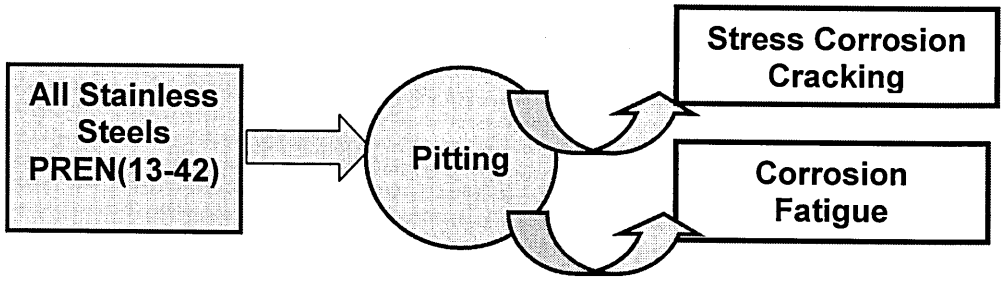

Figure:2.5 Schematic diagram of the role of pitting

The more the stainless steel is resistant to pitting the better it is for long term applications as pitting aggravates both stress corrosion cracking (SCC) and corrosion fatigue (CF) cracking which leads to the failure of engineering equipment. Therefore pitting is a localised form of attack resulting in pits which vary in size, shape, and density in the metal. Pitting of stainless steels involves several stages to occur in nature. It varies accordingly with the conditions of the stainless steels are

exposed. The Pitting occurs in three stages, consisting of nucleation, metastable growth and stable pit growth (Burstein et al, 1993). According to the authors pit nucleation is an unstable process and if a pit survives after the nucleation stage it enters to the metastable growth stage where pit growth is controlled through diffusion through a perforated film and finally, if it survives at that stage it will enter into stable pit growth region. As the pitting rate is different for every individual steel, it is essential to understand the contribution of various compositional parameters to justify the selection of particular steel for any industrial application, as every industrial metal or alloy is susceptible to pitting. Several authors (Smialowska, 1990; Newman, 1987) have studied this phenomenon for many decades and still found some unanswered questions. Most of their studies are restricted to the narrow range (25- 90^0C) of temperatures for a limited selection of steels. One of the main objectives of this study is to explore the temperature dependency of pitting susceptibility for a wide range of important industrial stainless steels.

2.4.1 Nucleation and growth of pits

The initiation of pitting is generally an unpredictable and a random event, as several identical samples of metal exposed to the same chemical conditions will neither corrode at the same time nor at the same points on the sample surface. It is well established that growth of corrosion pits in stainless steels exposed to chloride solutions involves two stages, the first stage was characterised as metastable growth followed by stable growth (Frankel et al, 1987; Issacs, 1989).

Metastable pit growth can be terminated at any time , where the pit surface repassivates and the current falls sharply. Pits which grow metastabily do not achieve stability, only when the potential is raised in the anodic direction does it achieves stability (Burstein et al, 1993). The studies by the same author proposed that pitting

of stainless occurs in three consecutive stages, the first stage is termed as nucleation and defined as unstable process. The second stage is termed as metastable growth, which is diffusion controlled process, provided by a perforated cover over the pit mouth. The survival of the pits without repassivation enters into the third stage where the pit growth is stable, and the stability is also a diffusion controlled with diffusion barrier provided by the pit depth alone.

The above mentioned studies do not explain the development of pits with respect to stainless steel oxidation which occurs at high temperature but the studies of (Evans et al; 1980) on 20% Cr/ 25%Ni Stainless steel oxidation tests were conducted in autoclaves at different test temperatures and they proposed a qualitative model.

The model explains that pitting is initiated when localised spalling of protective chromium oxide film occurs, followed by rapid oxidation of the chromium depleted substrate then proceeds with formation of iron rich oxide and spinels containing nickel, chromium and iron within the pit itself. A silica layer remains on the alloy surface acts as a diffusion barrier and with increase in attack the chromium concentration at the pit bottom reaches a critical value to reform the chromium oxide film. Once the chromium oxide film forms the pitting attack then ceases and a slow growth rate continues through the protective film at the base.

2.4.2 Role of chloride

Influence of chloride ions on properties of the passive film and their role in film breakdown is never completely understood. The studies of Kruger and McBee (1971) suggest that a passive film is thickened above the pitting potential in a chloride containing solution, and removal of Cl^- ions from the solution cause the passive film to return to its original thickness. Earlier Hoar (1965) assumed that inside growing

pits, a surface layer enriched in Cl^- ions maintains the active state of pits, which is supported by the studies of (Szklarska – Smialowska, 1971). Another possibility of nucleation of pits due to migration of both Cl^- and Fe^{2+} ions through the weakest points or defective sites of the passive layer, which in turn leads to salt layer formation was proposed by Janik-Czachor et al (1975).

The present study is interested in behaviour of chloride ions at high temperatures and their role in break down of the film

2.5 Pitting resistance equivalent number:

The pitting resistance equivalent number (PREN) has been introduced by the alloy producers as a tool for comparing stainless steels for their relative resistance to pitting. As the user of stainless steels has only a very limited knowledge of suitability of a specific steels for applications in the plant (Truman, 1987; Mori, 2004). It will allow the user to judge and select a material that is suitable for a particular environment and gives guidance about the alternate materials for various applications. Truman conducted experiments in seawater on different experimental steels at room temperature in order to define the PREN and is expressed as

$$PREN = \% Cr + 3.3\ \%Mo + 16\ N \qquad (2.7)$$

It is noticed from Eq 2.7 that chromium, molybdenum and nitrogen contribute to the pitting resistance of the stainless steels. For a user the main interest is not the relative effect of the individual elements with PREN but the sum effect on the pitting corrosion resistance. Although PREN is a simple form of expressing the three elemental influences on the pitting resistance it is considered as a useful index by the steel makers. Cleland (1996) has summarised several equations that exists for PREN

and they presented as below, one of the simplest equation 5 takes into account of only the effects of chromium and molybdenum

$$PREN = Cr+3.3Mo \quad (2.8)$$

Since most of the alloys existing contain nitrogen this equation does not consider the nitrogen so it has been ignored in the recent studies where as other formulaes presented in the literature are presented below

$$PREN = Cr+3.0Mo+12.8N \quad (2.9)$$

$$PREN = Cr+3.3Mo+13N \quad (2.10)$$

$$PREN = Cr+3.3Mo+16N \quad (2.11)$$

$$PREN = Cr+3.0Mo+27N \quad (2.12)$$

$$PREN = Cr+3.3Mo+30N \quad (2.13)$$

All these above equations are consistent with various sets of data, but it is difficult to compare as the test conditions vary from one another.

When calculating PREN values only one aspect is considered i.e. the influence of three elements, where there could be several other factors which could influence the pitting resistance of stainless steel. There are also elements not included which are know to have a negative effect on pitting resistance. One such element is sulphur, which in the form of sulphide inclusion can act as initiation site for pitting. In duplex stainless steels, the properties of the bulk reflect the properties of the individual phases, which depend on their chemical compositions. While in single phase alloys it is primarily given by the bulk composition. It has been frequently reported by various authors (Charles, 1991; Bernahrdson, 1991; Peterson, 1996) that the main alloying elements i.e chromium, molybdenum, nickel, and nitrogen are not evenly distributed in ferrite and austenite.

2.5.1 Applicability of PREN

The difficulty of using PREN in duplex stainless steels is as there are two phases, austenite and ferrite present with different compositions in these steels, and the elements involved in PREN are distributed between them. The diffusion rate of the alloying elements in ferrite are approximately 100 times faster than the corresponding values in the austenite and also ferrite is more enriched in chromium and molybdenum, which are known to enhance the promotion of intermetallic phases. As discussed by Charles (1991) the solubility in ferrite of elements like N, C, and Cu falls sharply with decrease in temperature, increasing the probability of precipitation during heat treatment.

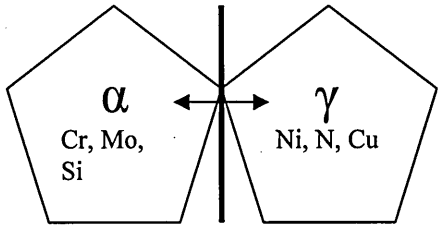

Figure:2.6 Partitioning of the major alloying elements in austenite and ferrite grains

It is noticed from the Fig:2.6 that alloying elements are not evenly distributed in duplex stainless steels. Cr, Mo, Si acts as ferrite stabilizers and tend to enrich in ferrite grains where as Ni, N, Cu acts as austenite stabilizers and austenite grains are enriched with these elements. Thermodynamic calculations were not consistent with PREN values as the increase in temperature can change the compositions and proportions of the two phases in duplex steels, as PREN for ferrite decreases with temperature that for austenite increases (Berhardsson, 1991). The ferrite phase is stronger in terms of corrosion resistance due to the higher molybdenum and chromium mass fractions while the nitrogen mass fraction in austenite is still too low

to result in a similar corrosion resistance. It is clear that PREN for each phase to be calculated separately and must consider the minimum value which every phase.

2.5.2 Limitations of PREN

The metallurgical condition and the effects of elements such as sulphur and copper have not been taken into account in PREN equation (Cleland, 1996). The PREN approach cannot supply a full explanation of the behaviour of the alloys because it does not take into account considerations of synergism between elements and considering single element in isolation, as strong synergism is found in case of austenitic stainless steels between Mo and N (Angelini et al, 2004). The use of PREN values should be kept to minimum and treating it as a good parameter for assessing the strength of the steels is at high risk (Alfonsson & Qvarfort,1991).It can be understood that PREN formulaes should be used for making a rough estimate of the pitting resistance of an alloy. The importance of the PREN values should therefore not be overestimated. Small differences in PREN values are irrelevant in practice (Weber and Uggowitzer, 1998). The same authors mention that increasing the nitrogen /nickel ratio has been proposed mainly in order to enhance the PREN of the bulk composition, one should have a closer look on its effect on the PREN of the individual phases

2.6 Pitting potentials

Pitting potential (E_P) is defined as the potential corresponding to an abrupt increase of the current above the passive current with increasing potential. The concept of a pitting potential or breakdown potential was proposed by (Brennert, 1935) for alloy steels, which characterizes the behaviour of passivable metals and alloys in chloride solutions. It is used as a electrochemical measurement of the pitting susceptibility of metals and their alloys to pitting in corrosion environments. This value can be

measured in the environment of interest for example in aqueous chloride, bromide , iodide and even in sulphuric acid solution. The values obtained depend on the composition and structure of the metal and the tests environment. Measuring the potentials when the pits tend to cause damage is useful for selecting materials for various applications.

Pitting corrosion has been influenced by different environmental parameters such as

- Temperature
- Chloride ion concentration
- Oxygen levels
- Chemical composition

The role of these parameters will be discussed individually in individual sections.

2.6.1 Techniques for measuring pitting potentials

2.6.1.1 Potentiodynamic polarisation

One of the electrochemical methods used for the determination of the pitting potential is the polarisation method.

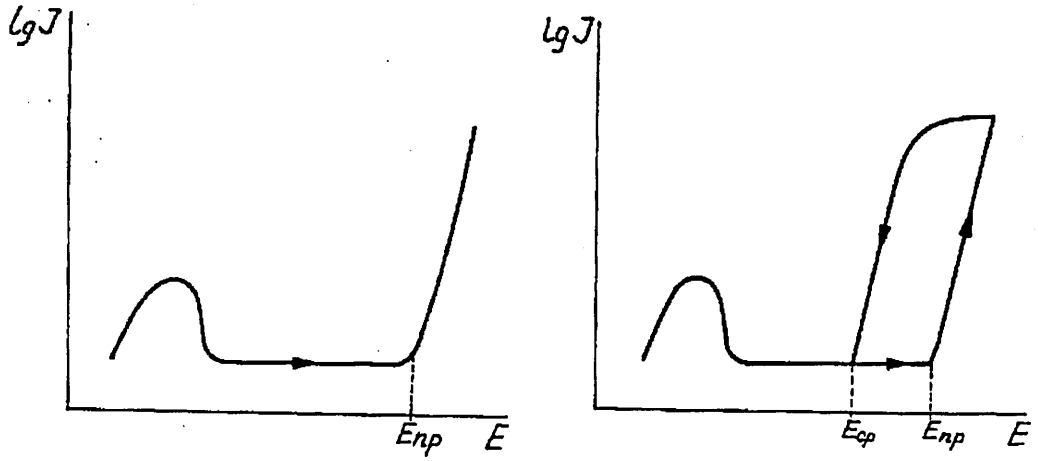

Figure:2.7 Schematic representation of the anodic polarization curves I vs E of a metal in solution containing aggressive ions obtained using a potentiostatic device a) Positive direction and b) backwards/negative direction (Smialowska, 1971)

There are two variations in this method a) by holding the specimen at each assigned potential until a constant current is established or b)Potentiodynamic method by changing the potential gradually at a constant rate. Using this method two characteristic potentials can be measured 1) pitting potential 2) repassivation potential as shown in Fig:2.7. This method allows to monitor the change in the current density with potential driving from the corrosion potential in the positive direction and then allows to reverse the loop to observe the drop in the current values where the pits tend to repasivate. In Fig 2.7 E_{np}, potential corresponding to rapid increase in of the current due to pit nucleation and E_{CP}, potential corresponding to the current drop caused by repassivation of pits.

2.6.1.2 Scan rate

All the potentiodynamic tests can be conducted at different potential scan rates but how far these scan rates influence the pitting initiation is not yet clear (Smialowska,1996). However, influence of scan rate has been summarised by Smialowska (1986) and was reported that scan rate does have influence on the pitting potentials for high chromium and molybdenum steels, whereas in case of ferritic steels it did not show significant effect. Also it was also noticed that chemical composition of metal or alloy has a significant influence on the scan rate. The pitting potential values at rapid and intermediate scan rates was reported by Manning (1980) on austenitic stainless steel and results were explained based on the different rates of passive film formation. However this study was conducted at a constant scan rate for all conditions.

2.6.2 Critical pitting Temperature

Measurements of critical pitting temperature (CPT) can be used to determine the material susceptibility to pitting. Stainless steel product manufacturers use this

parameter to promote their product against the CPT values. CPT tests are conducted in 10 wt% $FeCl_3$ $6H_2O$ in 900mL of distilled water according to the ASTM G 48, where the temperature is increased in steps of 2.5^0C and increase in the current density value at certain temperature value is recorded as CPT for that particular material. At the end of the test the sample is examined for weight loss and localised attack. Furthermore along with pitting potential, critical pitting temperature (CPT) values are well known parameters used to characterize the pitting resistance of alloys correlate with the composition of stainless steels with Cr, Mo, and N as shown below

$$CPT\ [^0C] = -41 + 2.5\ \%Cr + 7.6\ \%\ Mo + 31.9\ \%N \qquad (2.14)$$

2.6.3 Effect of alloying elements

It is well established that chromium, molybdenum, nitrogen and nickel are the main alloying elements required for high pitting resistance in stainless steels (Sedriks, 1987). Truman (1987) in his study mentioned the relationship between alloy content and pitting potential is not linear, involving a transition above a certain PREN value, which is due to the addition of chromium, molybdenum, and nitrogen individually or in a combination as shown in Fig: 2.8

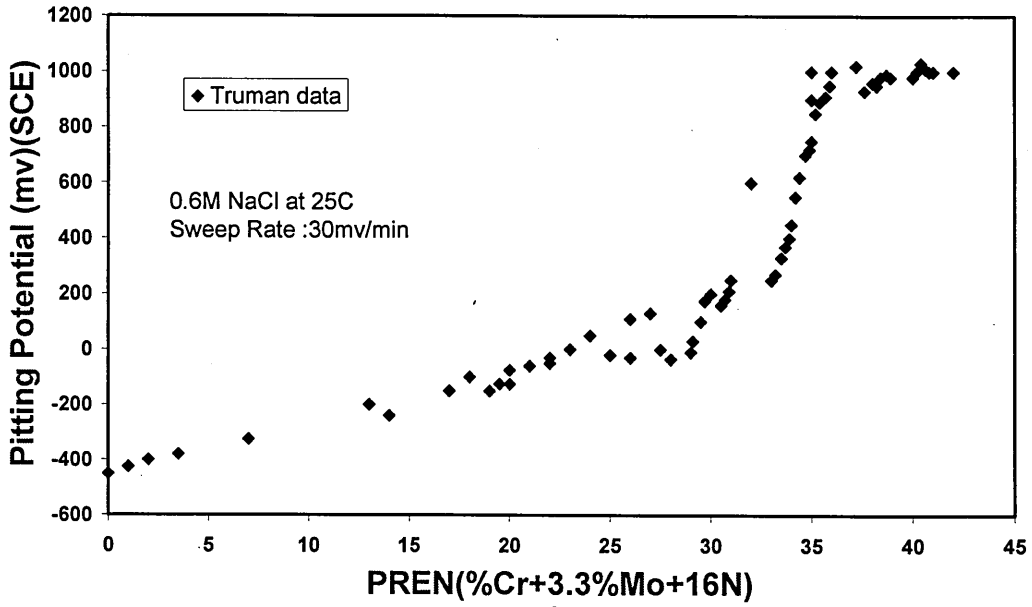

Figure:2.8 Pitting potentials measured at 25^0C in 3.5wt%NaCl for different PREN

As shown in figure the transition occurred around PREN value of 32 which suggests that increase in alloying elements does increase the pitting resistance. But the increase in PREN is directly related to the increase in cost. So it was not always a good idea to enhance the composition as it becomes very expensive product. Among the expensive compositional elements nickel tends to be at higher price so the stainless steel makers found an alternative solution by adding nitrogen and molybdenum. Earlier study of Horvath and Uhlig (1968) has shown that increase in chromium content of the iron chromium alloys in a deaerated 0.1N NaCl solution at room temperature shifts the pitting potentials to more noble direction as in Fig 2.9.

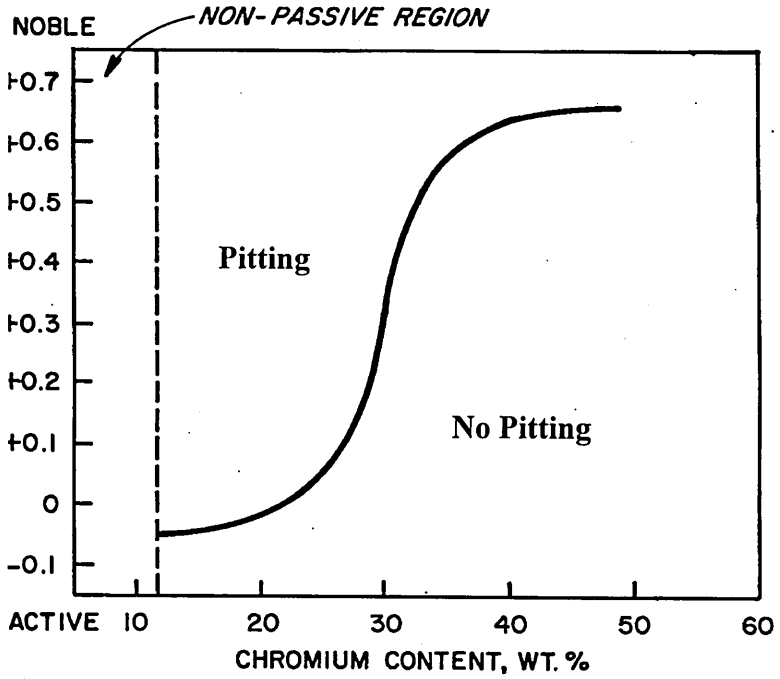

Figure:2.9 Effect of chromium content on pitting potential of iron-chromium alloys in a deaerated 0.1N NaCl solution at 25^0C (Horvath and Uhlig, 1968)

Lorenz and Medawar (1969) studied the effect of chromium and molybdenum on several austenitic, ferritic alloys in artificial seawater and proposed a following relation ship between pitting potential, and these alloying elements as

$$(1200 - E_{np})^2 = 2.54 \times 10^{-6} - 90 \times 10^3 (\%Cr + \% Mo) \qquad (2.15)$$

and they mentioned that in chloride solutions, the presence of chromium is essential if molybdenum is added to improve pitting resistance and in the absence of chromium the addition of molybdenum has no effect. The addition of the alloying elements depends on the microstructure of the stainless steels. In order to achieve higher PREN the addition of nitrogen and molybdenum play an important role. As increase in PREN achieves duplex and super stainless steel grades with higher resistance to pitting. Compared to the standard duplex stainless steels the second generation duplex stainless steels also called as super duplex stainless steels are well made of high nitrogen content which is an essential element to improve the pitting resistance. The Nitrogen content has a positive impact in maintaining the stability of duplex microstructure particularly in the heat affected zones (Combarde, Audouard, 1991) . These new super duplex stainless have lower nickel contents for the purpose of economic design, along with standard duplex steels these materials have already replaced the austenitic steels in many industrial applications for there excelling corrosion resistance and weldability (Francis et al, 1997; Spence and Warburton, Warburton et al, 1995). Recent study of Merello et al (2003) on thirty three experimental duplex alloys in NaCl solution at 25^0C to establish a relationship between chemical composition and pitting resistance of duplex steels found an exponential relation ship between pitting potential and chemical composition as given below

$$E_p = 2.94 \exp (0.14 PREN_{16}) \qquad (2.16)$$

The relationship was determined using the experimental results survey done by the Merello et al will be useful in designing new low Ni - high N steels based on the results shown in Fig 2.10

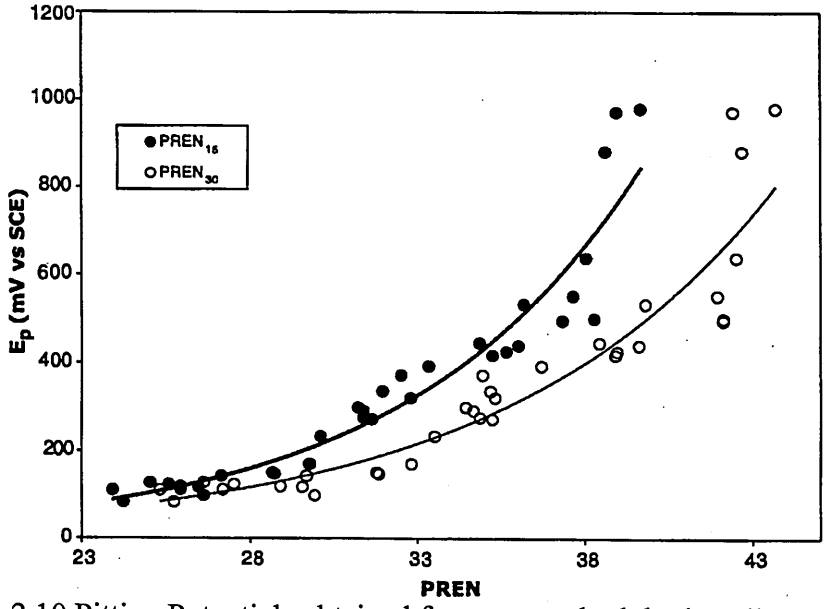

Figure: 2.10 Pitting Potentials obtained for non standard duplex alloys against $PREN_{16}$ and $PREN_{30}$ values at 50^0C (Merello et al, 2003).

Study on these non standard duplex steels has shown that at least 1 % Molybdenum is required to achieve high pitting resistance. All though it was a significant study to establish a relationship, the drawback was it is determined at room temperature. As most of these duplex steels are used in acidic environments and find increasing applications at high temperatures it is important to recheck the properties at various temperatures. The scope of this kind of relationship is very limited, so it is important to determine the behaviour of these duplex materials at higher temperatures. Apart from chromium a number of other alloying elements can have a significant beneficial effect, the present study will focus on the strong beneficial effects due to molybdenum plus nitrogen additions which has now been utilised in the development of new generation duplex stainless steels. It was noticed that addition of molybdenum in presence of nitrogen content have shown significant influence on the pitting potential which tells that a kind of synergism is maintained when these elements are together as shown in Truman's study.

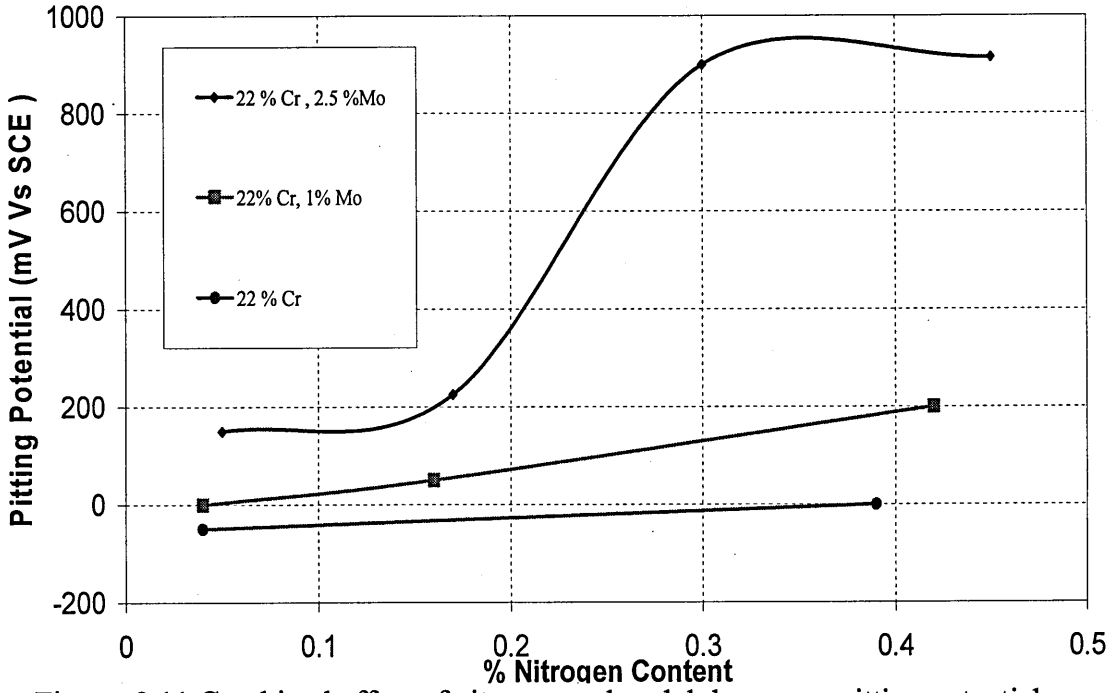

Figure: 2.11 Combined effect of nitrogen and molybdenum on pitting potential values at 25^0C in 3.5 wt % NaCl solution.(Truman,1987)

2.6.3.1 Nitrogen and Molybdenum effect

Nitrogen alloying has been introduced into austenitic stainless steel initially because it enhanced the strength and it results in reduction in the amount of nickel required to maintain the austenitic structure, also nitrogen is cheap and readily available alloying element, (Jargelius and Wallin, 1986). The addition of nitrogen to austenitic steel allows to decrease the wt% of nickel only to a certain limit around 0.32% (Bayoumi and Ghanem, 2005). Different mechanisms and theories have been proposed to suggest how nitrogen operates, in steel. Nitrogen modifies the ratio or composition of carbide phases which acted as pit initiation sites in a 18Cr 5Ni 10Mn steel (Janik-Czachor et al, 1975). Truman et al (1977) speculated that a nitride might be formed during dissolution in high nitrogen steels due to the availability of atomic nitrogen on the surface of the stainless steel and inhibit pit growth, this phenomenon was agreed by Bandy and Van Rooyen, (1983). The studies on 17 – 25Cr 22Ni1.5Mo Steels by Osozawa and Okato (1976) detected the presence of ammonia ions after the

pitting tests conducted in 20% ferric chloride tests suggested that nitrogen consumes protons and increases the pH in the early stages of pit growth and promotes repassivation which follows an equation

$$N + 4H^+ + 3e^- \rightarrow NH_4^+ \qquad (2.17)$$

This phenomenon was partly confirmed when Jargelius and Wallin conducted studies on 20Cr 25Ni and 20Cr25Ni4.5Mo Steels with varying nitrogen contents up to 0.210wt% found that improvement in pitting resistance was due to formation of ammonium ions within pits and crevices and thereby facilitating repassivation.

The results demonstrate the beneficial effect of nitrogen additions on pitting and crevice corrosion resistance in NaCl solutions, particularly for the molybdenum alloyed steels. Solution analysis confirmed that nitrogen is present in the form NH_4^+ ions, raising the pH close to the surface and facilitating repassivation. Nitrogen incorporation in the passive film was found in the studies of Truman (1977).

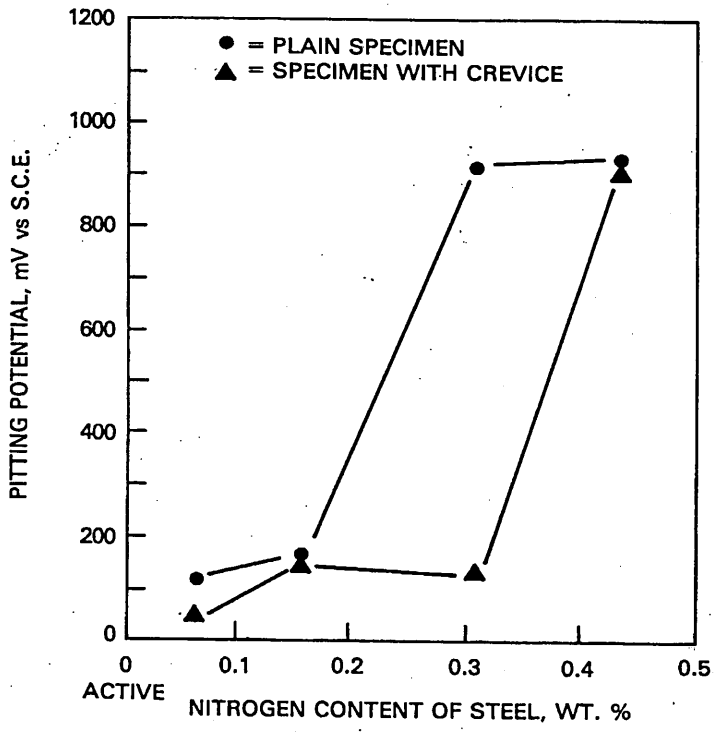

Figure:2.12 Effect of nitrogen content of steel on the pitting potential of Fe- 22Cr - 20Ni-4Mn-2.8 Mo-0.03C-0.01S stainless steel in an aerated aqueous solution containing 0.6M NaCl and 0.1M $NaHCO_3$ (Truman et al, 1977).

Evidence of nitride presence in the inner part of passive film near the passive film/alloy interface was found by Sadough Vanini et al (1994) in the studies of electrochemical behaviour of austenitic stainless steels. Olefjord and Wegrelius (1996) concluded that nitrogen segregates anodically to the metal- oxide interface during passivation, they also confirmed that chromium nitride is not formed and the enrichment of nitrogen increase with the potential. They go on to say that low nitrogen containing steels were more susceptible to pitting compared to high nitrogen steels at 65^0C, and the composition of passive films formed at room temperature are independent of the nitrogen content of the steel. Ives et al (1991) have suggested that nitrogen might form ammonium that combines with different oxidants to form less active compounds which inhibit pit growth. Newman and Sharabi (1987) proposed that, the slow reaction of nitrogen with protons during anodic dissolution, allows nitrogen to block anodic dissolution. The effect of nitrate on pitting of stainless steels

was studied using a microelectrode by Newman and Ajjawi (1986) found that nitrate passivates salt covered surfaces but not salt free surface thus suggesting that passivation depends in nitrate to chloride ratio. A more recent study (Lothongkum et al, 2006) concerning the effect of nitrogen on corrosion behaviour of 28 Cr -7Ni duplex stainless steel in 3.5wt% NaCl solution has shown that an increase of nitrogen as an alloying element increases the corrosion potential in acidic solutions but not in neutral and basic solutions. It was also said that ammonia formation can happen to increase the pitting corrosion resistance as well as the nitrogen enrichment in oxide/metal interface. Earlier Lu et al (1993) pointed out that the formation of nitrides hinder the dissolution of iron and reduces the acidification in pit sites, and also nitrides inhibits the transpassive dissolution of molybdenum in the passive surface leaving molybdenum to stay on the passive surface. They also suggested that chromium and molybdenum nitrates are more stable in acidic solution than in neutral solutions which may accelerate the anodic segregation of chromium and molybdenum during localised corrosion, and tend to form a salt layer at the pit. Nitrogen has shown significant effect on formation of intermetallic phases that are formed during high temperature aging of these materials. Since σ phase precipitation takes place in duplex steels which causes significant damage by reduction of toughness and ductility, the influence of nitrogen play an important role. Shang Huang and Chang Shih (2005) have studied the effect of nitrogen on precipitation of duplex steel and found that increase in nitrogen content lowers the content of σ phase in duplex steel.

The beneficial effect of molybdenum in various studies can be summarised (Montemore et al, 1999) as, enrichment of molybdenum in the passive film, molybdenum was found to be present in the inner layer of the passive film,

molybdenum thickens the passive film and stabilizes chromium oxide by the presence of Mo^{6+}, Molybdenum retards corrosion by the formation of molybdenum compounds. In a detailed study on Fe-Cr -Mo alloys presence of molybdenum has increased the pitting potentials in chloride solutions in such way suggests that it adsorbs with Cl^- and blocks Cl^- adsorption (Maximovitch et al, 1995). The study (Montemore et al, 1999) of capacitance measurements in oxide films grown in a furnace at higher temperature has shown the presence of molybdenum does not influence the thickness of the oxide film and Mo enriched the film with chromium oxide and traces of molybdenum was not present in the outer layer of the film but was to be in the inner layer of the film. Olefjord and Wegerelius (1996) have explained that the growth rate of pits formed on the Mo - containing steels is lower than on the Molybdenum free alloys due to enrichments of molybdenum and other alloying elements in their metallic state on metallic surface. Study by French workers Lemaitre et al (1993) reported the role of molybdenum in the pitting resistance of stainless steels as, molybdenum in steel or dissolved in the solution as molybdate ions improves the resistance to localised breakdown of the passive film and also confirmed that solubility of sulphide inclusions is modified by molybdate ions in the presence of dissolved oxygen. Certainly most of the above mentioned studies were conducted on different steels with varying molybdenum contents in the steels it is interesting to notice whether molybdenum influence only in chloride or in any other solution. One such kind of study by Kaneko and Issacs (2000) conducted on both austenitic and ferritic steels in chloride and bromide solutions have recorded higher pitting potentials for austenitic steels with increase in molybdenum content compared in ferritic steels. According to the authors large increases in the pitting potential was found in the chloride solutions rather in bromide solutions. Qvafort (1998) observed

that molybdenum influences the early stage of pit propagation and a thick porous layer of molybdenum rich oxide is precipitated on the pit walls in the study on 6Mo steels. The same author reported that molybdenum rich oxide will decrease the corrosion rate and favours repassivation of metastable pits. Since the alloying elements influence the pit initiation these kinds of observations cannot give full evidence of the influence of molybdenum and further study is required in detail at higher temperature about the stability of this molybdenum rich oxide. However, it is unclear the role of molybdenum in the steels at higher temperatures. One of the objectives of this study is to check if higher molybdenum containing steels were stable in wide range of chloride and temperatures.

2.6.3.2 Effect of Copper , Tungsten:

Since copper and tungsten were added to the duplex and super duplex stainless steels for compositional benefits it is interesting to know what these elements contribute. Firstly it is well known that copper has a beneficial effect on the pitting resistance in sulphuric acid environments however its role in chloride solutions is not yet clear. Bernahardsson (1991) reported that addition of copper has significantly improved the resistance to pitting corrosion in H_2S0_4 up to 45^0C, and it always interesting to know how addition of copper has on phase balance of these materials. Combrade and Audouard (1991) has highlighted that Cu + Mo accumulate in ferrite whereas Cu + N accumulate in austenite phase. Below is a summary of influence of copper on improving the pitting resistance in chloride solutions highlighted in the recent review (Sorisseau et al, 2005).

1. Copper inhibits the sulphide inclusions by forming copper sulphide.

2. Formation of metallic copper surface film will inhibit the steel dissolution on the surface.

The negative effects of copper are :

a) Copper allows to lower the chromium content of passive film

b) it promotes the chromium carbide precipitation

c) Increase anodic dissolution of the steel.

Garfias - Mesias and Sykes (1998) conducted study on 25%Cr Ferallium alloy SD40 duplex stainless steels with different copper contents and concluded that CPT (Critical Pitting Temperature) was not improved by addition of copper, and reported pitting in the ferrite phase, so at present it cannot be concluded that either has beneficial or detrimental effect. On the other hand very limited studies exist on the role of tungsten in case of duplex stainless steels. One of the earlier study by Chen and Kuo (1990) on iron has shown that tungsten improves the passivation range in acidic environments. In the case of Zeron100 super duplex stainless steel, one of the alloys that is investigated here in this study has shown that addition of tungsten about 0.5 to 1.0 wt% tungsten gave the optimum microstructure and corrosion resistance (Francis, 2000). Francis highlighted the fact that the combined effect of tungsten and copper in this alloy as achieved excellent corrosion properties in sulphuric and hydrochloric acids. But in case of tungsten containing Fe18Cr alloy it was reported that it had a detrimental effect on the pitting potential in aqueous electrolytic solution (Brookes and Graham, 1989) however to review the effect of these elements at high temperatures is beyond the scope of this study.

2.7 Effect of environment

All stainless steels are sensitive to chloride rich environments, with temperature and dissolved oxygen playing an important role in the environment assisted failure process. They are very often exist in a plant and are often difficult to completely control or eliminate from the system. Frequently the investigations carried out to determine the influence of these parameters is very restricted to a simple parameter or restricted to one alloy. A detailed study of these combination of factors is necessary for full understanding and the author believes that these parameters influence collectively in any plant rather than on their own. A general review of these critical factors will be discussed separately in the following sections.

2.7.1 Observed chloride effects

The severity of pitting process is related to aggressive halide ions, such as the chloride ion in the aqueous environment. The aggressiveness of pitting caused by halide ions in terms of pitting potentials was found to be in the order of chloride > bromide > iodide for stainless steels under different experimental conditions and alloy condition so consecutive decisions on materials selection can be safely based on corrosivity of Cl^- environment (Kaneko and Issacs, 2000; Katsumi and Hosoya, 1995). The environments in industries are polluted with or contain chloride ions, and it is considered as one of the primary species for the root cause of failures that occur in various components. It is known to be the most aggressive species as it can damage the passive film formed on the stainless steel more easily. The influence of this damaging species on the passivation behaviour of different alloys has been studied widely at room temperature. A critical chloride concentration exists for all metals to undergo pitting. This critical concentration varies with composition of stainless steels. Large concentrations of chloride ions will cause local damage of the

passive film more easily, and produce an increase of the anodic current density in the passive range (Smialowska, 1986; Sedricks, 1976). Chloride ions are increasingly absorbed or adsorbed at the surface, whereby the pitting mechanisms involve penetration of chloride ions through the passive film. A schematic diagram showing the progressive changes that a chloride ion can cause can be seen in the Fig 2.13 observed in polarisation scans. It is evident that as the chloride ion concentration increases, E_p decreases indicating that for most alloys and environments the chloride ion is the most effective agent in initiating pitting. As it can be noticed that passivity range can be extended with decrease in chloride concentration.

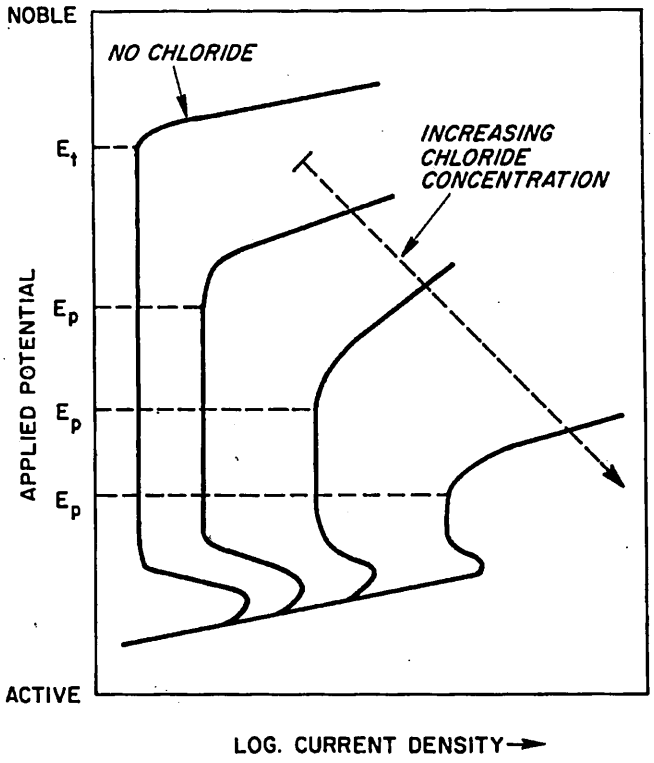

Figure:2.13 Schematic representation of effect of chloride concentration on polarisation curve (Sedricks, 1996)

A simple relationship between the pitting potential, E_P and the concentration of chloride ions was established from the previous studies (Strehblow, 1977; Wang et al, 1988) as

$$E_P = A - B \log [Cl^-] \qquad (2.18)$$

Where A and B are constants and depend on various factors mentioned above. The values of B obtained by various authors have been listed (Smialowska, 1986) for different metal and alloy conditions. The contributing factors to the effectiveness of chloride ions in reducing the E_p values are its high mobility, its small size, and permitting incorporation into the passive film and form its ability to soluble metal – chloride complexes (Frankel, 2004). Studies of Wang et al (1988) on 304L stainless steel, found a linear relationship between pitting potential (E_{pit}) and Log [Cl^-] for various temperatures.

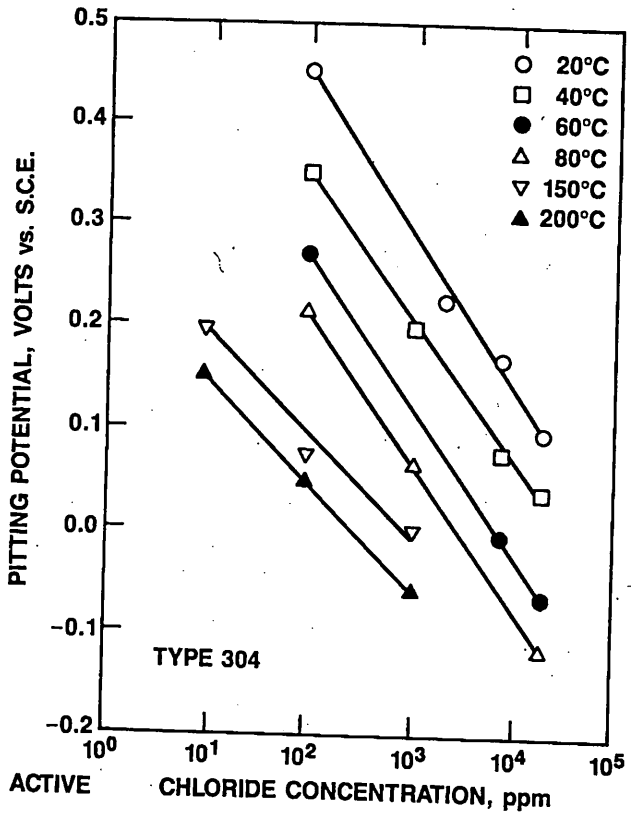

Figure:2.14 Pitting potential Vs log [Cl^-] concentration in aerated solutions at various temperatures. (Wang et al, 1988)

Similar relationship was noticed for carbon steel in the study conducted by Ergun and Turan (1991) in different chloride solutions at room temperature and concluded that the effect of chloride ions on the pitting potential and protection potential of

carbon steel is to decrease linearly with logarithmic chloride ion content as shown in Fig:2.15.

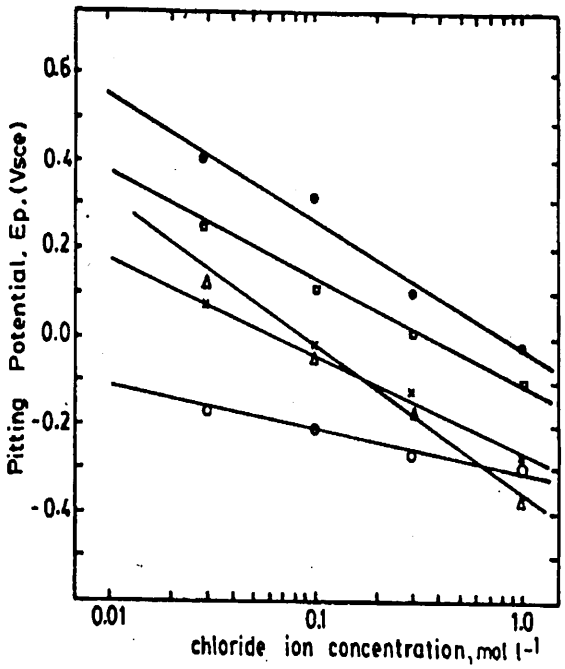

Figure:2.15 The influence of chloride ion concentration on the pitting potential (Ergun and Turan, 1991)

It was pointed out by the authors that, though there is a presence of weak passive film on carbon steels the presence of high concentrations of adsorbed chloride ions at the metal sites will prevent growth of passive film and results in establishments of active pits. This chloride dependence was even found in the case of duplex stainless steels shown in earlier study by Miyuki et al (1984) conducted in $C0_2$ – Cl^- environments with and without H_2S at elevated temperatures for two commercial duplex stainless steels with 22%Cr, and 25%Cr. As shown in Fig 2.16 pitting potentials values decreases with an increase of the chloride concentration in $C0_2$- Cl^- environments, specifying that 25 %Cr chromium steels have superior corrosion resistance, and increasing chromium have significant effect on the pitting resistance

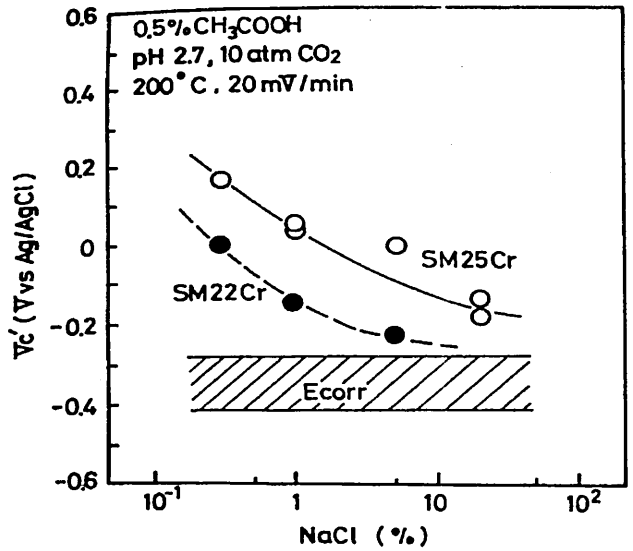

Figure:2.16 Effect of chloride concentration on 22%Cr and 25%Cr steels at 200^{0}C (Miyuku et al, 1984)

This kind of phenomenon is not only characteristic of high temperatures it does occur even at room temperature as shown in Fig 2.17 for 316 stainless steel.

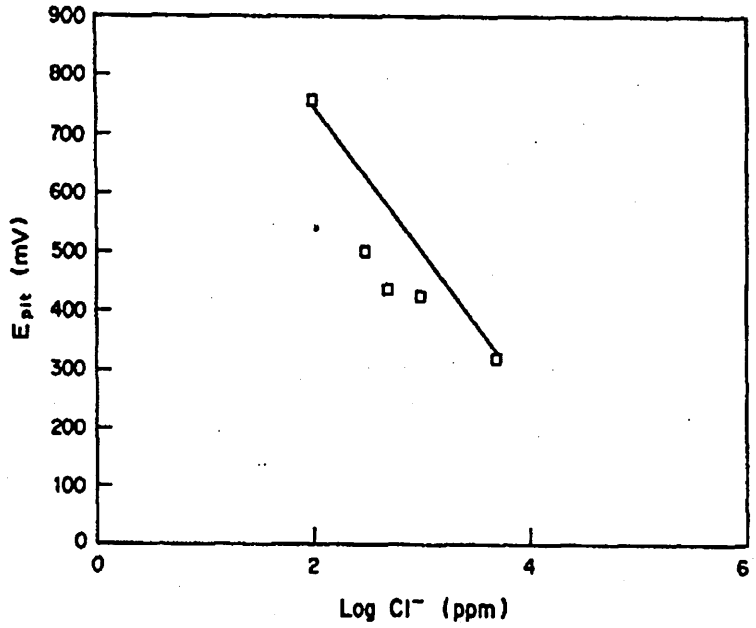

Figure:2.17 Pitting potentials vs log [Cl$^-$] at 20^{0}C and pH 4.

It is important to discuss the characteristics of the oxide film formed in different chloride solutions. Stewart (1987) pointed out that oxide film thickness is directly dependent on chloride concentration for 304L stainless steel. The current study has shown that 10ppm chloride is sufficient to nucleate stable, propagating pits

in the long term immersion tests. It is clearly indicating that a critical chloride concentration exists for all the steels that can cause pitting. Earlier, the concentration of chloride ions in pits was investigated by Mankowski and Smialowska (1975) on 18Cr -12Ni -2Mo -Ti austenitic stainless steel, in a solution containing 0.5N NaCl +0.1N H_2SO_4. They found that Cl^- concentration inside the pits was much higher than the bulk solutions, after they analysed the solutions in the pits which had grown for 30- 60 mins. According to the authors the low pH achieved inside the pits was due to the high chloride concentration inside the pits results from the hydrolysis of corrosion products. They also believe that the concentration of the Cl^- ions within pits changes with the composition of the film covering the pits such as convexity of film thickness, and finally the rate of pit growth decreased with increase in chloride concentration accumulating within the pits, indicating that pit growth is controlled by diffusion. However, less detailed information was available with the combination of temperatures especially above 90^0 C.

It is paramount to explore the effect of Cl^- concentration on E_P at different temperatures, and moreover it is of interest of this study to review the high temperature aqueous corrosion in chloride environments although other environments promote pitting. With increase in chloride concentration the tendency to pit increases resulting in the decrease of the pitting potential values up to a certain temperature range (25-130^0C) above this range it has been noticed (Cragnolino, 1987) that in some cases that E_P tend to increase and there is a weak dependence of E_P on chloride concentrations above 130^0C. A few relationships have been proposed to establish the relation between E_{pit} and $[Cl^-]^n$ for steel with PREN 19 and it is given by the expressions

$$E_{Pit} = 1.00 - 0.15 \,.\log C_{Cl^-}\,[ppm] \qquad (2.19)$$

at 20^0C and the equation is valid for 10- 10000ppm Cl^- ,even the same study also determined a relationship at 80^0C as given below (Wang et al ,1988)

$$E_{pit} = 0.75 - 0.15.\log C_{Cl^-} \text{ [ppm]} \quad (2.20)$$

The above conclusions were made from a study at room temperature but it is interesting to know the behaviour of these chloride ions at various temperatures on various stainless steels. It is a primary objective of this study to determine the critical concentration of chloride and determine the breakdown potentials for various temperatures in an environment to facilitate the materials selection process, and define threshold conditions to avoid pitting

2.7.2 Observed temperature effects

Temperature is one of the critical factors that effects a localised corrosion process. Localised corrosion tends to accelerate with increase in temperature and the pits act as stress raisers in many situations. It is well known (Smialowska, 1987) that resistance against localised corrosion decreases as temperature increases. The extent of this decrease i.e. temperature dependence of pitting potentials varies widely with change in composition of stainless steels as well corresponding temperature range in which the alloy was studied. The temperature at which the pitting corrosion starts is defined as critical pitting temperature (Brigham and Tozer, 1973). As corrosion is an activation controlled chemical reaction, the rate of is affected by temperature. The increase in temperature of the solution causes the pitting potentials to attain more active values. The rate of pitting would increase with increase in temperature according to arrhenius relationship (Semino et al, 1979). Most of the recent temperature dependence studies discussed below are restricted within a narrow temperature range of 25^0C- 90^0C with limited compositional changes of the stainless steels. It is important to estimate the pitting potential for any stainless steel in order

to prevent from localised corrosion the type of electrolyte has significant influence along with temperature to estimate the pitting corrosion of particular alloy in an environment which will be discussed in further sections.

The effect of temperature on different compositional alloys such as 17Cr, 18Cr10Ni and 18Cr10Ni 0.3Mo was studied by Szklarska-Smialowska (1971) who found a linear relationship exists between pitting potential and temperature. It was observed that for 18 Cr10Ni0.3Mo pit was independent of temperature and reaches a constant value above 70^0C. Another study conducted (Semino et al, 1979)using potentiostatic scratching technique on corrosion resistant alloys in 0.5M NaCl + 0.1M $NaHCO_3$ indicated that temperature dependence is consistent with the studies in the literature.

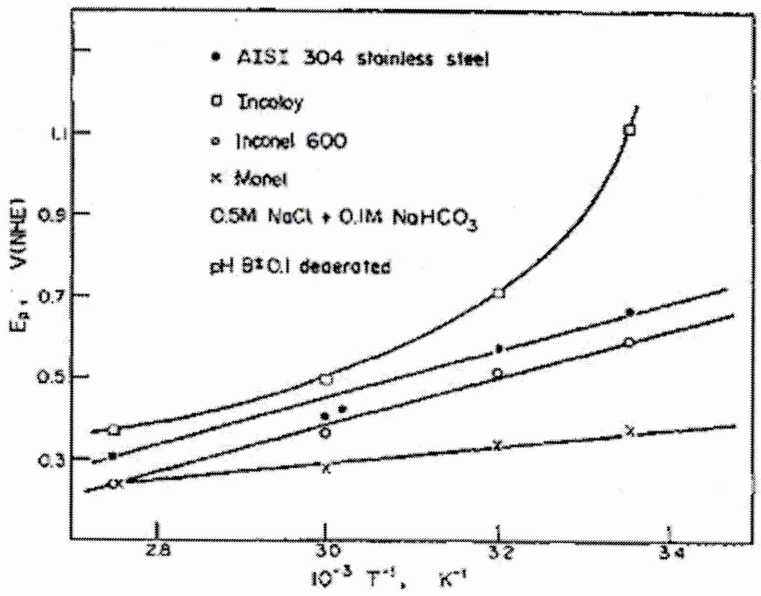

Figure:2.18 Pitting potentials Vs temperature in 0.5M NaCl + 0.1M $NaHCO_3$ (Semino et al, 1979)

As shown in Fig:2.18 pitting potentials became more negative with increase in temperature. Again in this study, although it made an attempt to study most corrosion resistant steels it was discussed for very limited steels, neither it explains neither compositional effects nor temperature kinetics. Cragnolino and Sridhar (1991) have examined the effect of temperature on the electrochemical parameters of Alloy 825

which is one of the candidate container material for nuclear waste disposal flasks. They found an inverse temperature effect in 6ppm chloride solution. Examination of the samples tested showed pitting in the range of 30 to 80^0C and interestingly no pitting was observed at 95^0C. The same authors also found that a weak dependence of temperature on pitting potential occurred in 1000ppm chloride solution and further investigated in 10000 ppm chloride and observed strong dependence of pitting potential with temperature. While many authors restricted the temperature effect studies to 304 and 316 steels in chloride solutions, Cristofaro et al (1997) continued their investigation on passivation behaviour of a super duplex stainless steel in a boric-Borate buffer solution with and without chloride and observed rather unusual behaviour as the temperature increase from 25^0C to 60^0C. They did not produce a decrease in the pitting potential and explained the result on the basis of stability of the passive film before the pitting corrosion occurred. A recent study by (Park et al, 2002) on the chloride dependence of pitting potentials at various temperatures observed that the presence of chloride influenced the pit growth rate and decreased the pitting potentials. They also found that an increase in chloride has altered pit morphology, and the role of temperature was to aid stable pit growth and prevent repassivation. It is well known that manganese sulphide inclusions play an important role in the pitting of low alloy steels, even in case of 304l Park et al have shown that with an increase in temperature both the dissolution of manganese sulphide inclusions and the metastable pit growth were accelerated.

So far the temperature dependence studies discussed were below 90^0C, however there were very few studies that exist above this range. One of the studies of Manning and Duquette (1980) on pit initiation in single phase and duplex 304L stainless steels containing delta ferrite in 100ppm Cl^- solution was conducted over

the temperature range (25-289^{0}C). The study showed a linear dependence of pitting potential with temperature as shown in the Fig 2.19

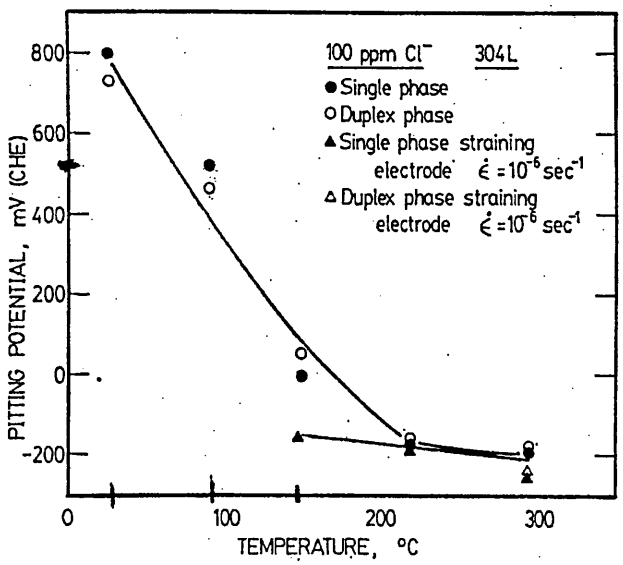

Figure:2.19 Pitting potentials of single phase and duplex 304L alloy as a function of temperature in 100ppm Cl$^-$. (Manning & Duquette study, 1980)

and concluded that the oxide film on stainless steels can undergo compositional change or physical structure modification behaving like a p-type semiconductor at room temperature and n-type at high temperature. Wang et al (1988) who reported rather a similar effect when they conducted a study on 304 stainless steel at (25-200^{0}C) in wide range of chloride concentrations (10-19000ppm) and found a linear relationship. The increase in temperature was observed to shift the pitting potentials to less anodic with increase in chloride concentration indicating that 304 stainless steel is sensitive to temperature in aggressive environments as shown in Fig 2.20. According to Wang et al two possible mechanisms might contribute to the fact that pitting resistance decreases with increase in temperature, firstly the film porosity is increased with increase in temperature, secondly the passive film undergoes an intrinsic modification of its chemical composition or physical structure, resulting in variation in density of vacancies or voids in the passive film. It seems the second proposed phenomenon supported by Manning et al as they argued that passive film

undergo change from p-type to n-type. But Smialowska is of the opinion that at elevated temperatures, the chemisorption rate of the chloride ions on the metal surface becomes more pronounced.

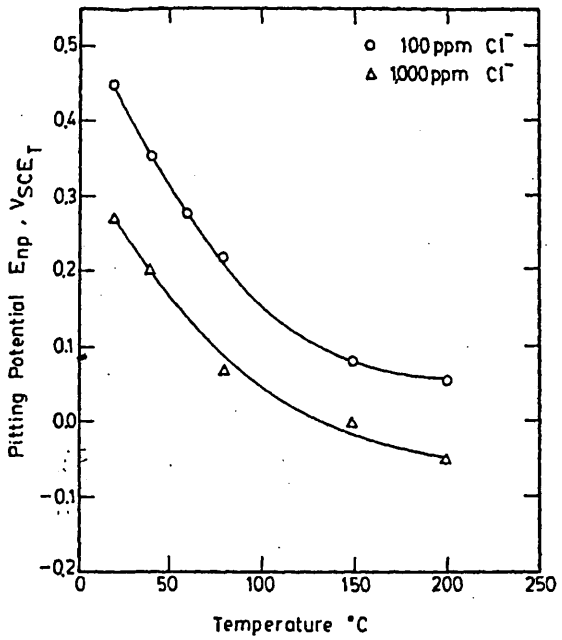

Figure: 2.20 Pitting Potential Vs Temperature in aerated solutions containing 100 and 1000ppm Chloride solutions (Wang et al, 1988)

In 1981 Lin et al noticed that the pitting potential of type 304 stainless steel sensitized for 12 hrs at 650^0C in 0.01M NaCl solution had no significant change in the pitting potential values above 150^0C unlike the linear dependence below 150^0C. It is clear from few studies that have been reviewed that a critical pitting temperature exists for each individual alloy and differs with environment. For example the study on the pitting behaviour on 904L stainless steel in 0.6M NaCl + 0.1 M Na_2SO_4 chloride and sulphate solution showed that 60^0C was the critical pitting temperature above which there was a drastic decrease in the pitting potential values (Ruijini et al, 1989). It can understood that low chromium steels have weak passive films as well as they have more inclusions that the high chromium duplex materials and the increase in temperature or chloride solution will definitely contribute to the dissolution of

manganese sulphide inclusions (Park et al, 2002). One of the studies (Sriram and Tromans, 1989) on two duplex steels in chloride solutions showed that the pitting potential and the selective phase attack was dependent upon partitioning of the elements Cr, Mo and N between the two phases.

In summary until now no theory has been satisfactorily proposed to describe the effect of temperature on the pitting potential of stainless steels . However it is believed that this temperature effect may be related to changes in the kinetics of passivation, repassivation, diffusion rates, and dissolution rate of alloy in the passivating state as it was shown all of them vary with temperature (Semino et al, 1979). As very limited information is available on the solution compositions within pits at elevated temperatures it is difficult to mechanistically understand the pit passive film breakdown at elevated temperatures, moreover above150^{0}C a qualitative change in the composition structure of the passive film occurs and observations made at room temperatures are irrelevant.

This study is conducted on wide range of stainless steels in chloride and temperature combinations to establish a relationship that can accurately predict pitting conditions in commercial grades of steel.

Repassivation Potentials or Protection Potential:

In 1960-1961 studies carried out by Cebelcor led to the concept of protection potential or repassivation potential which is more negative than pitting potential. Below this potential existing pits do not grow and these values can be determined using cyclic polarisation curves discussed in chapter 3. A very recent study (Abd El Meguid et al, 2007) on 254SMO stainless has shown that protection potentials does not depend on temperature up to 80^{0}C as shown in Fig 2.21. The same study has also shown the linear dependence and decrease linearly with log [Cl^-] for this particular

steel. Both pitting and protection potentials for this particular steel are related to the below relationship.

$$E = A\text{-}B\log [Cl^-] \qquad (2.21)$$

It can be noticed from the Fig 2.21 protection potentials are more positive than pitting potential values.

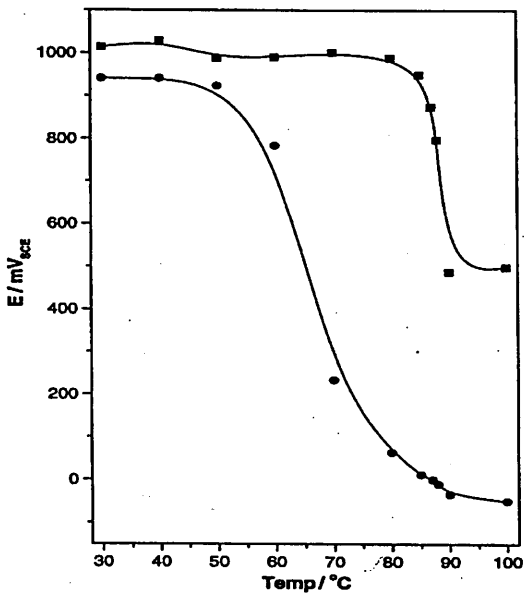

Figure:2.21 Effect of temperature on breakdown potential (E_P) and protection potential (E_{Prot}) for 254 SMO stainless in 4%NaCl solution (Abd El Meguid et al, 2007)

Pourbaix (1972) highlighted the significance of the protection potential in pitting, and stress corrosion cracking as these phenomenon can be eliminated by keeping the electrode potential below a given critical value, called the protection potential. He mentioned that where as the pitting potential very much depends upon both the pH and the chloride content the protection potential is independent of both pH and chloride content.

2.7.3 Dissolved oxygen

Dissolved oxygen is a major contributing factor to the natural corrosion of stainless steels. Oxygen is a part of electrochemical corrosion reaction occurring at

the interface between the aqueous phase and the metal surface. Therefore, the corrosion of a steel is directly proportional to the oxygen content in the water. Oxygen solubility will vary with many factors such as temperature, partial pressure, and electrolyte concentration. Increase in temperature reduce the solubility of oxygen, but increasing the partial pressure of oxygen increases the solubility of oxygen. Concentrated electrolytes have a tendency to decrease the oxygen solubility in water.

The presence of oxygen is necessary for the formation of protective oxides on the stainless steel surface(Fe_2O_3, Cr_2O_3), but in case of near neutral environments (pH 5-9) oxygen provides a cathodic reactant that increases the corrosion rates from 2 to 5 mpy under stagnant conditions (Stansbury and Buchanan, 2000). In the absence of dissolved oxygen i.e. in case of deaerated water the corrosion rate is greatly reduced as the stainless tend to have a uniform protective magnetite film (Fe_3O_4) on the surface, which isolates the base metal from water and reducing corrosion. Otieno-AlegoV et al (1995) studies on low alloy steel used in steam turbine environment have shown that the changes in the polarisation curve depend on the concentration of cathodic reactants like oxygen in the corrosion system of iron in aerated alkaline system. The phenomenon was explained based on the four cases where oxygen levels are treated as low oxygen level will initiate active corrosion in cathodic region, moderate oxygen allow to form a stable passive film to form with minimum corrosion, reduction in oxygen level will minimise corrosion and finally high oxygen level causes the film to be damaged at less anodic potentials with subsequent localised corrosion.

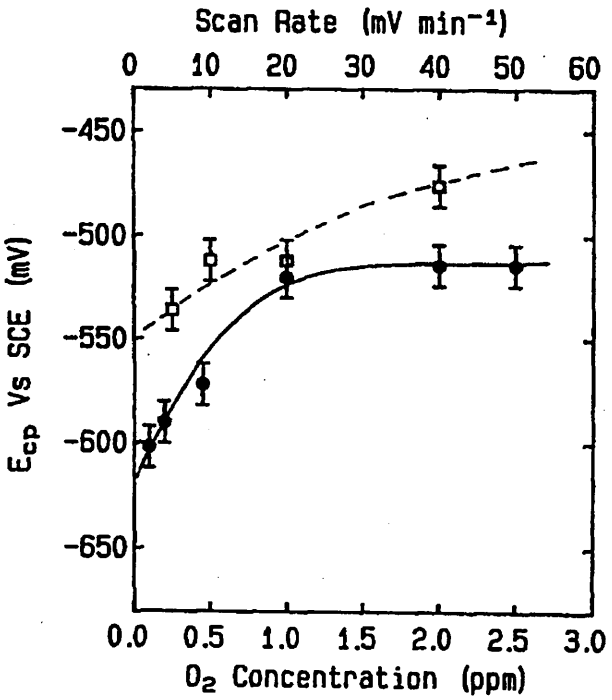

Figure:2.22 Showing variation of E_{CP} (Critical pitting potential) with scan rate and oxygen concentration for a low alloy steel (Otieno-Alego.V et al, 1995)

The results of the above study shown in Fig 2.22 established that increasing oxygen concentration drives the anodic reaction at a faster rate, and at low levels of oxygen it resulted in low/negative pitting potentials values as a result of tendency to form a weaker film. A recent study on the effect of dissolved oxygen on the passive behaviour of stainless steels concluded that dissolved oxygen provides only the necessary potential for passivation and provides no chemical species for passivation (Raja and Jones, 2005)

2.7.4 Pit growth rate and morphology

Numerous studies exist on pit growth kinetics and pit growth rates on metal at room temperature, but there is a scarcity of quantitative data concerning the newly developed alloys at temperatures higher than 90^0C. It is well known that the rate at which corrosion pits grow in depth is described as an power law function by

$$d = at^n \qquad (2.22)$$

where d is the depth of the pits and a, n are constants. Different values for n are reported for different metals. Mostly for stainless steels the value of n was found to be 0.75 (Smialowska and Mankowski, 1972). It was reported for alloy 600 that in NaCl solution the pits grew in depth proportional at $t^{0.3}$, $t^{0.5}$, and $t^{0.7}$ at 100, 150 , and 250^0C (Smialowska et al, 1987). These kind of measurements are useful as they allow the prediction of the pit depth and allow estimation of the remaining life of the component. It is of interest to know how the pits on super duplex stainless steels will grow compared to other materials.

Once the pits grew faster at higher temperature the pit morphology changes. SEM observations were usually made on the samples to study the pit density as well as pit morphology. Three distinctive type of pit morphology was noticed in the study (Smialowska et al, 1987) of alloy 600 for three different temperatures at 100, 150, and 250^0C. At 100^0C the pits were covered with original passive film and contained corrosion products near the pit bottom and on the surface. With the increase in temperature to 150^0C, a shallow form of pits were associated with a thick corrosion deposit, which is not easily removable, with further increase in temperature up to 250^0C it was noticed that a red brown film /deposit was present and with cap shaped pits and after etching the pits were connected into trenches. However we will discuss the pitting morphology for wide range of stainless steels at different temperatures in chapter 5 of this thesis.

2.8 Stress Corrosion Cracking (SCC)

Definition: Stress corrosion cracking (SCC) is defined as the growth of cracks under the combined influence of a non cyclic stress and a reactive environment (Sieradzki & Newman, 1987). Usually the environment is an aqueous solution and for the purpose of understanding this study the review restricts it to chloride solutions.

2.8.1 Introduction

Stress corrosion cracking is a phenomenon in which time dependent crack growth occurs when the necessary electrochemical, mechanical and metallurgical conditions exist, (Jones). Like pitting, SCC is determined by two electrochemical reactions, anodic and cathodic in combination with mechanical stress. The chemical composition of the environment, chloride levels, pH, and composition of the metal will influence these reactions and can dominate one of these two partial reactions. The interest in this topic is due to the fact that duplex stainless steels and super duplex stainless steels offer remarkably good SCC resistance in chloride environments compared with austenitic steels. In the following sections, the phenomenon of SCC and its assessment will be described. Also the environments where SCC occurs and different mechanisms of the observed laboratory and service failures are highlighted.

2.8.2 Testing methods

The objective of conducting SCC testing in the laboratory is to provide information within a short period of time which cannot be obtained from service experience, and also to estimate the remaining life or predict the total life of the component in service. Before conducting an SCC test programme a suitable test method should be selected based on the parameters of interest. Since a wide variety of test methods are available for the measurement of SCC susceptibility they sometimes gives inconsistent results

and little or no correlation with actual failure cases. The test method selected depends on the type of specimen used for testing and feasibility of the laboratory testing machine. The different kind of specimens are C-ring specimens, bent beam specimens, O-ring specimens, and tensile specimens. The applicability of these specimens and the test procedures are discussed elsewhere, (ASTM G38, G49, Sedricks,1990). The applied stresses vary in all these specimens and these specimens are chosen on the type of particular type of service application.

In the present study tensile specimens are used to conduct SCC testing as the author feels that is the appropriate testing method with available laboratory test machines and the versatility offered by this kind of test method.

2.8.3 Slow strain rate testing(SSRT):

These tests are also called as constant extension rate tests, or low strain rate tensile tests as the specimens used to conduct these tests are tensile specimens and are subjected to constant extension mainly used to determine the tensile properties in air and can also be adapted in an environment of interest, according to ASTM G49. These tests are frequently used to evaluate the influence of various metallurgical and environmental variables. Some of the advantages of using this test technique is that the stress pattern is uniform and simple. In these uni axially loaded specimens the stress can be generated by choosing one of these parameters like constant load, constant extension, or increasing load or strain. Also more importantly it is easy to define the maximum applied stress on the specimen during the test. One should realize that these kind of tests are significantly influenced by the cross section area of the specimens. Although large specimen correspond to more of the components used in service, they cannot be machined form the available raw material product forms and also difficult to handle in the laboratory testing (Sprowls). Therefore specimens

less than about 10mm (0.4in) in gauge length and 3mm (0.12in) in diameter is not recommended for tensile testing ASTM E8. All the SSRT tests are conducted at a critical strain rate as it is one of the most significant variable in SSRT tests. If the strain rate is too high the metal undergoes ductile failure and if it is too low the film on the metal undergo repassivation or film repair and SCC may not occur, so it is of paramount to select the appropriate strain rate before starting SCC tests programme. Typical strain rates range from 10^{-5} to 10^{-7} depending on the alloy environment system.

2.8.4 Stress - Strain curves

One way to approach the monitoring of the behaviour of materials under the action of tensile stress is by means of tensile test. Specimens with defined dimensions are subjected at a predetermined strain rate, between the crossheads of tensile machine and the valued of the load for all the extension values is recorded. Usually the data recorded is load/ extension curve in a graphical form, however the data is converted to an engineering stress –engineering strain curve. The load is divided by original cross section area, whilst extension is converted into strain by the relationship, Eq 3.3. The schematic stress-strain curve is shown in Fig 2.23

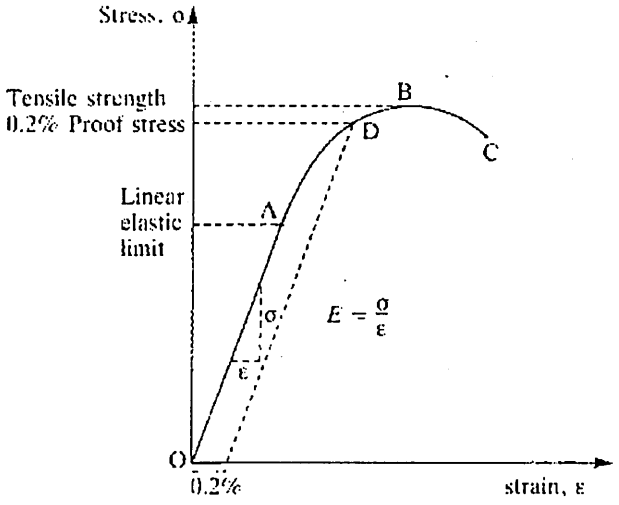

Figure:2.23 Schematic diagram of typical stress/strain curve (Trethewey,1996)

As shown in Fig 2.23 during the initial period the stress-strain relationship is linear and elastic. As the increase in stress above point A, a situation where it reaches point B the material begins losses its cross-section gradually at one point along its length an effect known as necking. The stress at point B, point of necking is known as ultimate tensile strength. Further increase in strain leads to decrease in stress indicated by point C and then specimen breaks after this point. The two ends of the broken specimens are joined to measure the reduction in area after failure. This reduction in area is a measure of ductility, the greater the elongation and greater the ductility of the material. The materials under some conditions fail at very earlier stages than at point C, which doesn't have any necking such type of failure have brittle manner. The main concern for engineers is that this type of failure is brittle because the components can fail without prior warning which results in economic loses. One of the objectives of determining the stress-strain behaviour is to identify regions /conditions that cause these brittle failures so that necessary measures can be implemented in the plant to avoid SSC.

2.8.5 Assessment of SSRT test results:

The SSRT test conducted in different environments will respond differently ,the assessment is made with a test conducted in a inert environment, see Fig 2.24 .The ultimate tensile strength and the % elongated has been reduced in the corrosive environment compared to an inert environment.

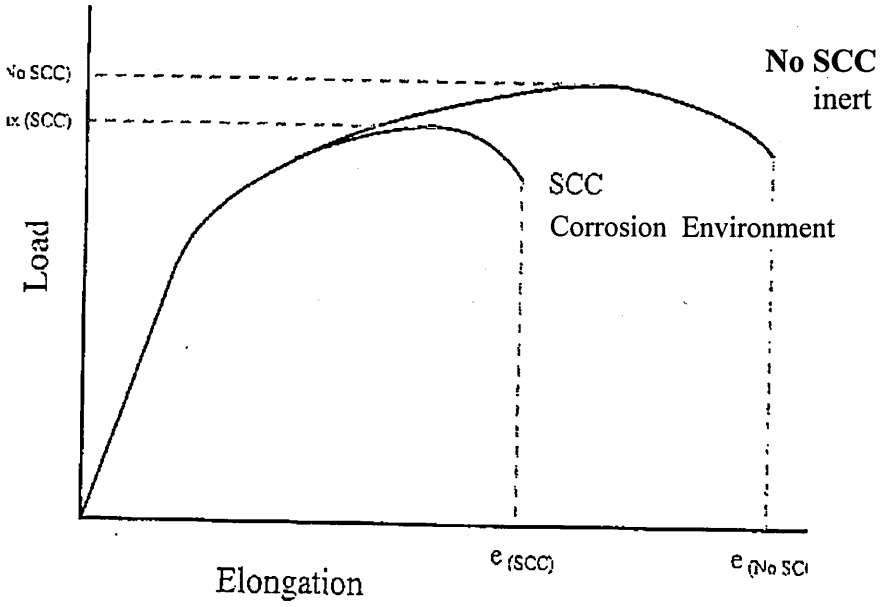

Figure: 2.24 Schematic representation of load –extension graph (Davis)

The test results are assessed based on

- Ductility, assessed by percentage reduction in area
- Maximum tensile load to failure
- Time to failure
- Fracture mode, by observing failed specimen
- % SCC fracture, % ductile fracture

The control of various environmental factors will effect the SSRT test results. The aim of this project was to understand the effect of environmental parameters and try to determine critical SCC conditions that can compare the data from the other studies, and the Ep data from this study.

2.8.6 Environmental Factors influencing SCC behaviour:

The SCC of susceptible alloy is dependent on environment it is exposed. Environments that cause SCC are usually aqueous solutions but not necessarily in

every case, there exists a specific range for all the environmental parameters that can cause cracking. These include but are not limited to the following

- Temperature
- Applied Potential
- Solution concentration
- Oxygen concentration
- pH

As SCC involves crack initiation/nucleation and crack propagation stages it is important to notice that changing any of these environmental parameters can affect the rate at which SCC occurs (Davis). A detailed study of these parameters may methods to reduce the rate of crack propagation in service. Since the present study investigates the SCC in DSS the literature review will focus mainly on the SCC of DSS and SDSS. However in case of non availability of results in the literature on these steels it will discuss general effects and mechanism for other materials.

2.9 Models of SCC

A) Anodic dissolution models:

Anodic dissolution models suggest that SCC is caused by three steps

1. Rupture of passive film by slip steps
2. Crack propagation due to anodic dissolution
3. Environment in the crack tip becomes acidic, enhancing crack propagation.

A) Slip dissolution model[Hoar;1962]:

This model assumes that a passive film will rupture locally due to a gliding process at active slip planes. As a result the passive film is broken and locally destroyed due to application of a critical strain. The important feature of this model is a sequence of transient anodic dissolution followed by repassivation. The localised plastic

deformation at the crack tip concentrates film rupture and dissolution occurs at that region permitting crack propagation. The figure illustrates that a) rupture of film is achieved through the active slip plane. Since it acts like a transient and repassivation of the film takes places, the repassivation kinetics remain important in the slip dissolution model. Metal corrodes until repassivation occurs.

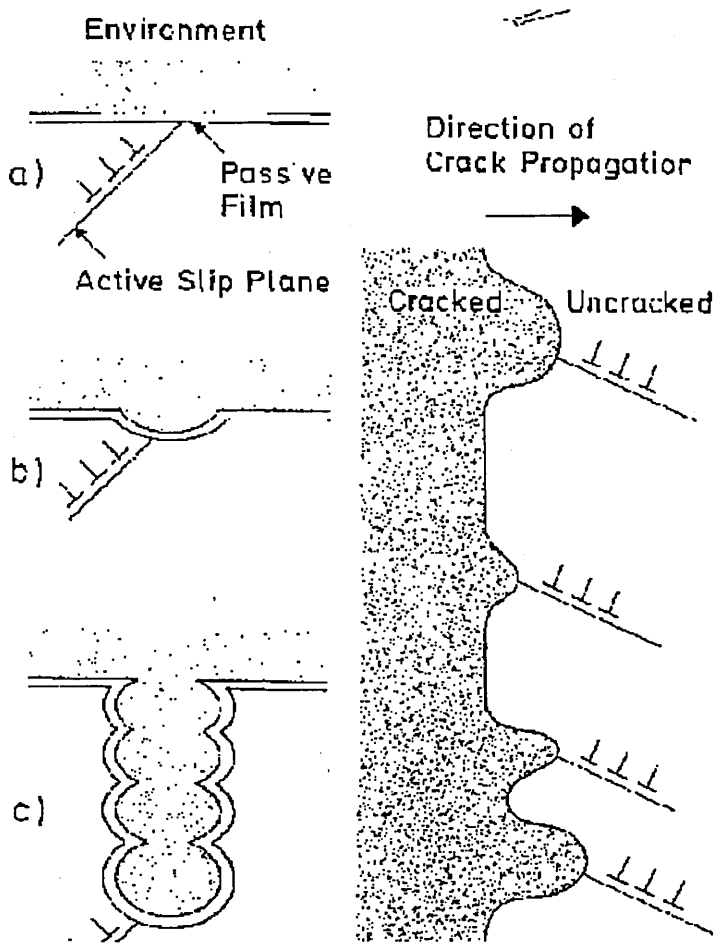

Figure:2.25 Schematic representation of slip dissolution model.(Hoar, 1962)

B) Stress Assisted intergranular corrosion or Brittle film model[Vermilyea,1977]:

This model assumes that a brittle or mechanically weak film exists on the surface produced by the environment. Fig 2.26 will be able to explain the fundamental steps to demonstrate the model.

The initial step with a grain boundary and a surface film produced by the environment will grow preferentially along grain boundaries as in (a). This grain

boundary film is continuous shown in (b), in case of absence of tensile stresses the depth of travel of such a film along the grain boundary into the metal will be limited by the transport across the film. When stressed this film is assumed to fracture at some critical depth fig (c). The brittle crack is arrested by plastic deformation when it enters the metallic substrate as shown in (d).The bulk solution has gained access to the metal and the process is repeated as shown from (e) to (h).

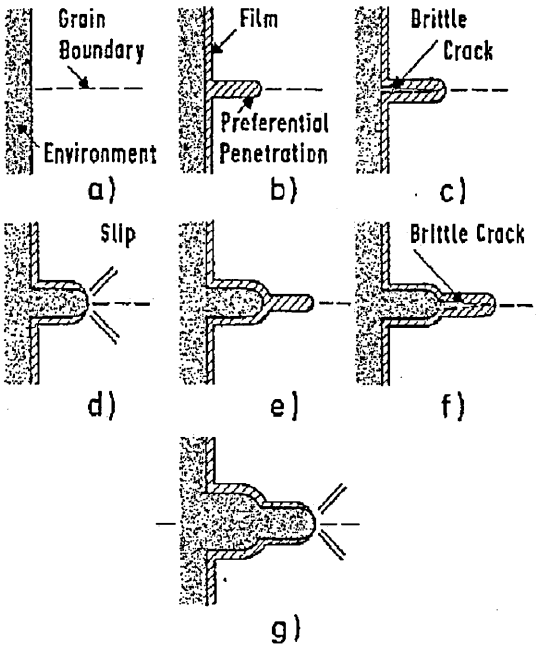

Figure:2.26 Schematic representation of brittle film model for SCC, (Vermilyea,1977)

C) Tunnelling model[Swann;1965]:

This model is based on microscopy evidence which starts with the formation of many corrosion tunnels at slip steps. These tunnels weaken the metal and lead to ductile rupture. The model supposes that tunnelling will commence again and ductile rupture be repeated. This model belongs to group of discontinuous crack propagation. The process begins with the rupture of thin protective film under the action of the applied stress, dislocations move to the surface forming to the slip steps, secondly the metal atoms exposed after the fracture of the film to the corrosive environment which allows Cl^- ions to concentrate at slip steps and delay repassivation of the protective

film, this enables corrosion pits to elongate and ultimately form tunnels (Swann, 1965).

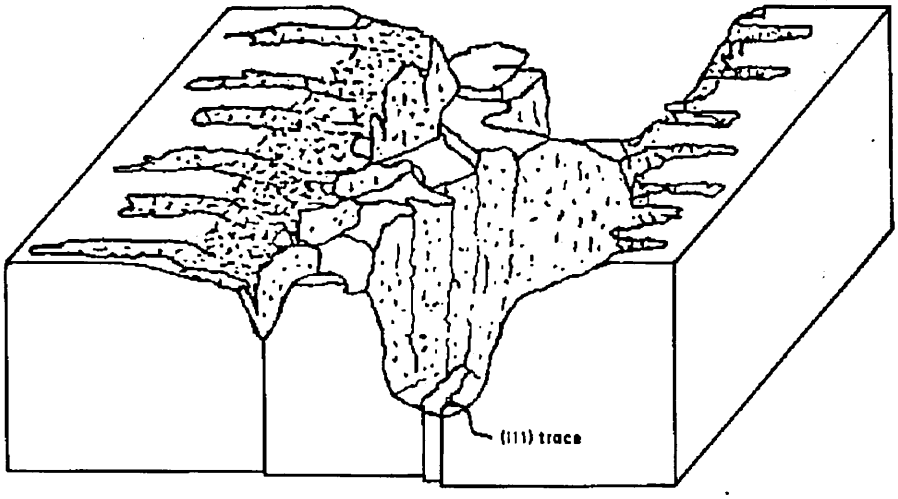

Figure 2.27: Corrosion tunnelling (Swann,1965)

D) Surface Mobility mechanism[(Galvele; 1987)]**:**

This model proposed by Galvele (1993) is based on the assumption that stress corrosion crack propagation is due to the capture of vacancies by the stressed lattice at the tip of the crack as shown in Fig 2.28 below.

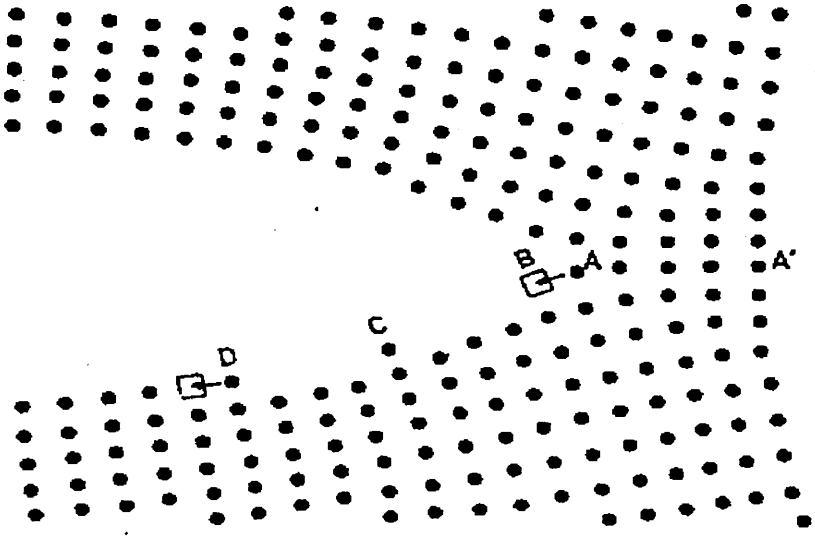

Figure: 2.28 Surface mobility cracking mechanism. Stresses at the crack tip will favor A-B exchange, introducing a vacancy at the tip of the crack (Galvele,1987)

According to this model the environment plays a dual role that it increases the surface self diffusivity of the metal or alloy and on the other hand it assures a free

supply of vacancies to the metal surface. Basically a high surface mobility is achieved if the passive layer has a low melting point and Galvele claims that if the melting point of the film is below 800^0C rapid crack propagation is possible.

Factors influencing SCC:

The critical factors that influence the SCC in general are crack growth /propagation rates and crack coalescence will be discussed briefly that are relevant to this study. In order to estimate the crack growth in terms of crack velocity a relation was established between current density and crack velocity and is given by

$$da/dt = I_a . M/zFd \qquad (2.23)$$

where da/dt is crack velocity, I_a = anodic current density CD, M = atomic weight of the metal= valency of the solvated species, z = valency and F= Faraday constant (Parkins, 1987). Another factor that determines the crack propagation rates is crack tip strain rate. Congleton et al proposed a relationship, if multiple cracks exist on a gauge length and it is given by the following expression

$$\epsilon_{CT} = \frac{75}{N} \epsilon_{app} + \frac{a}{5} \ln \frac{1000}{N} \qquad (2.24)$$

Where N= number of cracks, ϵ_{app} = applied strain rate and a= crack velocity, ϵ_{CT} = crack tip strain rate. Ford defined the crack tip strain rate in a SSRT as

$$\epsilon_{CT} = 5\, \epsilon_{app} \qquad (2.25)$$

But this expression does not consider the number of cracks in the specimen. Once the crack are initiated crack coalescence play a significant role to produce larger cracks. This phenomenon was discussed in detail by Parkins and Singh (1990) and highlighted that the rate of coalescence increases relative to the rate of nucleation of new cracks, and the number of effective cracks becomes effectively constant, i.e coalescence consumes as many cracks as are nucleated in a given interval of time.

2.10 SCC of Duplex stainless steels

The failures in the offshore industry due to hydrocarbon contaminant incidents led to HSE in the UK to reviewing the current understanding of the conditions that cause stress corrosion failures and the applicability of the duplex stainless steels in order to support the safe usage of duplex stainless steels. Cottis and Newman,1993 have reviewed the stress corrosion resistance of duplex stainless steels and pointed out that inadequate data exists in the temperature range of 60-130^{0}C and the situation is unclear. Most of the work related to the stress corrosion cracking susceptibility of duplex stainless steels have usually been studied only in hot concentrated chloride solutions (150^{0}C) and the failure modes have been characterised in terms of time to failure or cracking velocity (Ghoshal et al, 1993; Hochman et al,1977; Jargelius et al, 1991; Hsuang et al, 2000) The applicability of this data is very limited as most industrial applications don't experience such an aggressive environment especially when it is in contact with the stainless steels.

Since large amount of data concerning duplex stainless steels exists was related to the effect of concentrated $MgCl_2$, the current work was initiated to study the behaviour in low concentrated chloride solutions and as function of other parameters such as applied potential, oxygen concentration, chloride concentration and temperature in order to get the overview of the failure mechanism involved by varying each of these parameters.

2.10.1 Mechanisms of cracking in DSS

Although Stress corrosion failures of duplex stainless steels in various chloride and CO_2/H_2S environments have been reported in the literature, still there is lack of general agreement. Ghoshal et al, (1987) studies have shown the stress corrosion cracking (SCC) susceptibility of a duplex stainless steel, U-50 in deaerated 1N NaCl

solution was dependent primarily on potential rather than pH of the solution. The cracking mechanism involved in the failure of U-50 was selective dissolution of austenitic phase leading to failure. Once the cracking potential is attained the austenite became more anodic to the ferrite phase and underwent preferential dissolution of the austenite phase this phenomenon was confirmed in the same study by X-ray diffraction analysis. In the constant load tests conducted by Hochman et al 1977 in 44% $MgCl_2$ at 153^0C it was clear that failure of duplex stainless steels involves a kind of synergism corresponds to the improved performance compared to single phase austenitic and ferritic steels. It was noticed that austenite was 10mV more noble than corresponding ferrite, and then indicates that ferrite grains cathodically protect the austenite. The same phenomenon was observed by Jargelius et al, (1991), when they conducted studies on alloys with constant composition and found ferrite was cathodic to austenite, which in turn acted as a crack arrester. Crack propagation in duplex stainless is found to be complex and various studies have concluded different mechanisms and very few are in general agreement. Studies conducted by Van Gelder et al (1987) on duplex stainless steel in H_2S /CO_2/Cl^- environment using the slow strain rate technique at 160^0C concluded that the mechanism of SCC in duplex stainless steel is slip-step emergence /anodic dissolution for initiation and hydrogen embrittlement was associated with the propagation of cracks. Van Gelder et al state that the propagation of cracks in ferrite was noticed in their studies and it could be hydrogen embrittlement as it is known that the ferrite phase is more susceptible to hydrogen embrittlement than the austenite. In a comparative study (Jargelius et al, 1991) of three different duplex stainless steels 2304, 2205 and 2507 in boiling $MgCl_2$, LiCl2 and $CaCl_2$ solution at 100^0C and 150^0C have noticed that austenite is cathodically protected by the ferrite

phase, and the crack path followed primarily in the ferrite phase at all test conditions. This mechanism of cracking in the ferrite phase has a similarity with the study of Van Gelder et al (1987). It was noticed that in case of SCC of DSS the cracking morphology varies showing transgranular in case of ferrite and intergranular in austenite- austenite grain boundaries.

2.10.2 selective phase attack

The concept of selective or preferential dissolution has raised in case of failure modes of duplex stainless steels where there are two grains with different microstructures and due to difference in chemical composition between the two constituent phases. The selective attack occurs in wide range of environments which involves not only chloride environments but also in H_2SO_4/HCl which was studied recently on 2205 duplex stainless steel (Hsuang et al, 2006).The similar phenomenon was studied (Symniotis et al, 1998) earlier for a duplex stainless 2377(22Cr 5ni 0.15N) in 4N H_2S0_4 + 0.1N HCl, by using potentiostatic weight loss measurements of individual phases and have shown that galvanic effect exists between the two phases, ferrite being anodic to austenite.

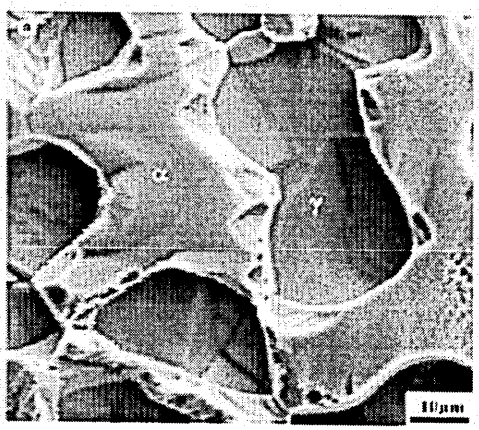

Figure: 2.29 SEM micrograph showing the selective attack of 2205 DSS after potentiostatic etching at $E_{\gamma Max}$ = -250mV(Hsuang et al, 2006)

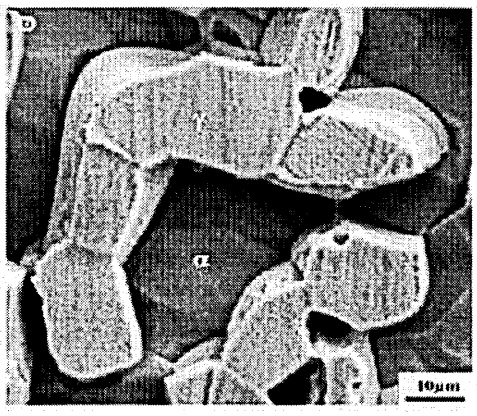

Figure:2.30 SEM micrograph showing the selective attack of 2205 DSS after potentiostatic etching at $E_{\alpha Max}$ = -315mV ;(Hsuang et al, 2006)

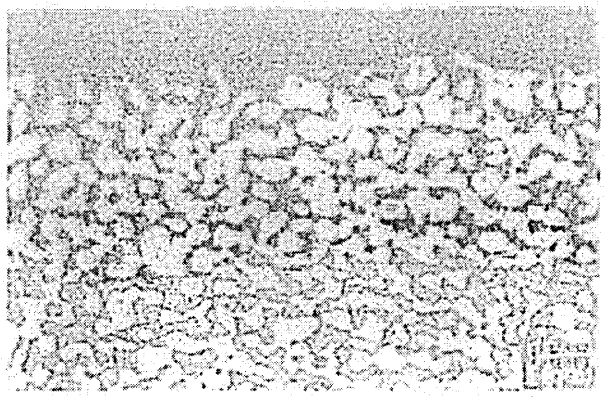

Figure:2.31 Selective dissolution of ferrite (darkened phase) after 15 hrs exposure to 1M H_2SO_4 + 0.2M NaCl at 60^0C (Symniotis, 1991;1998)

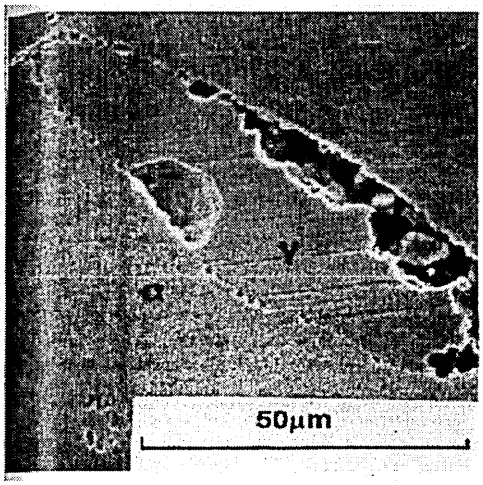

Figure:2.32 SEM micrograph showing preferential pitting of austenite in cast steel in 1MNaCl solution at free corrosion potential. Pits initiate at α – γ interface and propagate into γ region. (Sriram and Tromans, 1989)

2.10.3 Role of applied potential

It has been established for a long time now that applied potential plays a major role in the corrosion of stainless steels. Recognition of the importance of the electrochemical potential as one of the critical controlling parameters in SCC initiation or in SCC failures has resulted in the increase use of tests with potentiostatic control. Anodic polarisation curves discussed in ASTM G 5 provide reasonable predictions of the critical potential ranges controlling the SCC in a identical environment system, Parkins (1980). The importance of the controlled potential SSRT tests in determining the susceptibility of SCC is highlighted by Cottis and Newman (1993), according to them boiling solutions for SCC testing without any potential control is misleading. In their view boiling solutions are deficient in oxygen and the electrochemical potential is set by cathodic reactions like hydrogen evolution. In case of duplex steels it is more even important as the potential can be more influential (Nagno et al, 1981) in determining the attack of the two individual phases austenite and ferrite. One way of studying the stress corrosion behaviour is to conduct Slow Strain Rate experiments (SSRT) under controlled potentials either cathodic or anodic. The potential at which the stress corrosion cracks start to initiate or occur in stainless steels is termed as stress corrosion cracking potential (E_{SCC}). Studies on 22% Cr duplex stainless steel in boiling $MgCl_2$ environments have shown that cracking is accelerated by anodic polarisation and retarded by cathodic polarisation Sakai et al (1982). The mechanism of failures alter based on the applied potential like if the failure occurs at anodic potential it might correspond to the film breakdown due to chloride ion or slip induced film breakdown, if it is negative potential it might be due to hydrogen entry resulting in hydrogen embrittlement. Thus it is important to note that for every steel in operation has a critical E_{SCC} above

which it starts to lose its strength and ultimately failure occurs independent of the loading conditions.

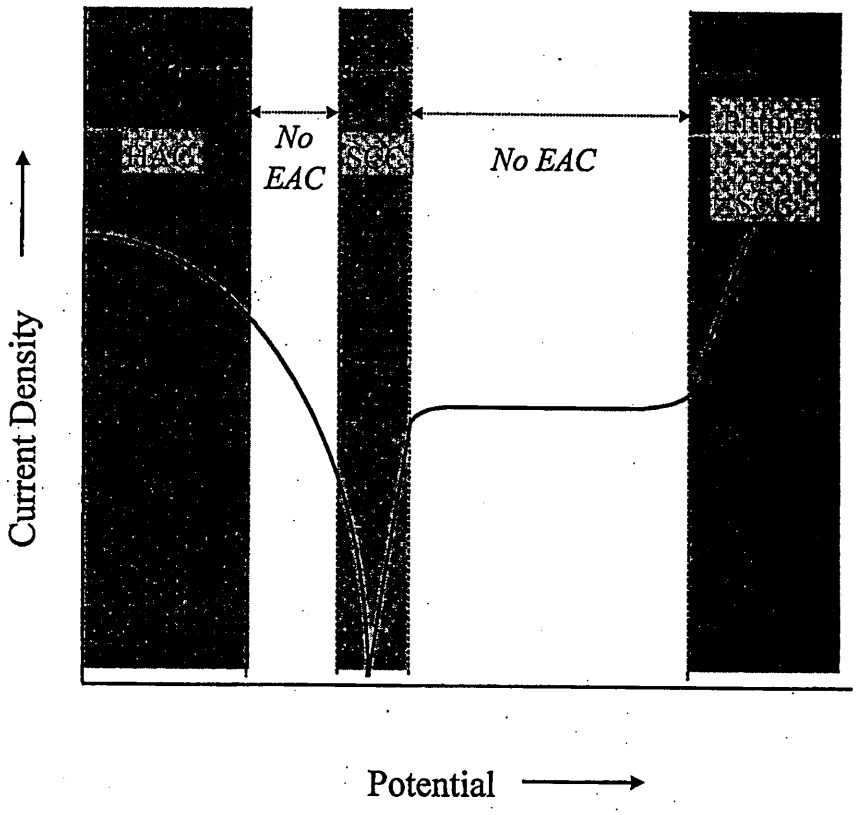

Figure: 2.33 Effect of applied potential on current density (Wen- ta -Sai etal, 2000)

The applied potential allows the material to fail not only due to small strain but also at a constant applied stress. The studies of Sand known et al (1993) on alloy 255 under constant load of about 90% yield strength in boiling $MgCl_2$ have shown that a critical cracking potential (E_{CC}) of -380 mV SCE above which the material failure occurred. In the recent work (Wen –Ta-Sai et al 2000) on 2205 duplex stainless have proved the role of applied potential in environmental assisted cracking behaviour indicating that 2205 duplex stainless steel is susceptible to SCC in 26wt% NaCl solution at room temperature in a narrow potential range of -380 to -500mV SCE near to corrosion potential as shown in Fig2.34.

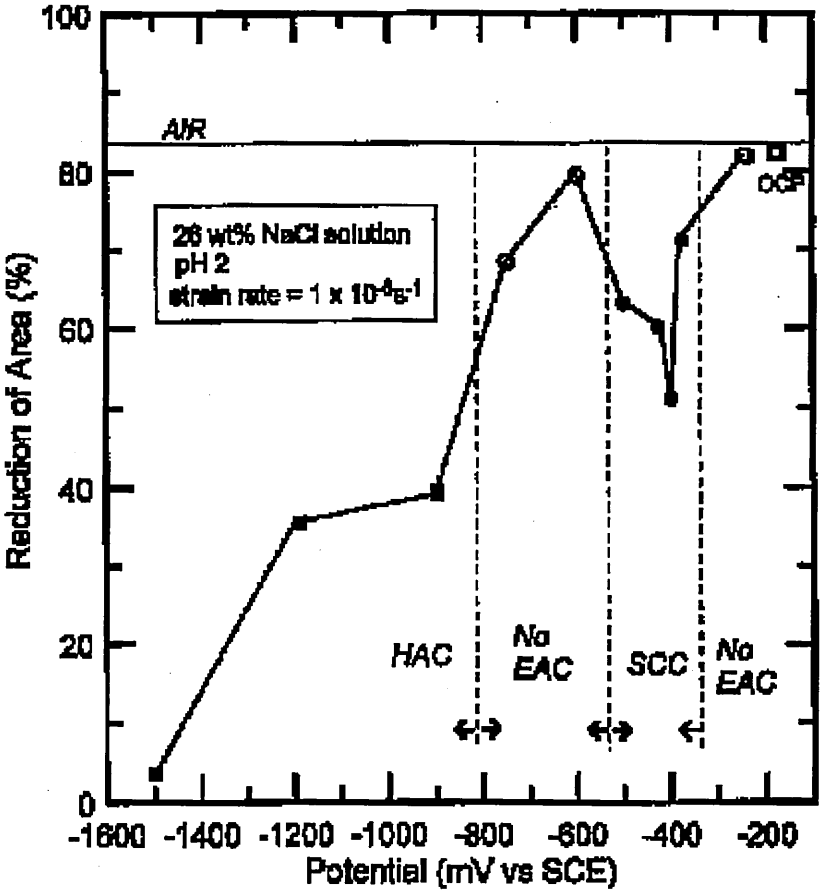

Figure:2.34 Effect of applied potential on ductility on change of % reduction in area of 2205 duplex stainless steel after slow strain rate in 26 wt %NaCl solution of pH2 (Wen-Ta-Sai et al, 2000)

In another study conducted by the same author in 2205 duplex stainless steel but at different environmental conditions, temperature 90^0C and 26wt% NaCl has shown that critical cracking potential was around –160mV above which loss of ductility is predominant as shown in Fig 2.35.

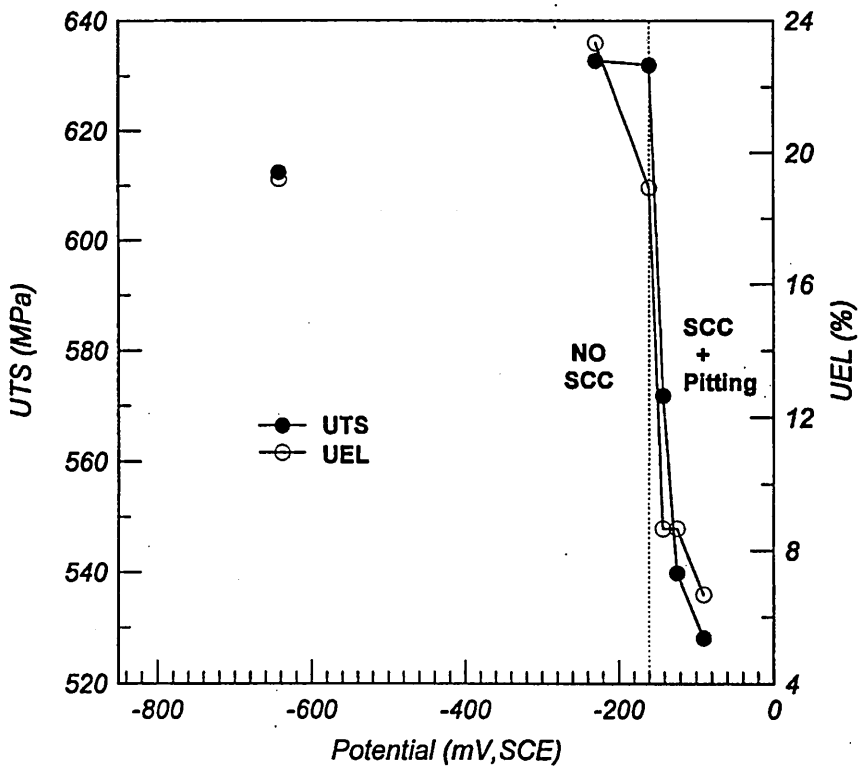

Figure: 2.35 Showing the Effect of applied potential on the change of reduction in area of 2205 duplex stainless steel after slow strain rate in 26wt% NaCl solution of pH 2. (Wen- Ta Sai & Ming –Shan Chen, 2000)

Fig 2.35 shows the effect of applied potential on tensile strength and elongation for 2205 duplex steel and mechanism of failure was found to be pitting corrosion assisted anodic dissolution. Same author also investigated the effect of applied potential on high nitrogen steels, P900 and P 900N in 1 wt% NaCl solution found that at, + 500mV and +650mV (SHE) that SCC was occurred by pitting corrosion. The results were explained by analysis of the electrolyte solution which turned yellow in colour at higher applied potentials and corrosion products were formed at the bottom of the cell. It was found that significant amount of NH_4^+ exists in all the solution, which suggested that after dissolution of iron it formed NH_4^+ ions from the dissolved nitrogen.

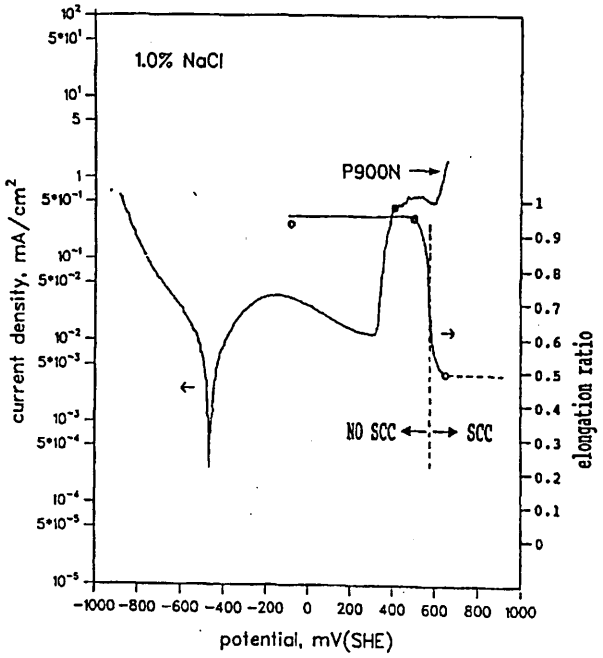

Figure:2.36 Variation of the ratio of percentage of elongation with potential of P900 (Wen -Ta- Sai et al, 1993)

The repassivation kinetics of the passive film play an important role in failure process and applied potentials has significant influence on these potentials.

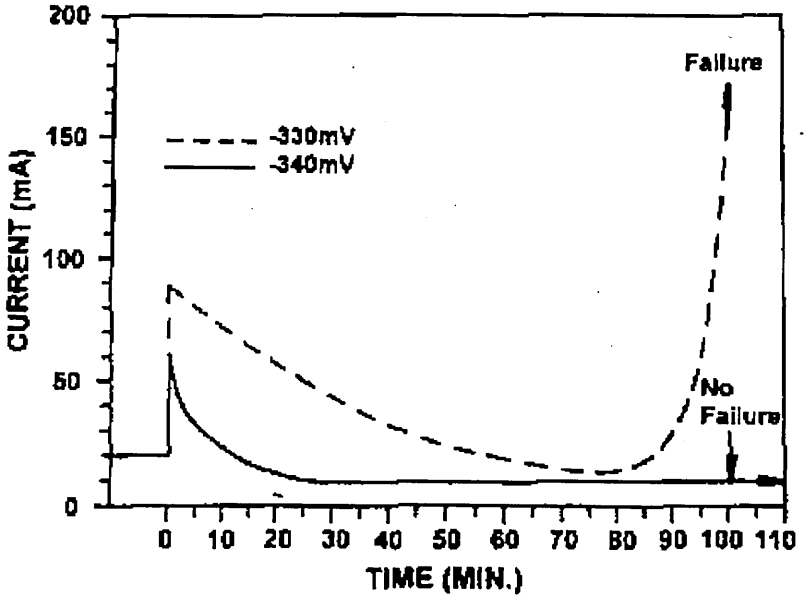

Figure: 2.37 Effect of applied potential on the current Vs time curve of mill annealed alloy 255 loaded to 90% of the yield strength in boiling $MgCl_2$ solution.(Kwon and Kim, 1993)

Fig 2.37 shows that repassivation rate depends on the potential and can be represented using the current – time curve under potentisatic conditions and it can be

noticed from the Fig 2.37 for alloy 255 in boiling 35% $MgCl_2$ solution (Kwon and Kim, 1993). The results show a significant point that magnitude of the anodic current induced by the film breakdown and repassivation of the alloy 255 are extremely sensitive to the applied potential as shown in Fig 2.37 in boiling magnesium chloride solutions.

2.10.4 Chloride concentration effect on SCC

SCC occurs in wide range of environments, however chloride ions are considered as the aggressive species involved in the corrosion phenomenon in case of stainless steels. High chloride concentrations and low pH are at least necessary to initiate cracking (Herbsleb and Poepperling, 1980). These environments are achieved through the concentrated magnesium chloride solutions which are frequently used for determining the susceptibility of high alloy steels SCC. It is very rare that SCC can occur in other halide environments.

The chloride environment has a potential impact in the failure process. It is explained by the fact that chloride ions have the ability to accelerate anodic reactions, Fontana (1987) described such a mechanism where oxygen in the surface is responsible to maintain passivity. In chloride containing solutions the solubility of oxygen is limited and therefore chloride ions migrate to the surface easily and involves in film breakdown process. It can be concluded that high mobility of chloride ions compared with halide ions will definitely contribute to its aggressiveness.

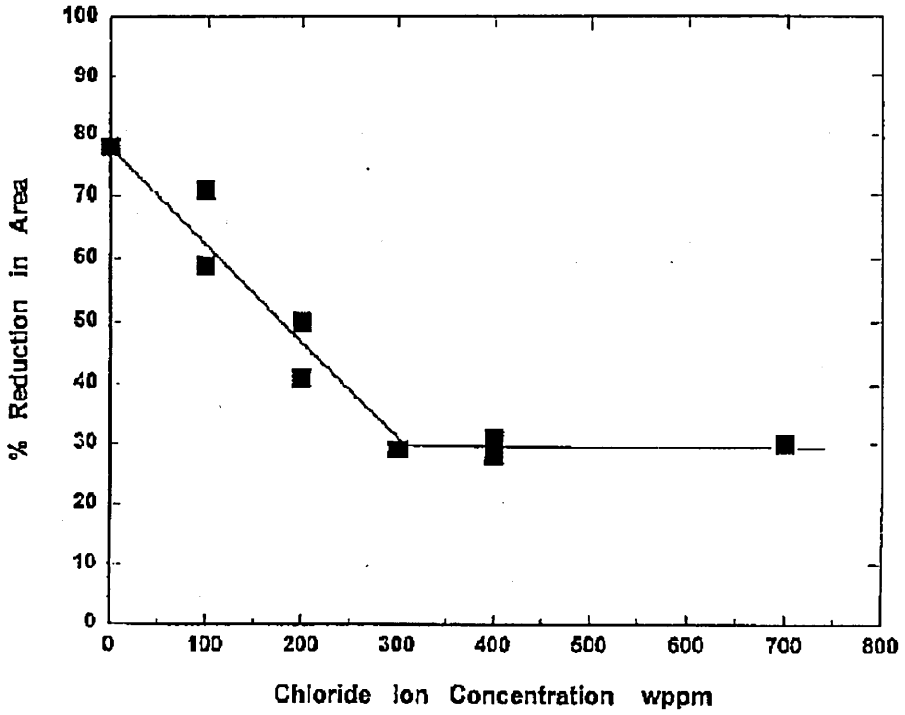

Figure:2.38 Effect of chloride concentration on ductility of duplex steel saturated with hydrogen sulphide (El – Yazgi.A.A & Hardie.D, 1998)

An example of the influence of chloride ions on ductility was shown in Fig 2.38, for experiments conducted in neutral aqueous solution having chloride concentrations from 0 to 700ppm and saturated with hydrogen sulphide, indicating that chloride ions play a significant role. As it can be noticed in Fig 2.38 that an increase in Cl^- level beyond 300ppm has little or no influence on the steel, which proves that a critical concentration is enough to cause damage above which there is not much significant influence on the SCC behaviour in case of duplex steels. In another study on the SCC susceptibility of a duplex steel in H_2S / CO_2/ Cl^- environment by Van Gelder et al (1987) showed that, the SCC mechanism of duplex stainless steel involve a combination of repetitive slip step emergence/anodic dissolution and hydrogen embrittlement only when the temperatures are higher than 80^0C at free corrosion potentials. The results demonstrate that cracking did not occur at room temperature in the environment studied, and indicated that cracking was more severe in transverse specimens compared to longitudinal specimens, indicating

that orientation has an influence on the SCC behaviour of stainless steels. None of the above mentioned investigations were carried out in dilute environments at intermediate temperatures and it was one of the objectives of this study to investigate SCC in 15ppm Cl^-.

2.10.5 Role of temperature:

It is well know that SCC in general occurs above 60^0C in austenitic stainless steels, and it is considered as the lower threshold limit for SCC initiation (Cottis & Newman, 1992). The influence of temperature on SCC behaviour in most cases is that an increased temperature increases the risk of SCC to occur. As it was observed in the case of pitting, with increase in temperature the pitting susceptibility tends to increase, in a similar fashion it has an influence on the crack density and the observed crack velocity. Temperature does effect the SSRT tests results as, it will influence the maximum stress (UTS) and the elongation decreasing with increase in temperature. A recent study (Maeng et al, 2005) on turbine blade steels has confirmed this kind of observation. It was observed that with increase in temperature from 50 – 150^0C a drastic decrease in the ductility was noticed, with not much further decline above 150^0C, see Fig 2.39.

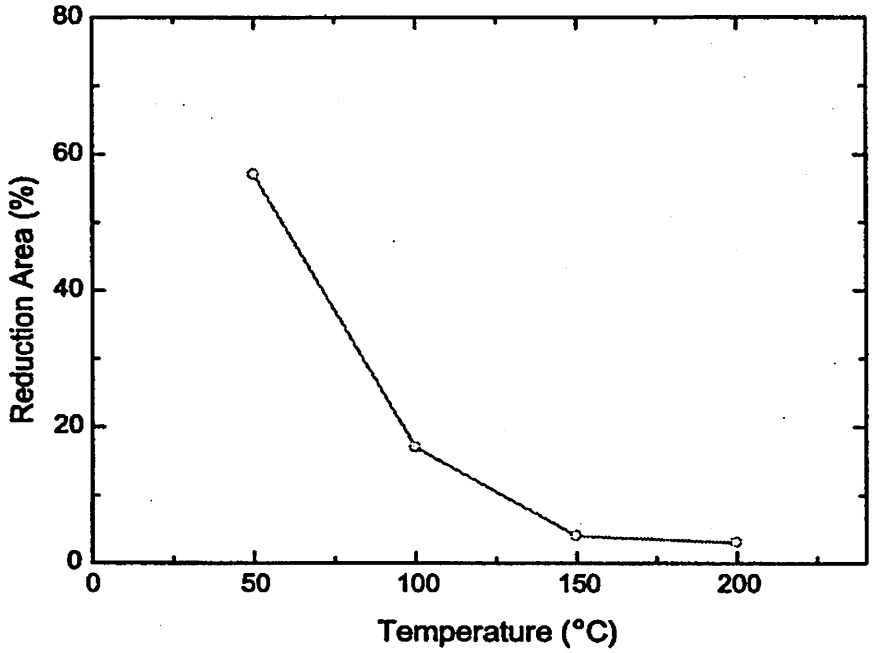

Figure: 2.39 Reduction in area (%) of the 3.5NiCrMoV steel tested in aerated water (Maeng et al, 2005)

This shows that there is little deformation around the fracture surface at higher temperatures. The degree of temperature influence decreases with increase in temperature. It was confirmed through the studies of Andresen and Ford (1980) that crack propagation reaches a maximum at 200^0C and becomes lower above this temperature. In this way temperature does influence crack propagation in the SCC process.

In sour environments, a comparison of two duplex steels revealed that with increase in temperature both density of pit formation and number of secondary cracks tend to increase (El –Yazgi & Hardie, 1998). The study has shown that in NACE –01-77 solution that cracking was observed along the austenite/ferrite interface and was explained by the fact that these sites act as hydrogen traps and there is a higher diffusivity of hydrogen in ferrite compared to austenite.

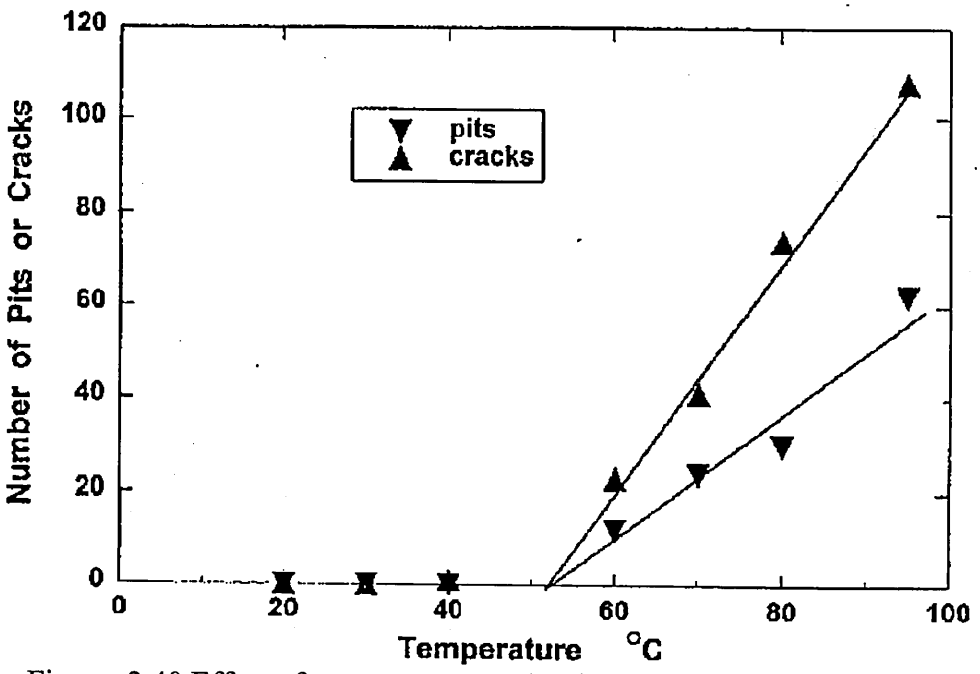

Figure: 2.40 Effect of temperature on density of pits and cracks in sour environments (El – Yazgi & Hardie, 1998)

These kind of systematic observations are useful to assess the influence of temperature on the failure time by estimating the number of significant cracks and pits on known gauge length to estimate failure times.

2.10.6 Dissolved oxygen effect:

The studies on the susceptibility of DSS and SDSS to stress corrosion cracking under different dissolved oxygen conditions do not exist, however in order to understand how dissolved oxygen influences the SCC behaviour on different stainless steels will be reviewed. The strength of the oxygen-metal bond is not the same at all parts of the metal, as the bonding strength vary in case of weak areas the possibility of oxygen ions being replaced with chloride is regarding as the cause of pitting by Rosenfeld (1967). Dissolved oxygen in aqueous solution does not allow chloride to dissolve completely and allows the aggressive species on to migrate to the surface and cause localised breakdown (Fontana, 1987). In most cases there will be critical dissolved oxygen concentration above and below which it will influence the SCC process. The

concentration of the dissolved oxygen is an important parameter in nuclear power stations, especially studies do exist on 304L and turbine blades materials. One of the studies on the oxygen acceleration on intergranular SCC process was conducted by Clarke and Gordon (1973) on sensitised Fe – Ni –Cr alloys found that between 0.2 – 3 to 5 ppm oxygen acceleration does dominate, whereas above that at between 5 to 100ppm oxygen there is no dependence. The study has summarised and related to some of the following effects that could cause the oxygen acceleration

a) The supply of oxygen to the specimen surface may be diffusion controlled and thus directly dependent on concentration.
b) Increase in the electrochemical potential caused by oxygen may oxidize chromium contained in the surface film to Cr^{+6} state, through the formation of $CrO_4^{=}$ ions.
c) The electrochemical driving force for the crack propagation phase is related to the difference between the bulk surface potential and at the oxygen depleted crack tip, and can lead to anion concentration in a potential gradient.
d) A small drop in pH caused by larger oxygen additions may accelerate anodic dissolution during the initiation phase.

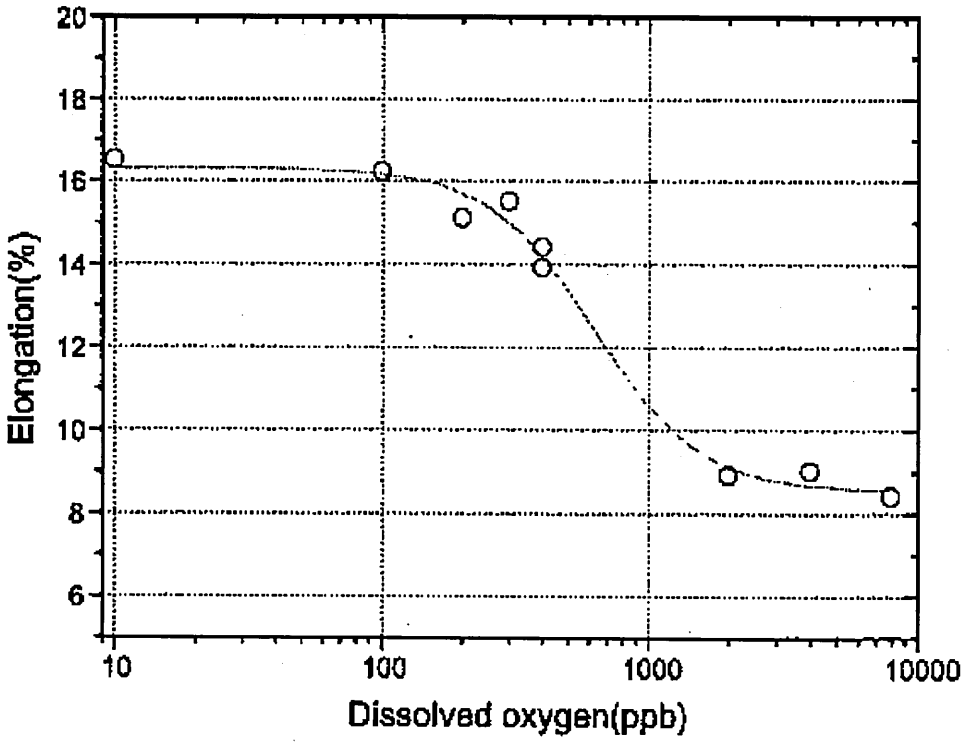

Figure: 2.41 Effect of dissolved oxygen on % elongation (Maeng et al, 2005)

These oxygen levels are very important in reactor environments, as the dissolved oxygen influence the electrochemical potential, achieving low levels of oxygen will shift the stainless to a region where the IGSCC will not occur (Weeks et al, 1985). But how far this theory applies to the failures associated with internal chloride stress corrosion cracking in duplex stainless steels (topside pipe work) is not clear. It was highlighted in an HSE review (Leonard, 2003) that the mechanism of duplex stainless steel failure in deoxygenated environments needs to be investigated. It was pointed out by Kangas and Nicholas (1995) that the most reliable tool to measure the SCC susceptibility of duplex steels is through pressurised autoclave testing, where temperatures and chloride concentrations can be controlled. For this purpose a detailed investigation has been carried out to assess the mechanism of failure in Zeron100 SDSS.

CHAPTER 3

Experimental

3. Introduction

This chapter will discuss the experimental procedures, material composition, together with environmental parameters that are used to generate the required results which are highlighted as part of the objectives of this project. Different test techniques that are used to determine the resistance of the alloys to pitting and stress corrosion cracking tests are discussed in separate sections.

3.1 Materials

The alloys used in this investigation have different chemical compositions and based on their crystal structure they are classified as martenstic (FV520B, FV566), austenitic (304L, 316), ferritic (430), Super austenitic (Uranus 65), duplex (2205, Ferallium alloy 255) and super duplex stainless steels (Zeron100). These grades were chosen because of their wide range of applications in the industry mentioned below.

- Fv520B and Fv566 are used as turbine blade materials in power industry.
- 304l and 316 grades are used for pressure vessels and pipelines.
- Ferritic steels are used as creep resistant material applications in the power industry.
- Uranus 65 is used for nitric acid tanks.
- Duplex grades 2205 and Ferallium alloy 255 are used for the processing of more corrosive hydrocarbon sour gases and liquids in Oil and gas industry,
- Finally super duplex grade Zeron100 is used in Umbilicals, pipelines, topside flow lines for aggressive environment in oil and gas.

3.1.1 Chemical composition

The chemical composition of the materials tested was presented in the table 3.1

Grade	Cr	N	Mn	Si	Mo	Ni	P	S	Cu	Nb	V	C	PREN**
Zeron100	25	0.3	1.0	1.0	4.0	7.0	0.03	0.01	1.0			0.03	43
2205	23		2.0	1.0	3.5	5.5	0.03	0.02				0.03	33
F255	25	0.18			3.0	6.0	0.03		2.2				37.78
Uranus65	24.97	0.026	0.56	0.19	0.106	19.6	0.023	0.001	0.154	0.2		0.012	25.73
304l	17.57		1.73	0.37	0.068	8.5	0.037	0.0015	0.001		0.043	0.029	19
Fv520B	13.56		0.75	0.39	1.44	5.45	0.023	0.006	1.67	0.26		0.057	18.3
Fv566	11.73	0.028	0.75	0.25	1.71	2.76	0.011	0.003			0.30		17.8
12%Cr	11.62				0.6								13.6
Fv566a	11.38	0.031	0.61	0.29	1.53	2.50	0.021	0.002			0.28		16.9

Table 3.1 Show the chemical composition of the materials tested for the current study

All these materials were supplied in various product forms and test samples were made only from longitudinal direction with respect to rolling direction and are produced in circular discs.

3.1.2 Microstructure

The microstructure of the various materials used in this study is shown below. All the crossectional views are in longitudinal directions and different etchings were used to view the microstructure they are a) Electrolytic 10% KOH for duplex steels, b) electrolytic 10% oxalic acid for austenitic c) Villella's for 10 secs martensitic steels.

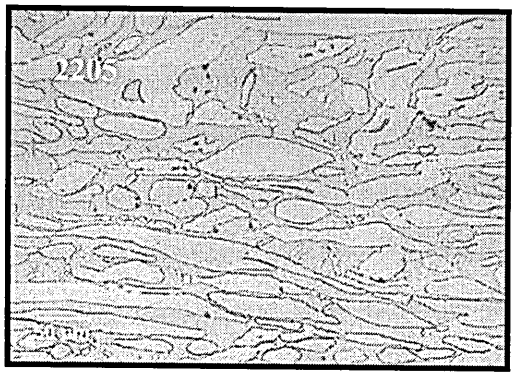

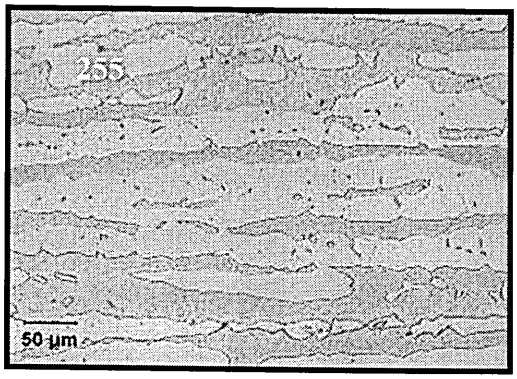

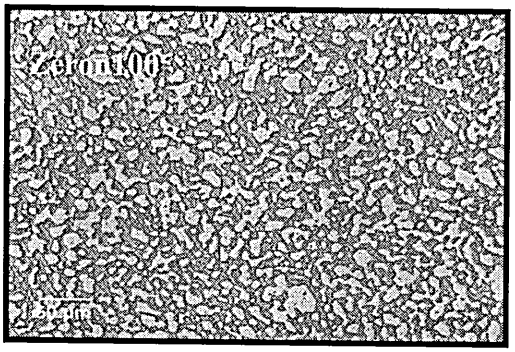

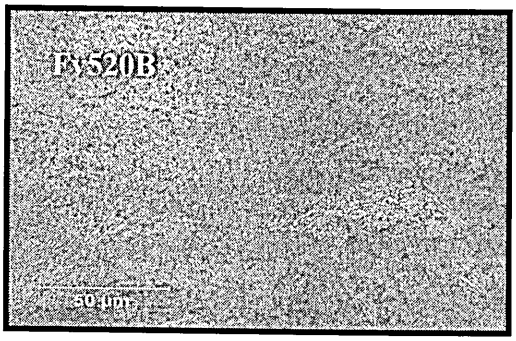

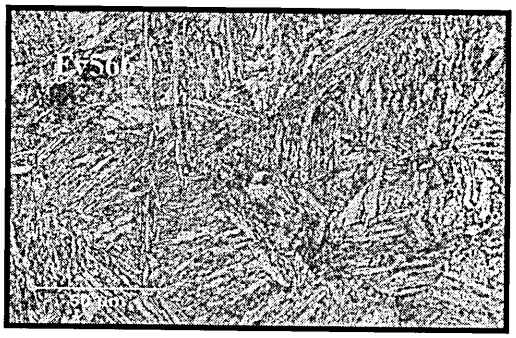

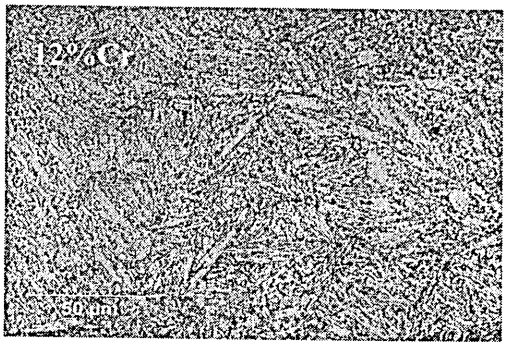

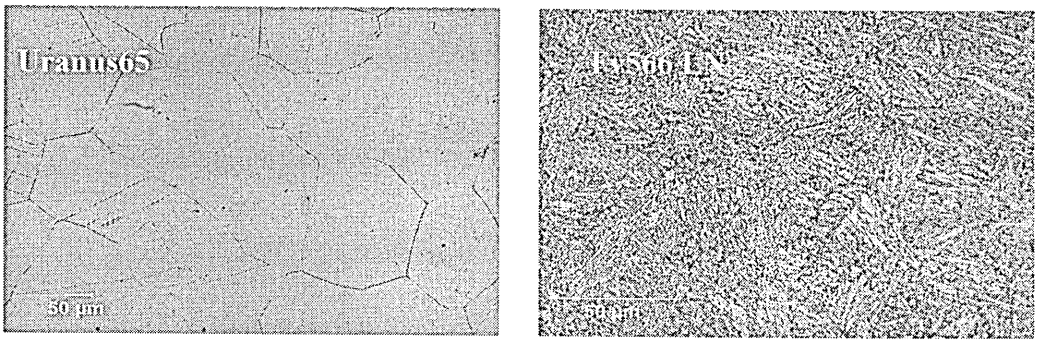

Figure 3.1 Microstructures of the materials used in the present study

3.1.3 Heat treatments

The heat treatment condition for Zeron100 was solution annealed at 1100^{0}C for 60 minutes and water quenched and the resulting mechanical properties were presented in the tabular form below.

3.1.4 Mechanical properties in air

The tensile properties of materials tested were given in the below table:

Material type	Temp ^{0}C	R_P 0.2 MPa	R_m MPa	EL %	ROA %	CvImpact J	Hardness HRC
Zeron100	20	598	823	38	81	306	24.2
2205	25	450	620	25	31		31
255	25	560	800	30			
304L	25	170	485	40			
12%Cr	25	711	908	19.5			

Table 3.2: Mechanical properties of various steels

3.2 Localised Corrosion Tests

Localised corrosion (Pitting) tests were carried out in order to determine the susceptibility of stainless steels to pitting using cyclic polarisation potentiodynamic technique. The main advantage of with this kind of testing is the opportunity to

investigate corrosion phenomenon in the solution of interest and the parameters that are evaluated from these tests are 1) Pitting potential, E_P 2) Repassivation potential, E_{rp} 3) Free corrosion potential, E_{corr} 4) Critical current density, I_{crit}. All these measurements were made at temperatures ranging from 25^0C to 170^0C in autoclave system with a constant flow rate.

3.3 Potendiodynamic polarisation:

Potentiodynamic polarisation technique has been in practice for long time and was known to be reliable and most useful approach to make current-potential measurements. This technique only indicates the relative resistances to pit initiation but has the advantage of giving results in a reasonable time period. A three electrode cell arrangement has been used to perform the tests at room temperature.

To discuss the effect of temperature on pitting corrosion, it is important to consider the critical potentials characteristic of pitting corrosion and environment. These measurements were conducted using a cyclic and linear sweep rate of 30mV/min, which gives a reasonable compromise between speed and accuracy. Potential sweeps are conducted in the potential range of -800mV to +800mV, in various electrolytes 15 - 10000ppm chloride levels at different temperatures.

3.3.1 Sample Preparation:

The main drawback with electrochemical testing for localised corrosion resistance is sample mounting. It is extremely difficult to mount a sample with an insulated electrical contact and controlled surface area without introducing a crevice at the sample-mount interface. It is also not possible to reproduce the crevice of exact geometry repeatedly for all the samples as the crevice corrosion occurs at lower potentials rather than pitting, underestimating pitting resistance of the materials.

In order to overcome these problems, in the present study the material was machined to 12mm diameter discs with 5 mm thickness and the discs were mounted in epoxy resin, spot welded with nickel-chrome wire on the back of the unpolished surface for an electrical connection. The wire is sealed with heat shrinkable plastic using hot air gun.

Figure: 3.2 Automatic Ecomet variable speed grinder- polishing machine.

The specimens are then allowed to dry overnight and then polished using automatic Ecomet variable speed grinding and polishing machine shown in Fig:3.2 was used to polish the samples in order to maintain consistent surface finish across the samples tested. Not only it produces flat surfaces it has an advantage of producing more than one sample at a time. A series of silica carbide emery papers of various grits (120-1200) microns were used in that order and then further polished with diamond paste up to 1μm and washed with soap water, rinsed with acetone and dried in hot air. The specimen is separated from the epoxy setting using two coatings of lacquer and dried with hot air in order to prevent crevice attack.

3.3.2 Electrochemical procedure:

The potentiodynamic polarisation curves experiments were conducted following the ASTM G5 and cyclic potentiodynamic curves were determined using a potentiostat.

A conventional three electrode system was used inside in an autoclave that can withstand temperatures of up to 200^0C. The purpose of using autoclave is to study the temperature dependence on corrosion behaviour in dilute chloride solutions. A potentiostat (ACM instruments, UK) was used to control the electrode potential inside the autoclave. The potential of the working electrode was measured via silver - silver chloride (Ag-AgCl 0.25MKCL) reference electrode and saturated calomel electrode (SCE) when the tests were performed in the room temperature. The auxiliary electrode was platinum (Pt) sheet, placed as close as possible to the working electrode in order to avoid any ohmic drop.

The flow rate of the solution inside the autoclave was gravity feed. The connections were insulated again with heat shrinkable shrink and connected to the leads of potentiostat. Once the autoclave is sealed it is heated up using Eurotherm which controls the temperature of the solution, and can be adjusted for desired level measured using thermocouple placed inside the autoclave. After each test the autoclave was rinsed with deaerated water so that any salt particles will not get settled in the corners of the tubes connected to autoclave and to maintain uniform conductivity of the solution. At the end of each test, sample of solution was collected to measure the conductivity and pH of the solution after the test. The o-rings were replaced with new o-rings after every three tests to ensure the safety by avoiding any leaks or pressure drops to run the experiment.

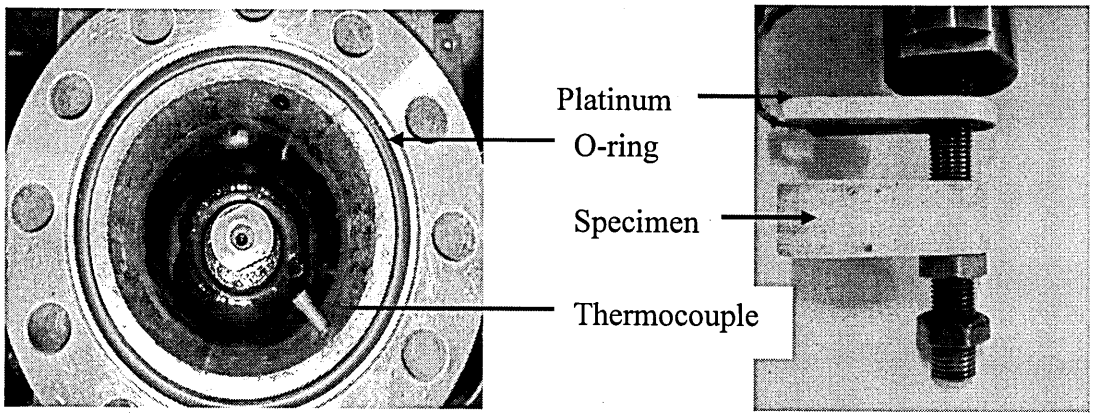

Figure 3.3: Showing a) the open section of the autoclave b) modified design for polarisation

3.3.3 Environment:

Potentiodynamic polarisation curves were conducted in various chloride solutions 15, 100, and 1000ppm chloride. The salt was weighed and was calculated to prepare required levels of chloride solution from NaCl. The salt was mixed in deionised water with conductivity of 0.1 micro Siemens. The solution was transferred to the overhead tank on the test rig and then used to fill the autoclave.

3.3.4 Measurements:

The electrode potential was scanned from the cathodic (-800mV) to the anodic direction (until the current values reach $10mA/cm^2$ at a scan rate of 30mV/min. From the polarisation curves corrosion current density (I_{Corr}) and corrosion potential (E_{Corr}) were obtained from polarisation curves using the tafel slopes. The potential at which the current density increases dramatically was defined as pitting potential (E_p).

Cyclic scans tests were done under similar conditions but the test was reversed when the current value reached a value of $10mA/cm^2$. Once cyclic curves were determined, pitting potentials, passivation current density(I_p) and repassivation potentials(E_{rp}) were calculated as these parameters were characteristic for defining localised corrosion resistance of a material. A calibrated orbisphere is used to measure the oxygen levels of the tank. Nitrogen is purged into the tank after the end

of the test in order to protect the surface of the specimen and to do controlled oxygen level experiments. All the above mentioned measurements were performed using an Ag/AgCl (0.25MKCL) reference electrode.

3.3.4.1 Silver/Silver Chloride reference electrode

When reference electrodes are used at temperatures over the range of 25 - 175^{0}C requires thermodynamic stability compared to the use at room temperature. The detailed reviews of (Macdonald et al (1975, 1978, 1979); Danielson (1983)), have established that for most of the high temperature and pressures tests in autoclaves Ag/AgCl reference electrode is used to measure the potential of the working electrode. These reviews highlighted the design and performance of Ag/AgCl reference electrodes in high temperature/high pressure aqueous solutions, and reasons for their argument was K^+ and Cl^- ions have equal mobilities even at higher temperatures, and Ag-AgCl/Cl^- electrode is the only one that exhibits predictable thermodynamic behaviour over the wide range of temperature range (25 - 275^{0}C) in aqueous solutions. However, Scott and Bamford (1985) have discussed a lot of key issues regarding the development and use of the reference electrodes and some of the key elements worth mentioning. They addressed the practical problems could be

1) The retention of the soft silver coating in a suitable electrically isolated pressure fitting.
2) Maintainence of a constant chloride activity around the sensing element.
3) Loss of electrical continuity due to air bubble formation.
4) Body materials of adequate strength up to 200^{0}C capable of insulating the electrode from the metal of pressurised water system.

Keeping in view of the above precautions and problems, in the present study the electrode was prepared. The silver rod after chloridising was placed in the PTFE tube

where it is filled with 0.025 M KCl solution, using a syringe and then assembled with anti expulsion bracket in place in order to avoid the expulsion of silver rod at high pressures. The reference electrode was maintained such that it is prevented from any loss of electrical conductivity and leakage of KCl into the test solution. Frequent checks have been made by comparing the potential difference with a saturated calomel electrode maintained at room temperature. The difference was observed to be around 53 mV in a given test solution, and varied within a range of 2mV. The electrode was stored in a solution of KCl after the tests so that it was not dry before use. Standard pressure fitting are used to retain the stainless steel tube when used at high pressures. Care was taken to avoid formation of air bubbles, which might break the electrical conductivity.

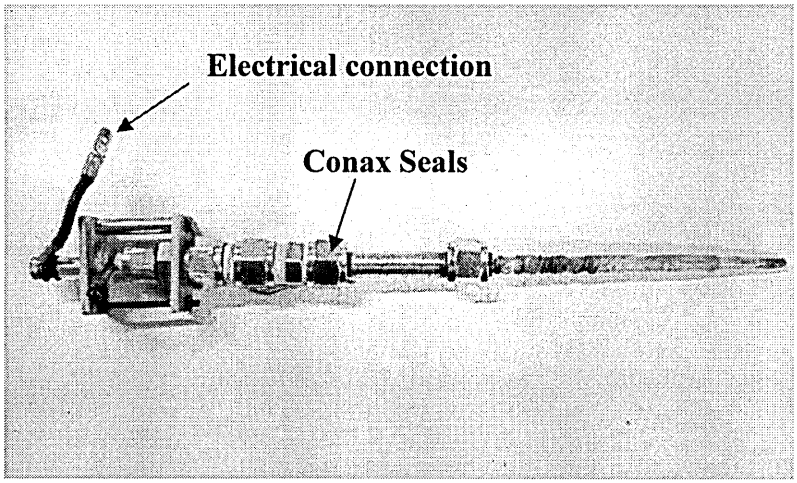

Figure: 3.4 Reference electrode used in the current study

The electrode is always mounted in the horizontal direction to avoid bubble formation in the electrode. It was made sure that reduction of ohmic drop between the reference electrode and the test specimen by placing the zirconia plug as close as possible to the specimen.

3.3.4.2 Pitting potentials

Pitting potential or breakdown potentials were measured from the polarisation curve to assess the relative performance of the various steels investigated in the present study as function of temperature. The pitting potential was measured when the abrupt increase in the current density was noticed during the polarisation scan and was recorded digitally using ACM software. All the values were recorded against Ag/AgCl electrode unless stated.

3.3.4.3 Pit Depth

In order to measure the pit depth, the working electrode (specimen) was held at a constant potential 10mV above the pitting potential measured from polarisation curves at various time 1 to 1000mins in order to measure the pit depth dependence with time. Once the specimen is held for constant length of time it was examined with optical as well as SEM for to measure the pit diameter and shape and the depth measurement were carried out using Stylus marker instrument.

3.4 Slow strain rate tests

Slow strain rate tests are a well known and common laboratory test used in order to study the stress corrosion resistance of an alloy in aqueous solutions in a quick time. The tests were conducted by applying dynamic strain to the tensile test specimen, usually 10^{-6} - 10^{-8} s^{-1}, and the material is subjected to plastic deformation until final failure. Data was recorded on the computer controlled Dennison-Mayes machine operated by Rubicon software. All the SSRT tests were conducted in a 2L capacity autoclave in order to study the performance and behaviour of the materials in corrosive environment under controlled potentiostatic conditions. The maximum stress (UTS) and % elongation (El) were obtained from these curves, while %

reduction in area (RA) was measured after the test. Since reduction in area factor proved to be the most sensible susceptibility index, it is used a criteria in the presentation of results and reference will be mainly made to this parameter.

3.4.1 Materials

The alloy used for the majority of the SCC investigation is Zeron100 super duplex stainless steels and few tests were conducted to judge the relative performance of the 2205 and Ferallium alloy 255 duplex stainless steels. The steels were produced as a round bar of 12mm diameter of which the samples were made by slicing the bar with a thickness of 5mm and surface area of 1.13cm^2.The material supplied by Weir Materials UK is solution annealed at 1100 ^{0}C for 60 minutes and water quenched. All the materials were supplied in wrought product forms.

	C	Si	Mn	P	S	Cr	Mo	Ni	W	Cu	N
2205	0.03	1.0	2.0		0.020	23	3.5	5.5			
255	0.05					25	3.0	6.0		2.2	0.18
Zeron100	0.024	0.24	0.51	0.024	0.0004	25.10	3.75	6.86	0.55	0.61	0.23
Zrn73266	0.018	0.24	0.86	0.025	0.0005	25.10	3.52	6.85	0.54	0.52	0.221

Table: 3.3 Show chemical composition of materials for SSRT tests

3.4.2 Specimens

All the specimens used to conduct SCC tests were standard slow strain rate tensile specimen with a gauge length of 17.27mm and diameter 3.68mm and an overall length of 110mm machined with axis parallel to the longitudinal direction of the bar and the guage lengths were polished to 0.5μm to remove the machining marks on the specimen surface. The engineering drawing of the specimen was shown below, and the identical geometry was used for entire SSRT tests conducted in various

conditions. The specimens were grounded using 600 and 1200micron emery paper and further polished using the 1 and 0.5μm diamond paste.

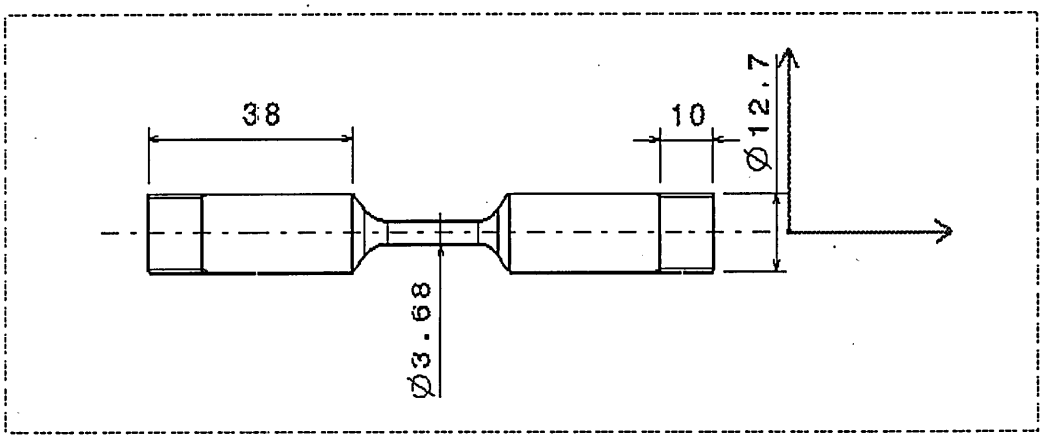

Figure: 3.5 SSRT specimen geometry

3.4.3 Environment

The environment used to conduct the SCC tests was chloride solution prepared using deionised water. The analytical grade sodium chloride was weighed and mixed in the deionised water to achieve the required concentration 15 to 10000wppm Cl^- (pH = 6.5) and subsequently mixed in 20litres equivalent in the tank. Once the salt solution was filled into the tank nitrogen and oxygen were sparged alternatively into the tank until 8 ppm oxygen level is attained. The oxygen concentration in the test solution was measured using the 3200 model oxygen analyser.

3.4.4 Testing machine:

The schematic view of the autoclave and the water loop setup is shown in the Fig 3.7. The autoclave was made of 316 stainless steel with 2L capacity and designed to withstand maximum operating temperature less than 200^0C. The autoclave has two half's of cylindrical cell which can be closed with screws by an O-ring seal placed between them. It incorporates a thermocouple which monitors the temperature inside

the autoclave sealed in a conax fitting, a reference electrode (Ag/AgCl electrode), and platinum cylindrical mesh counter electrode around the specimen. The connections to the electrodes inside autoclave were through conax fitting situated on the head of the autoclave. The autoclave has inlet and outlet tubes to allow continuous bubbling of oxygen and nitrogen during the tests. The water inlet tube connected to the autoclave was connected to the over head tank and the autoclave was filled by gravity feed. Once the autoclave is filled with the solution, then passes through the chiller, a copper block into which the cooling coil was inserted was fitted in water loop system, so that it can feed the chilled water to the entire system reducing the risk of damaged flow lines. The test solution is heated or cooled to the desired test temperature (from 25 to 170^{0}C) using 600W band heaters that were tightly fixed to the autoclave before the potentiostat is switched on, or before straining is applied to the sample. The autoclave is wrapped with glass wool for insulation and found to be very efficient at high temperatures as it prevents any heat loses.

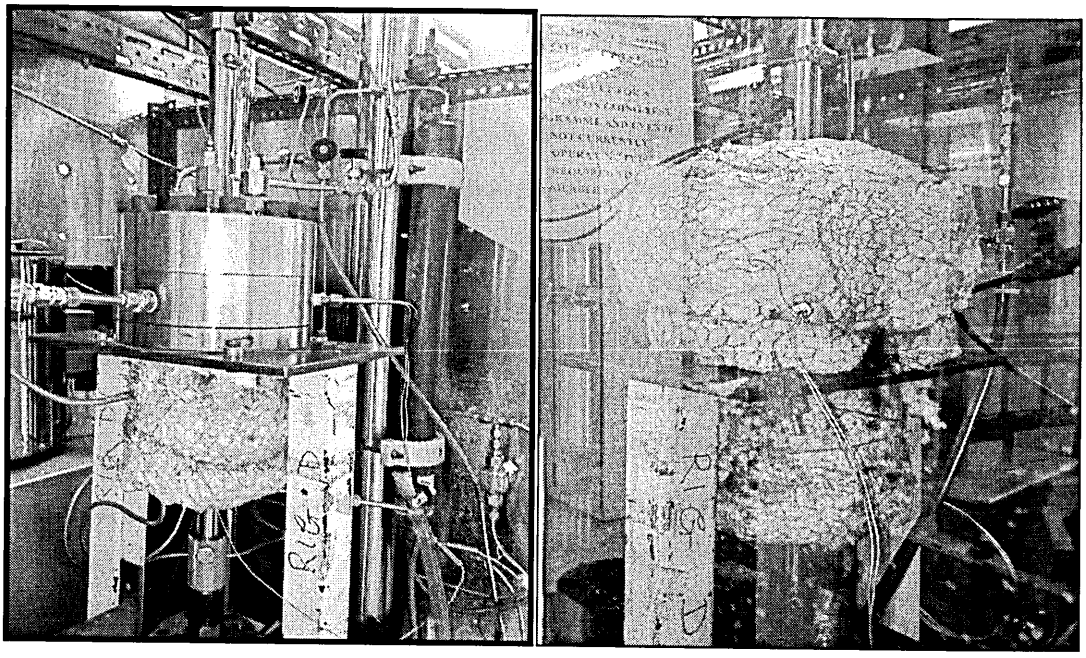

Figure: 3.6 Show the autoclave when in closed position a) before the test b) during the test covered with glass wool and safety screen in position.

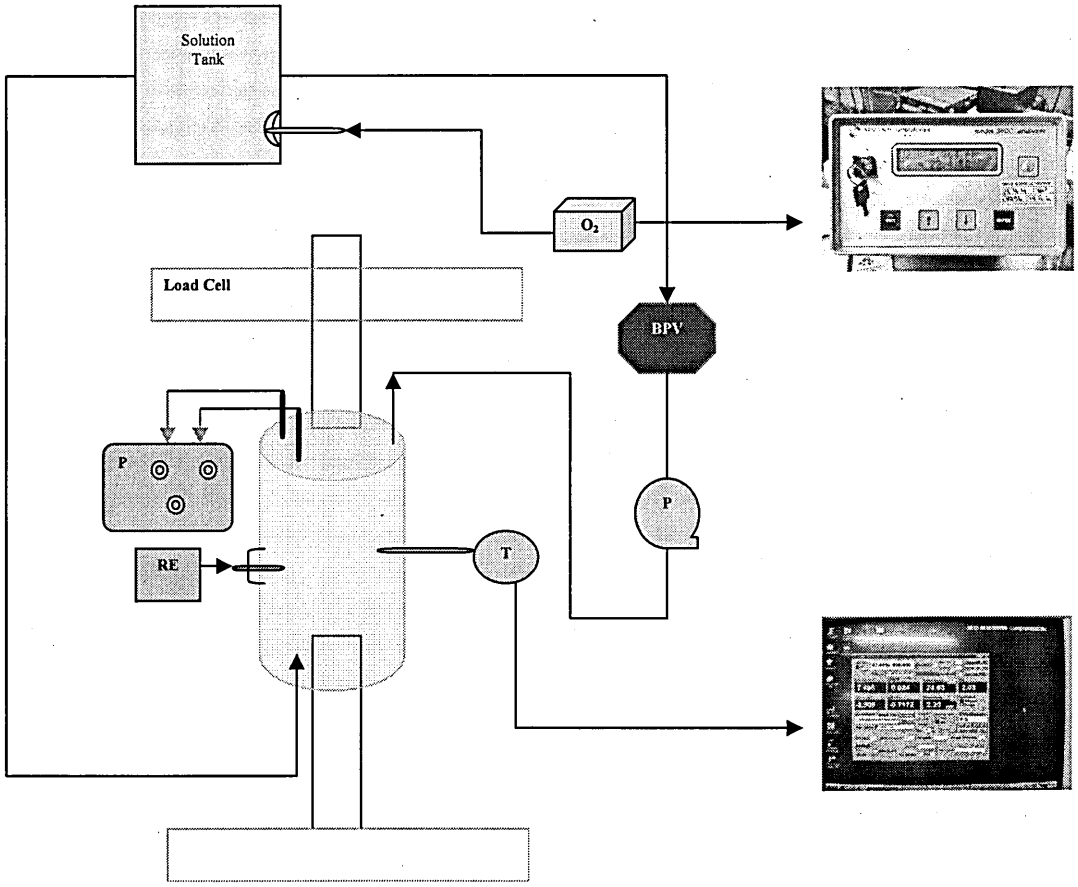

BPV – Back pressure Valve
P – Pump
RE – Reference electrode
T - Thermocouple
P – Potentiostat
O_2 – Orbisphere

Figure 3.7 Showing schematic view of the water loop connected to

Bran and Luebbe pump was used to pressurise the autoclave to prevent the water to become steam above 100^0C. The water enters the inlet of the pump from the overhead tank also connected to the orbisphere to measure the oxygen levels. The tank was sealed and all the inlets and outlets of the tank are frequently checked in order to avoid leaks. The autoclave when pressurised was designed to withstand 560psi. The back pressure regulating valve was used to control pressure inside the autoclave so that water is not turned to steam. The principal advantage of using this set up is it allows to control several parameters at the same time in individual experiments.

3.4.5 Potential control

The Specimen was subjected to constant strain under constant anodic potentials applied using ACM GILL AC potentiostat. The potentiostat is computer controlled and the data generated is digitally recorded in the ACM software from it can be reproduced. The shoulders of the specimens are insulated with PTFE heat shrink and made sure that the electrical connections from the potentiostat is subjected to the guage length not passing through the specimens to the loading bars. In order to prevent from short circuit the specimen is separated from the loading bar with a thin sheet of inert material like PTFE plastic so that the applied voltage stays within the guage length and also the circular sheet of platinum, an auxiliary electrode was placed around the guage length with a provision to insert reference electrode. This kind of setup produced excellent and consistent results throughout the previous studies conducted by Atkinson and Clive (1999).

3.4.6 Strain rate

Strain rate is the critical parameter and defines the severity in order to conduct the SSRT tests. The straining was achieved in a hard tensile machine at a cross head speed that produced a strain rate of 1×10^{-6} /S^{-1}. The extension of the specimen was monitored using external LVDT extensometer connected to Rubicon data logger. All the SSRT tests are carried out under constant strain rate unless otherwise specified.

3.4. 7 Calculation of %RA, Stress, and Strain.

One way to measure the loss of ductility is to measure **percentage reduction in area** (%RA) of the material exposed to the service conditions. In the present study the ductility is measured as change in the area of the gauge length near the fracture surface. The initial gauge length is denoted by (L_O), initial diameter as (D_O), initial

area A_O before the fracture and final gauge length (L_F), final diameter (D_F) and final area (A_F) after the failure are considered. The percentage reduction in area is calculated using the equation

$$\% \text{ Reduction in area} = \frac{Changeinarea(\Delta A)}{Originalarea(A_o)} \tag{3.1}$$

Stress is defined as force per unit area. The load values obtained from load-extension plotted during the slow strain rate test are divided by the area of the specimen and calculated using the equation

$$Stress = \frac{force(N)}{Area(mm^2)} \tag{3.2}$$

All the stress values were quoted in MPa in the stress - strain curve.

Strain (Є) is defined when the material undergoes deformation as a result of applied stress. It is a dimensionless quantity and can be calculated using the formulae below

$$\epsilon = \frac{l - l_0}{l_o} \tag{3.3}$$

The above equations are used in order to produce the stress -strain curves in the present study.

3.5 Fracture surface examination

After the SSRT tests the fracture surfaces are examined under optical and scanning electron microscopy. After finishing the pitting and slow strain rate tests the specimens were sectioned parallel to the gauge length and mounted in the Bakelite. The specimens were then polished from 120 - 1200 grit silicon carbide paper, fixed on a grinding wheel followed by polishing on 6 μm and 1 μm finish paper. The specimens were then examined for pits and cracks and photographs were taken using the optical microscope.

3.5.1 Optical microscopy

Microstructure, cross sections and etched samples were examined under optical microscopy after the end of the test. The specimens were polished in conventional manner using silica carbide grits up to 1200microns and then further polished on diamond polishing on both 6μm and 1μm rotating wheels. The resultant microstructure was photographed using Carl Zeiss optical microscope with digital camera arrangement.

3.5.2 Scanning electron microscopy

After potentiodynamic polarisation and SSRT tests the surface of the specimen were examined under Philips Xl40 scanning electron microscopy operated at 20kev with varying spot size and working distance. Specimens were cleaned and dried in order to prevent charging up. The cross sections of the specimen was mounted in conductive bakelite and then polished to 6μm to 1μm for further inspection.

To study the microstructure electrolytic etching was carried out on the samples depending on the constituent phases. Electrolytic etchants have been widely used in this study as they are simple in composition and can be used safely producing excellent results superior to chemical etchants. Electrolytic etchants are generally recommended for selective etching of specific phases, because many of them are quite specific in their attack of the sample surface, which is useful in identifying the phases Michalska & Maria (2006). In case of duplex stainless steels the etchant used was 10% potassium hydroxide electrolytically treated 3-9 Volts for 10 secs, this allowed the ferrite phase to darken preferentially.

CHAPTER 4
Results

4.0 Introduction:

In this chapter will shall discuss the results and explain the final outcome of the research carried out by the author. The test programme was carried out and compared with the limited data available on pitting and stress corrosion areas, highlighted in the literature review. The data from the present study is discussed with the published data in the literature in chapters 5 & 6.

The data of the polarisation studies carried out at room temperature is presented in section 4.1 and polarisation studies conducted in an autoclave facility are reported in sections 4.1.2. The chloride effect on polarisation curves is shown in section 4.1.4, chemical composition effects on polarisation curves is demonstrated in section 4.1.4.1 and pit growth rate is presented in section 4.1.5.

Stress corrosion cracking (SCC) tests conducted using the slow strain rate technique (SSRT) is presented in section 4.2. Including applied potential effect (section 4.2.1), chloride effect (section 4.2.2), temperature effect (25 - 170^0C) (section 4.2.3), dissolved oxygen effect (section 4.2.4), and composition effect in section (4.2.5). All the results are presented in the form of graphs and tables and referred in discussion.

4.1 Potentiodynamic polarisation results:

4.1.1 Polarisation test data at 25^{0}C

Polarisation curves determined by potentiodynamic polarisation technique using experimental procedure explained in the chapter 3 are shown in Fig 4.1.

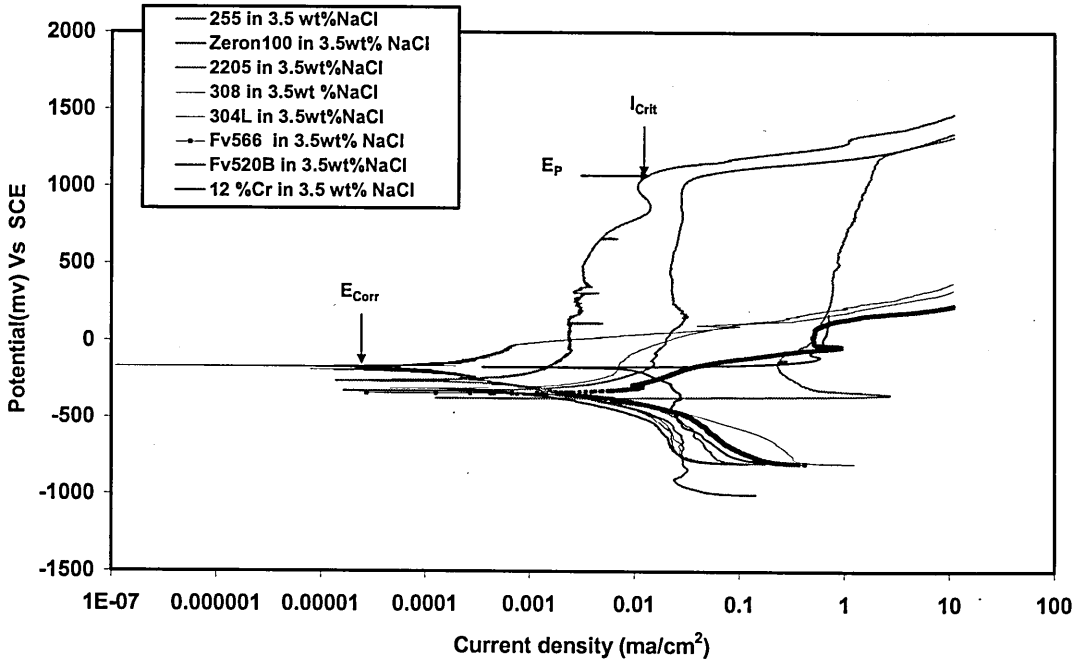

Figure 4.1: Polarisation curves of different steels tested at room temperature in 3.5 wt % NaCl solution, the electrochemical parameters E_P, I_{CRIT}, & E_{corr} are indicated in the graph are recorded for different chloride solutions.

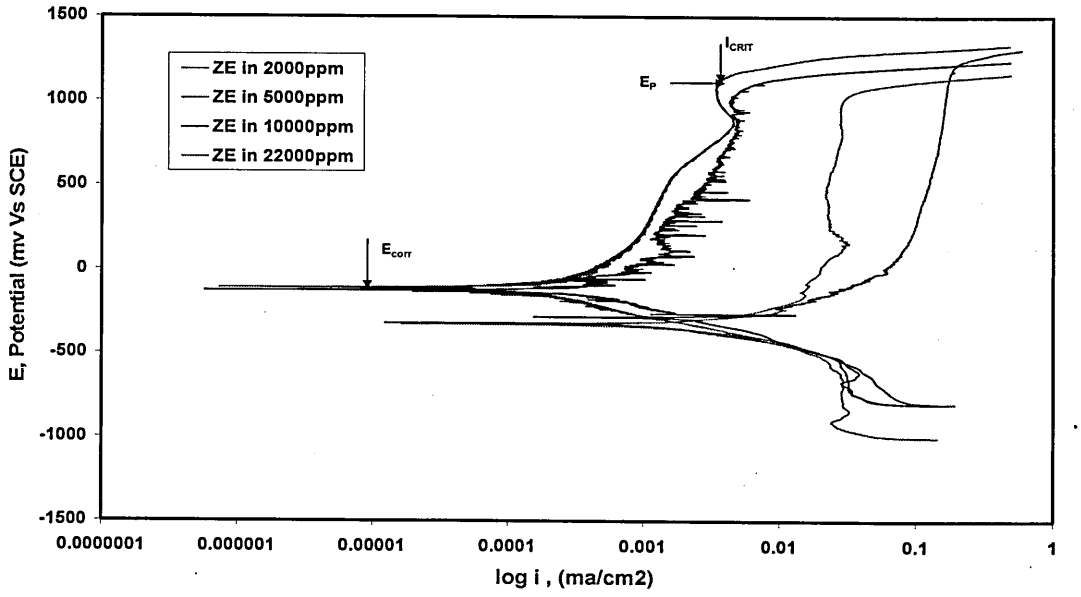

Figure 4.2: Polarisation curves of Zeron100 in different chloride solutions at 25^{0}C showing transpassive behaviour as they are below CPT and high potential values.

For comparison, identical conditions were maintained to generate the relevant data needed for this study. Electrochemical parameters highlighted in the Fig 4.1 and 4.2 are presented in tabular form and this data generated from the polarisation curves is used to rank the stainless steels against the pitting resistance. The pitting/breakdown potential values recorded are plotted against the chloride concentration in Fig 4.3.

Material	PREN	Temp^{0}C	[Cl]level in ppm	O_2 level in ppm	E_p in mV Ag/AgCl	I_{crit} @ E_P mA/cm^2	E_{corr} mV Ag/AgCl
12%Cr	13.6	25	22000	8	-109	0.001	-304
12%Cr	13.6	25	10000	8	51.48	0.19	-342
FV520B	18.3	25	22000	8	-181	0.02	-341
FV520B	18.3	25	10000	8	-34	0.001	-192
FV566	17.8	25	22000	8	40	0.02	-370
FV566	17.8	25	10000	8	86	0.008	-225
304L	19	25	22000	8	-113	0.007	-311
304L	19	25	10000	8	340	0.001	-105
304L	19	25	5000	8	330	0.40	-326
304L	19	25	2000	8	415	0.07	-86
18/13/1	20.3	25	22000	8	-24	0.0007	-161
18/13/1	20.3	25	10000	8	119	0.36	-352
18/13/1	20.3	25	5000	8	275	0.006	-217
18/13/1	20.3	25	2000	8	288	0.001	-88
Uranus65	25.73	25	22000	8	1163	46.93	-123
Uranus65	25.73	25	10000	8	1032	0.006	-153
Uranus65	25.73	25	5000	8	1249	1.50	-116
Uranus65	25.73	25	2000	8	1229	1.58	-99
2205	33.74	25	22000	8	1092	0.014	-257
2205	33.74	25	10000	8	1205	0.032	-220
2205	33.74	25	5000	8	1131	0.004	-146
2205	33.74	25	2000	8	1094	0.005	-98
Alloy255	37.78	25	22000	8	1204	2.255	-369
Alloy255	37.78	25	10000	8	1048	0.004	-106
Alloy255	37.78	25	5000	8	1216	0.18	-253
Zeron100	41.16	25	22000	8	1044	0.033	-321
Zeron100	41.16	25	10000	8	1077	0.0055	-110
Zeron100	41.16	25	5000	8	1230	0.20	-324
Zeron100	41.16	25	2000	8	1158	0.004	-114

Table 4.1: Results of the test programme conducted in various chloride concentrations at 25^{0}C to measure critical electrochemical parameters Pitting potentials (E_P) , Free corrosion potentials (E_{CORR}) , Corrosion current density (I_{Crit}) for wide range of PREN.

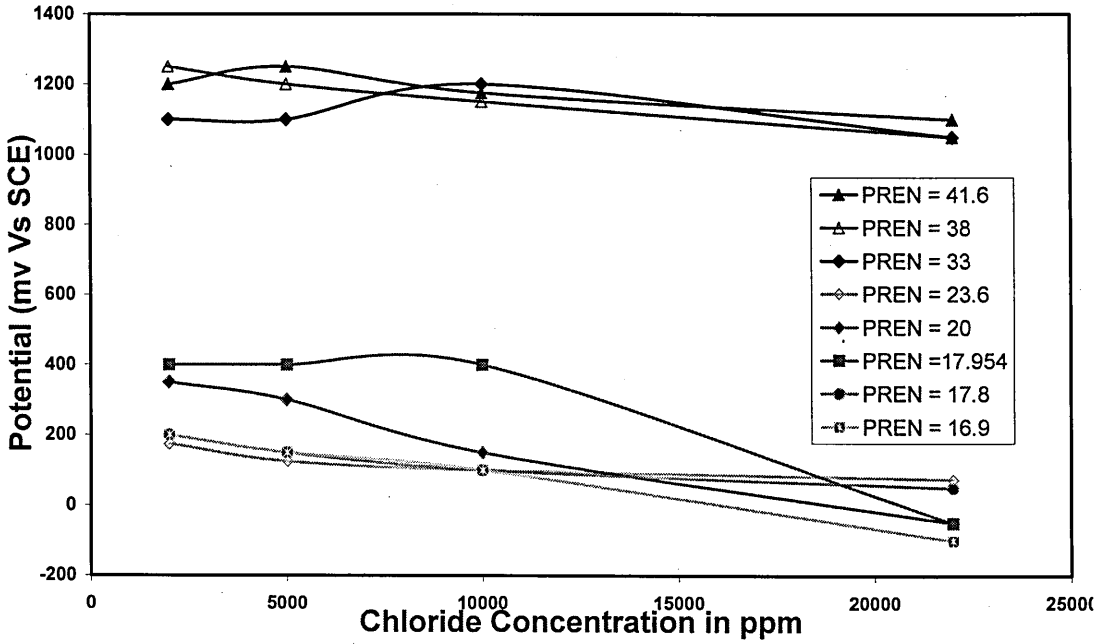

Figure: 4.3 The effect of chloride concentration on wide range of PREN showing that PREN has significant influence on pitting potentials on the tests conducted at room temperature, with two groups of data, standard stainless steels PREN <33, duplex >33

4.1.2 Polarisation test data at various temperatures:

The extension of polarisation technique from room temperature to a different range of temperatures has been produced using the experimental technique described in chapter 3.

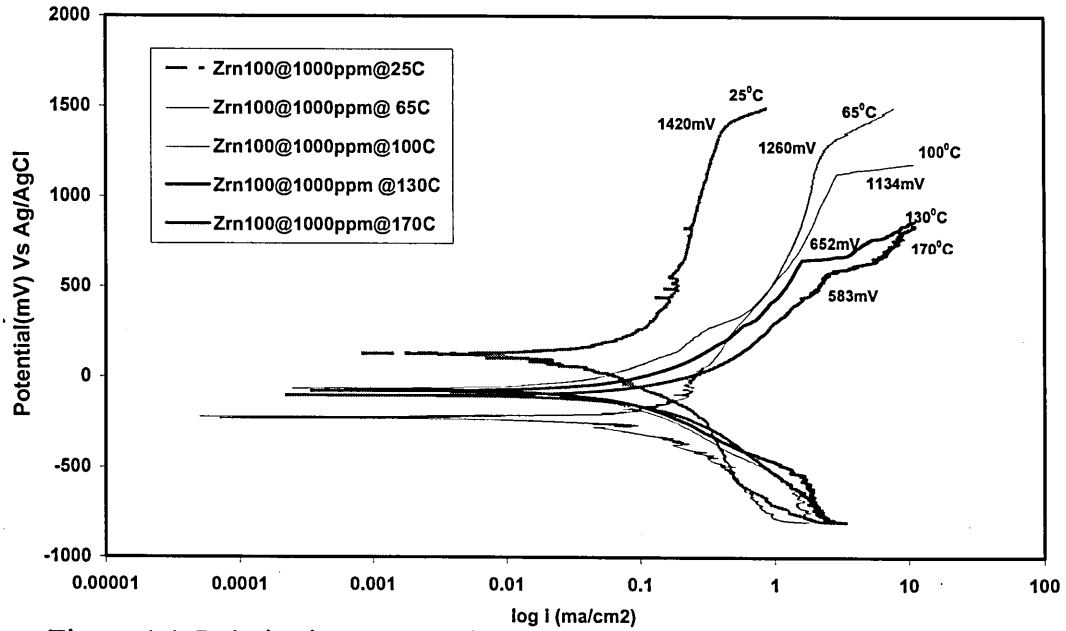

Figure 4.4: Polarisation curves of Zeron100 showing the change in various electrochemical parameters with change in temperature.

The results from all the tests conducted for different steels at different conditions has been presented in table 4.2

Material	PREN	Temp^{0}C	[Cl]level in ppm	O_2 level in ppm	E_p in mV Ag/AgCl	I_{crit} mA/cm^2	E_{corr} mV Vs Ag/AgCl
12%Cr	13.6	65	1000	7-8	-22	0.32	-401
12%Cr	13.6	95	1000	7-8	-169	0.31	-450
12%Cr	13.6	150	1000	7-8	-254	0.51	-468
304L	19	65	1000	7-8	-50	0.34	-480
304L	19	95	1000	7-8	-80	0.45	-478
304L	19	130	1000	7-8	-43	0.89	-406
304L	19	150	1000	7-8	-65	0.52	-376
304L	19	170	1000	7-8	-29	0.79	-359
Uranus65	25.73	130	1000	7-8	153	0.90	-360
Uranus65	25.73	150	1000	7-8	25	0.67	-352
Uranus65	25.73	170	1000	7-8	25	0.91	-332
2205	33.74	65	1000	7-8	794	0.61	-494
2205	33.74	95	1000	7-8	322	0.72	-432
2205	33.74	130	1000	7-8	109	0.785	-330
2205	33.74	150	1000	7-8	215	1.14	-377
2205	33.74	170	1000	7-8	178	1.27	-313
Alloy255	37.78	65	1000s	7-8	608	1.50	-402
Alloy255	37.78	95	1000	7-8	370	2.18	-474
Alloy255	37.78	130	1000	7-8	129	0.95	-577
Alloy255	37.78	150	1000	7-8	126	0.75	-351
Alloy255	37.78	170	1000	7-8	187	1.65	-473
Zeron100	41.16	65	1000	7-8	1314	2.76	-215
Zeron100	41.16	95	1000	7-8	1134	2.92	-63
Zeron100	41.16	130	1000	7-8	652	1.78	-61
Zeron100	41.16	150	1000	7-8	411	2.25	-307
Zeron100	41.16	170	1000	7-8	583	2.74	-100

Table: 4.2 Test conditions and values of pitting potentials (E_P), free corrosion potentials (E_{Corr}), critical current density (I_{Crit}), conducted in 1000ppm chloride in autoclave.

The results obtained at different temperature for various stainless steels in 1000ppm chloride solution are plotted in the Fig: 4.5. The very high breakdown potentials that were recorded for Zeron100 at 65^0 and 95^0C will correspond to the transpassive behaviour of this alloy at those conditions. The values noticed at 25^0C (Table 4.1) for

duplex and super duplex materials represent that these alloys exhibit transpassivity below CPT.

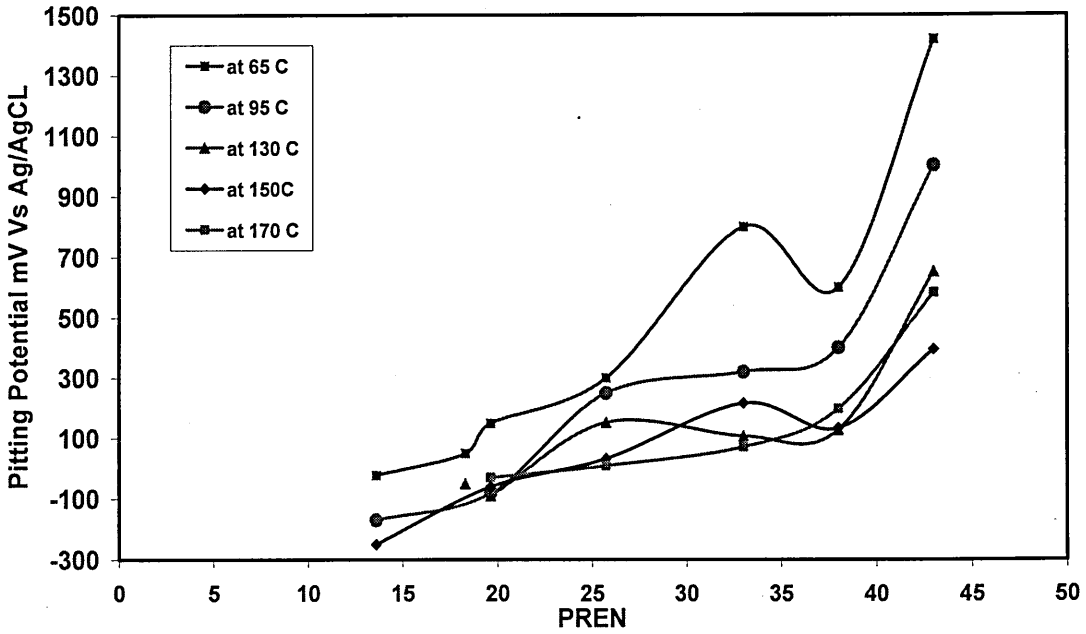

Figure: 4.5 showing the pitting potentials for wide range of PREN at various temperatures in 1000ppm chloride solution in most cases. Increase in PREN has shown higher pitting potential values.

4.1.3 Polarisation test data for various chloride levels at 130^{0}C:

An example of the effect of chloride concentration on different electrochemical parameters is determined using the potentiodynamic polarisation test set up in an

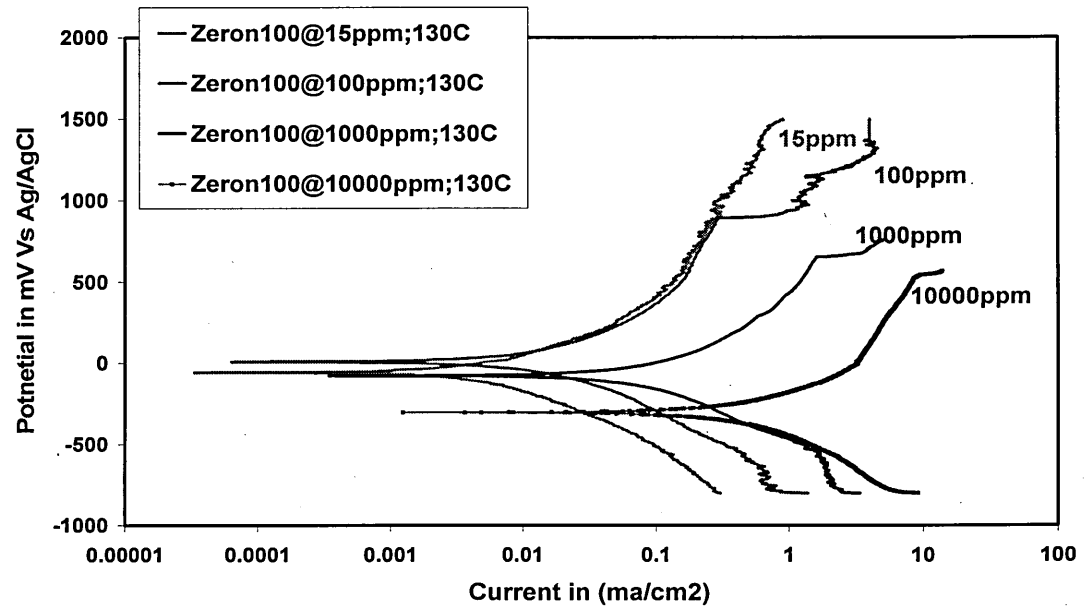

Figure: 4.6 Polarisation curves for Zeron100 conducted at 130^{0}C in various chloride solutions.

Autoclave conducted at 130^{0}C is shown in Fig 4.6. As shown in Fig 4.6 at various chloride concentrations the tests were conducted at 130^{0}C and the results are presented in table 4.3

Material	PREN	Temp^{0}C	[Cl]level in ppm	O_2 level in ppm	E_p in mV	I_{crit}	E_{corr}
12%Cr	13.6	130	15	7-8	143		-76
304L	19	130	15	7-8	228		
Uranus65	25.73	130	15	7-8	534	0.074	-198
Uranus65	25.73	130	10000	7-8	-26	1.85	-411
2205	33.74	130	15	7-8	849	0.071	-147
2205	33.74	130	100	7-8	475		
2205	33.74	130	10000	7-8	33	2.43	-386
Alloy255	37.78	130	15	7-8	1068	0.11	-72
Alloy255	37.78	130	100	7-8	545		
Alloy255	37.78	130	10000	7-8	97	2.81	-333
Zeron100	41.16	130	15	7-8	1400	0.74	-28.69
Zeron100	41.16	130	100	7-8	892	0.29	18.614
Zeron100	41.16	130	10000	7-8	541	9.30	-299

Table 4.3: Test data conducted at 130^{0}C in 15, 100, and 1000ppm chloride levels is presented in order to use the data to discuss the effect of chloride on PREN.

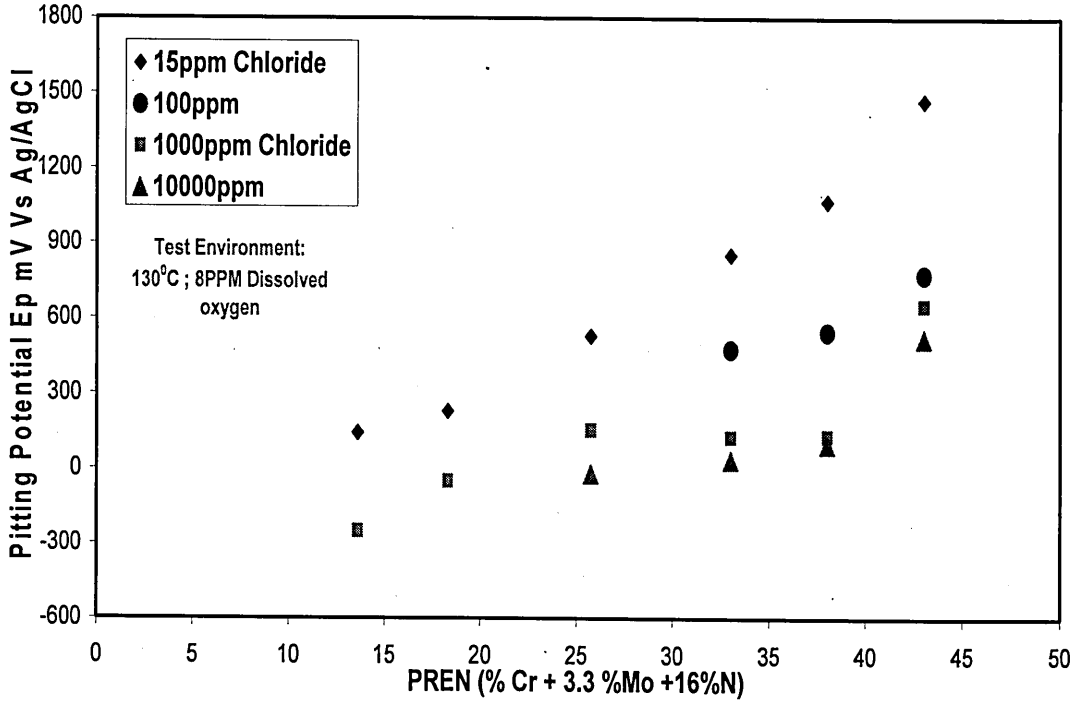

Figure: 4.7 Effect of chloride concentration (15, 100, 1000, 10000ppm) on pitting potentials for wide range of PREN at 130^{0}C in 8ppm dissolved oxygen.

4.1.4 Effect of Chemical Composition on Pitting Potentials:

The individual effects of chloride concentration, temperature on pitting potential values obtained from the polarisation curves were plotted in Fig: 4.8 to Fig 4.11.Only the results that are relevant in the discussion were presented in this chapter.

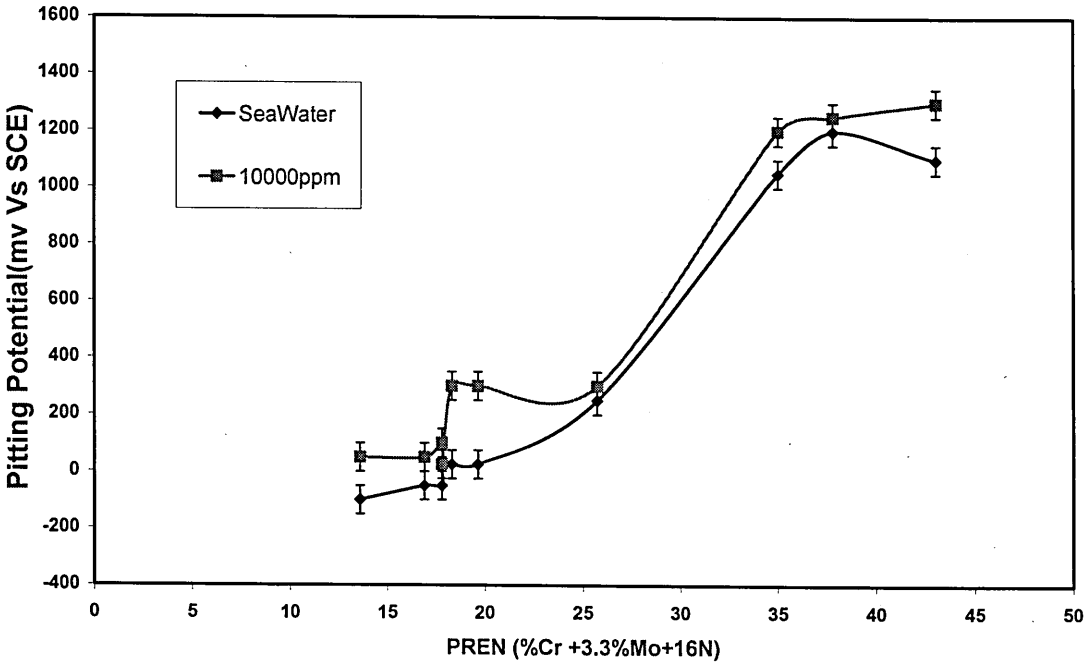

Fig: 4.8 Graph shows the effect of chloride concentration on chemical composition w.r.t pitting potentials in 3.5 wt% NaCl conducted in room temperature.

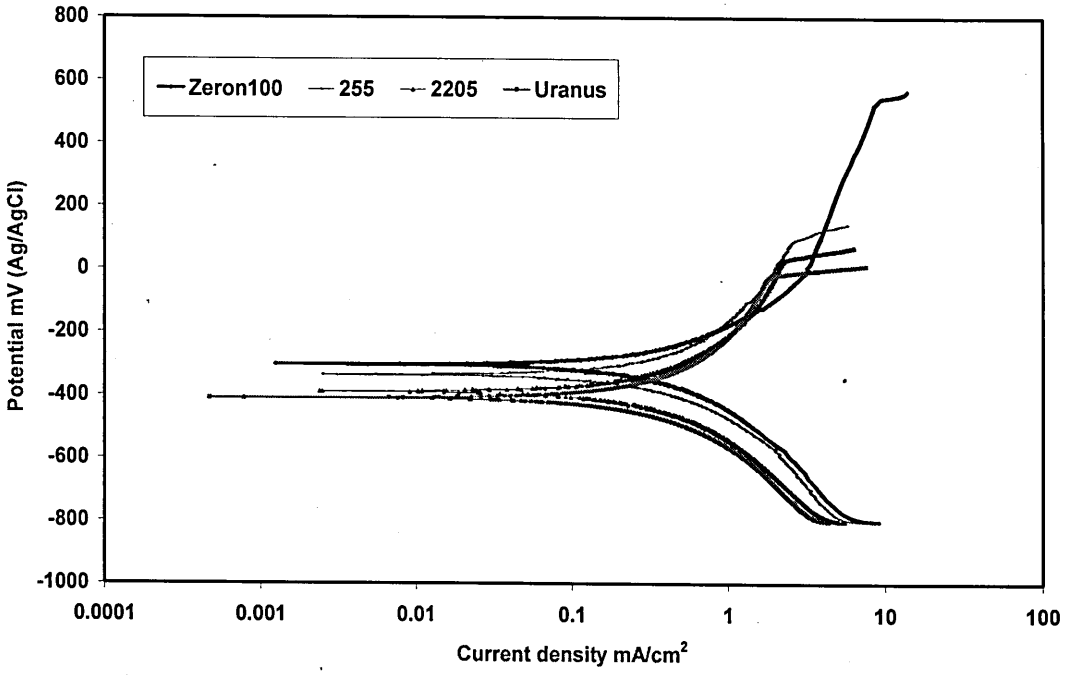

Figure: 4.9 Polarisation curves conducted in 10000ppm chloride at 130^{0}C in autoclave for different PREN.

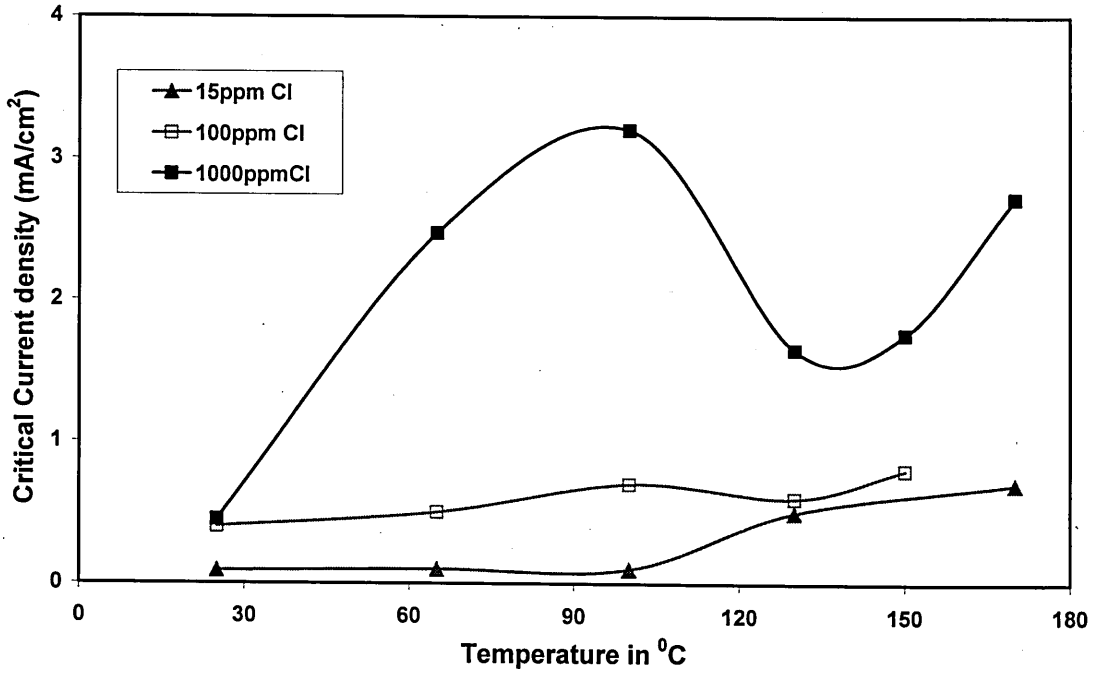

Figure: 4.10 Effect of temperature on critical current density for Zeron100 conducted in 15, 100, 10000ppm chloride levels at various temperature in an autoclave.

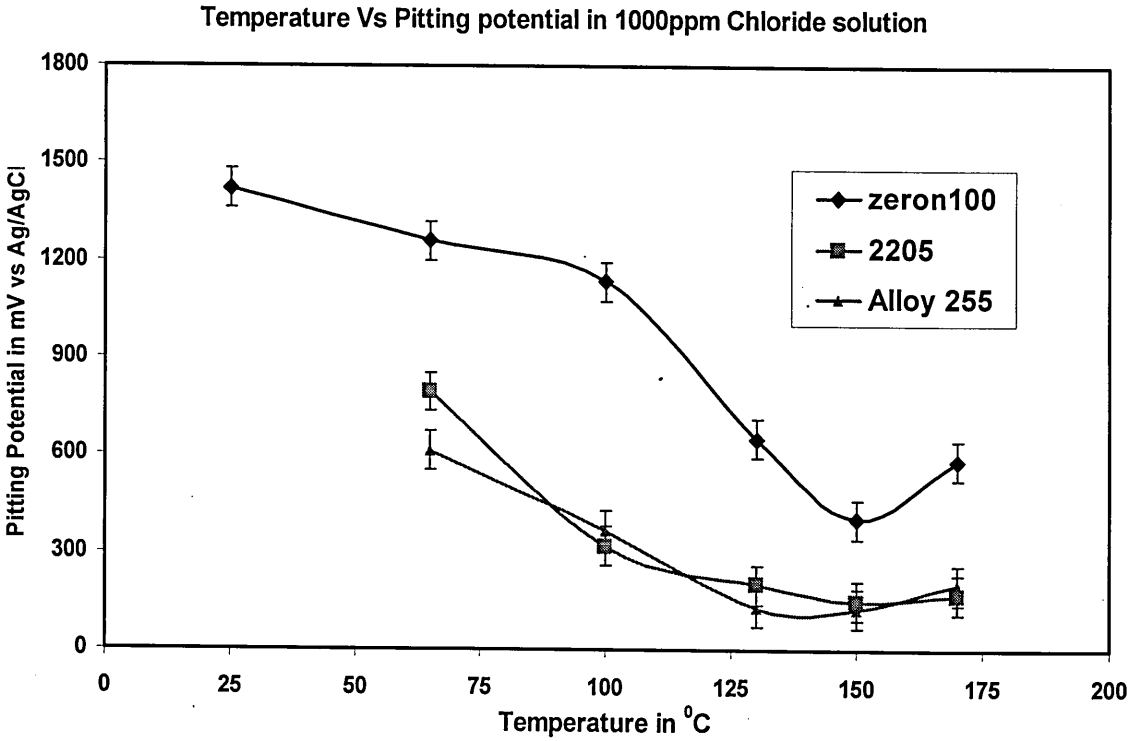

Figure: 4.11 Comparison of pitting potential values for 2205, alloy 255 duplex steels with Zeron100 super duplex stainless steel in 1000ppm chloride and 7-8 ppm dissolved oxygen.

4.1.4.1 Effect of chemical composition on Repassivation potentials:

The results of cyclic potentiodynamic polarisation are shown in Fig 4.12.The important parameter that is recorded from these results is E_{rp} (repassivation potentials).

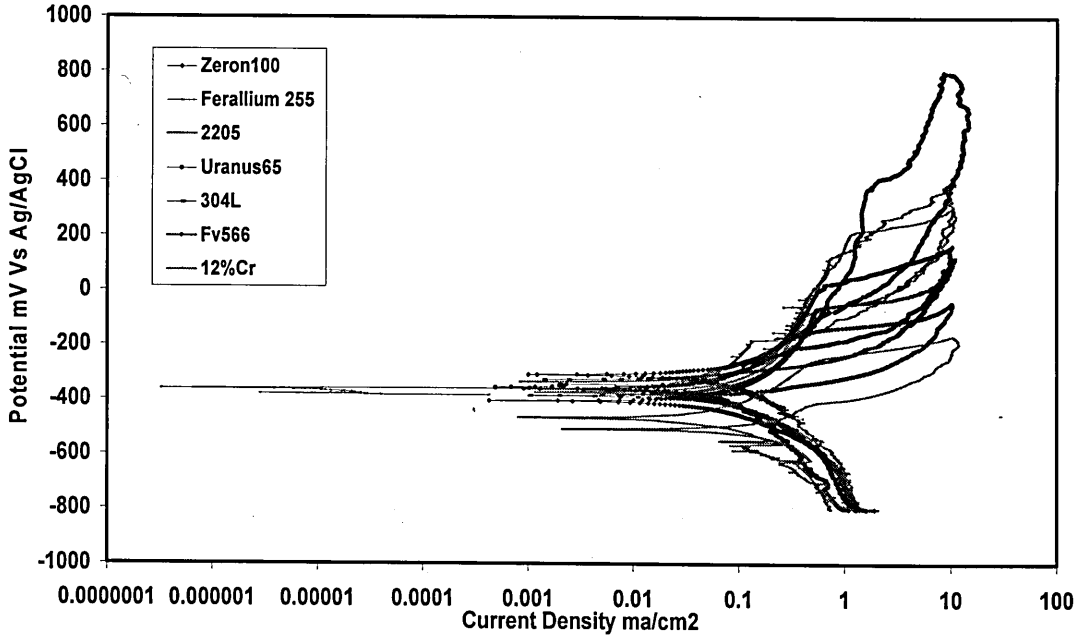

Figure: 4.12 cyclic potentiodynamic polarisation curves of various steels conducted in 1000ppm chloride solution at 150^0C in 8 ppm dissolved oxygen.

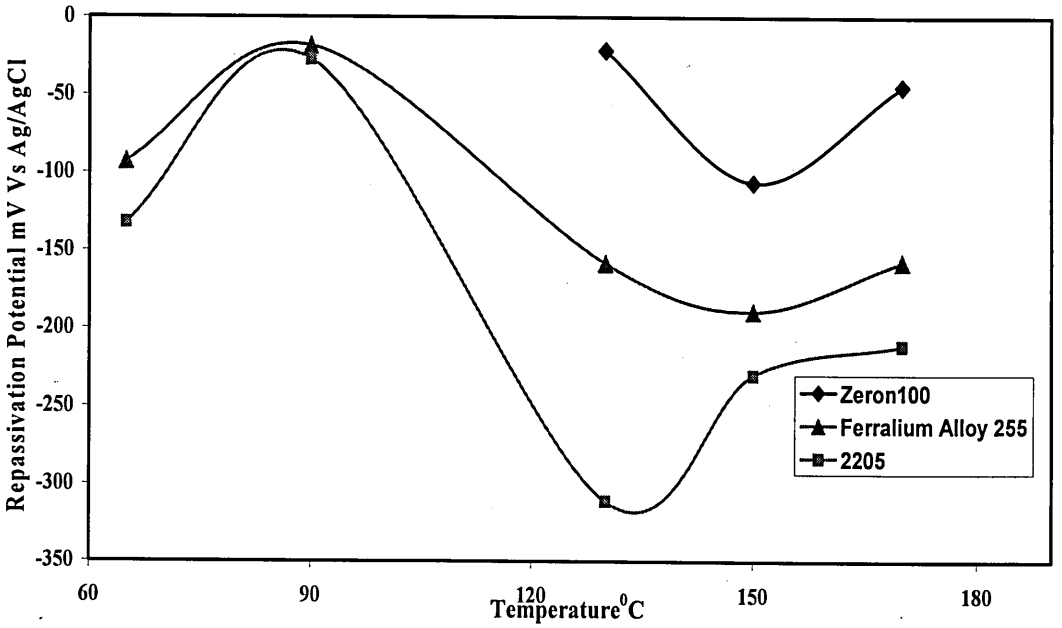

Figure: 4.13 Comparison of repassivation potentials of three types of duplex stainless steels in 1000ppm chloride solution at various temperatures in 8ppm dissolved oxygen.

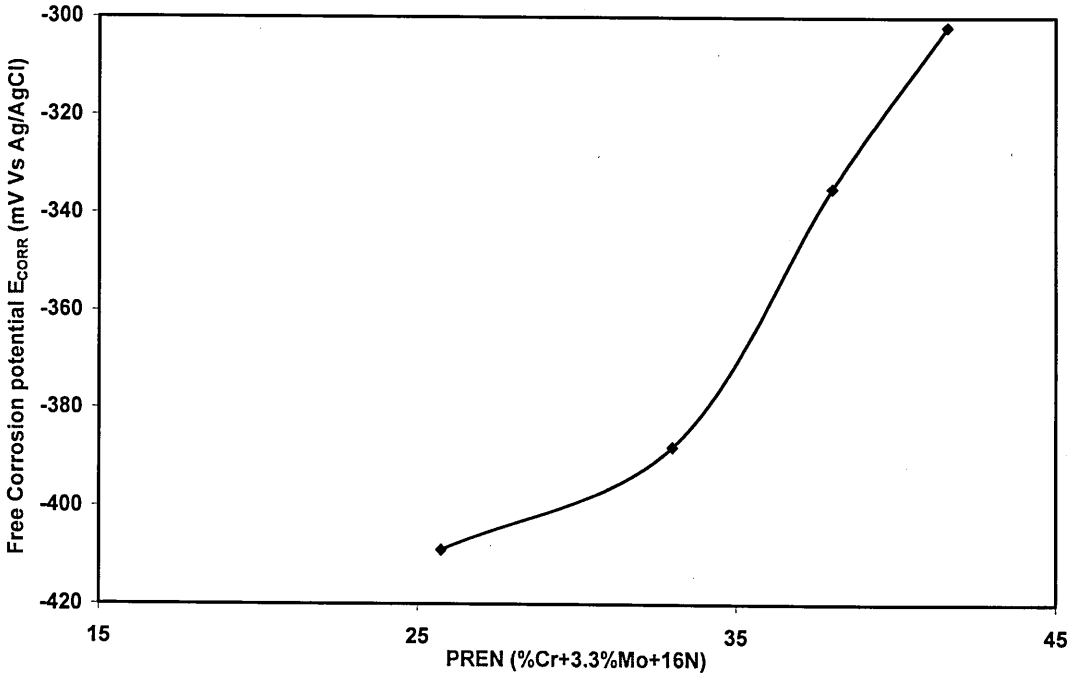

Figure: 4.14 Relationship of between free corrosion potential and chemical composition in 10000ppm chloride conducted at 130^0C.

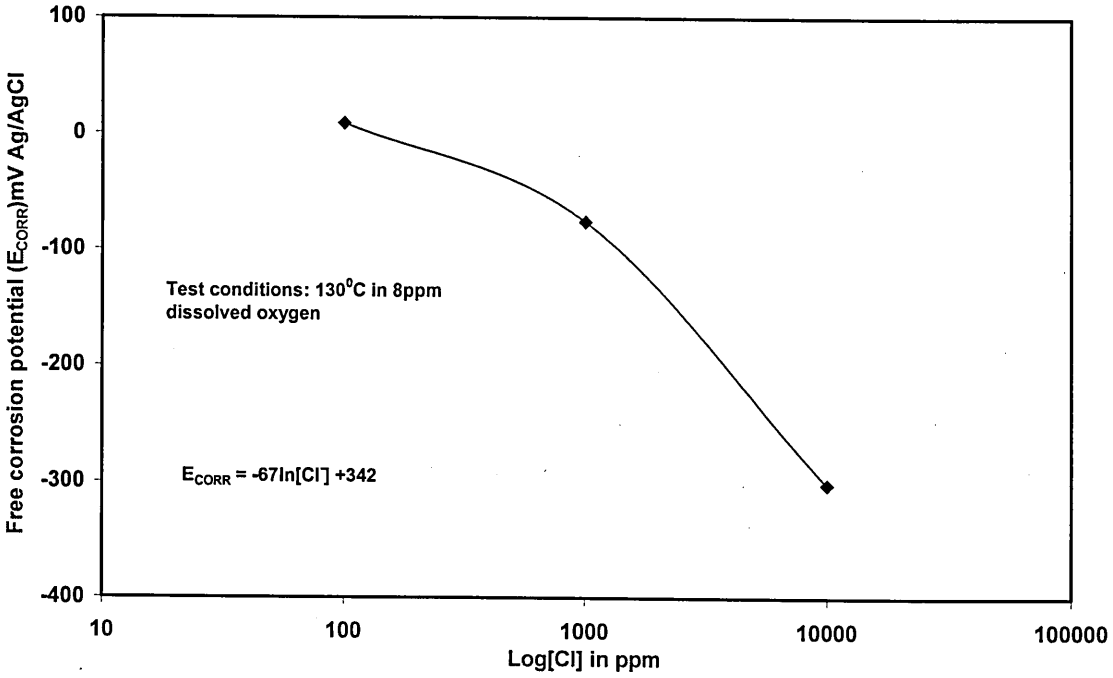

Figure: 4.15 Relationship between free corrosion potential and Chloride concentration.

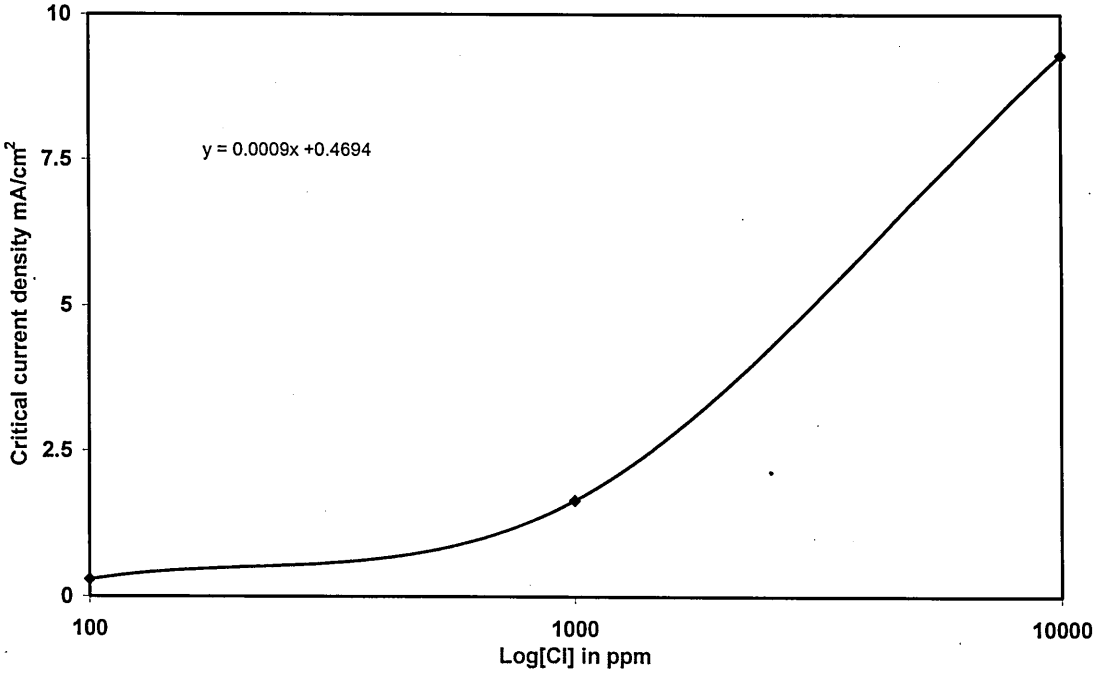

Figure: 4.16 Relationship between Chloride concentration and critical current density for pitting for Zeron100 at 130^0C.

4.1.5) Pit growth rate:

The pit growth rate is determined for Zeron100 in 1000ppm chloride solution

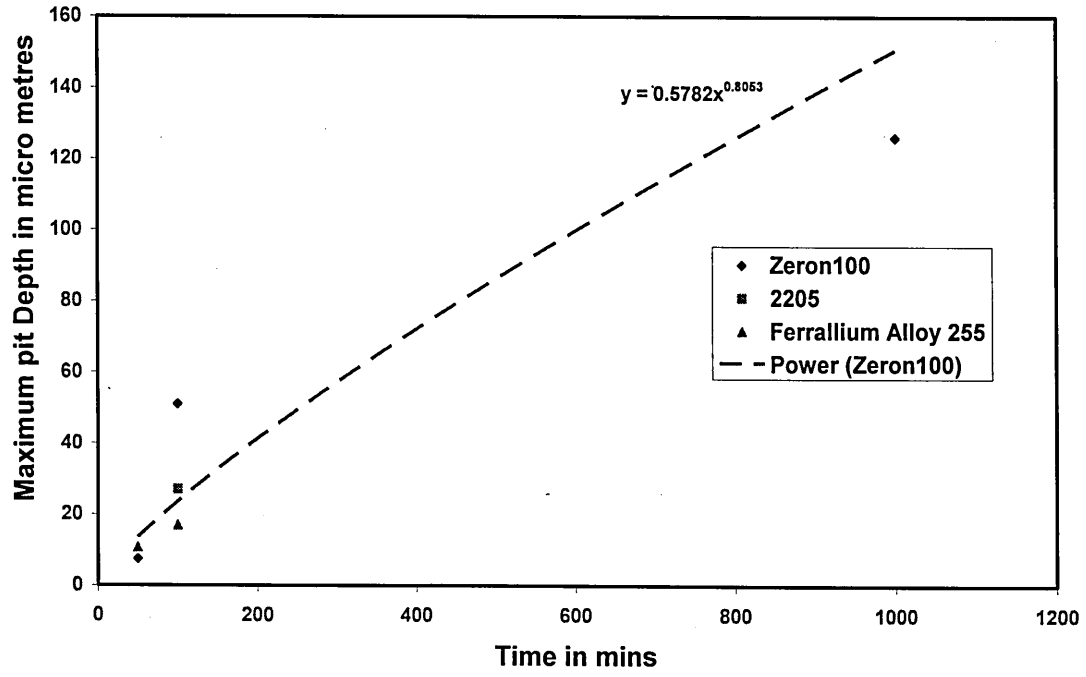

Figure: 4.17 Variation of pit depth was determined for Zeron100 for various times in 1000ppm chloride solution at 130^0C.

4.2 Introduction to SCC tests:

The slow strain rate tests were carried out in order to determine the SCC resistance of the super duplex stainless steel (Zeron100). The test conditions were varied in order to see the effect on the failure mechanisms and the tests results are presented in figures and tables that are discussed in chapter 6. The tensile strength, percentage elongation and percentage reduction in area are plotted with respect to applied potential, chloride concentration, temperature and dissolved oxygen.

4.2.1) SSRT results:

The slow strain rate technique (SSRT) is used to conduct the SCC tests in an autoclave at different applied potentials have allowed to produce stress - strain graphs as shown in Fig 4.18-4.22.

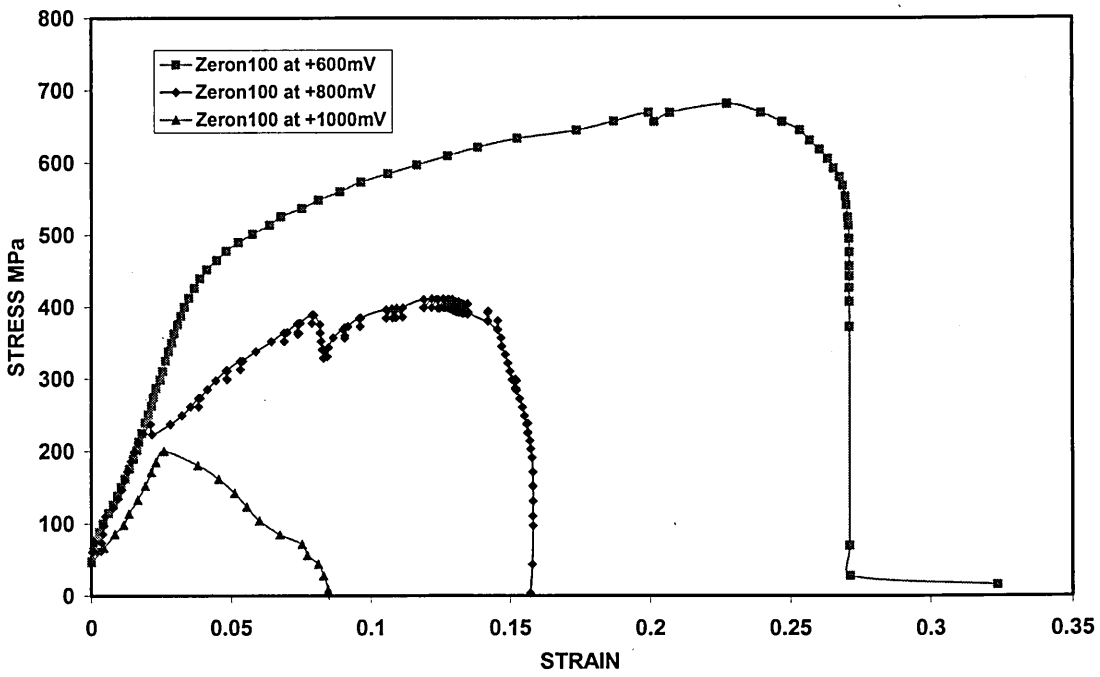

Figure: 4.18 Effect of applied potential on the stress strain curves of Zeron100 SDSS in 1000ppm chloride solution and 8ppm dissolved oxygen.

Specimen ID	strain rate S^{-1}	Temp ^0C	[Cl^-] level in ppm	O_2 level in ppm	Applied Potential in mV	%RA
ZRN13	$1 x10^{-6}$	130	1000	8	500	40
ZRN14	$1 x10^{-6}$	130	1000	7.6	600	18
ZRN15	$1 x10^{-6}$	130	1000	7.9	800	12
ZRN16	$1 x10^{-6}$	130	1000	7.3	1000	4

Specimen ID	strain rate	Temp ^0C	[Cl] level in ppm	O_2 level in ppm	Applied Potential in mV	%RA	Critical Current density (mA/Cm^2)
ZRN01	$1 x10^{-6}$	130	15	8	0	82	-221.788
ZRN02	$1 x10^{-6}$	130	15	7.6	400	81.5	73.077
ZRN03	$1 x10^{-6}$	130	15	7.9	800	29	155.735
ZRN04	$1 x10^{-6}$	130	15	7.3	1200	10	360.357
ZRN05	$1 x10^{-6}$	130	15	7.9	600	30	125.103
ZRN07	$1 x10^{-6}$	130	15	8.0	500	87	99.219

Table 4.4: Showing the data collected from SSRT tests conducted in 15, and 1000ppm chloride solutions at various controlled potentials in 8ppm dissolved oxygen.

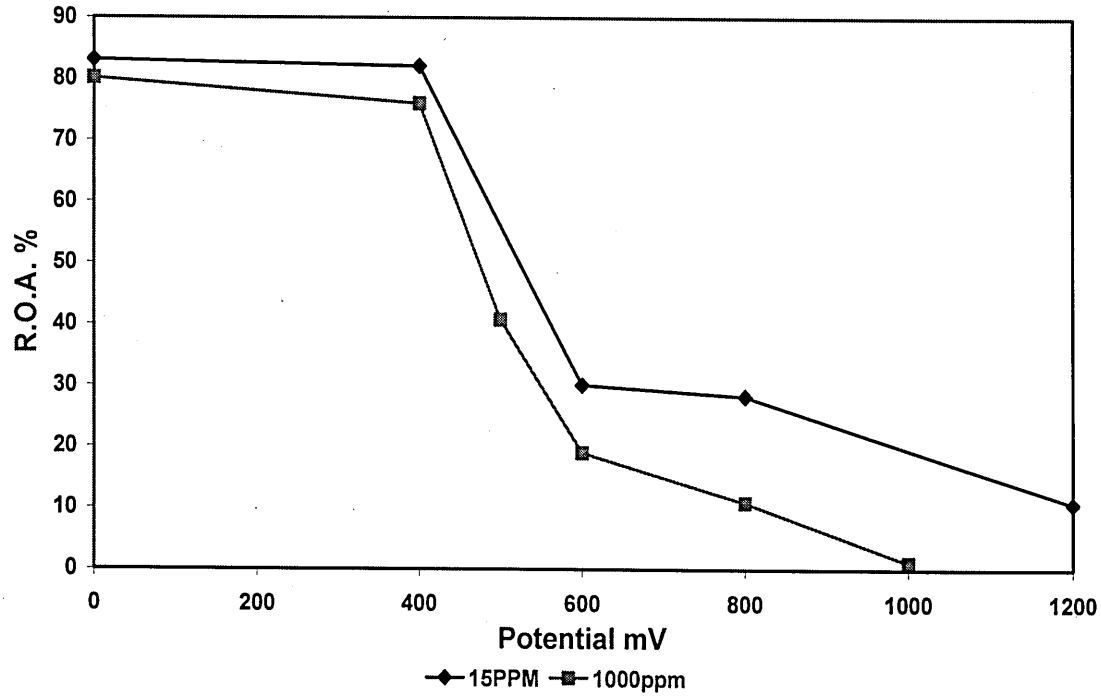

Figure: 4.19 Effect of applied potential on the ductility in two different chloride solutions conducted in 8ppm dissolved oxygen using SSRT technique

4.2.2) Effect of chloride on SCC of duplex stainless steel:

The effect of chloride concentration on SCC behaviour of Zeron100 is shown in Fig:4.20.

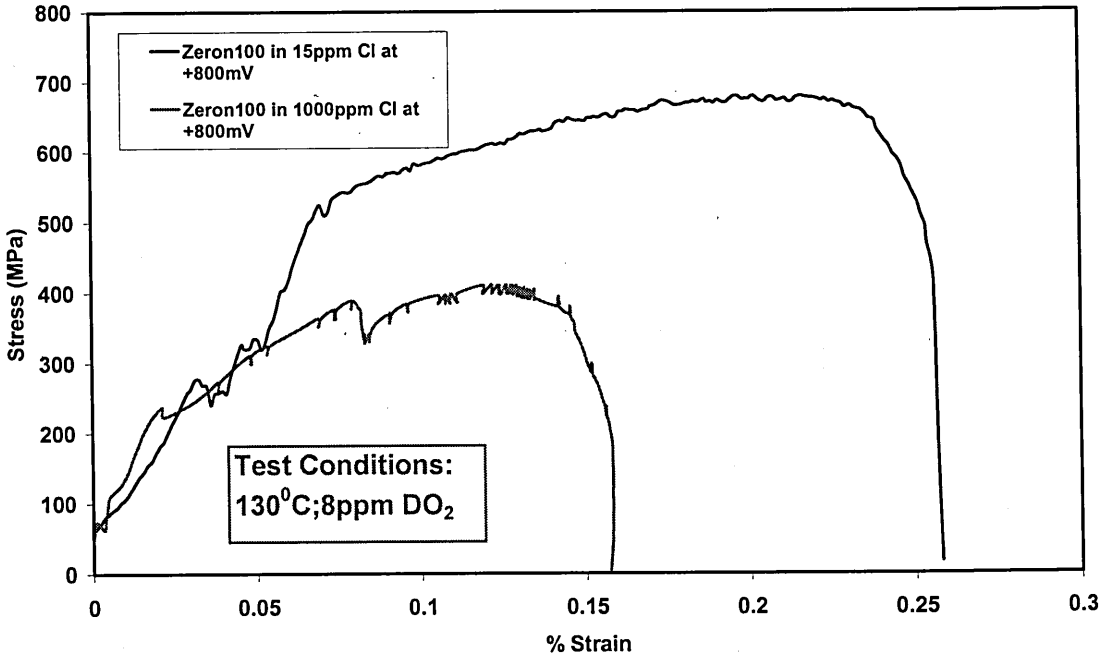

Figure: 4.20 SSRT tests results of Zeron100 in 15 and 1000ppm Chloride at +800mV, 130^{0}C; in 8ppm dissolved oxygen

These results are used to discuss the chloride effect on the mechanical paramters.The measurements made after the failure are shown in table 4.5 .

strain rate	Temp ^{0}C	[Cl] level in ppm	O_2 level in ppm	Applied Potential in mV
1 x10^{-6}	130	15	8.8	+800
1 x10^{-6}	130	100	7.6	+550
1 x10^{-6}	130	1000	7.9	+800

Table 4.5: Results of SSRT tests conducted in different chloride solutions

4.2.3) Effect of temperature on SCC behaviour

The role of temperature on the SCC of Zeron100 is evaluated using SSRT technique and one of the advantages of studies conducted in autoclave is to control the temperature of the solution in the autoclave therefore controlling test conditions. The role of temperature is discussed in the chapter 6 and its influence of the fracture behaviour. The results shown in table 4.6 are recorded from the experimental results.

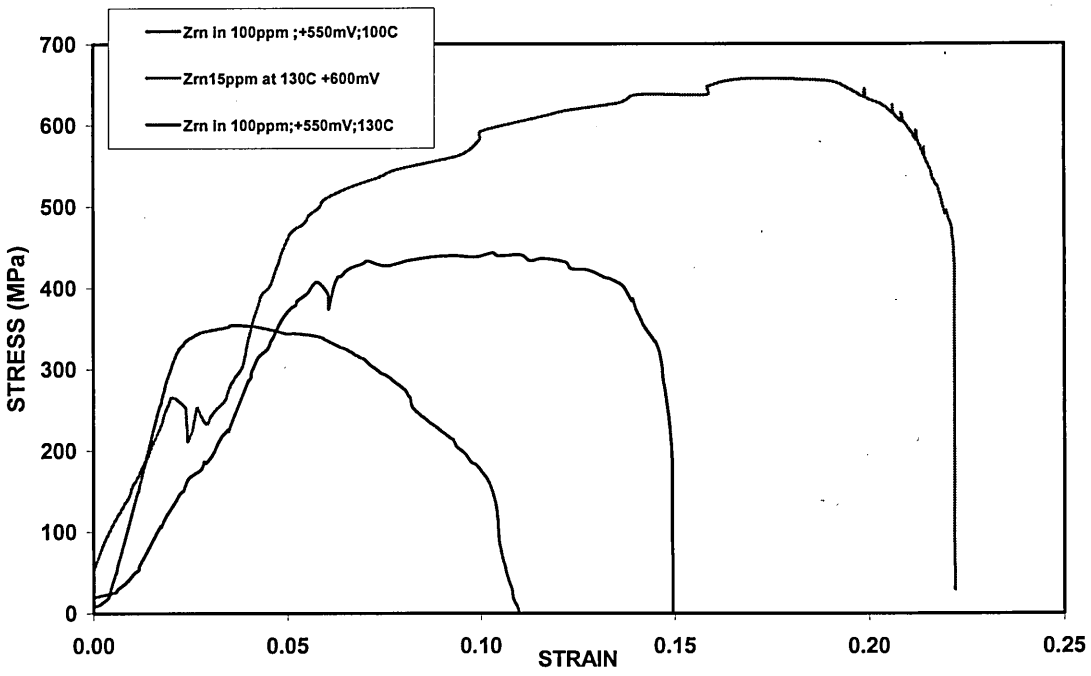

Figure: 4.21 Effect of temperature on SCC behaviour of Zeron100 in 15,100 chloride solutions at +600 and +550 mV in 8ppm dissolved oxygen

specimen ID	strain rate	Temp ^{0}C	[Cl] level in ppm	O_2 level in ppm	Applied Potential in mV
Z1	1 x10^{-6}	100	100	8.8	+550mV
Z2	1 x10^{-6}	130	100	8.3	+550mV

Table 4.6: Showing the test conditions of Zeron100 for the tests conducted at two different temperatures 100 and 130^{0}C in 100ppm chloride solution.

4.2.4) Effect of Dissolved Oxygen on SCC

Dissolved oxygen measured using obi sphere is used to control the appropriate oxygen levels and the SSRT tests are conducted on Zeron100 in order to find the mechanism of failure. The effect of dissolved oxygen is shown in Fig: 4.22 and the results are presented in table 4.7.

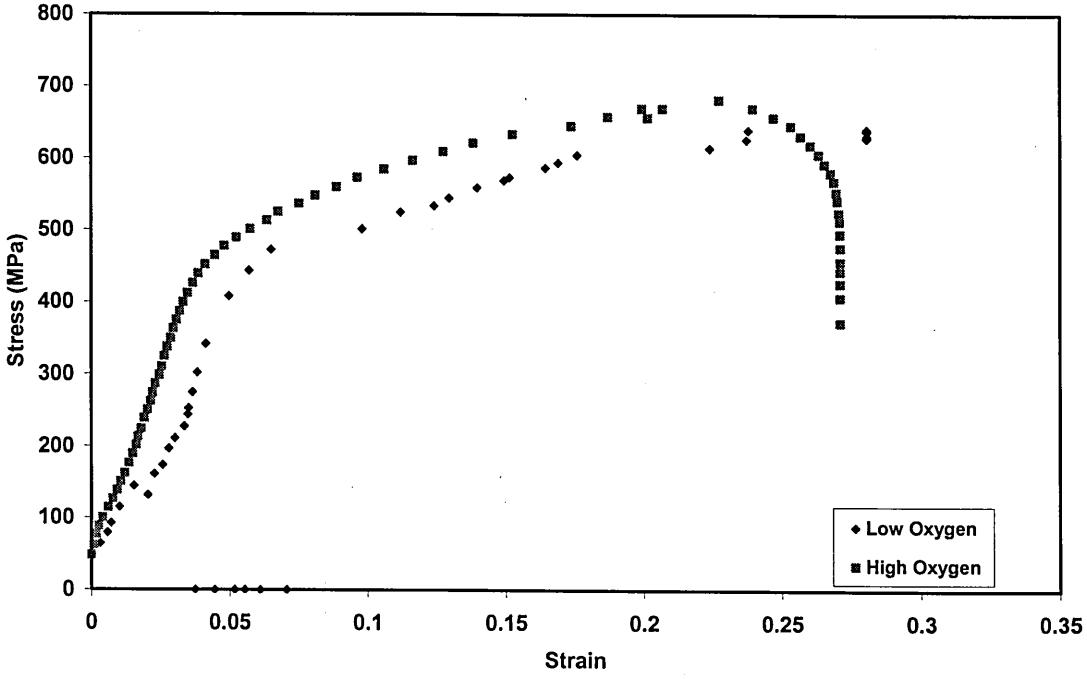

Figure: 4.22 The effect of dissolved oxygen on slow strain rate response of Zeron100 conducted in 8ppm and <20ppb oxygen.

specimen ID	strain rate	Temp ^{0}C	[Cl] level in ppm	O_2 level	Applied Potential in mV Ag/AgCl
Z16	1 x10^{-6}	130	1000	<20ppb	+600
Z17	1 x10^{-6}	130	1000	8.0ppm	+600

Table 4.7: Showing the test conditions of Zeron100 for the tests conducted at two different oxygen levels conducted at 130^{0}C in 1000 ppm chloride solution.

4.2.5) Comparison of performance of duplex steels:

The relative performance of different kind of duplex stainless steels is measured on their response to the slow strain rate response plotted on stress - strain graph. The results of the tests are presented in Fig 4.23 and Table 4.8.

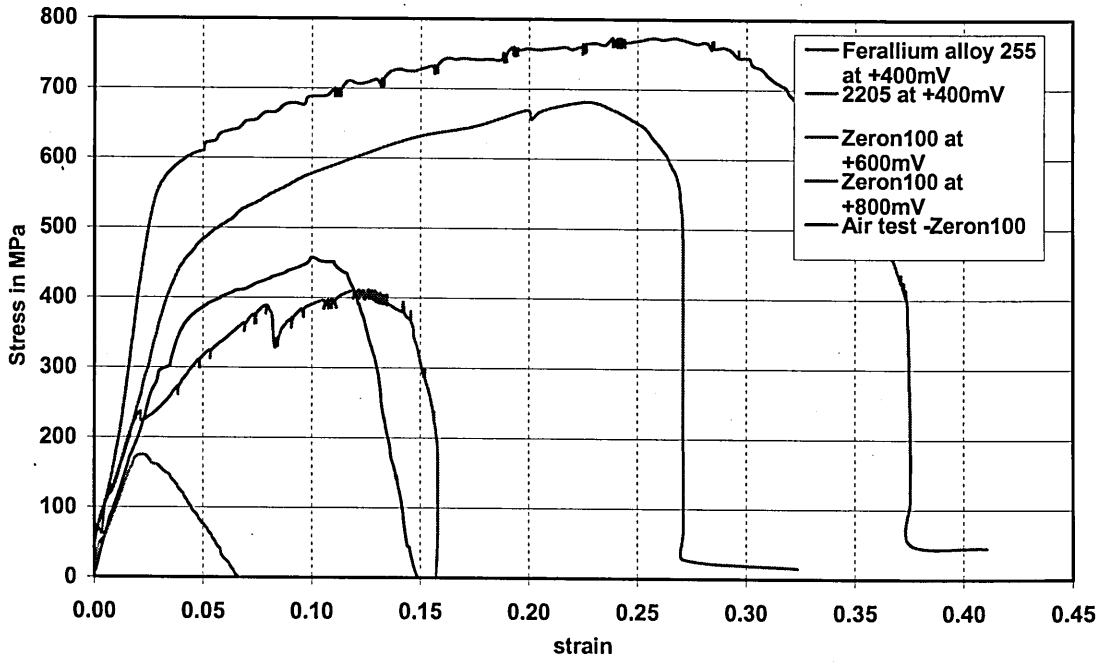

Figure: 4.23 Comparison of the Zeron100 SDSS with 2205 and Ferallium alloy 255 duplex stainless steels in 1000ppm chloride in 8ppm dissolved oxygen.

PREN type of Duplex steel	strain rate	Temp ^{0}C	[Cl] level in ppm	O_2 level in ppm	Applied Potential in mV
Zeron100	1 x10^{-6}	100	100	8.8	+550
2205	1 x10^{-6}	130	1000	7.6	+400
255	1 x10^{-6}	130	1000	7.9	+400

Table 4.7: Showing the test conditions of Zeron100, 255, and Ferallium alloy 255 for the tests conducted at conducted at 130^{0}C in 1000 ppm chloride solution.

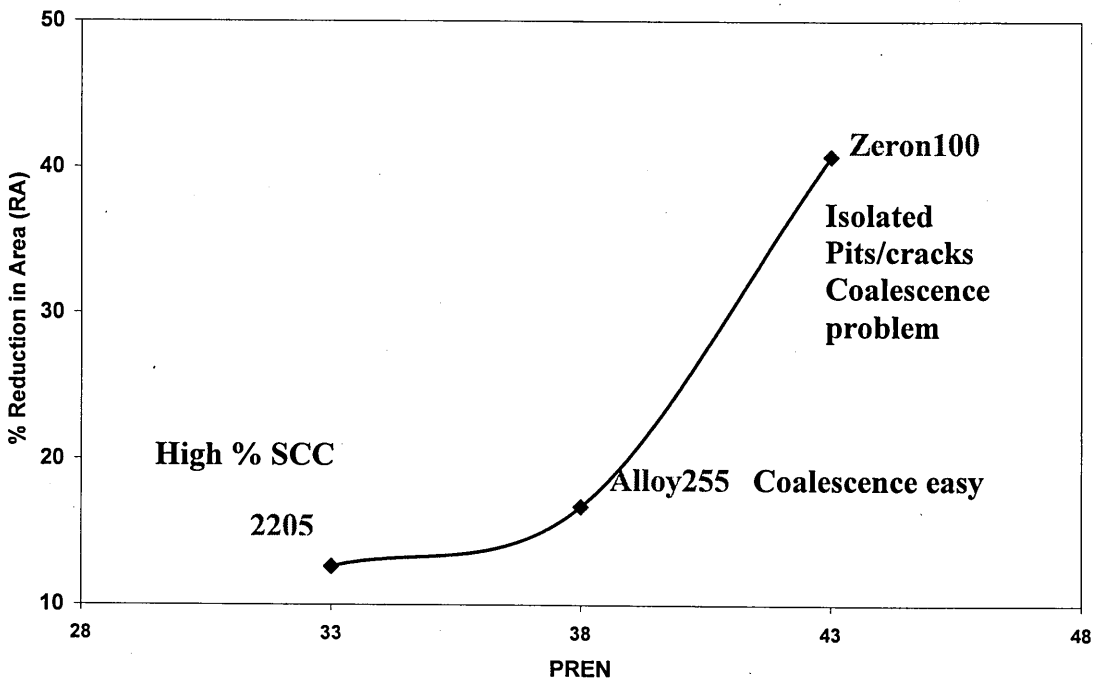

Figure: 4.24: Showing the variation of % ROA for different duplex stainless steels for the tests conducted in 1000ppm chloride solution in 8 ppm dissolved oxygen.

CHAPTER 5

Overview of environmental parameters effecting pitting potential

5.0 Introduction:

The aim of this chapter is to discuss the influence of chemical composition, temperature and chloride concentration on the pitting behaviour of stainless steels. The validity of PREN as a material selection criterion has been discussed based on the results obtained from this study. A universal pitting equation has been proposed to predict pitting by correlating PREN, temperature and chloride concentration with the data obtained from experimental potentiodynamic polarisation studies. Pit initiation and pit growth rate test results for Zeron100, Ferallium alloy255 and 2205 duplex steels are discussed. A three dimensional mathematical model was developed to predict pitting in engineering alloys. Applicability of this model has been verified with experimental results from the literature and this study.

5.1 Interpretation of Potentiodynamic polarisation data:

Potentiodynamic polarisation tests carried were conducted to measure pitting potential values. Pitting potentials increase with increase in chemical composition for wide range of materials at 25^0C in 3.5wt%NaCl as shown in Fig 4.1.Truman et al (1977) believed that the addition of nitrogen and molybdenum together improved the pitting corrosion resistance of stainless steels. It increased availability of nitrogen in the atomic form at the surface which favours the formation of nitride in the metal, and when dissolved could form nitrogen based ions in the electrolyte such as NH_4^+, NO_3^-, which could inhibit the pit growth. Nitrogen addition to the alloys without molybdenum didn't show resistance to pitting as shown in Fig 5.1, but with increase in addition of molybdenum a considerably greater influence on the pitting potential values is observed as shown in Fig 5.1. The current study also fits in with this trend as it has shown the improvement with increase in Mo & N when tested in 1000ppm chloride solution.

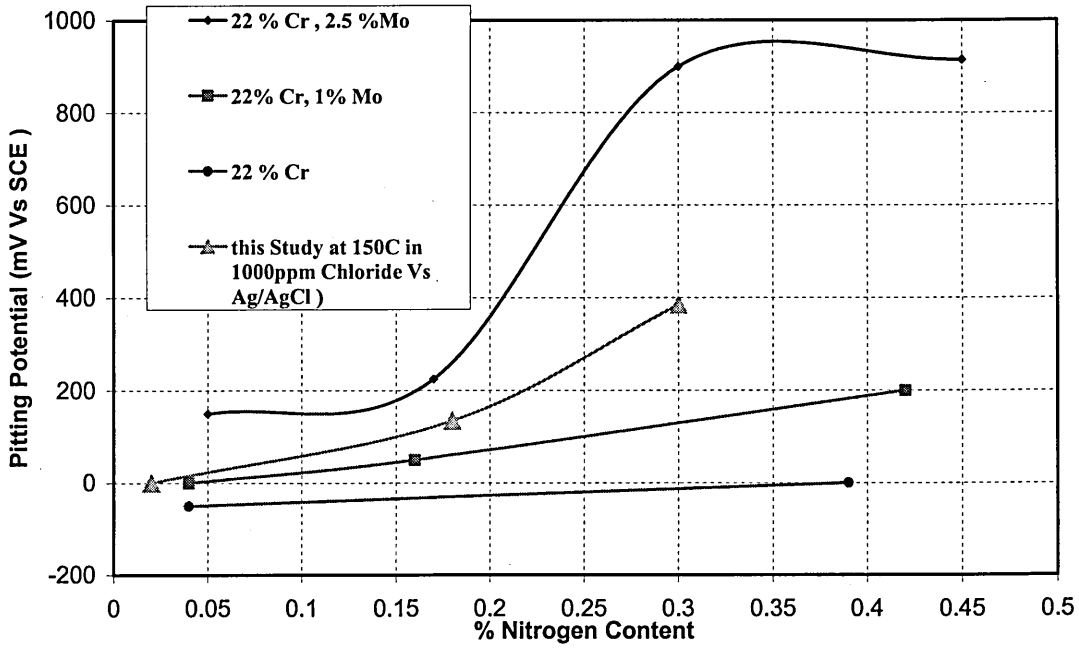

Figure 5.1: Influence of Nitrogen and Molybdenum on pitting potentials

A systematic and thorough investigation of Jargelius Peterson (1999) on the different nitrogen content austenitic stainless steels has proposed that the critical pitting temperature (CPT) increases with nitrogen additions, and the dominant effect of nitrogen is associated with repassivation. The same author is also in agreement with different possible mechanisms concluded by various authors (Truman et al, 1977; Osazawa et al, 1976; Bandy et al, 1983) that surface accumulation of nitrogen and pH buffering by NH_4^+ formation can explain the role of nitrogen in improving the corrosion resistance. Besides these mechanisms, various conclusions were drawn on the beneficial effect of nitrogen viz it decreases the passive current density (Bandy et al, 1986), modifies carbide phases (Janik-Czachor et al, 1975), causes incorporation of nitrogen beneath the film (Olefjord et al, 1985), improvement of the dissolution behaviour of Fe, Cr, or Mo (Clayton and martin, 1988). On the other hand, it was reported (Zagoriski and doraczynska, 1976) that nitrogen containing 17 Cr -13Ni-2.5Mo austenitic stainless steel has shown less corrosion resistance compared to the alloy without nitrogen. These proposed mechanisms refer mostly to a narrow temperature range of 25 - 65^0C in seawater environment.

In order to check some of this phenomena, this study started with an investigation of a few engineering alloys that covered a wide PREN range and produced the data at room temperature in different chloride levels to compare with the original Truman data. This was presented in table 4.1. The results obtained in this study were consistent with the observations of Truman and introduction of PREN with his study was a landmark which will certainly help the stainless steels users, for materials selection at room temperature. However when the current study extended the investigations above room temperature, it was noticed that some of the benefits of nitrogen and molybdenum interactions which are discussed in chapter 2 seems to

be less evident. As it was noted in the potentiodynamic polarisation results shown in Fig 4.4 an increase in temperature was found to decrease the observed pitting potential values. This trend was observed for all materials and a range of testing was conducted to produce the results for different PREN and some of the key results were plotted in Fig 5.2.

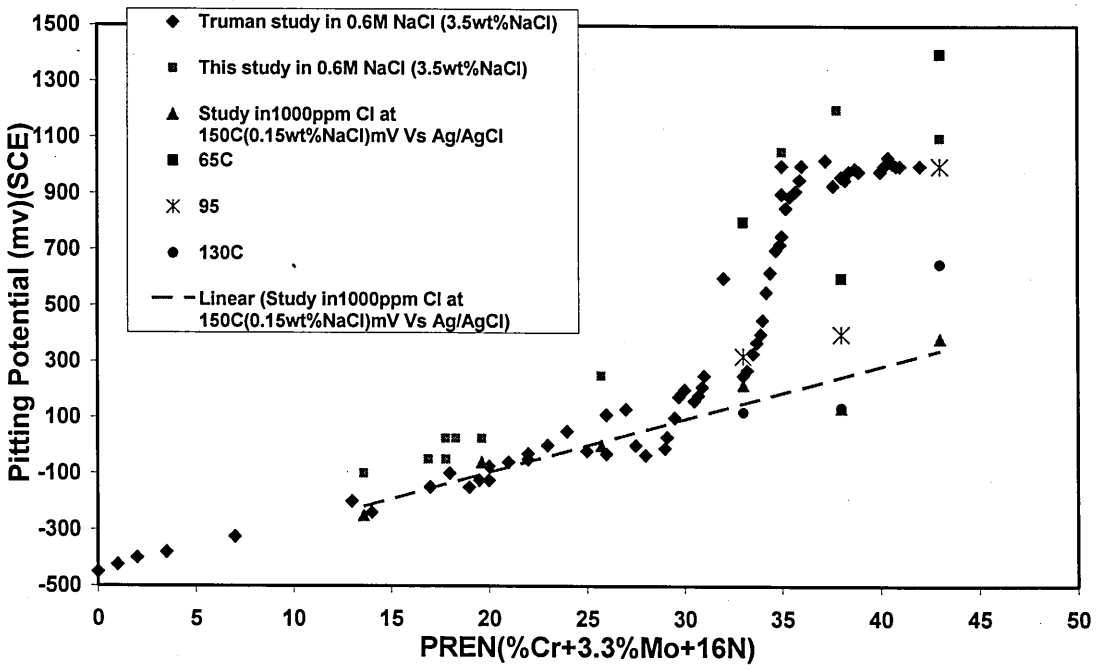

Figure: 5.2 Comparison of original Truman study with the present study.

The results show that with increase in temperature, there are two extremes of behaviour. The upper bound is the band of SDSS very resistant to pitting at 25^0C in sea water. The composition elements N, Mo, Cu, W, are all influential in these materials. Lower bound behaviour is seen in non DSS and on extrapolation to PREN >33 give a reasonable fit to the 150^0C, 1000ppm Cl^- SDSS data. This lower bound is clearly strongly influenced by the chromium level and possibly reflects the amount of Cr_2O_3 and protectiveness of the oxide film. It was noticed that with increase in temperature even in very dilute chloride solutions there was a massive potential change (pitting potential decreases with increasing temperature) and a condition was reached where the SDSS upper shelf disappeared. The Mo-N beneficial effect is

clearly progressively more unstable above 150^{0}C. These expensive materials mainly depend on these elements, but unfortunately they cannot contribute much to the pitting potentials for wide range of temperatures. It clearly shows the superiority of a chromium oxide film formed on the stainless steel surfaces, it exists in low grade steels and is not very temperature dependent compared to DSS and SDSS. The diffusion of nitrogen from metal to the solution could not have happened as it acts as an inhibitor and prevents from pitting (Truman et al, 1977). Clearly that is not the case with these SDSS, the current study do not agree with it, one could argue only with the measured properties of the film formed in these SDSS at 150^{0}C. However performing oxide film measurements is beyond the scope of this study. However a detailed study was performed for different chromium steels and the temperature dependence is discussed in the following sections which might help to interpret the rate controlling processes and might help for material selection.

5.2 Temperature effects on pitting potentials:

Single cycle polarisation curves in 1000ppm chloride solution (0.006M NaCl) at 150^{0}C for Zeron100, Ferallium alloy 255, 2205, Uranus 65, 304L, Fv566 and 12%Cr in that order were shown in Fig 4.12. All the materials have free corrosion potentials varying between -250 to - 450mV Vs Ag/AgCl and pitting resistance decreased in that order mentioned. The results were produced at 65^0, 95^0, 130^0, 150^0, & 170^{0}C using similar technique and were presented in table 4.2 for convenience. The potential at which pits initiate (E_p) was determined by the rapid increase in the current density in the forward scan. Zeron100 showed the longest passive region indicating that pitting of this particular material is not very easy to initiate. On the other hand, Ferallium alloy 255, which has shown highest pitting potential at room temperature has recorded lower potential values, once the temperature is increased.

The pitting potentials, measured from polarisation curves in 1000 ppm chloride is given in Fig 5.3 plotted as a function of temperature for the steels tested to show the profound effect of temperature on pitting. Malik et al (1995) has done a systematic study on different combinations of temperature and chloride concentrations. The data collected from that study was plotted in the same Fig and found that the values recorded through this study were consistent with the published work as shown in Fig 5.3.

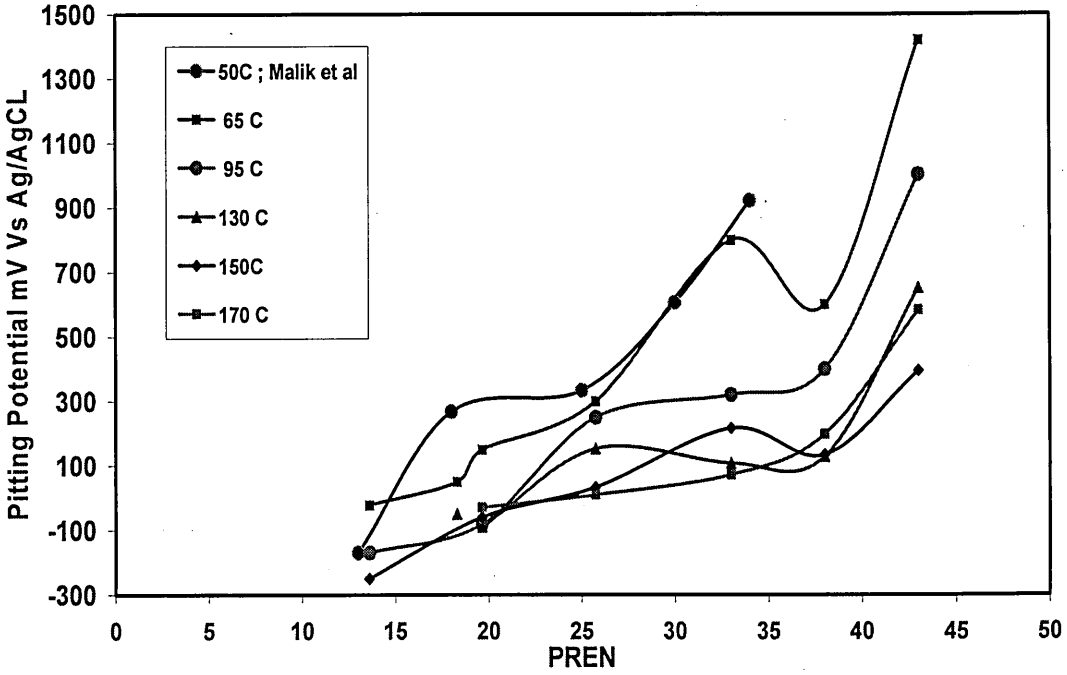

Figure 5.3: Variation of pitting potentials with temperature in 1000ppm Cl^-

As it is evident from Fig 5.3 that as the temperature is increased the duplex stainless steels (DSS) and super duplex stainless steels (SDSS) PREN >33 are losing their potency gradually when compared with conventional low chromium steels. The difference in magnitude of change in their pitting susceptibility remain less in low alloyed steels, but where as in the expensive materials DSS & SDSS the enhanced benefit remains unstable for wide range of temperatures. From the results in this dilute chloride solution, it is important to note that DSS and SDSS grades were found susceptible to pitting.

Clearly the dependence of the pitting susceptibility in these materials does exhibit the temperature induced change of protective passive film properties for the conditions tested. Temperature influence on these films has been discussed in few studies, according to (Manning et al, 1980) film porosity has been observed to increase with increase in temperature or the passive film itself might undergo change in the composition or physical structure resulting in the variation of density of voids or vacancies in the film (Wang et al, 1988). These are supported by the observations of incorporation of chloride ions in the film (Manning et al, 1980) and change of passive film from p-type at room temperature and n-type at high temperature (Wang et al, 1988). The kinetics of pit generation on stainless remains complicated at high temperatures, it involves two process a) pit initiation and b) pit propagation. The absorption and segregation of Cl^- ions on the weak spots of the passive film, causing the passive film to be locally destroyed and the second process is that the pits develop and propagate because of anodic dissolution (Smialowska and Murkowski, 1972). According to the results shown in Fig 5.3 two mechanisms might contribute differently across the PREN range. For PREN above 33 where the duplex steels achieves higher potentials at all temperatures, it is likely that there might be a delay in the initiation of pits, due to the formation of metastable pits characteristic to these steels. On the other hand inclusions play an important role in determining the pitting susceptibility of stainless steels (Sedricks, 1987). The steels below PREN 33 could have more inclusion as the sulphur and manganese content of these materials remains high and has more temperature effect. Hence they have a greater influence on the pitting potential values for the materials PREN below 33. With increase in temperature or chloride concentration the metal dissolution occurs at MnS inclusion sites and these lower alloyed stainless steels tend to pit more easily compared to the

high chromium steels. Detailed large scale and microelectrochemical investigations showed that strong effect of temperature on the anodic metal dissolution during metastable pitting leads to higher current transients and also facilitates transition from metastable to stable pitting which is the reason for the decreasing pitting potential values with increasing temperature (Matsch and Bohni, 2000).

The experimental results shown in Fig 5.4 indicate that critical current density required to cause pitting increase with increase in chemical composition at a constant temperature in chloride solutions. This indicates the resistance of the passive film which require high potential thus high current values to cause pitting.

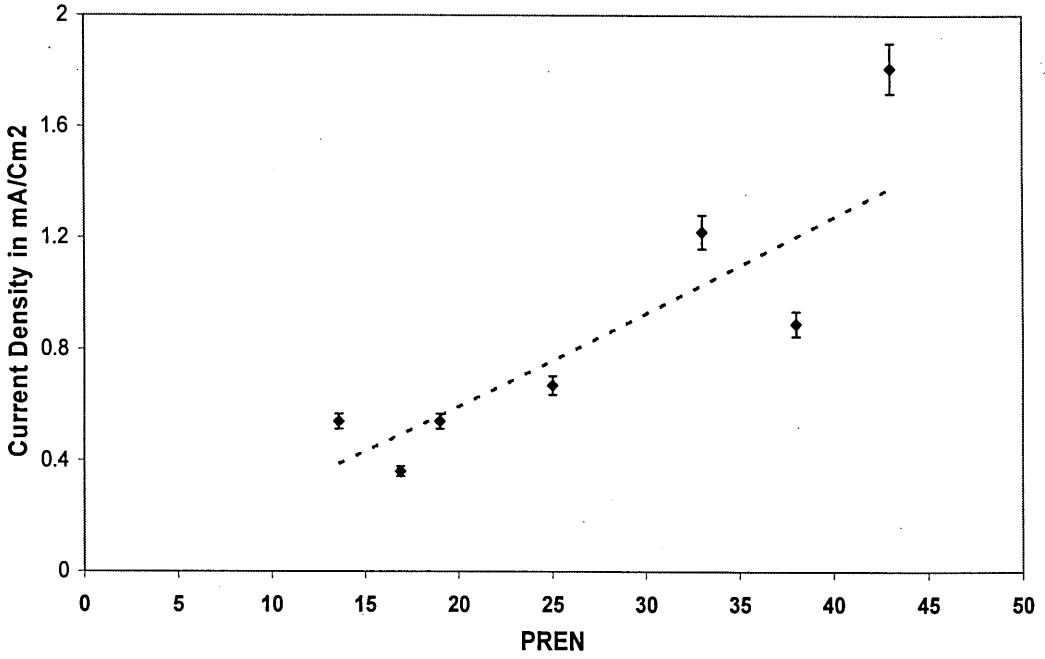

Figure: 5.4 Variation in Critical current density (E_{CRIT}) on PREN at 130^0C

5.3 Chloride concentration effect on pitting potentials:

It has been confirmed through various studies that the initiation of pitting is due to the result of the breakdown of a passive film caused by aggressive chloride ions. The critical chloride concentration at which chloride induced pitting becomes evident and rises with temperature. The influence of combination of temperature and chloride on

2205 duplex steel is shown in Fig 5.5. It shows the interaction of these two parameters exist in similar manner such that both can influence individually and together on the pitting susceptibility. For many metal and alloys pitting potentials a logarithmic function of Cl^- concentration is observed at room temperature (Smialowska, 1987) as

$$E_P = A - B \log [Cl^-] \quad (5.1)$$

The precise relationships for all materials tested in this study will be discussed later in this chapter.

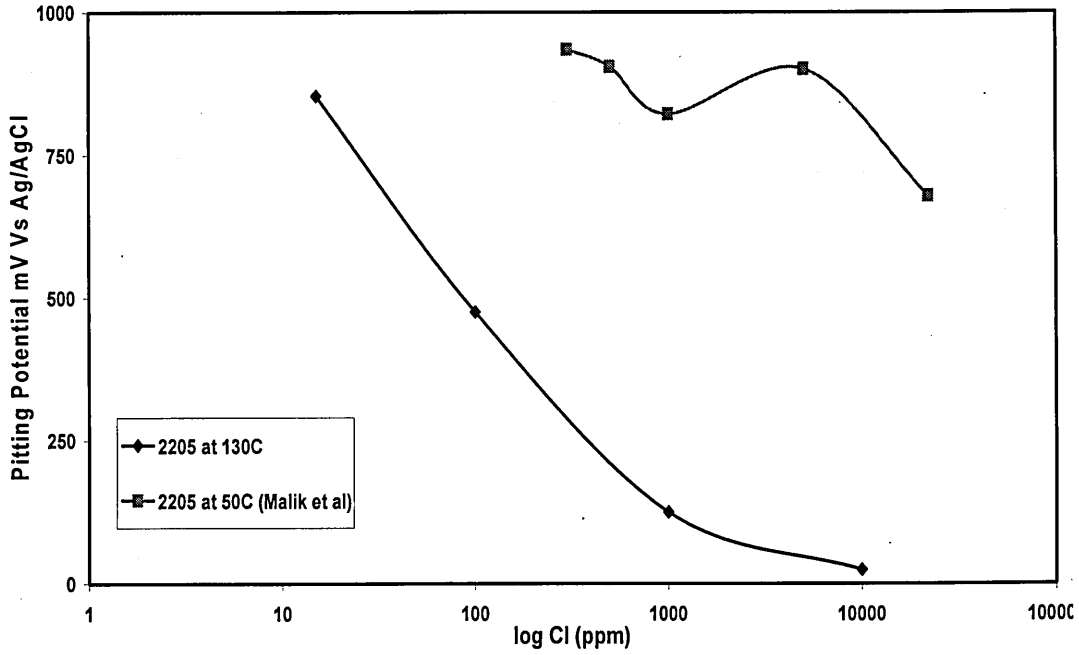

Figure: 5.5 Effect of temperature and $[Cl^-]$ on pitting potentials for 2205 duplex

The effect of chloride concentration on the polarisation curves conducted at 130^0C for Zeron100 is shown in Fig 4.6. Starting from the free corrosion potential, a passive region is associated in all the three chloride concentrated solutions 15, 100 and 1000 ppm. A pronounced increase in the current density values was observed at a critical potential values for 100 and 1000ppm, but it was not observed in case of 15ppm chloride. The density of pits increased with increase in chloride concentration. Pits formed in 1000ppm chloride have visible deposit on the pit surface as shown in SEM

images in Fig 5.8, where as pits formed in 100 ppm chloride were typically with sharp edges and free of any visible deposit. With increase in chloride concentration to 10000ppm the pits formed on Zeron100 were more polished and depth of pits was found to be decreased as shown in Fig 5.7.

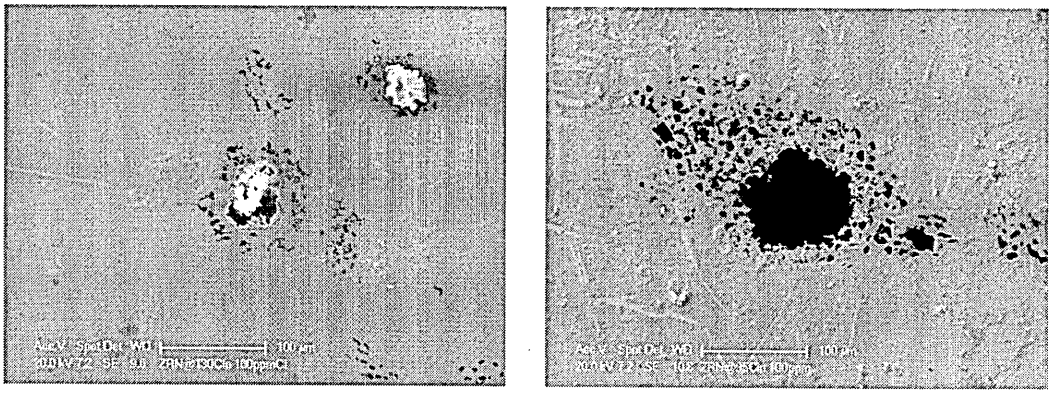

Figure: 5.6 Pit shapes formed in a) 1000ppm and b) 100ppm chloride solution.

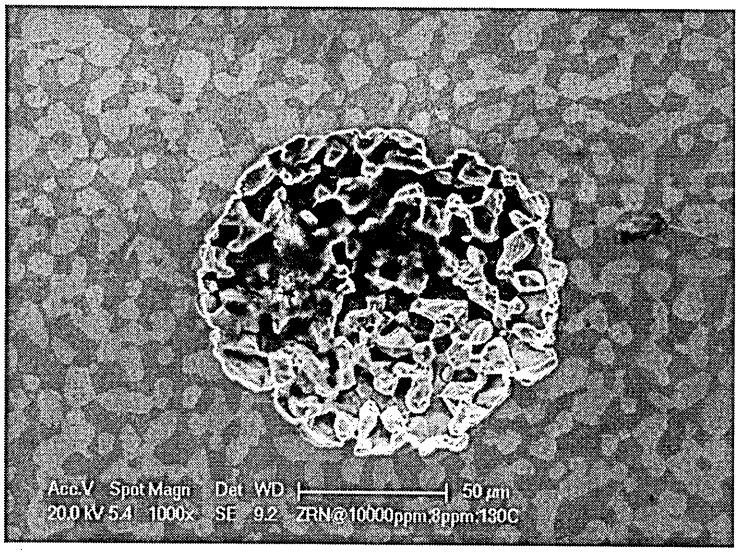

Figure: 5.7 Pitting at high chloride concentration at 130^0C in 8ppm dissolved oxygen.

One of the earlier studies in 0.5N NaCl + 0.1N H_2SO_4 solution reported (Sriram and Tromans) that the chemisorption rate of chloride ions increases with increase in temperature, and due to this at higher temperatures breakdown of the passive layer occurs sooner at lower potentials. According to this author (Sriram and Tromans, 1989) at constant potential the value of density of pits formed increase with increase

in temperature, this was because as at higher temperatures more sites are available for pit nucleation which is consistent with the present study. Detailed study on the effect of chloride on pitting potentials has been performed in this study has shown that the least potential value that can be achieved for the Ferallium alloy 255 was -275mV shown in Fig 5.8. It is understood from this study that increase in chloride from 15 to 1000ppm has caused significant damage and increase from 1000 - 10000 ppm chloride concentration didn't show any drastic change in the pitting potential values indicating that a critical chloride concentration of 1000ppm is enough to cause significant damage at realistic potentials.

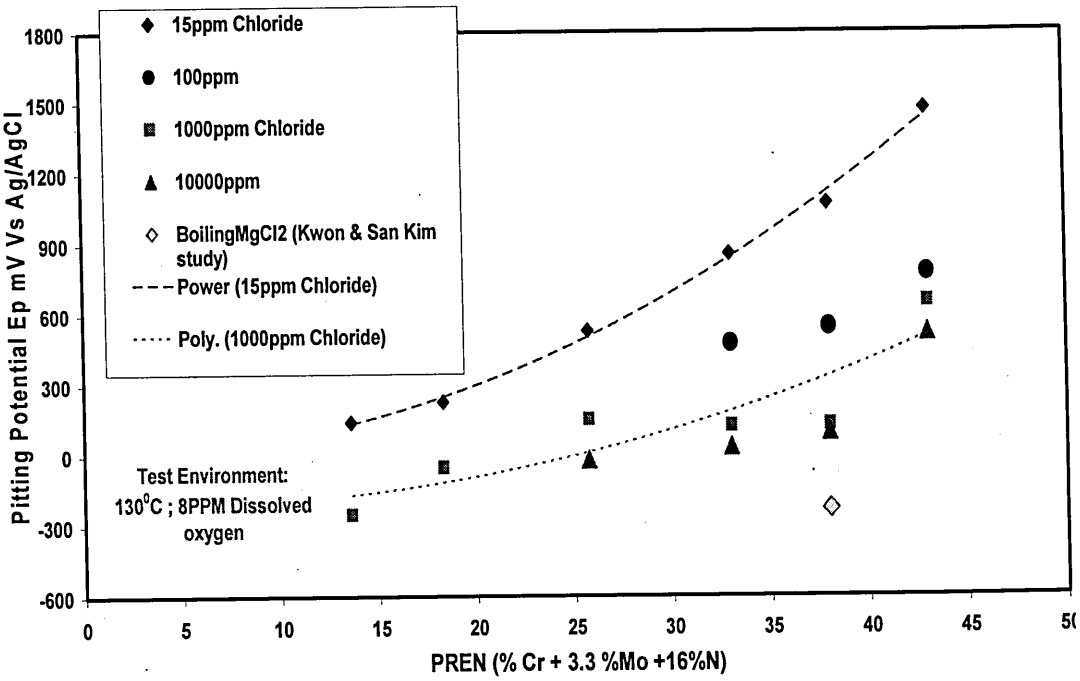

Figure 5.8 Chloride effect on pitting at 130^{0}C in 7- 8 ppm dissolved oxygen

5.4 Repassivation Potentials:

An important parameter after pitting is initiated is the repassivation potential .It is defined as the potential at which pits repassivate is termed as repassivation potential (E_{rp}) or Protection potential and was determined from the potential at which the crossover of the reverse scan to the forward scan occurs. Thus based on Fig: 4.13 at 150^0C E_{rp} of Zeron100 was near -100m$V_{Ag/AgCl}$ and –175m$V_{Ag/AgCl}$ for Ferallium alloy 255 followed by 2205 at -225 m$V_{Ag/AgCl}$. The results indicate that above 90^0C the strong decrease in repassivation potential towards negative direction, indicating that the corrosion rate will be higher above 90^0C. Above 150^0C all the three steels tend to have more positive repassivation potentials. On the other hand the temperature studies on alloy 825 (Cragnolino and Sridhar) produced an increase in the repassivation potential above 90^0C, in contrast to these duplex steels conducted in 1000ppm chloride solution. These authors also highlighted that repassivation potential depends on the maximum current density attained through the forward scan. The difference between Ep and E_{rp} values (E_p - Erp) certainly is large for the duplex stainless steel compared to the austenitic steels. A large difference exists even below 100^0C, which indicates that at ambient temperature pitting conditions are established because it is difficult for the active pits to repassivate. The polarization curves enabled record all the repassivation potentials in this study as shown in Fig 4.12 by the reverse scan, unlike in some studies where it is not well defined due to the pit number, size and degree of occlusion of already grown pits (Cragnolino, 1987). The difference between pitting and repassivation potentials at 150^0C in 1000 ppm Cl^- solution is shown in Fig 5.9 and the relationship between E_p, PREN and E_{rp} is

$$\mathbf{E_{rp} = 12\ [PREN] - 570,} \qquad \mathbf{(5.2)}$$

$$\mathbf{E_P = 18\ [PREN] - 460} \qquad \mathbf{(5.3)}$$

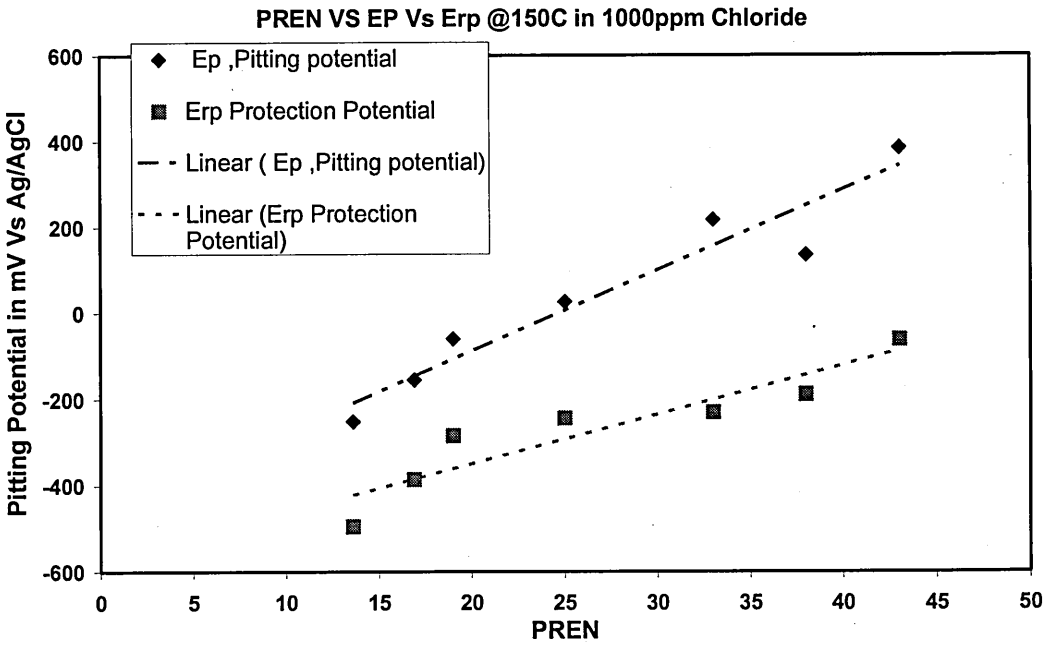

Figure: 5.9 Pitting and repassivation plotted for various steels for tests conducted in 1000ppm Cl^- at 150^0C in 8 ppm dissolved oxygen.

The difference between pitting and repassivation potentials has increased with increase in PREN indicating that repassivation of passive film has a critical potential value, Increasing in composition will not change the repassivation by significant amount. The established relation ships in this study will allow to estimate the safe operation potentials for wide range of materials operating at 150^0C.

5.5 Pitting morphology:

From the observations that pitting potentials tend to decrease with increase in temperature the contribution of the pitting morphology to this observed phenomenon might draw useful information. Pit shapes in 2205 are found to be similar, but above 150^{0}C it was noticed that pits have polished edges compared to sharp edges at lower temperatures.

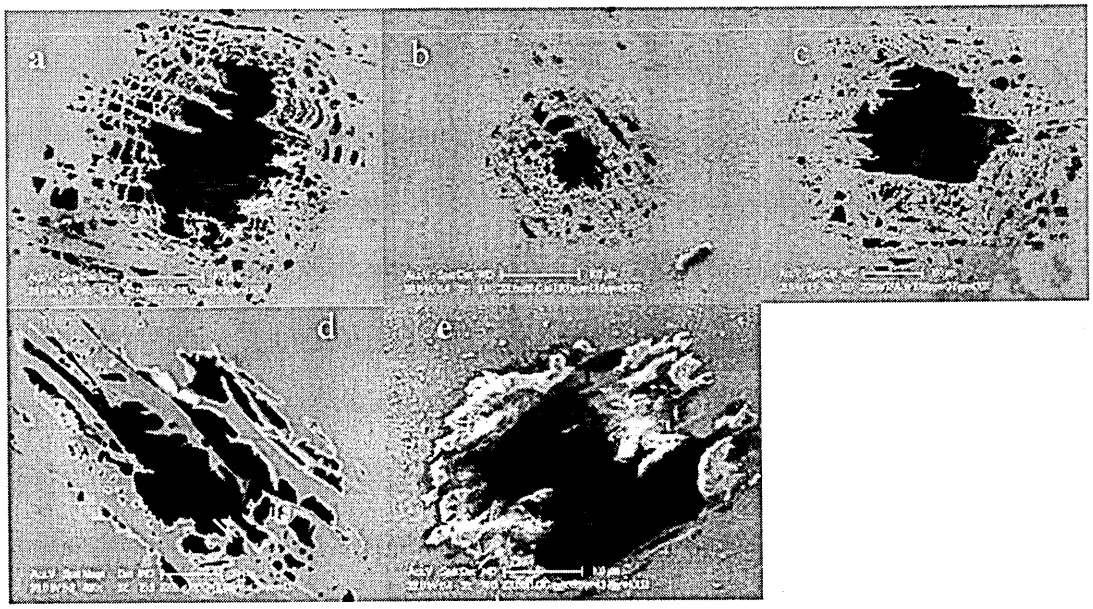

Figure 5.10: Pit shapes formed at different temperatures in 2205 duplex stainless steel a) 65^{0}C b) 95^{0}C c) 130^{0}C d) 150^{0}C e) 170^{0}C after cyclic polarisation test in 1000ppm Cl and 8ppm dissolved oxygen.

It was noticed in several studies that above critical temperatures some alloys exhibit increased resistance to pitting over a certain range of temperatures. One of the investigations on Nickel in 0.1N NaOH + 0.1M NaCl has shown an increase the resistance to film breakdown above 125^{0}C i.e. pitting potentials increase with increase in temperature (Postlethwaite et al, 1974).The increase in temperature does alter the type of pitting attack and these kinds of observation can be linked to the form of attack that takes places and the pitting morphology. Likewise it was observed (Postlethwaite et al, 1974) that a change in temperature altered the pit

morphology from deep pitting attack to a process where general corrosion occurred and a thick layer was removed from the surface. It was observed in the present study on all stainless steels that a hard dark brown type corrosion deposit was formed on the surface of the metal at higher temperatures. When the specimen was removed from autoclave at ambient a very thick oxide layer was present. This might influence the pit density where only few large deep pits were present at low temperatures and a greater number of pits, less deep, and smaller in size are formed at higher temperatures. Undoubtedly thicker films were observed at higher temperature and these might contribute to the pitting resistance above a certain temperature.

Pit Initiation in Duplex stainless steels:

Pits were always observed to be randomly distributed along the metal surfaces, however for duplex stainless steels consists of two phases there are conflicting observations on the relative pitting susceptibility of each phase. Preferential pitting of either one of these phases or their interfaces may occur in these materials due to the difference in the partitioning of alloying elements between them. Cr and Mo enriched in ferrite phase and the nitrogen enhanced with austenite phase and this caused the ferrite phase to preferentially dissolve was noticed in the studies of (Sriram and tromans, 1989). Symniotis (1995) argued that preferential dissolution depends on electrochemical potential; austenite was dissolved if the applied electrochemical potential is more than passivation potentials and ferrite was dissolved if applied potential is less than passivation potential. In the present study on Zeron100 SDSS, shown in Fig 5.10, reveals that austenite - ferrite interface is more susceptible to pit initiation, and further growth was noticed in austenite. Very few significant complete pits were formed in ferrite regions. This study was consistent with the observations of Siow et al (2001) on 2507 and 2205 steels.

Although their studies were at room temperature it might be possible to link to the current study.

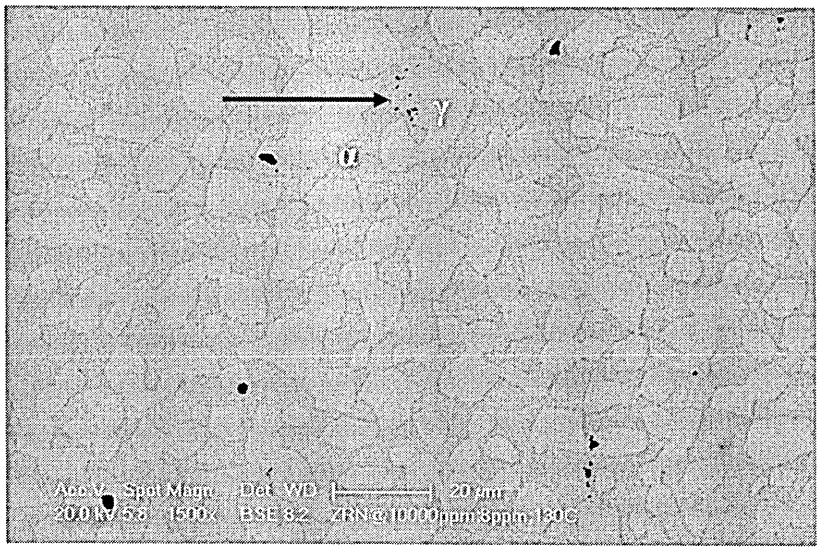

Figure: 5.11 Early stages of pit initiation in Zeron100, test conducted in 10000ppm chloride solution, and 8ppm dissolved oxygen at 130^0C.

Similar mechanism might exist both at room temperature and even at 130^0C in chloride solutions. It is widely accepted that phase boundaries are more susceptible to corrosion, compared to the individual grains, as the phase boundaries might be chromium depleted and thermodynamically more active due to carbide formation.

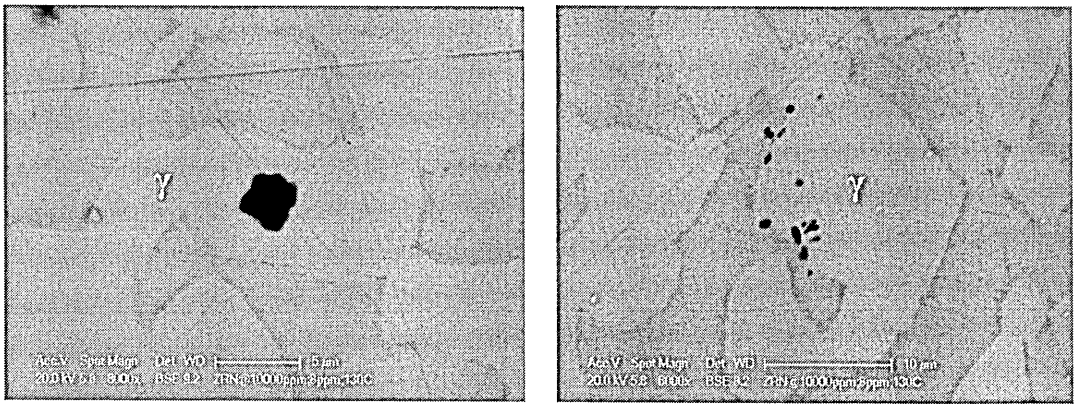

Figure: 5.12 Pit initiations in Zeron100 in chloride solution found to occur predominantly in austenite and austenite/ferrite interface.

The role of inclusion in this kind of pit initiation observation can be completely eliminated as these steels are very clean and contain less sulphur, most probably intermetallic phases might play a role but 10%KOH cannot distinguish these phases

from austenite and ferrite. Fig 5.11 shows that the composition of these austenite grains in Zeron100 was not resistant to pitting corrosion or due to the diffusion of nitrogen that is already settled in this phase may not exist under those test conditions. As nitrogen is an austenite stabilizer and can dissolve as a solid solution element in austenite more than in ferrite (Lacombe, 1993). Nitrogen increases corrosion resistance more than chromium does in austenitic steels (Charles, 1991) and the local PREN will definitely be higher for austenite grains than ferrite grains in nitrogen alloyed duplex steels. So the duplex stainless steels without nitrogen will pit in the austenite phase and in those with nitrogen should pit in ferrite phase, which makes it clear that in hot solutions the nitrogen may not be stable in austenite phase and is involved in pitting as shown in Fig 5.11. Micro electrochemical measurements, (Perren et al 2001) have shown that PREN is a reliable method to assess the corrosion resistance of the individual phases of a SDSS and notice that in strong acidic environments the austenite phase has been susceptible to pitting.

Further evidence to support this conclusion that pitting depends on the individual phase composition in duplex materials is that, Ferallium alloy 255 has shown equal susceptibility in both the phases as shown in Fig 5.12. Pitting was observed more in the individual grains rather in the α / γ interface. This shows that the composition of the local phases might be similar and this particular steel has got more copper and which might segregate differently into the individual phases in this steel.

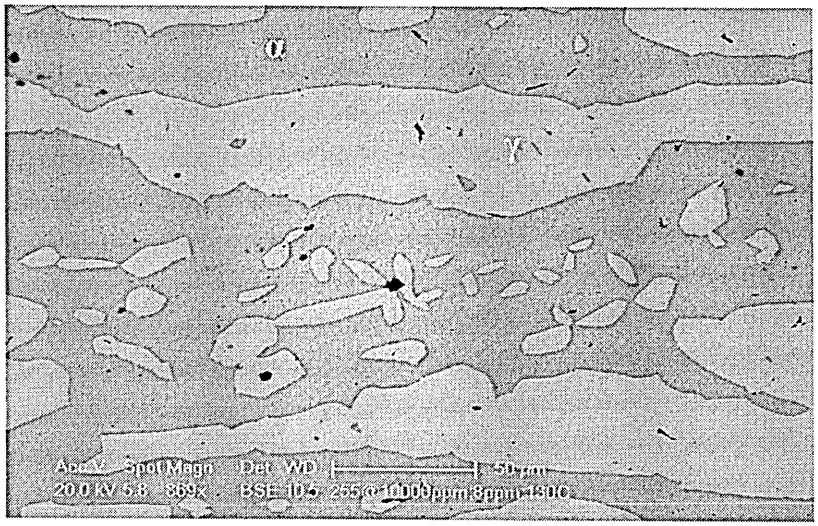

Figure: 5.13 Pit initiation in Ferallium Alloy 255, showing the equal distribution of pits in both Austenite and ferrite phases.

However the effect of phase composition on the pitting was studied by Garfias - Mesias et al, (1996) on annealed duplex steel and found that ferrite phase was preferential to pitting and further promoted the idea that bulk PREN is not recommended and local PREN of individual grains is more acceptable to assess the pitting resistance.

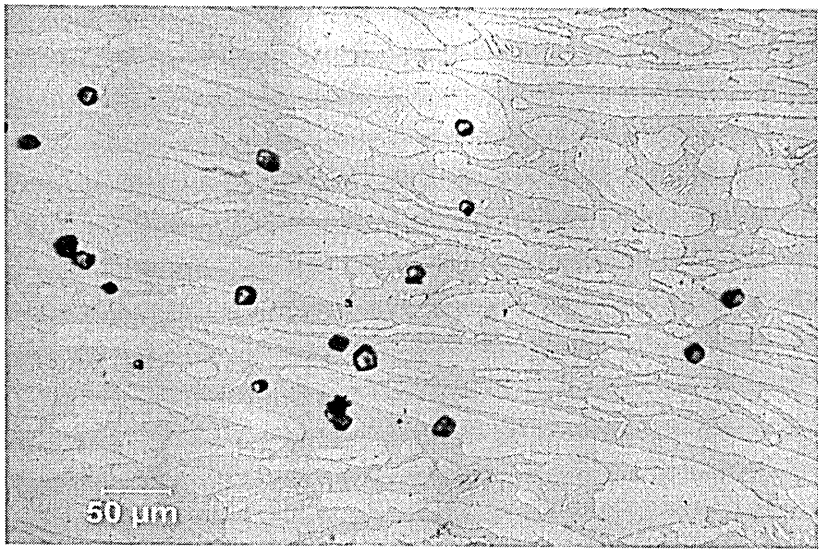

Figure: 5.14 Pit initiation in 2205 duplex steel showing α / γ interface is susceptible to pitting at 130^0C in 10000ppm chloride solution and 8ppm dissolved oxygen

Unlike Ferallium alloy 255, 2205 duplex steel is susceptible to pitting at α / γ interface similar to Zeron100 SDSS. Previous studies (Siow et al, 2001) also have observed similar behaviour in 2205 duplex steel.

From these observations it shows that percentage of ferrite and austenite along with local compositional alloying elements play an important role in the assessment of the pitting initiation in these materials. Most recent study has concluded that nitrogen increase the corrosion resistance of austenite (Lothongkum et al, 2006). However this study has shown that pitting initiation in these duplex steels is not temperature dependent as long it is chloride environment it shows pitting at α / γ interface and further into austenite grains for newly developed Zeron100.

Pit growth rate:

It was pointed out earlier in the literature review, the pit growth rate depends on the materials and follows an expression of the form

$$d = at^n \qquad (5.4)$$

Where d is depth of a pit, a & n are constant, and t is the time.

Changes in pit depth were plotted in Fig 4.17 shows that pit growth at 130^0C in 1000ppm chloride solution follows power law as in Eq (5.4) form even for super duplex stainless steels (Zeron100). It was found that the value of n = 0.8, and value of a = 0.58. The n value will depend on the temperature and the chloride concentration; however a detailed study (Smialowska et al, 1987) at three temperatures on alloy 600 revealed an absence of temperature dependence. It still remains unclear, how the pitting process varies with temperature, but one could predict the n value by linking it to pit morphology as it varies with increase in temperature. A detailed study on the passive film properties would be useful to interpret the dependence of n value on temperature. It was found for Zeron100 that

the pit density tended to decrease with increase in temperature and the shape of the pits was more polished compared to sharp and crystallographic edges at low temperatures. The pit growth kinetics depends on temperature and local pH inside the pit bottom in this newly developed alloy. It is known that a growing pit itself acts as local electrochemical cell, by transforming the bottom of the pit as anode and the surrounding walls of the pit and surface of the metal as the cathode (Payer and Staehle, 1972). The large cathode areas with small anode areas will contribute to the high rates of pit growth. This pit growth depends on the metal and environments. A high chloride concentration produces high pit growth rates. But it is not always necessarily high chloride environments prevail in certain applications. Even high temperatures don't necessarily produce higher pit depths as it was proved in the studies on Alloy 600 (Smialowska et al, 1987) where pit depth decreases with increase in temperature. The determination of the dependence of pit growth on time in dilute chloride solution for Zeron SDSS is vital information, when one considers that pits play an important part in environmental assisted crack growth process of SDSS. This kind of quantitative information is important to evaluate the performance of this steel, which will substitute conventional steels in the new generation plants where more aggressive environments exist. The influence of pits on the SCC process will be discussed in the chapter 6.

The role of corrosion potential gradients to concentrate cations in a crack or crevice is well established and through hydrolysis process reduces pH inside the pit. The present study in dilute environments (15ppm Cl^-), show effect how the ion drift process operates, probably to form concentrated salt films before the pit initiation stage. The continuous effect from 15- 20000 ppm Cl^- indicates that it is a single

process over the whole concentration stage. Tests in boiling $MgCl_2$ are unnecessarily aggressive for some service applications.

5.6 Mathematical models for prediction of pitting potential

Introduction:

Although extensive work has been devoted to understand the phenomenon of localised corrosion, in chloride solutions there is still an uncertainty for engineers to predict the occurrence localised corrosion and prevent failures in industrial plants. The use of pitting resistance equivalent number gives a rough estimate for predicting the susceptibility for various steel compositions at room temperature. However, there is a considerable amount of uncertainty regarding the usage of this factor as a criterion in the selection of materials for wide range of temperatures. It is of paramount importance to quantify the data and provide a general usable mathematical model to avoid failure due to pitting. For this reason by combining the individual effects of primary contributing factors on pitting potential an attempt has been made to develop a mathematical model that correlates the pitting potential with simultaneous changes in PREN, temperature, and chloride levels. Due to the inherent difficulty observed in assuming that the controlling parameters for pitting as independent variables various relationships are drawn to establish a universal pitting equation (UPE). The variables considered in the development of the model were found from the experimental data.

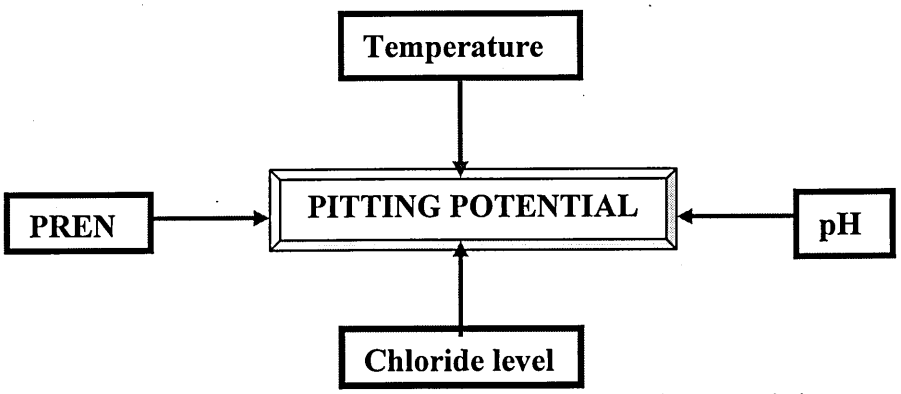

Figure: 5.15 Schematic diagram showing factors that influence pitting potentials

All potentials recorded are with respect to the standard silver/silver-chloride (0.025M KCl) electrode and chloride concentrations are in ppm, and temperature is in ^{0}C. Factors in PREN are 3.3 for molybdenum and 16 for nitrogen. Pitting potentials at high temperatures are generally difficult to determine, and very few people in practice are familiar with the concepts of electrochemistry. Therefore development of mathematical/empirical models to predict this value will be of great importance.

a) Relationship of pitting potential and chloride at 25^{0}C

In the studies conducted at room temperature the pitting potentials was found to be a logarithmic function of chloride concentration which indicates that an increase in chloride concentration shifts the pitting potential values in the negative direction which can be expressed in the form as shown below

$$E_P = A - B \log [Cl^-] \qquad (5.5)$$

A summary of results obtained through this study determining the values of A, and B is presented in tabular form

Steel type	Relation	Valid for
FV566	$E_P = 232.55 - 0.0149\log[Cl^-]$	$10^3 > Cl^- < 2X10^4$; PREN 16.5-16.9
Fv520B	$E_P = 193.07 - 0.07 \log [Cl^-]$	$10^3 > Cl^- < 2X10^4$;PREN 17 –17.8
304L	$E_P = 518.42 - 0.0237\log [Cl^-]$	$10^3 > Cl^- < 2X10^4$; PREN 17.8 – 18
18/13/1	$E_P = 384.91 - 0.0202 \log[Cl^-]$	$10^3 > Cl^- < 2X10^4$; PREN 19-20

Table: 5.1 Relations between, Pitting potential E_P and $[Cl^-]$

The relationships for the four steels PREN <20 are valid as the critical pitting temperature for these materials is around 25^{0}C. The very high breakdown potentials recorded for duplex and super duplex does not relate to pitting as the CPT values vary from 60- 80^{0}C and these steels are transpassive at these potentials.

It appears from the results that pre-logarithmic factor has decreased for the steels with higher PREN>33 compared to the steels with PREN <33. Whereas it was opposite for A values, which tend to decrease with decrease in PREN values and increase with increase in PREN values. These kind of relationships were established in previous studies highlighted in the literature review and were obtained for limited PREN ranges. The relationships shown in Table 5.1 are applicable idea for material selection in chloride environments used at room temperatures but one should note that the high breakdown potential values that were obtained at room temperature for Uranus65, 2205, Ferralium alloy 255 and Zeron100 super duplex correspond to transpassive behaviour of these alloys. As these highly alloyed materials has CPT above 40^0C. Not only are these relationships useful for the steels determined in this study, but the data can be extrapolated for the steels for materials outside the range.

From the results shown in Fig 4.8 it can be noticed that the relationship between PREN and E_P is non linear, for convenience to get best relationship the curve was divided into two different regions, for PREN<33 and for PREN>33.

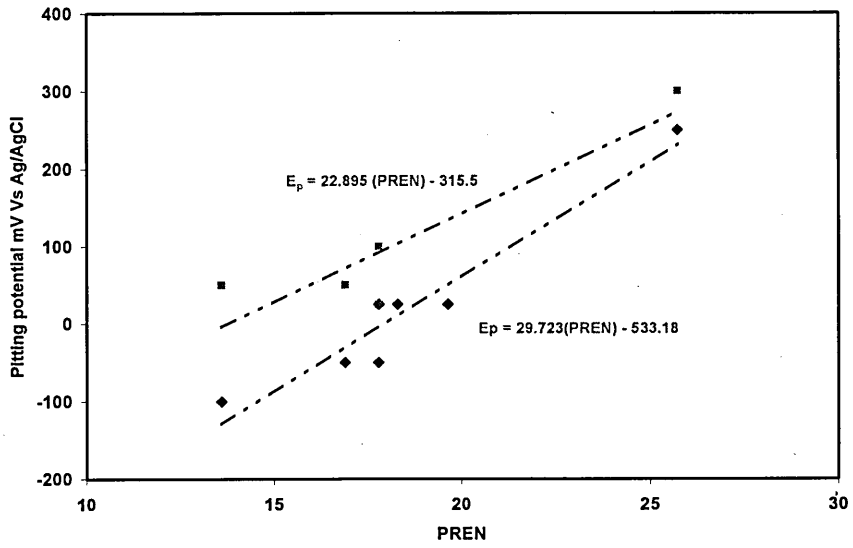

Figure: 5.16 Relationship between pitting potential and PREN <33 for predicting pitting potential in seawater and 10,000ppm, Chloride

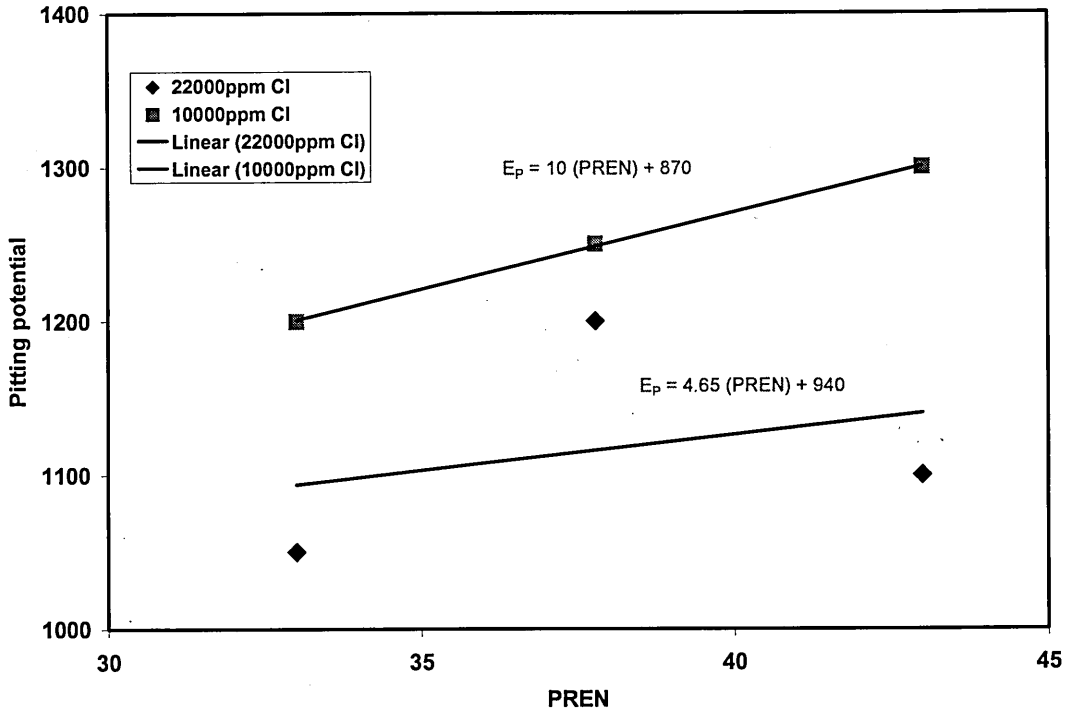

Figure: 5.17 Relationship between pitting potential and PREN >33 in 3.5wt%NaCl and 10,000ppm chloride level at 25^0C

From these relationships it is clear that pre PREN factor was less for higher PREN steels compared to the lower PREN steels as shown in Figure: 5.16.

Chloride dependence at 130^0C:

The effect of chloride ion concentration on the pitting potential was studied in pH 6 NaCl solutions at 130^0C for similar number of steels conducted at room temperature The relationship is given below as

$$E_P = (PREN)^2 - B \ln [Cl^-] \qquad (5.6)$$

The measured B values for wide range of PREN at various chloride levels were presented in the table determined from the Fig 5.17.

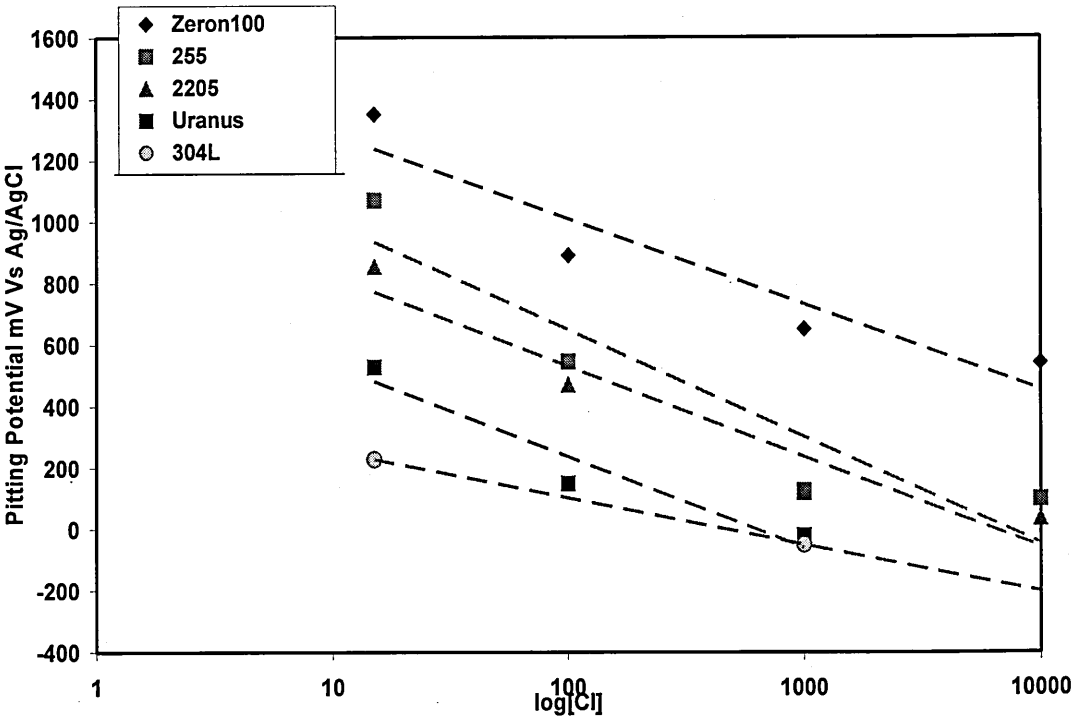

Figure: 5.18 Chloride dependence on the pitting potential values at 130^{0}C in 8ppm dissolved oxygen

PREN	B values
18.3	66
25.7	128
33.0	127
38.0	150
41.6	135

Table: 5.2 Represents B values for calculating Pitting potentials at 130^{0}C in 8ppm dissolved oxygen

B values were obtained from the trend lines in Fig 5.18. An example of the usage of this mathematical model equation is validated for Zeron 100 stainless steel with PREN 41.6 and the results are shown in Fig 5.19. It can be noted that the very small difference in prediction can be obtained from the proposed expression and it should be valid for various other super duplex steels such as 2507, (UNS S32750) and Ferallium alloy 255 (SD50). The equation was verified for Zeron 100 as it was tested

in wide range of chloride concentrations, which would allow to verify the proposed expression in many conditions.

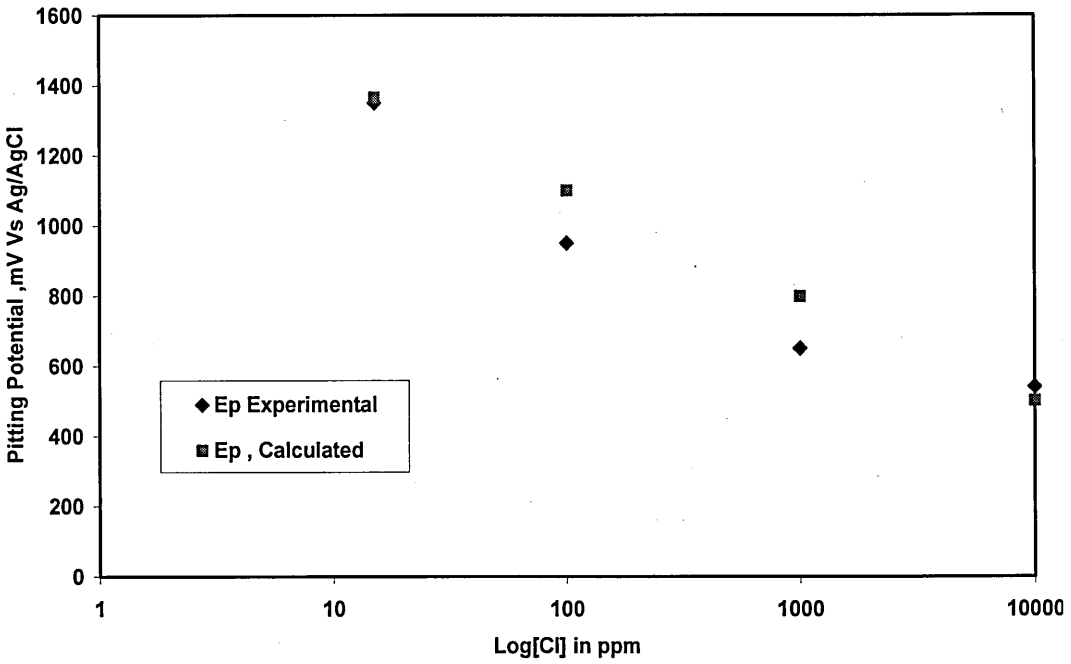

Figure: 5.19 Log [Cl^-] Vs pitting potentials, checked for Zeron100 at 130^0C

The model validations shown in Fig 5.19 indicate high degree of good correlation for both experimental and predicted values. The significance of the results shown in Fig 5.19 is that, no studies exist on this kind of super duplex stainless steels under these conditions and the proposed equation is valid for even higher chloride concentrations with higher accuracy which is of interest and one such result was plotted for alloy 255 in Fig 5.10 was -300mV (Ag/AgCl), the lowest pitting potentials observed for that particular steel.

b) Relationship of pitting potential and temperature:

To determine the dependence of pitting potential on temperature in constant chloride solutions and pH values, temperature was controlled and changed from 25 ^{0}C to 170^0C. The data was plotted as shown in Fig 5.20, linear dependence was observed

i.e increase in temperature does decrease the pitting potential values linearly for all PREN for tests conducted in 1000ppm chloride solution.

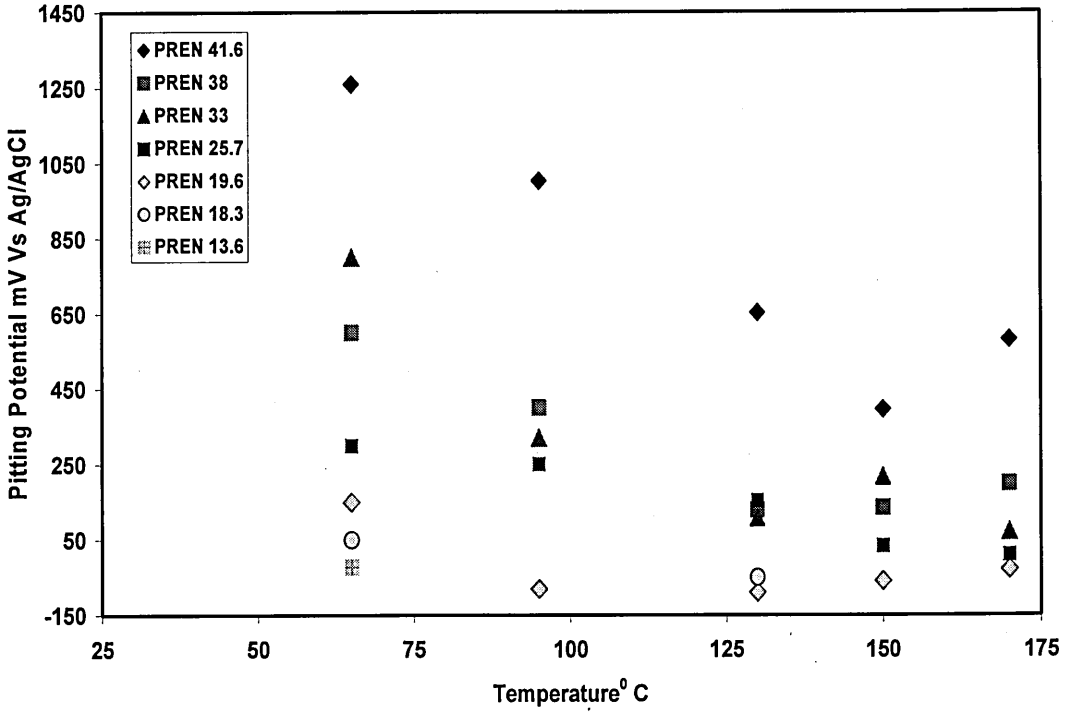

Figure:5.20 Effect of temperature on pitting potentials for wide range of PREN investigated in 1000ppm chloride and 8ppm dissolved oxygen

Pitting potential and temperature can be related with an expression as

$$E_p = C - D\,[Temp^0C] \qquad (5.7)$$

Where the variables C and D are given in tabular form for different steels. It shows, C and D parameters of the linear expression indicate the significance of the effect of variables.

C	D	PREN	[Cl⁻] ppm
1700	7.7	41.6	1000
815	4.3	38	1000
512	3.0	25.7	1000
151	1.5	19.6	1000
115	2.5	13.6	1000

Table: 5.3 Values of C & D used to calculate E_P, temperature range (65-170), and 1000ppm Cl^-

C) Effect of chemical composition on E_P:

Since the relationship between chemical composition and pitting potential is a non linear fit, for convenience the results were divided into two different zones, one for PREN < 33 and the second one for PREN >33.

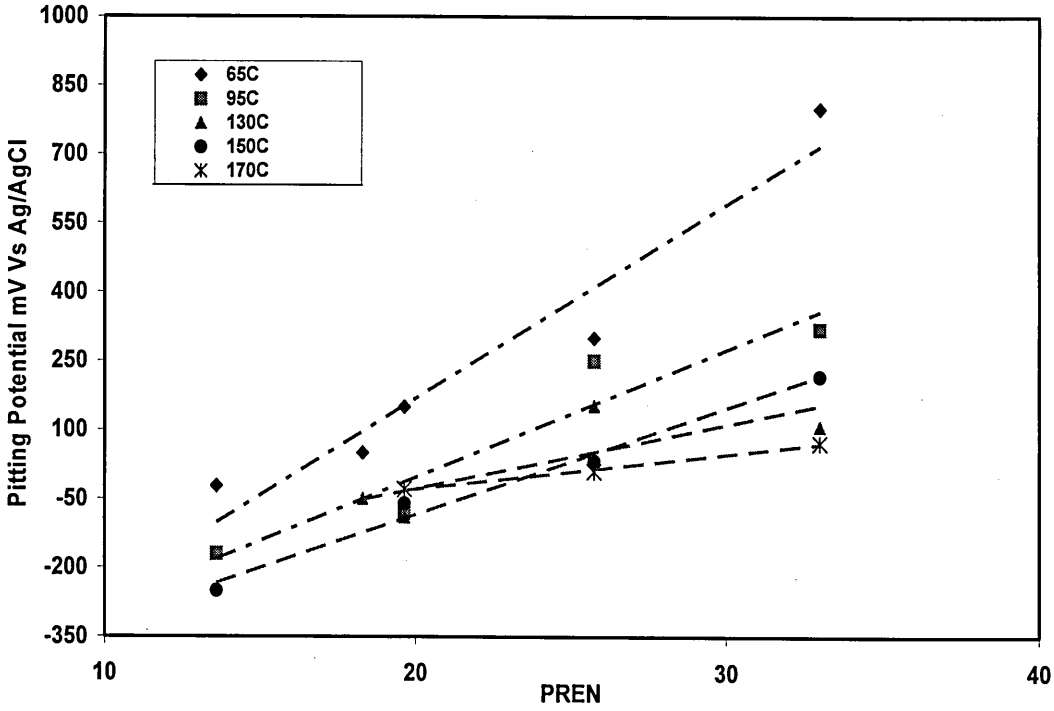

Figure: 5.21 Dependence of pitting potentials on temperature in 1000ppm Cl^- solution and 8ppm dissolved oxygen.

The decrease in pitting potential values with a decreasing PREN indicates the importance of the passive film formed in high chromium steels. Linear regression analysis has established the following relation between PREN and pitting potentials for different temperatures

$$E_P = E\,[PREN] - F \quad (mV) \qquad (5.8)$$

The values E and F do vary with change in temperature.

Temp^{0}C	E	F
65	42.24	675
95	27.74	560
130	13.94	307
150	23.24	550
170	7.54	180

Table: 5.4 Values of E & F determined to predict E_P for various PREN.

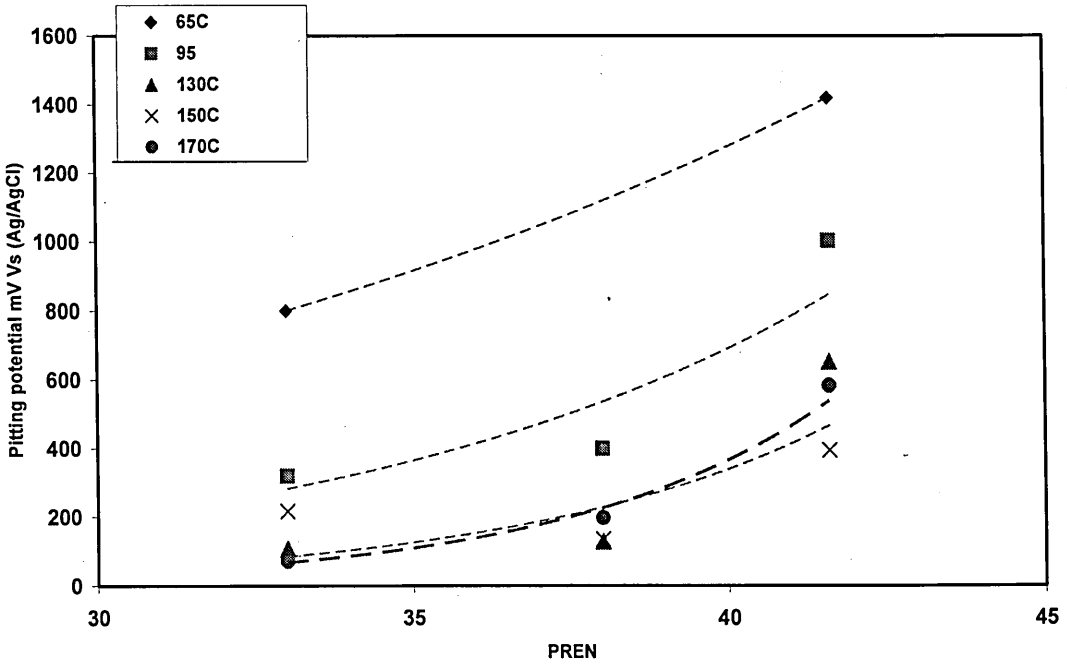

Figure: 5.22 Dependence of pitting potential values on temperature in 1000ppm [Cl^-]

The following relationship has been obtained from the data presented in Fig 5.15. An exponential relation exists for PREN above33 and is given below

$$E_P = G\, e^{L\,(PREN)} \quad (mV) \qquad (5.9)$$

As mentioned earlier since linearity is only given for PREN below 33, the Eq 5.10 will be able to predict the pitting potentials for all the duplex and super duplex steels. The factors G, and L has an influence in predicting pitting for these steels and a list of values that can be used to predict the pitting is given in table 5.5.

Temp^{0}C	G	L
65	88.45	0.0667
95	4.25	0.1273
130	0.122	0.1982
170	0.024	0.2406

Table: 5.5 Values of G and L to calculate E_P at different temperatures

Table 5.6 gives the values determined from the composition effect on E_P in 15 ppm chloride solution at 130^{0}C in 8 ppm dissolved oxygen.

PREN	E_P (mV) Vs Ag/AgCL
13.6	142
18.3	228
25.7	528
33.0	854
38.0	1069
41.6	1471

Table: 5.6 Pitting potentials in 15ppm [Cl^-] solution at 130^{0}C

The following power relation has been obtained between E_P and PREN: see Fig 5.23

$$\mathbf{E_P = 0.65\ [PREN]^{2.052}.\quad (mV)} \qquad \mathbf{(5.10)}$$

These kind of relationships are not reported in the previous works above 100^{0}C. As it can noticed even at 130^{0}C with increase in PREN the E_p value increases.

The values quoted in table 5.6 were plotted in Fig 5.23 to show the relationship between pitting potentials and PREN.

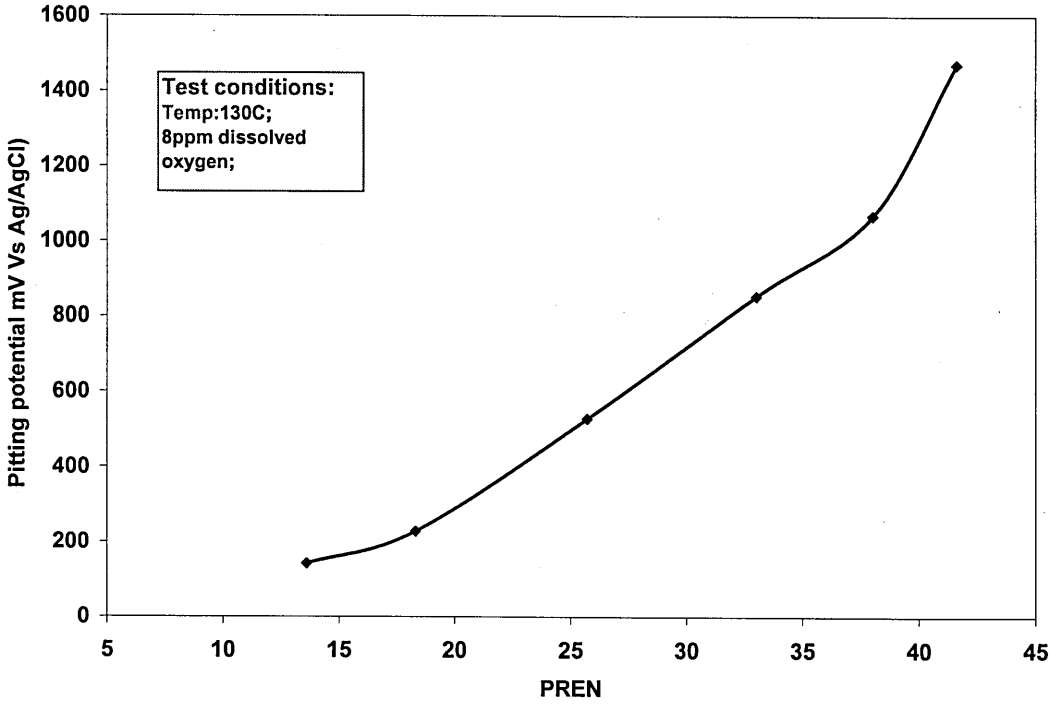

Fig: 5.23: Showing the relationship between pitting potentials and PREN in 15 ppm chloride at 130^0C.

Merello et al demonstrated a relationship between chemical composition and pitting potential values for non-standard duplex stainless steels and concluded that an exponential function can determine the pitting potential and can serve as a tool to design new non-standard low-Ni high – Mn-N duplex alloys. The present study focused on more dilute chloride solutions but at a temperature of 130^0C with a wide range of PREN, precise relationship was not found between pitting potential and chloride concentration in high temperature aqueous solutions. This data confirm that an increase in PREN values, results in higher pitting potentials especially with the duplex and super duplex stainless steels as their enhanced performance is due to addition of nitrogen and molybdenum, which increases PREN.

This study has obtained a power, and polynomial equations from the results shown in Fig 5.8, which allows an estimate of pitting potential values in 15 and 1000 ppm chloride solution, given by the following Eq (5.11) and (5.12).

$$E_P = 0.6399\ (PREN)^{2.0524} \quad (5.11)$$

$$E_P = 0.4733\ (PREN)^2 - 3.745\ (PREN) - 205.12 \quad (5.12)$$

The correlation coefficients (r^2) for the above two chloride levels were 0.9963 and 0.7833 indication that Eq (5.11) is the best fit compared Eq (5.12).The values obtained for pitting potentials of different alloys were against standard 0.025M (Ag/AgCl) electrode.

Only one parametric mathematical model exists to predict pitting potentials at present and it is restricted to a temperature of 65^0C and for one single composition of steel (Ergun and Balbasi, 1994).

The significance of this work is to predict pitting potentials for wide range of materials under different conditions. One should realise that linear models have given better fits than quadratic models. If too many parameters are used to fit the data, the compactness and the accuracy of the results have to be sacrificed. Study on remaining combinations of chloride at different temperatures for steels used in this study will definitely allow building a 3D model .However this study has shown some significant trends and will help a design engineer to predict pitting potentials of stainless steels.

In summary equation 5.5 is a simple description of the effect of chloride and composition of stainless steels, and the measured values through experiments were tabulated in table 5.1. The usage of this expression is restricted to room temperature and for various chloride solutions. Equation 5.6 links to three parameters, PREN, E_p and chloride levels at one single temperature, and table 5.2 will give necessary values to predict E_P for these conditions at 130^0C for different materials. Equation 5.7 is simplified description of effect of temperature on pitting and the factors involved and the values to be considered to calculate is given in the table 5.3. It allows the

stainless steels user or design engineer to estimate pitting potential and maximum temperature for a particular alloy composition. Unlike compositional effects (PREN) on pitting this is a linear effect like chloride on pitting potentials. It is valid for chloride solution of 1000ppm. Further work is required to study at different chloride levels for different temperatures which is beyond the scope of the current study. The effect of chemical composition on pitting potential at various temperatures is proposed in two different equations 5.8 and 5.9. For convenience the chemical composition is divided into two zones as PREN <33 and PREN >33. This is because of non linearity in the relationship. Above PREN >32 in all chloride solutions materials do not show a linear dependency. A linear fit for PREN <33 is proposed in the equation 5.8 and the factors involved in the table 5.4 and exponential fit has been obtained for the PREN>33, these two proposed equations fit practical measurements with good precision. The proposed formulas for different variables should be seen as a tool for the stainless steel user to choose the proper grade of material for his plant and to check maximum application ranges with respect to chloride concentration, temperatures for a certain steel. All the proposed expressions have produced very conservative and good correlations so they should have wide applicability.

Limitations of all the above relationships have not been considered for structural defects, intermetallic phases, all types of precipitates, and non metallic inclusions in the materials which have an influence on the pitting susceptibility, but the steels used were commercial grades from a range of steelmakers.

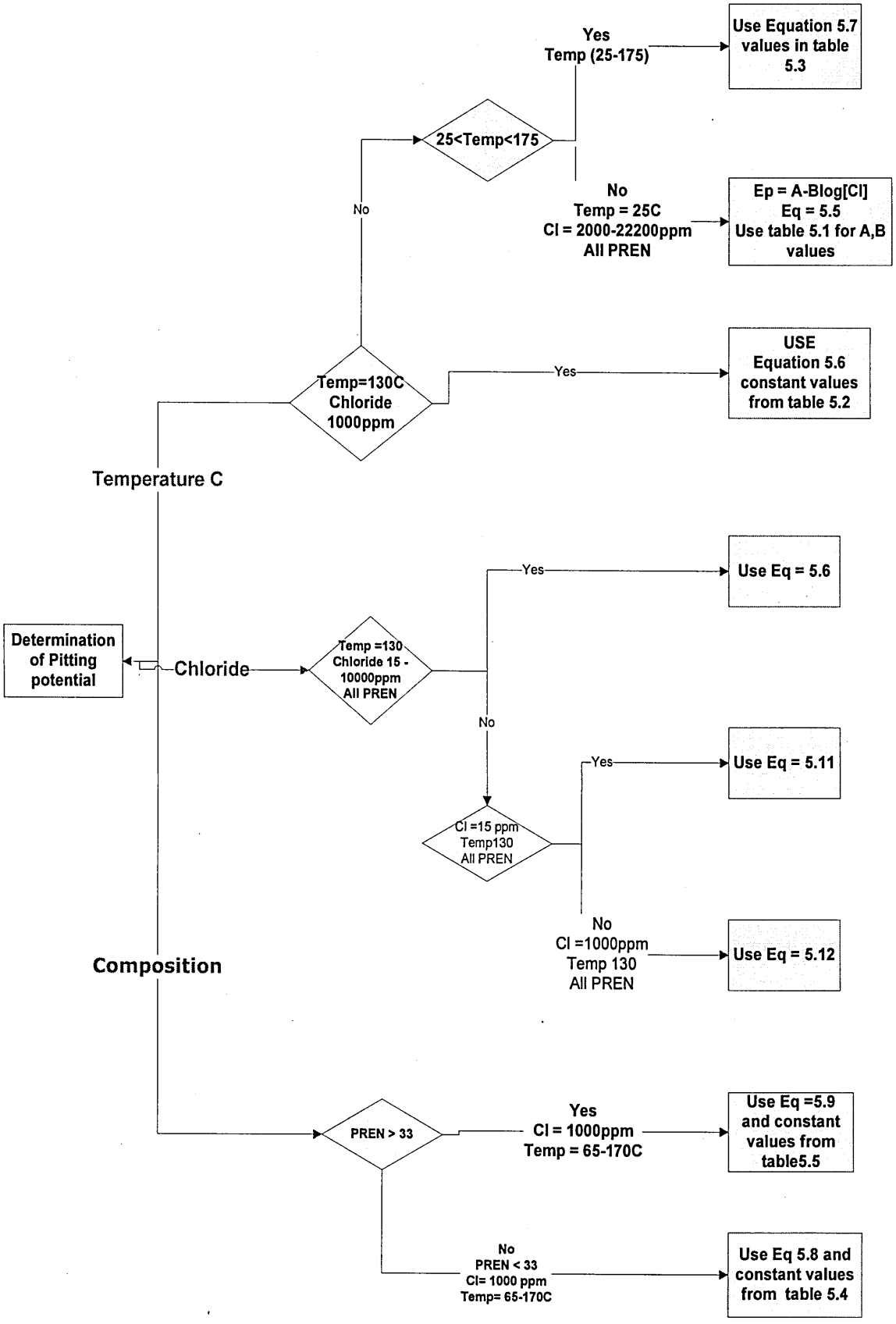

Figure 5.24: Decision tree Flow chart

CHAPTER 6
SCC of Zeron100 in dilute chloride solutions

6.1 Introduction:

This chapter discuss the key issues of the factor that influence SCC in the recently developed super duplex stainless steel in dilute chloride solutions and explain the mechanism of SCC in these SDSS. The SCC susceptibility can be evaluated by comparing the ductility of the specimens in the SSRT tests. The ductility can be measured by calculating the elongation and the reduction in area (%) of the specimens tested. The behaviour of SDSS is also compared with DSS to explain the superiority offered by the SDSS. The SCC susceptibility of the SDSS was dependent on applied potential, chloride concentration, Temperature and dissolved oxygen. The susceptibility increases with increase in the above parameters mentioned. The following section describes the individual effects based on the results shown before in chapter 4. The relationship between pitting potentials and stress corrosion potentials has been discussed in dilute chloride solutions for duplex stainless steels. Critical Potential vs chloride concentration maps were produced in order to estimate the failure region that can be possible in a plant.

6.2 Applied potential effect on SCC:

The SSRT technique was used to determine the stress - strain curves indicate the dependence of the failure time and tensile behaviour of Zeron100 SDSS on the applied potential compared with an air test. The applied potential effect has significant influence on the tensile properties of Zeron100 as shown in Fig 4.18. The SCC susceptibility of SDSS increase as the applied potential increases. Maximum stress and strain decreases as applied potential increases as shown in Fig: 4.18. At the applied potential of +400mV and potentials lower than 400mV showed in Fig 4.19 that the ultimate tensile stress and percentage of elongation were very close to that at 0mV. No evidence of SCC was evidenced from the SEM micrographs shown in Fig 6.1 below 400mV. The appearance of the fracture surface below +400mV showed ductile failure with large dimple/voids and extensive necking was witnessed shown in Fig 6.1 (a, b). No evidence of localised corrosion was observed below this potential on the specimen surfaces.

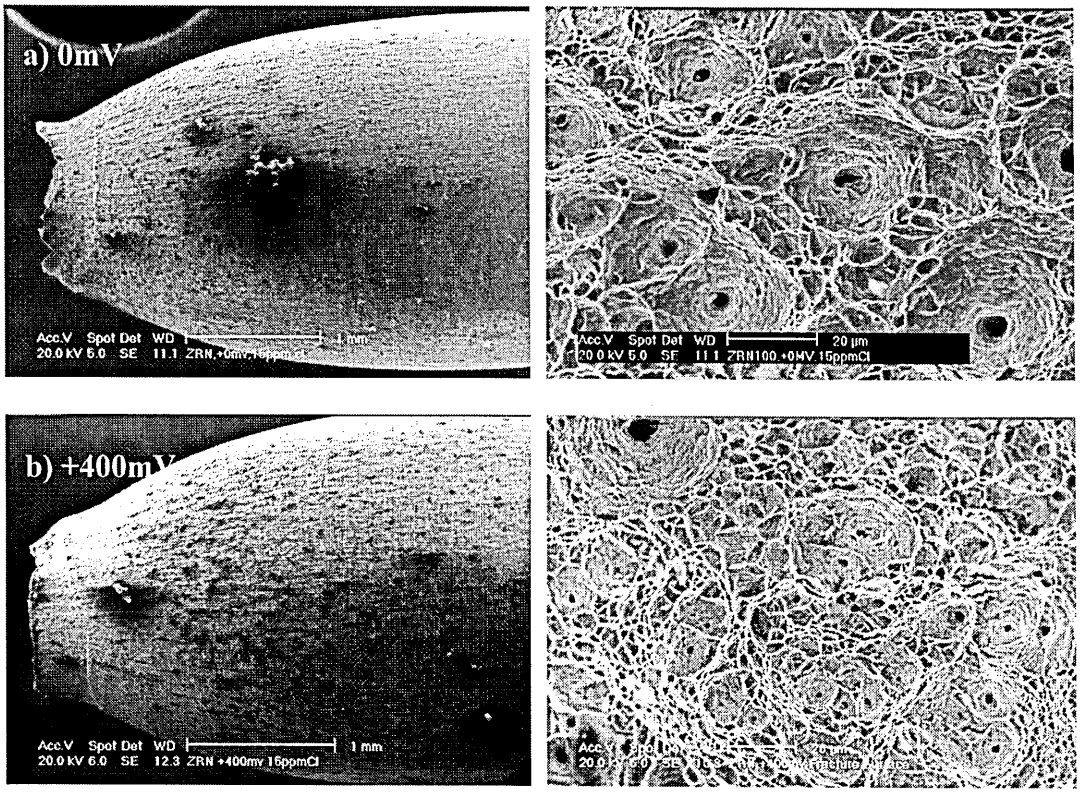

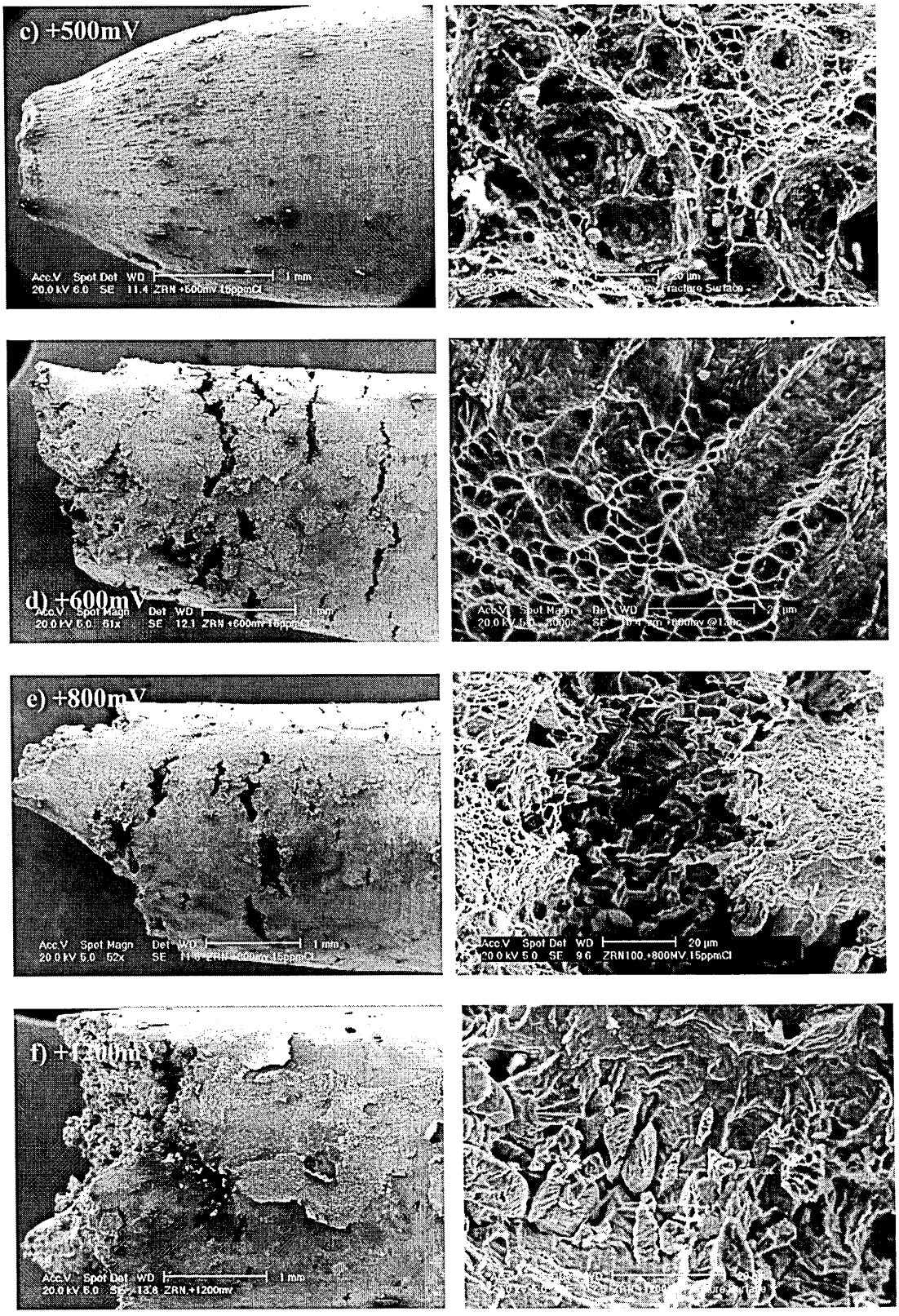

Figure: 6.1 SEM micrographs of the fracture surfaces of the specimens after SSRT tests conducted in 15ppm chloride at 130^0C in 8ppm dissolved oxygen, controlled applied potentials a) +0mV b) +400mV c) +500mV d) +600mV e)+800mV f)1200

At applied potentials greater than 400mV, the ductility has begun to drop which is measured as measure of percentage reduction in area. Dramatic decrease in the ductility was observed above this potential ad fracture appearance above 400mV have shown environmental assisted cracking. The fracture surface appearance on the sample surface for the test conducted at 500mV has shown, see Fig 6.2 (a) the initiation of environmental assisted fracture with evidence of localised corrosion but interestingly the ductility still exists and it does not have any effect on SCC susceptibility in the real life. Cracks have begun to initiate at 500mV but found difficult to link and importantly they did not play any significant role in the failure process. This potential value exists in Zone2, see Fig 6.3 and begun to give an indication of environment assisted cracking (EAC) type behaviour. The initiation of cracks and pits is shown in Fig 6.2 (a & b).

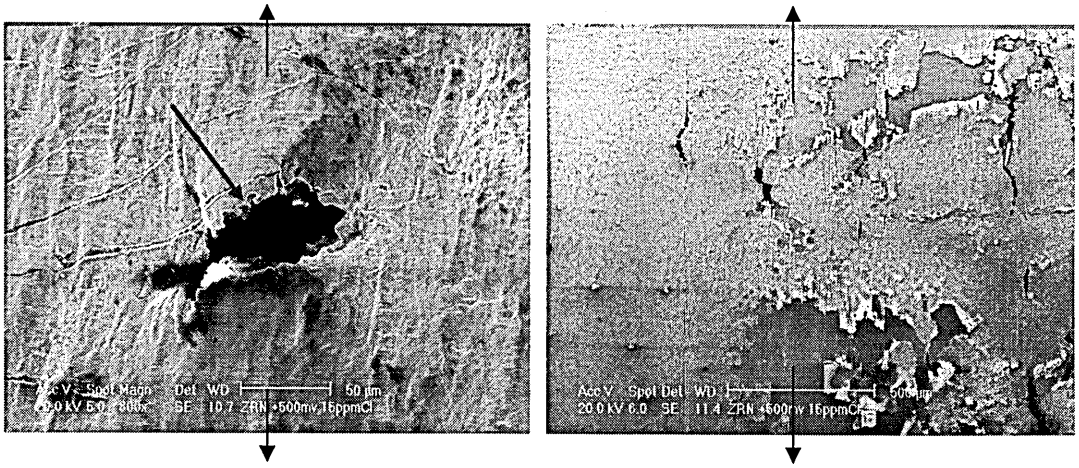

Figure: 6.2 a) Pitting corrosion and b) initiation of isolated cracks are noticed on the specimen surface, tests conducted at +500mV in 15ppm Cl, 8ppm DO_2.

However, at potentials greater than 500mV signs of SCC exists and visible on the surface of the specimen in the SEM micrographs. Significant number of cracks was found on the gauge length of the specimen at +600mV as shown in Fig 6.1 (d). The fracture mode was Finger/Tunnelling was witnessed and these were known to be the signs observed when the alloy is susceptible to SCC (Swann, 1965). Ductility at

these potentials is dramatically reduced along with ultimate tensile stress under this condition. The results indicate that a critical potential value exists, above which the failure time of Zeron100 decreases in this dilute chloride solution. The ductility (% ROA) declined with increase in the applied potential in the graph plotted as shown in Fig 6.3. Three Zones (Zone1, Zone 2, Zone 3) are identified that determine the failure type and behaviour as shown in the Fig 6.3.

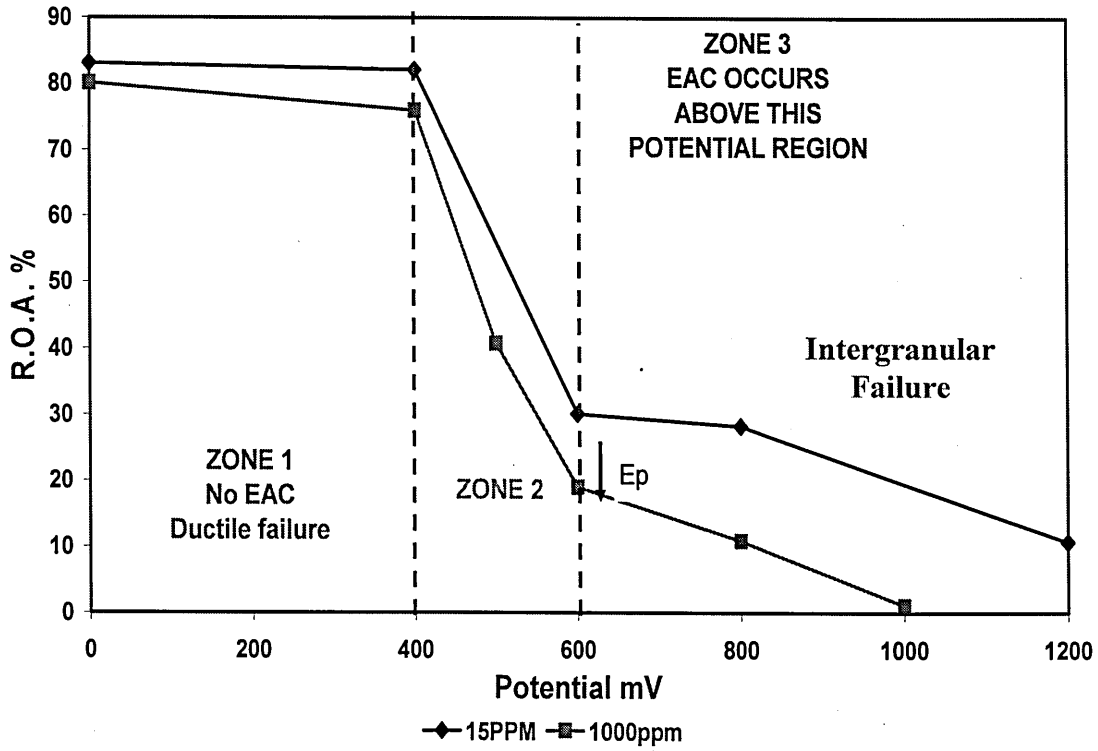

Figure 6.3: Effect of applied potentials on percentage reduction in area measured after the tests conducted in 15 and 1000ppm chloride levels at 130^0C.

From the Fig 6.3 it can deduced that a critical potential exists for SCC (E_{SCC}) in Zone 2 and the regions are identified in the plot in order to highlight the safe operational potential limits of SDSS. The ductility prevailed over the large range of potentials 0 to +500mV. The fracture surface of the tests conducted above +500mV had different fracture modes, such as tunneling/transgranular and intergranular fracture mode behaviour at higher potentials as shown in Fig 6.1 (e & f). It is interesting that crack density is reduced at higher applied potentials, and the possible reasons for this kind

of observation was highlighted by Parkins (1987) for the study conducted on pipe line steels and this study was in agreement with that observation. Parkins (1987) related the observation of number of short cracks with the crack tip strain rate, as with increase in number of short cracks on the SSRT specimen the crack tip strain rate decrease for a given applied strain rate. The expression proposed by Congleton et al (1985), to calculate crack tip strain rate is found to be a useful approach

$$\epsilon_{CT} = \frac{75}{N}\,\epsilon_{app} + \frac{a}{5}\,\ln\frac{1000}{N}$$

Where N= number of cracks along the gauge length, ϵ_{app} is applied strain rate and, a is crack velocity. As N increases the crack tip strain rate decreases, say for a few number of cracks to cause failure the cracks have to maintain the conditions helpful to grow. Although present study is focussed on single applied strain rate value it can be applied to the current study to calculate the crack tip strain rate for various number of cracks observed at various applied potentials.

Crack coalescence was predominant at higher applied potentials due to severe pitting was observed as shown in Fig 6.4. Excessive pitting that occurred on the specimen surface dominate the crack growth process. Pits tend to link easily and they will create less chance for the sharp cracks to grow.

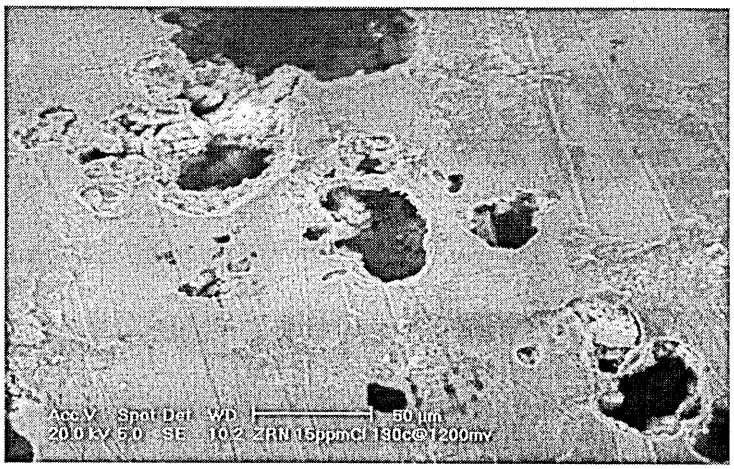

Figure: 6.4 SEM micrograph for test conducted in Zone3 where the intensive pitting is observed at +1200mV

Inspite of intergranular failure mode is observed on the fracture surface at these high applied potentials, pitting or uniform corrosion behaviour contributes a lot to the loss of cross section of these materials. Due to the extensive pitting the damage did not follow a sharp path instead it looks like galvanic attack, which assists crack coalescence. The results clearly indicate the superior performance of Zeron100 in these dilute chloride solutions compared to the duplex and austenitic steel grades, which fail at much lower applied potentials (Atkinson and Brashaw ;2003). This study also extends the controlled potential tests to 1000ppm chloride solution at 130^0C. Similar kind of role by the applied potential observed in 15ppm Cl studies was repeated even in case of 1000ppm chloride solution. Optical images of the failed specimens are shown in Fig: 6.5. As it was observed from the Fig 6.3 the loss of ductility was noticed above +500mV in these conditions. At low potentials mechanically induced cracks have occurred on the gauge length but as the potentials are increased the morphology of the short crack tends to change and it becomes apparent from these observations that EAC is occurring. Fig 6.3 gives a comparison of the minimum potentials for cracking and transition potentials from predominant ductility to transgranular SCC and intergranular SCC for the Zeron100 and the potential ranges indicated by dashed lines for cracking as a function of chloride concentration.

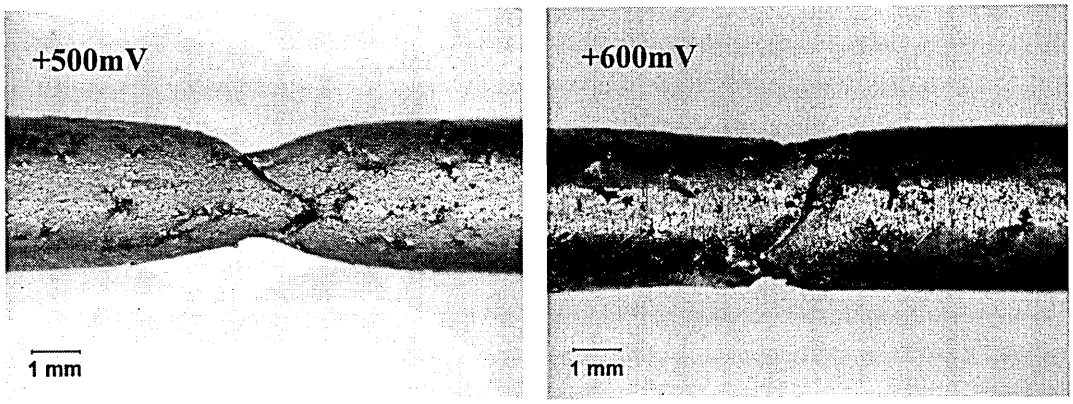

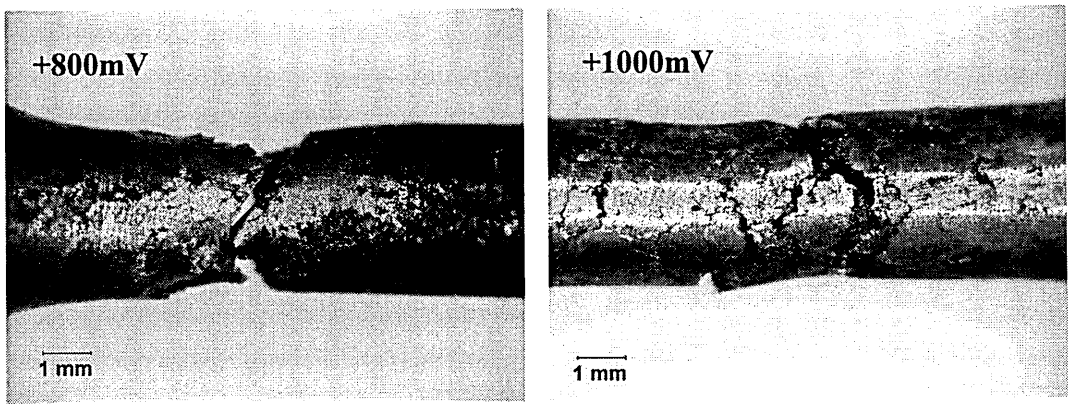

Figure: 6.5 Optical micrographs of SSRT tests conducted at different potentials a) +500mV b) +600mV c) +800mV & d) 1000mV in 1000ppm Cl^- solution at 130^0C in 8ppm dissolved oxygen.

The fracture appearance even in 1000ppm chloride has shown the decline of the ductility as the potentials are increased above critical stress corrosion cracking potentials (E_{SCC}) as has been mentioned earlier for 15ppm Chloride. The three Zones identified in Fig 6.3 has shown similar behaviour of Zeron100 under applied potential conditions. The percentage reduction in area was less in 1000pm compared to the values noted at 15 ppm chloride solution as shown in Fig 6.3. As the chloride concentration has a significant influence on the SCC behaviour it is obvious that 1000ppm chloride tend to decrease the failure time and the loss of cross section would be easier compared to the 15 ppm chloride solution. The influence of the chloride concentration is discussed in detail in the later section of this chapter.

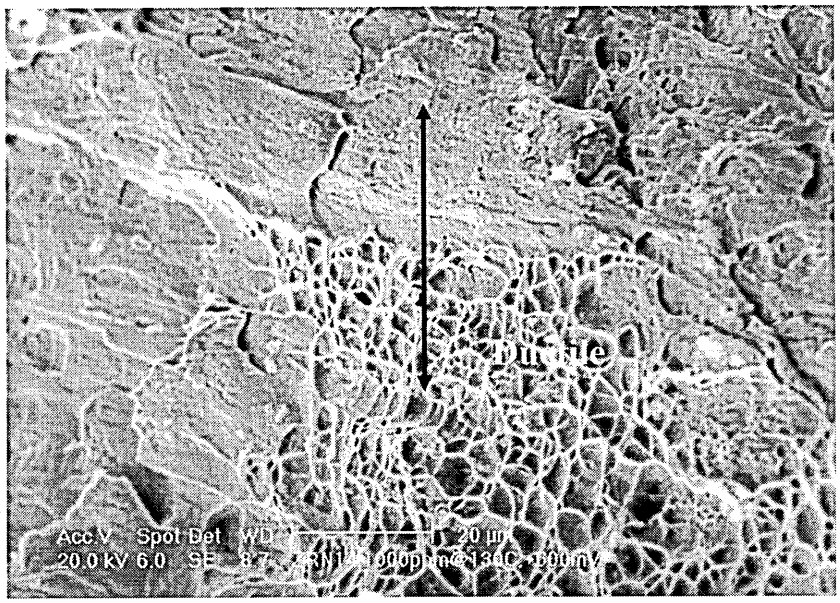

Figure: 6.6 Percentage of ductility is beginning to drop at +600mV in 1000ppm Cl^- level at 130^0C in 8ppm dissolved oxygen

The example of transition from ductility to intergranular fracture is shown in Fig 6.6 and 6.7 for the tests conducted at +600mV and +1000mV.

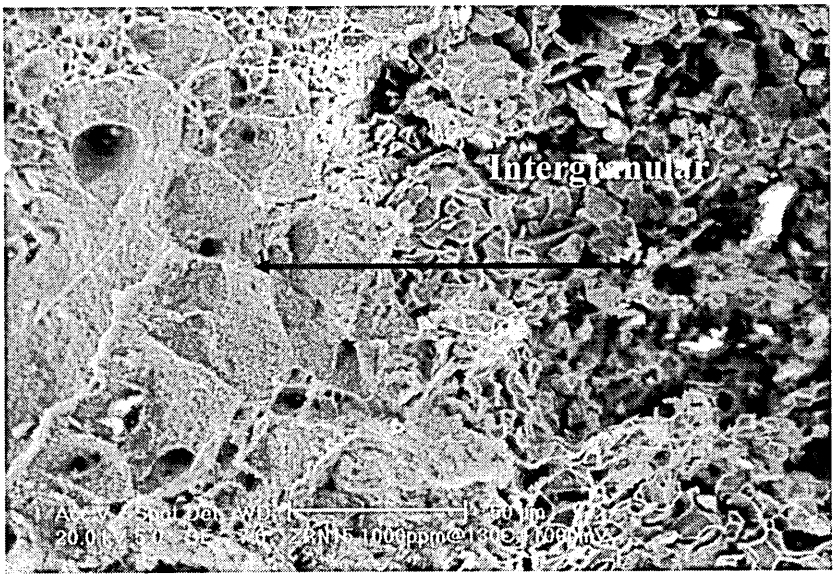

Figure: 6.7 Intergranular fracture mode is observed in 1000ppm Cl^- at 130^0C,+1000mV

As Zeron100 consists of two phase α (Ferrite) and γ (Austenite) it is highly resistant to stress corrosion cracking compared to the individual performance of austenitic and ferrite in the identical environments shown in the studies conducted by

Atkinson and Brashaw (2005). The potential dependence of SCC in duplex steels and the importance of studying the SCC susceptibility under controlled conditions has been highlighted, Cottis & Newman (1993). In their review they justified the importance of the controlled potential tests to judge the SCC behaviour of stainless steels. In their view the use of boiling solutions for SCC testing, without any potential control is not relevant to the plant operation, as solutions doesn't have oxygen and the electrochemical potentials are generated by means of different cathodic reactions like hydrogen evolution.

6.3 Applied potential effect on current density:

The present work has shown that for Zeron 100 SDSS there was a wide range of potential over which SCC can occur. Although at low potentials less than (+400mV) that crack growth is not excessive or any evidence of EAC has not seen, may be not the case if the temperature is increased.

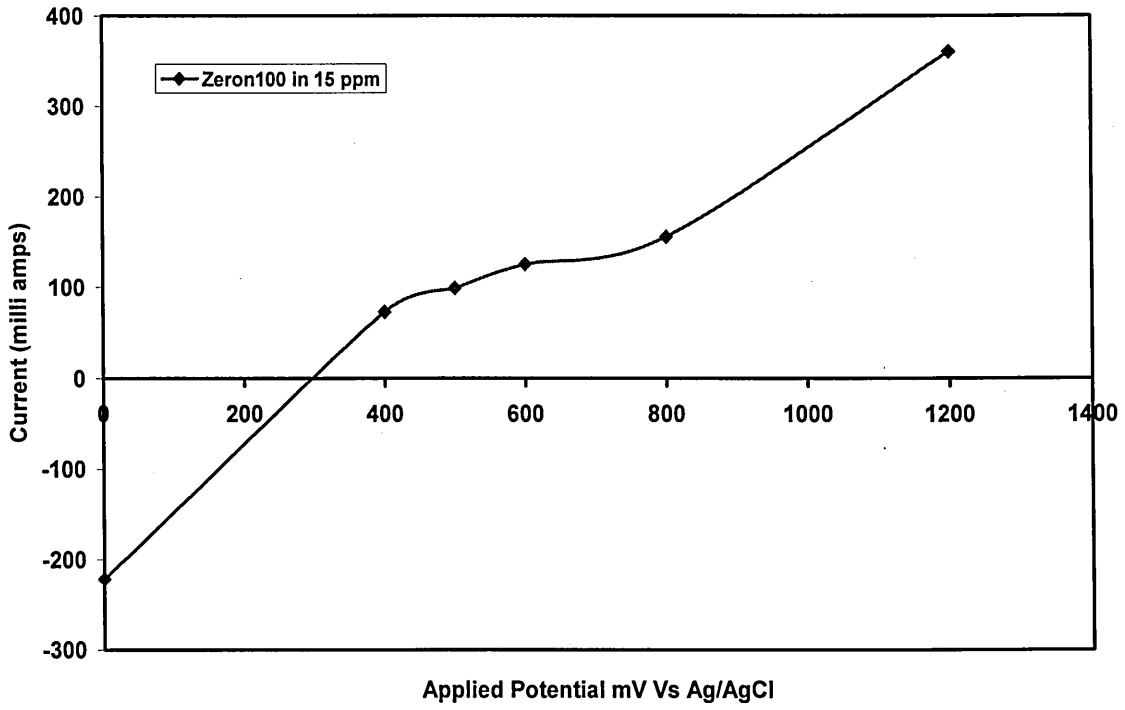

Figure: 6.8 The change in current values with applied potential recorded for Zeron100 in 1000ppm Cl^- solution during SSRT tests at 130^0C

6.4 Chloride effect on SCC:

Comparison of the SSRT test results conducted for Zeron100 at +800mV in 15 and 1000ppm chloride levels at 130^0C indicate that chloride does have influence on the failure of Zeron100 as shown in Fig 4.20. Increase in chloride concentration does reduce the failure time and less strain to failure is observed at higher chloride levels. The fracture surface observations show that the elongation is reduced by nearly 50% in 1000ppm Cl compared to 15ppm Cl at 130^0C at +800mV applied potential. The specimen gauge length showed severe pitting, which is associated with the higher anodic current density in 1000ppm Cl^- . The Cl^- concentration also had an influence on the maximum stress required to cause the failure, it was reduced by 40% in 1000ppm Cl^- solution compared to 15ppm Cl^-.

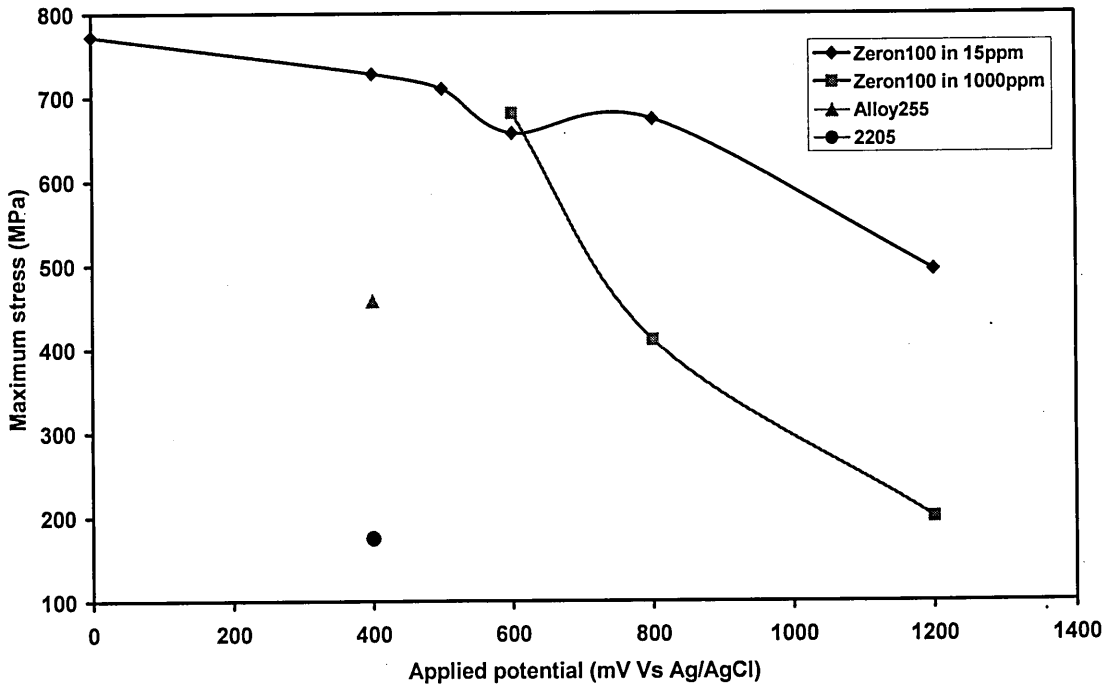

Figure: 6.9 No Effect of applied potential on the changes of the maximum stress required to fail after SSRT tests in 15 & 1000ppm Cl^- solution.

The coincidence of the critical potentials for 15, and 1000ppm chloride concentration levels seem to be between +500 to and 600mV Ag/AgCl as shown in Fig 6.3, which suggest that the chloride ions penetrate the film at these potentials under this

temperature and dissolved oxygen conditions. Alternatively, the change in chloride levels below 1000ppm doesn't seem to cause extra damage to the film.

6.5 Effect of chemical composition of steel on SCC in duplex stainless steels:

SSRT tests were conducted in the 1000ppm Cl^- environmental conditions, on two additional duplex stainless steels, 2205 and Ferallium alloy 255 to compare with Zeron100. The results shown in Fig 4.23 indicate that SCC resistance of Zeron100 is superior to the other two steels for these test conditions. Interestingly both 2205 and Ferallium alloy 255 have nearly identical pitting potentials, of +200mV (Ag/AgCl) under these conditions and yet Ferralium alloy 255 exhibits higher stress corrosion resistance when constant strain rate was applied as shown in Fig 4.23. Fractographic pictures show that the coalescence of cracks/pits occurred more easily in the case of 2205 compared to Ferralium alloy 255 and Zeron100 as shown in Fig 6.10 a) &d) and less galvanic attack was evident, see Fig 6.11

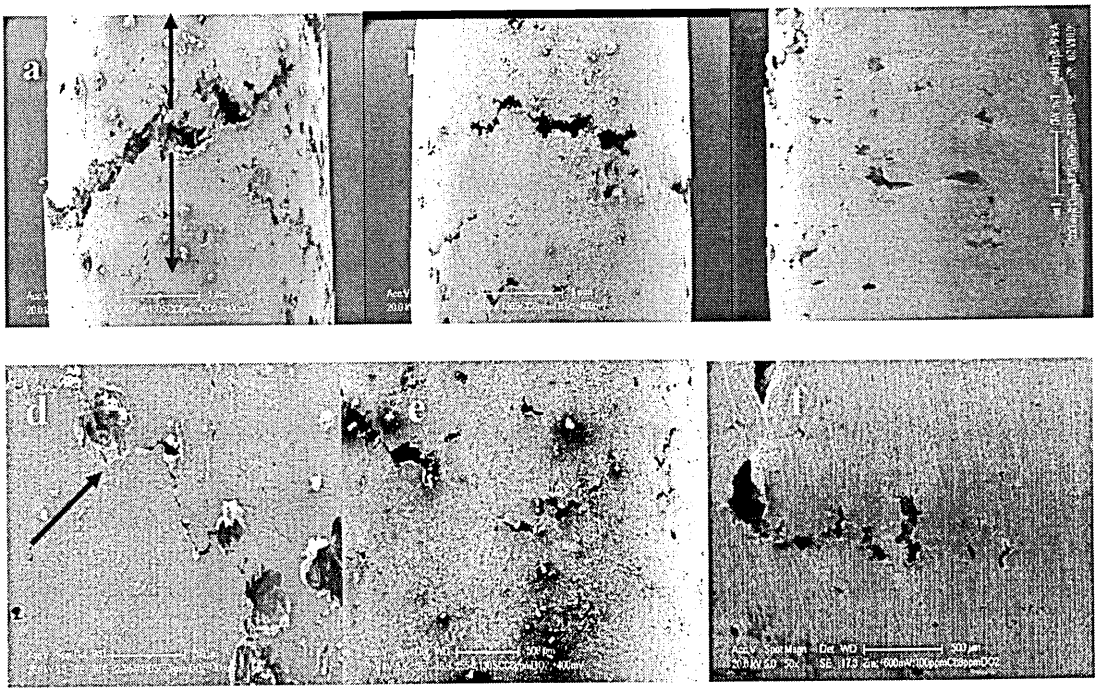

Figure: 6.10 SEM images of fracture surface across gauge length a) & d) 2205 b) & e) Ferallium alloy 255 c) & f) Zeron100 after SSRT test in 1000ppm Cl at 130^0C

Further work is needed to define the precise threshold conditions for Ferallium alloy 255 and 2205 steels. From this preliminary study it is likely to be close to +200mV and +400mV, with pronounced EAC greater than +400mV.

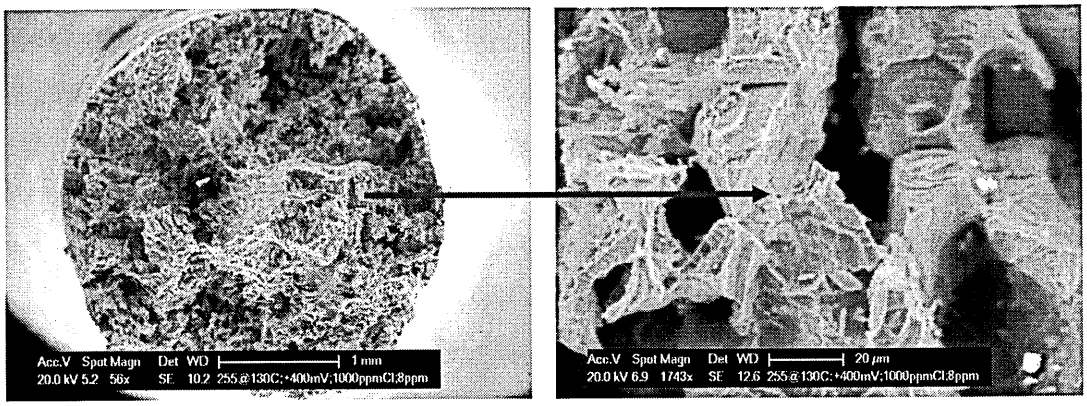

Figure:6.11 Fracture appearance of Ferallium alloy 255, showing intergranular fracture mode in the region A, test conducted in 1000ppm Cl^- at E_{app} of +400mV.

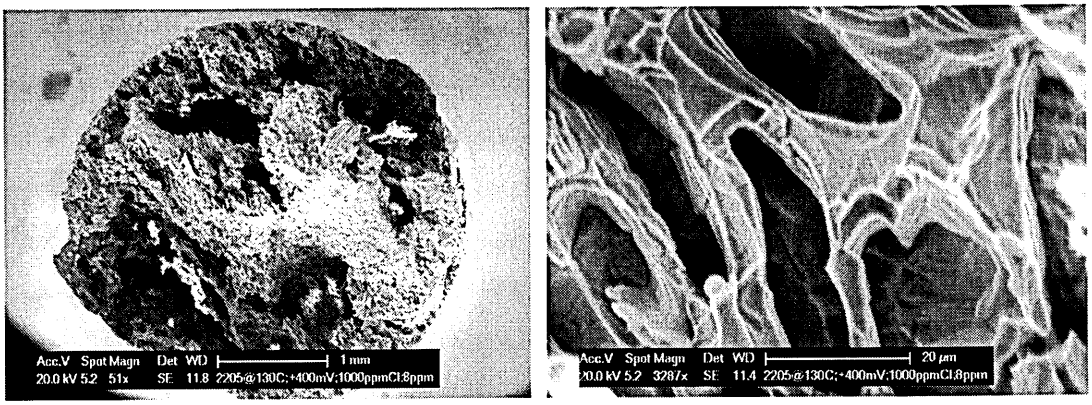

Figure: 6.12 Fracture appearance of ferallium alloy 255, showing intergranular fracture mode in the region A test conducted in 1000ppm Cl^- at E_{app} of +400mV.

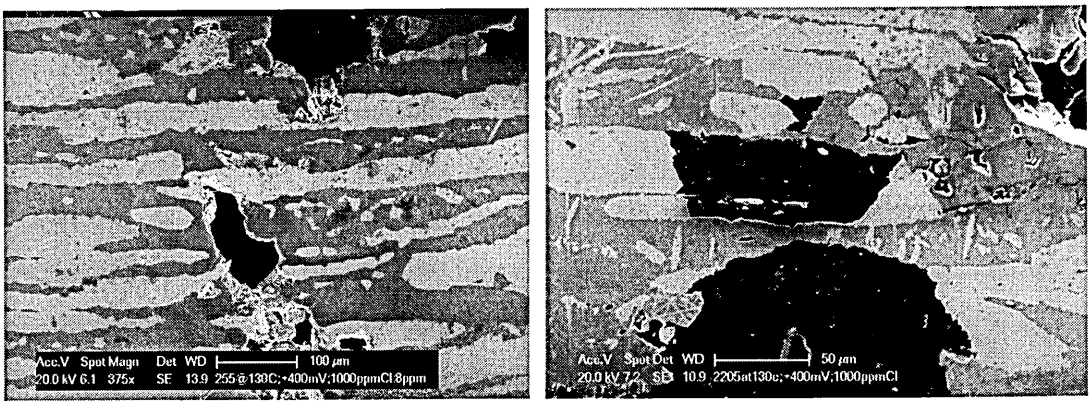

Figure: 6.13 Showing variation cross section images of the samples for the test conducted in identical environments haven't shown any sharp cracks path.

The observation that, under stress, passive film damage can occur at about 200mV below the conventional pitting potential (E_P), and should be considered in plant assessments.

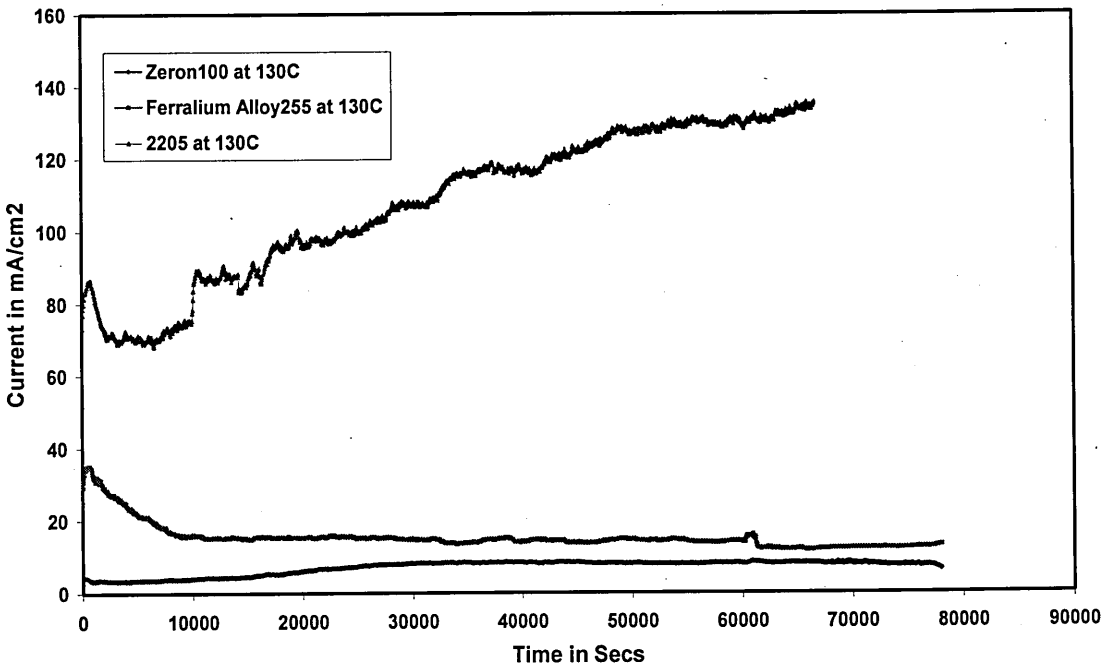

Figure: 6.14 Change in current values at constant potential of +400mV in 1000ppm Cl^- solutions.

The good performance of Zeron100 in SCC studies should not be surprising compared to 2205 and Ferallium 255 duplex steels as it has shown to have better oxide film properties. It was already been emphasized during the discussion of the preceding chapter that the attainment of proper oxide film composition and phase balance achieved due to the addition of nitrogen and molybdenum are operating excellently in this material. Moreover at constant potential for prolonged time under loading conditions, 2205 (low nitrogen steel) has shown noticeable current fluctuations, see Fig 6.14 and high current values compared to Ferallium alloy 255 (Medium nitrogen steel) and Zeron100 SDSS (high nitrogen steel). The change in current values are not easily distinguishable in case of Zeron100 as on the low nitrogen steel 2205. The observations in Fig 6.14 under loading conditions shows that film rupture upon loading has produced immediate anodic current values, which

should decrease with time as repassivation occurs. This kind of behaviour was noticed in all these three duplex steels but in case of low nitrogen steel (2205) the current values tend to increase over a period of time during the tests duration indicating no repassivation behaviour. This can be due to the weak film formed on the surface of 2205 duplex steel or the nitrogen added to this steel is not enough to promote repassivation as observed in alloy 255 and Zeron100. These large current values observed in 2205 will undoubtedly promote crack initiation and propagation process more easily.

The influence of nitrogen certainly has an influence and confirmed that it promotes the passivation behaviour in these nitrogen alloyed steels.

6.6 Dissolved oxygen effect:

The results of stress strain curves of Zeron100 SDSS conducted in 1000ppm Cl^- solution at 130^0C of two different dissolved oxygen concentrations, 8ppm and < 20ppb at a strain rate of $1x10^{-6}$ /sec are shown in Fig.4.22. The elongation in aerated water, (8ppm dissolved oxygen, DO_2) decreased by about 10 % compared to that in deaerated water. The fractographic images shown in Fig 6.15 and 6.16 indicate that much more necking in the deaerated water (<20ppb DO_2). Unlike chloride, which has an effect on stress levels required to cause failure, oxygen does not appear to have a severe effect on the mechanical stress required to cause failure. Although the length of the time to fracture increases at low dissolved oxygen. From the SSRT results and fracture morphology, it suggests that oxygen plays an important role in metal dissolution rather than on mechanical properties. As the maximum solubility of dissolved oxygen in water is about 8ppm at ambient temperature it is treated as the higher oxygen level in this case.

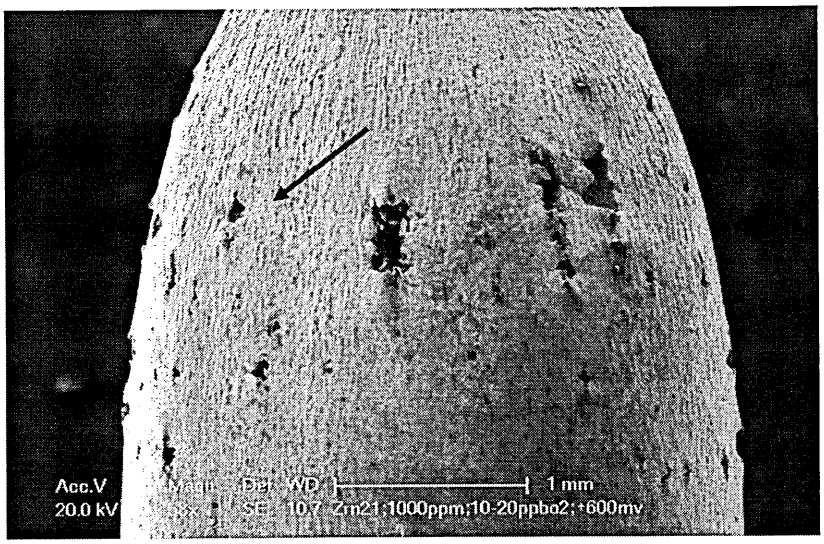

Figure: 6.15 Pits unassociated with no sign of linkage to cracks for the test conducted in 1000ppm Cl^- and <20ppb oxygen at an applied potential of +600mV

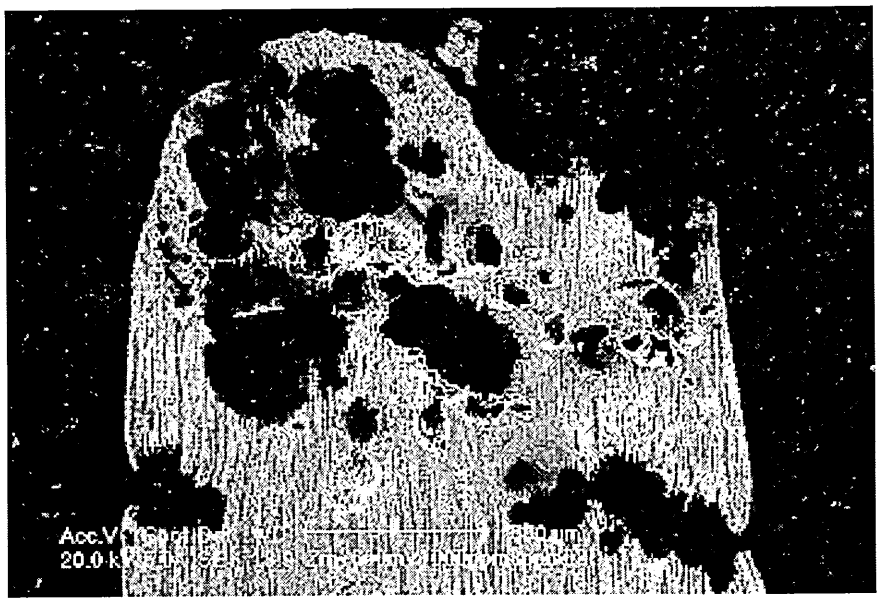

Figure: 6.16 Cross sectional view of the failed sample for the tests conducted at +600mV in 1000ppm chloride at 130^0C under high dissolved oxygen conditions.

Dissolved oxygen in the corrosion environment significantly influences the corrosion potential and it is well established, that effect of the O_2 content of water will determine whether an alloy is susceptible to SCC, which links directly the effect of O_2 on potential.

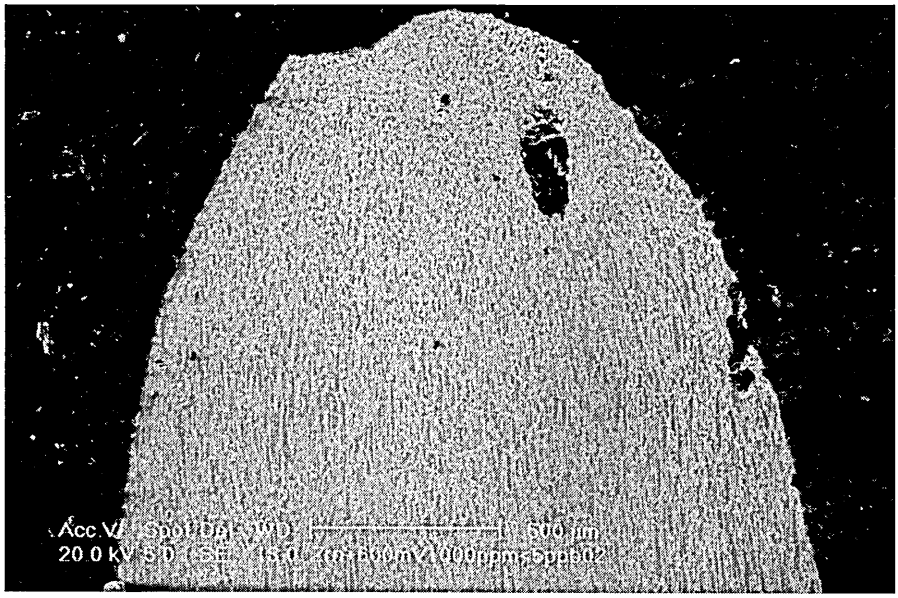

Figure: 6.17 Cross sectional view of the failed sample for the tests conducted at +600mV in 1000ppm chloride at 130^0C under high dissolved oxygen conditions

In the present investigation SCC susceptibility of Zeron100 SDSS is shown in Fig 6.16. The cross section appearance after the failures Fig 6.16 show that loss of metal rate increased with dissolved oxygen content. Moreover a ductile fracture mode can be witnessed from the fracture surface and from the cross section view as shown in Fig. 6.17

Increase in the corrosion potential and corrosion current density in aerated solutions also contributes to the rapid metal dissolution rate and accelerated time to failure compared to the deaerated solution. At higher oxygen levels the potential at the pit bottom is likely to be high compared to the bulk surface, which might also lead to high metal loss compared to deaerated solution. It is well known from the studies on turbine blade steels (Maneg et al, 2005) that oxygen mass transfer is proportional to the oxygen concentration in water and it can control the corrosion rate. However, it is important to consider that likewise in turbine blade steels, the SCC susceptibility and the relation to anodic metal dissolution at the crack tips follow a similar pattern with these SDSS.

The following reaction is often encountered as a cathodic reduction reaction when there is a high concentration of dissolved oxygen.

$$O_2 + 2H_2O + 4e^- \rightarrow 4OH^- \qquad (6.21)$$

The current for this reduction reaction increases with dissolved oxygen content available. When the dissolved oxygen content is high the higher the reduction current, also results in higher corrosion potentials in the anodic direction. Since a passive film is formed on SDSS during oxidation conditions, the corrosion current decreases as the corrosion potential is increased for a maximum period. Whereas for low grade stainless steels, where there is less chance of passivation the corrosion current tends to increase. The corrosion current and corrosion potential decreases if dissolved oxygen content decreases. It is illustrated by Congleton et al (1985) the combined influence of oxygen and temperature on the cracking potentials for A533B steel material and showed the maximum dependency on time to fracture can happen below oxygen content of 400ppb. Upon increase of the oxygen content above this level with corresponding change in temperature did not have significant effect on the measured ductility and there is a very little variation in % ROA. It is important that to investigate alloys that are used for specific applications to find the relationship between cracking susceptibity, temperature and O_2.

Therefore, when stainless steels including SDSS are surrounded by high dissolved oxygen the anodic metal dissolution at the crack tips tend to increase as the diffusion of oxygen molecules take place easily between the crack tip and bulk solution. This kind of rapid transport of oxygen molecules to the crack tip will increase the SCC susceptibility of Zeron100 or any other stainless steel in highly dissolved oxygen conditions. Due to this phenomenon a differential aeration cell created between the crack tip and the bulk solution turning the crack tips as anodes

and surrounding solution as cathode. The dissolved oxygen effect is independent of microstructure and even in the intermediate range type steel like 304 stainless has also seen similar effect in 100ppm Cl^- at 289^0C where the cracking potential in deaerated solution was -650mV (0.01N Ag/AgCl) and in case of aerated solution (2ppm DO_2) it was in the range of 0 to -100mV suggesting the significant influence (Andresen and Duquette, 1980).

In all these cases dissolved oxygen will be the rate controlling factor determining the intensity of these reactions and the attack on the metal. Dissolved oxygen in water acts as a chemical potentiostat. The facts of this are clearly demonstrated by the effects of various concentration of oxygen, altering the attack on the specimen. The magnitude of the potentials recorded depend on the potential change can prevent loss of materials. However limited access of dissolved oxygen from the bulk solution to crack tip can be achieved by measuring the oxygen content in the plant more frequently to prevent failures. The cracking can be prevented by lowering the potential in high oxygenated water and can make cracking to occur by increasing the applied potential in low oxygen water. From this little discussion it can be summarised that dissolved O_2 has an influence on the following critical parameters of an alloy in service

a) Cracking Susceptibility of an alloy

b) Crack Velocity

c) Time to failure

d) Cracking potential

e) Percentage reduction of area (% ROA)

f) Fracture mode.

6.7 Effect of Temperature on SCC of SDSS:

The stress strain curves of SSRT tests of Zeron100 which are conducted at 100^0C and 130^0C at a strain rate of $1x10^{-6}$ $/s^{-1}$ are shown in Fig 4.21. The elongation and the maximum stress decrease with increase in temperature. The variation of elongation was reflected in the fracture characteristics of the specimen. The fracture morphologies for the tests 100 & 130^0C is shown in Fig: 6.18

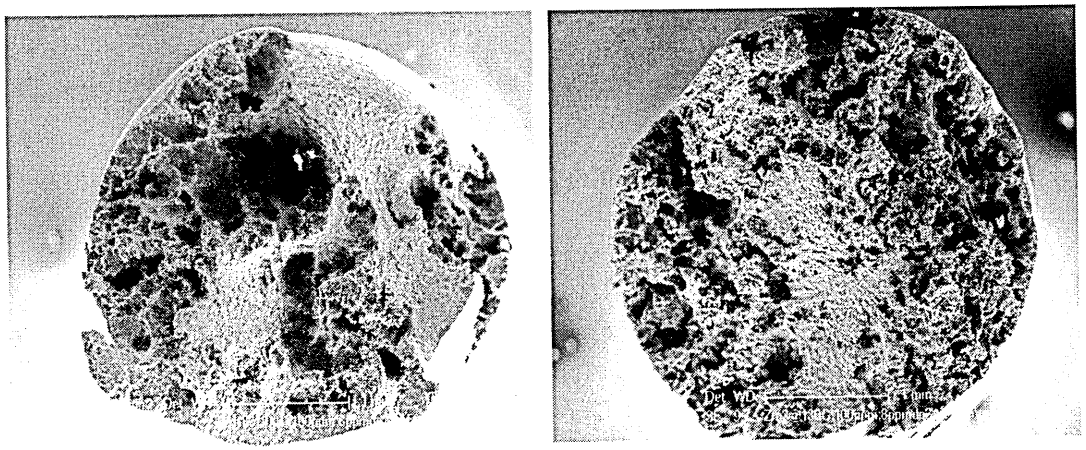

Figure: 6.18 Fracture surfaces showing a) ductility at 100^0C b) intergranular fracture at 130^0C in 100ppm chloride solution in 8ppm dissolved O_2 at +550mV.

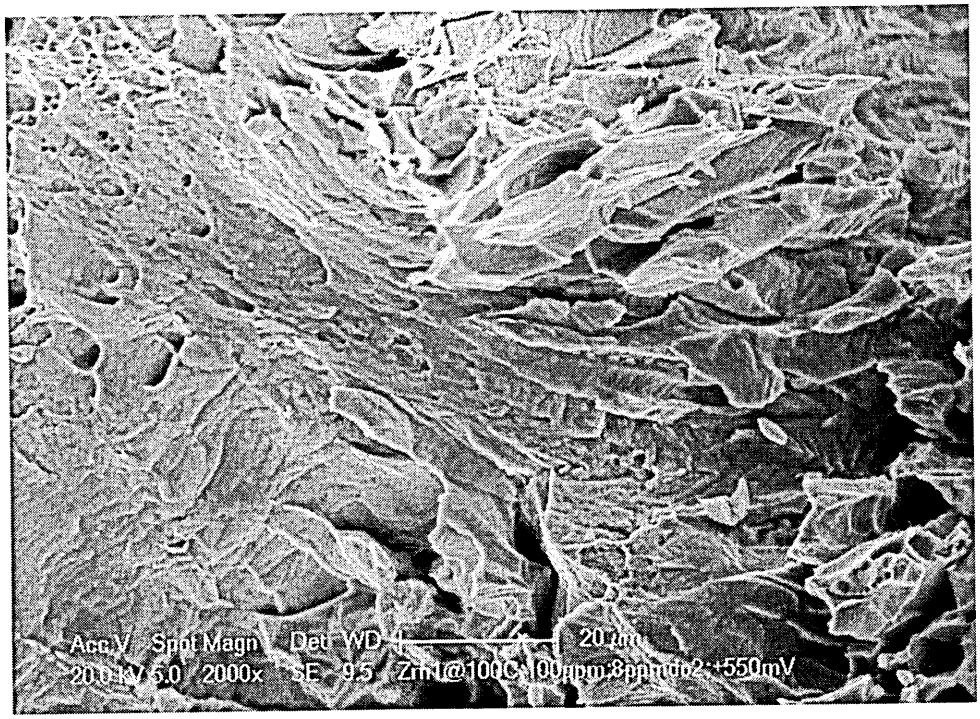

Figure:6.19 Fan shaped transgranular fracture mode observed at 100^0C in 100ppm Cl^- at +550mV applied potential (Ag/AgCl).

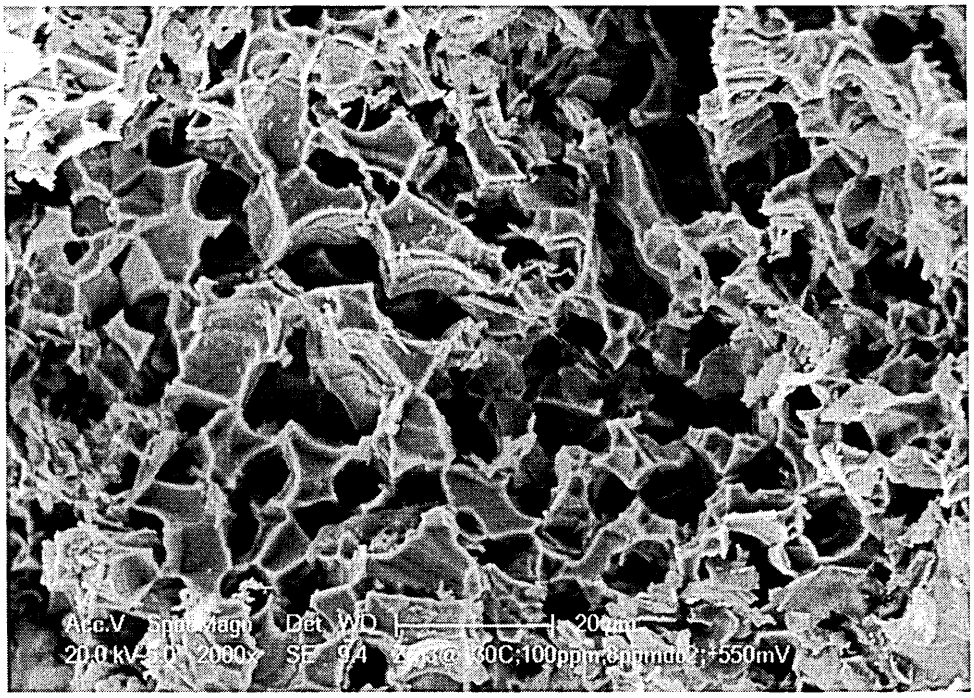

Figure: 6.20 Intergranular fracture mode observed in Zeron100 in 100ppm chloride solution at applied potential of +550mV

It is observed that a large deformation occurred around the fracture surface for the test at 100^0C. As temperature is increased to 130^0C the deformation tends to decrease as witnessed in SSRT curves shown in Fig4.21. Indication of degree of increase in brittleness was noticed as the temperature is increased.

Temperature is always known to play a significant part in the assessment of the SCC susceptibility of an alloy. In Fig 6.21, SCC cracks initiate perpendicular to the loading direction at 100^0C. As temperature increases, both the density of cracks and pit formation increase in 100 ppm chloride solutions. Plastically deformed regions are observed near the crack tips indicating possible slip step deformation process occur during the SCC of SDSS. It is evident from this result that SCC occurring at low temperatures is more stress dependent, as the applied stress is increased it allows the cracks to initiate and delay can occur before they link to final failure. On the other side, with increase in temperature to 130^0C aggressive pitting is observed which play an important role in the SCC process.

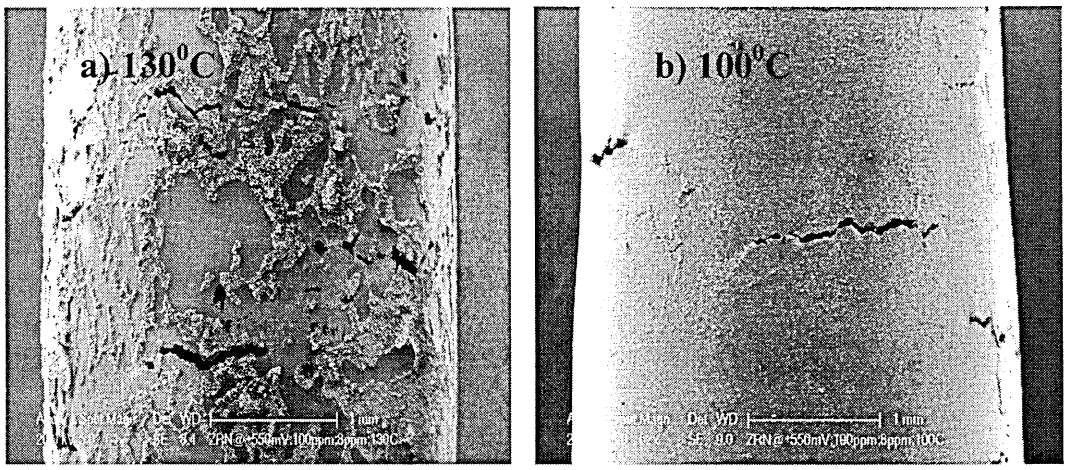

Figure: 6.21 Showing the difference in the attack on the samples under two different temperature conditions a) 130^{0}C b) 100^{0}C in 100ppm Cl solution; at +550mV

At 130^{0}C, shown in Fig.6.21 the nucleation of the cracks tends to become easier and more significant in the number of cracks formed on the surface. Thus it can be confirmed that temperature has a significant influence on the rate controlling step for initiation of SCC cracks. The high corrosion current values noticed at 130^{0}C indicate that crack growth rate is related to the current near the crack tips which allows the metal dissolution occur with ease compared to the one at 100^{0}C.

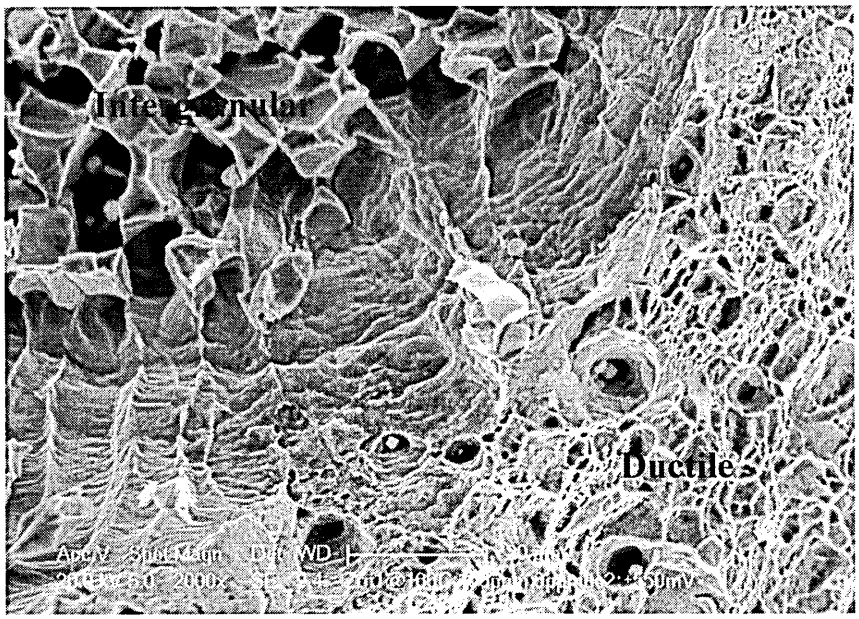

Figure: 6.22 Showing the transition from ductility to Intergranular failure mode; test conducted at 100^{0}C in 100ppm Cl$^-$; +550mV

Even at higher temperatures the transport of the ions on the metals to the bulk solution increase creating more acidic conditions near the crack tip.

One of the possible processes explained in the study of Maeng et al (2005) could have happened, which is due to the increase of transport rate of oxygen to metal surface from bulk solution, consequently increasing the reduction rate and anodic dissolution rate at the crack tips as temperature increases.

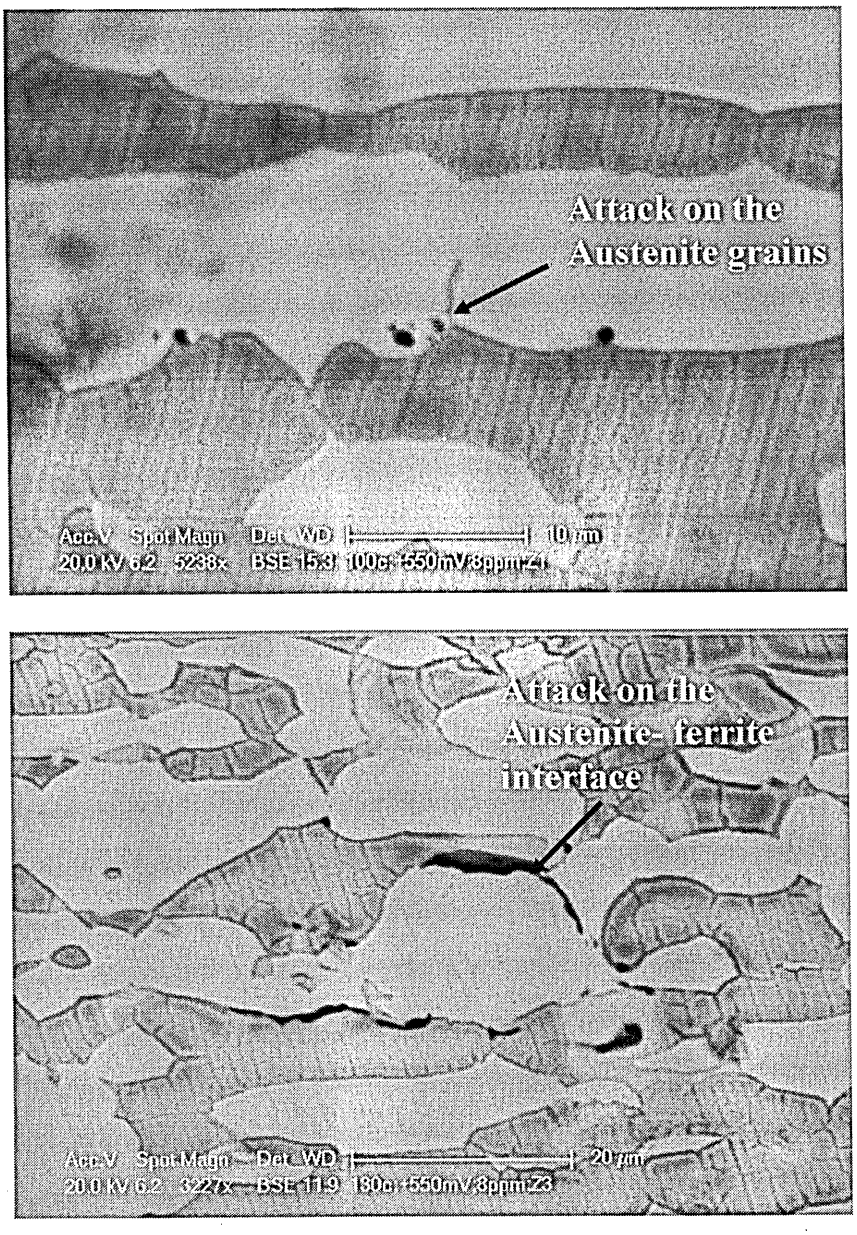

Figure:6.23 Showing the cross section images of the initiation of attack in Zeron100 SDSS in 100ppm chloride solution at a) 100^0C b) 130^0C with 8ppm dissolved oxygen

This kind of anodic dissolution can be controlled by reducing the reduction rate or the oxygen content in the solution to increase the failure time and the effect of dissolved oxygen is discussed later in this chapter.

The kind of temperature dependence is not only noticed in dilute chloride environments but it was also observed in sour environments by Van Gelder et al (1987). They concluded from their work that of all the environmental factors investigated temperature has a massive influence on the occurrence of SCC in duplex stainless steels in sour environments. Another study (El – Yazgi & Hardie; 1998) in sour environments has concluded that after pitting occurs small cracks tend to initiate and propagate by cracking of the ferrite and simultaneous dissolution of the austenite. Also with increase in temperature the cracks tend to get blunted by the accelerated corrosion reaction which agrees with the current study. Thus increase in temperature of the environment does alter the moment of the metal ions more easily compared to room temperature. Indirectly it can be said that temperature alters the passive film properties of the stainless steels and create more defect at high temperatures. Due to high chromium content in Zeron100 the passive film formed on it has got more resistance and stability to aqueous environments. Due to this outstanding protective film combined with additional metallurgical elements nitrogen and molybdenum it is believed to have high stress corrosion resistance. Unless the film cooperates to the metal dissolution it is often difficult to cause SCC in Zeron100

Relationship between critical potentials for stress corrosion and pitting:

The polarization curve obtained in the 1000ppm chloride solution suggests that passive film formed on the surface could play an important role in SCC evaluation. The polarisation curve indicates the crack initiation region and also highlights the

regions of rapid crack growth process. An example of polarisation curve related to this study conducted at 130^0C in 1000ppm chloride solution with a scan rate of 30mv/min is shown in Fig 6.24. It is important to note that polarisation curves depend on several parameters like surface finish, scan rate, temperature and dissolved oxygen. In order to make a consistent comparison the conditions are maintained as near as possible to the SSRT tests to establish a relationship. Since the polarisation curves are generated potentiodynamically it is often not consistent with potentiostatic test condition used for SSRT tests as the crack tip chemistry will be different to the bulk chemistry, which have an impact on the passivation behaviour of the material.

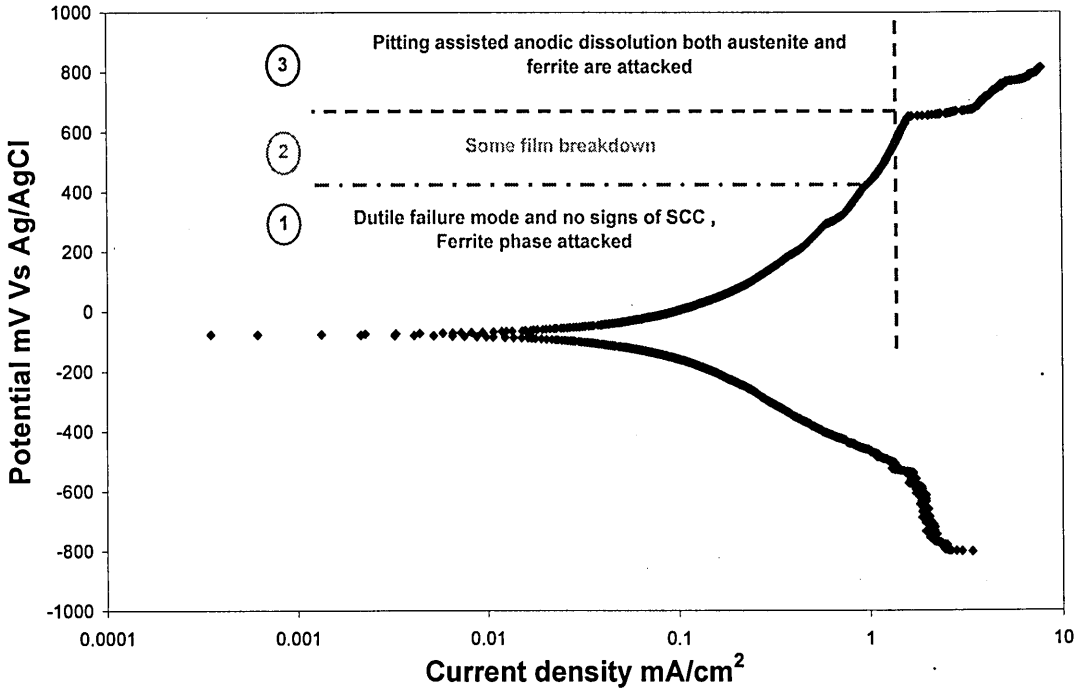

Figure: 6.24 Polarisation curve identifying the SCC behaviour of Zeron100

But one should remember that electrochemical data generated under identical polarization and SCC conditions would give useful knowledge in order to assess the EAC behaviour. As pitting is considered to be the dominant process in the stress corrosion of DSS in the previous studies (Wen-ta Sai et al, 2000), it is expected that a close relationship exists between the critical potentials for pitting and stress corrosion

even in case of Zeron100 SDSS. Fig 6.24 shows a relationship between the polarisation curve obtained at 130^0C in 1000ppm chloride solution in 8ppm dissolved oxygen and EAC regions in those conditions. The critical potential for pit initiation (E_P) is found to be +625 mV (as shown by inverted arrows in Fig6.3 from the polarisation curve. From Fig 6.3 it can be noticed that critical cracking potential for SCC to occur E_{SCC} = +500mV in 1000ppm chloride. The more positive value of E_P compared to E_{SCC} indicates the contribution of stress to crack initiation easier compared to the pit initiation. The study conducted in 35 % boiling $MgCl_2$ by Kwon and Kim (1993) on Ferallium alloy 255 duplex steel reported that critical cracking potentials for SCC to occur is negative value compared to the pitting potentials. Interestingly their study showed that critical cracking potential is close to the repassivation potential (E_{rp}) of growing pits in boiling $MgCl_2$ solutions, which means that cracks grow and pits repassivate at the same potential. In the current study the E_{rp} value in 1000 ppm chloride is found to be +150 mV which is a negative value compared to E_{scc} value, which implies that in case of SDSS and dilute chloride solutions pits tend to repassivate at very low potential values and cracks tend to initiate at more positive potential values.

According to the studies, of Ta Tsai and Shan Chen (2000) on 2205 DSS in 26wt% NaCl solution of pH 6.0 at 90^0C reported that critical potential for SCC, E_{SCC} was coincident with pitting potential determined under similar conditions. They also mentioned the importance of pits in initiation of SCC near the pitting potentials, but the repassivation potential is found to be very negative and they didn't try to comment on the E_{rp} values it seems that the link between E_{scc} and E_P only depend in certain chloride concentrations and temperatures. As it was found even in the case of present investigation on Zeron100 the E_{rp} values seems to be very negative similar to

the study for 2205 DSS. SSRT study on 304 stainless relating environmental and electrochemical variables on SCC resistance was reported (Andresen and Duquette 1980). The results of critical potential for SCC and the pitting potentials were found to be similar for 304 stainless steels in 100ppm Cl^- and they referred in their paper of the study (Hoar et al, 1965) to say that the coincidence of potentials could be the critical potential value for Cl^- ion to penetrate the film. On the contrast in case of 304 in 100ppm Cl^- at 289^0C mechanical film rupture has an insignificant influence on the SCC behaviour (Andresen and Duquette, 1980).

It should be pointed out that the a polarisation curves determined under similar conditions of SSRT tests give valuable information in the present investigation about the fracture mode observed in the SSRT tests, indicated by regions shown in Fig 6.24. Significant film breakdown can happen in the region 2 indicated by dashed lines, starting 200mV below E_P when the stress is applied during the SSRT tests. Below this region indicated as 1, ductile failure mode with no evidence of pitting was observed as discussed in the section. It is noted that above pitting potentials indicated by region 3, severe pitting assisted anodic dissolution was predominantly observed. Nevertheless these electrochemical measurements do give adequate information about SCC behaviour of any alloy.

It is clear from these few studies that a link between E_P and E_{SCC} might be alloy dependent, unless a systematic study is performed it is hard to establish a definite relationship, however from these limited studies it is important to realize the role of pitting in the loss of cross section of these SDSS. The film breakdown process appears to commence at about 200mV lower potential than the unstressed samples in the SSRT tests. The results in Fig 6.25 give a good relation between pitting and stress corrosion potentials under similar conditions.

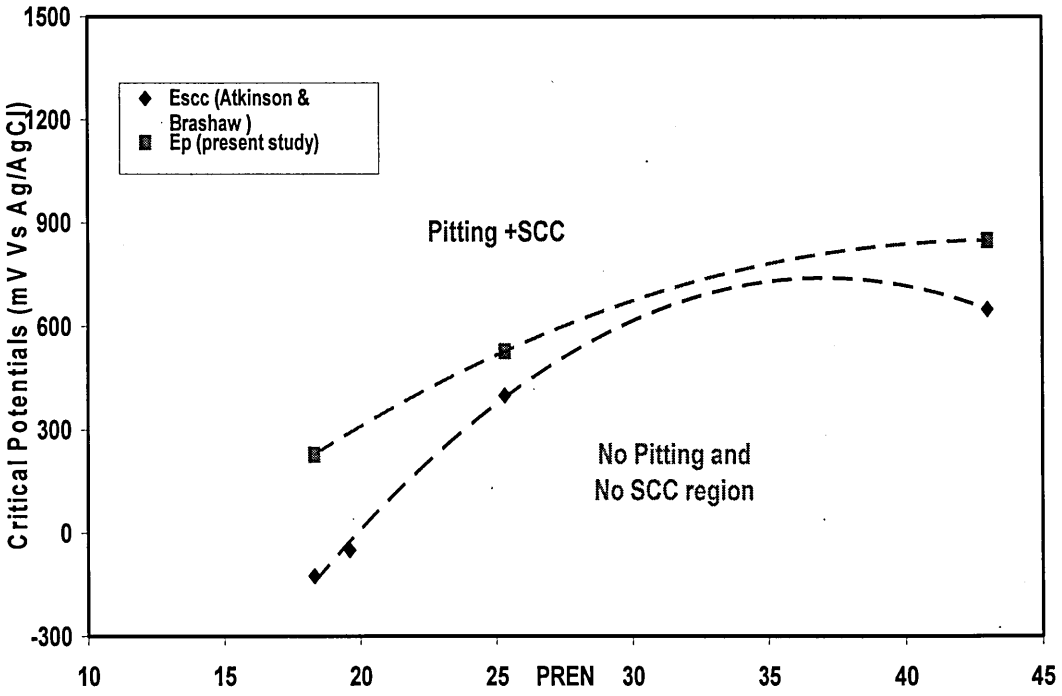

Figure: 6.25 Relationship between chemical composition and critical potentials for pitting and stress corrosion cracking potentials at 130^0C in 15 - 30ppm, Cl^-.

$$E_P = 86\,[PREN] - 0.99\,[PREN]^2 - 1020 \qquad (6.2)$$

$$E_{SCC} = 186\,[PREN] - 2.5\,[PREN]^2 - 2720 \qquad (6.3)$$

These empirical relations can be used by a plant engineer working in a power industry, as these tests conditions will represent conditions in the low pressure steam turbine. These equations will predict the critical pitting and stress corrosion potentials for wide range of materials in high purity water with very little contamination. So it is not necessarily determine for one particular material say FV520B or FV566 with lower PREN values that are commonly used as steam turbine blade materials, it also predicts the damage conditions for other materials used in steam flow lines, feed water to the boilers etc.

Crack Initiation in Zeron100:

Pits tend to act as a crack initiation sites for stress corrosion, but no direct studies exist on the role of pitting in stress corrosion of duplex stainless steels. Pits acts as stress concentration areas and they are most favourable areas for the crack initiation. Pits tend to form on the surface of the gauge length of the specimen tested near the pitting potential values as shown in Fig: 6.26 and indicated by arrows.

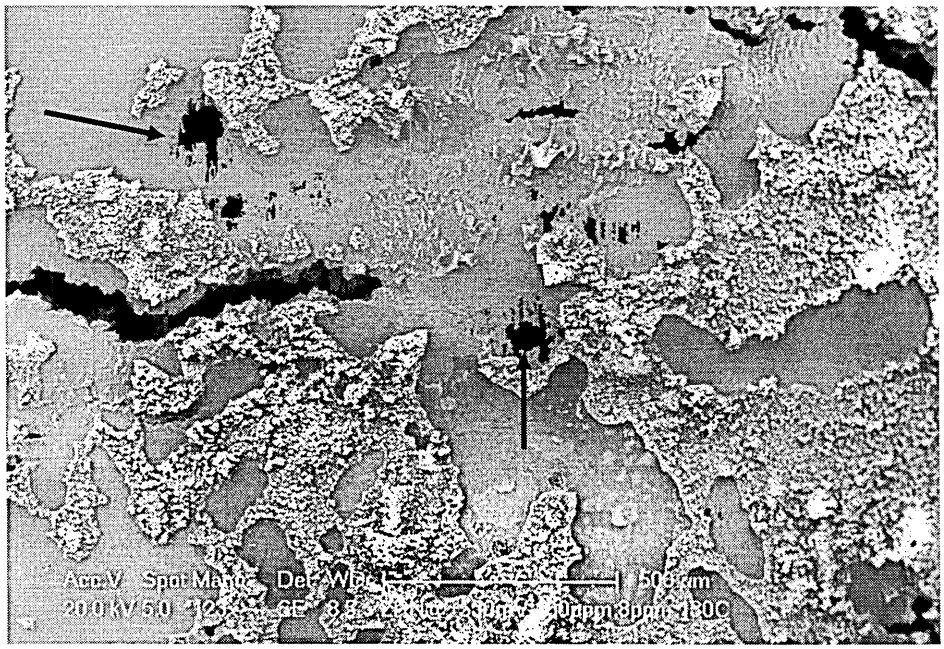

Figure: 6.26 Isolated pits formed on the gauge length of the SSRT sample near to the cracks for the test conducted at 130^0C in 100ppm chloride solution at +550mV

Direct observation shows few pits tend to involve with crack propagation, examples of it are shown in Fig 6.27 & 6.28, where the cracks are linked to the pits. Pits make the crack propagation process effective by changing the crack tip chemistry. Recently it has been reported (Shibata, 2007) that almost 30% of reported cases by corrosion failures, trouble is caused by localised corrosion which include mainly pitting and SCC in nuclear power stations. These kinds of statements do strengthen the importance of current study in simulated power plant conditions.

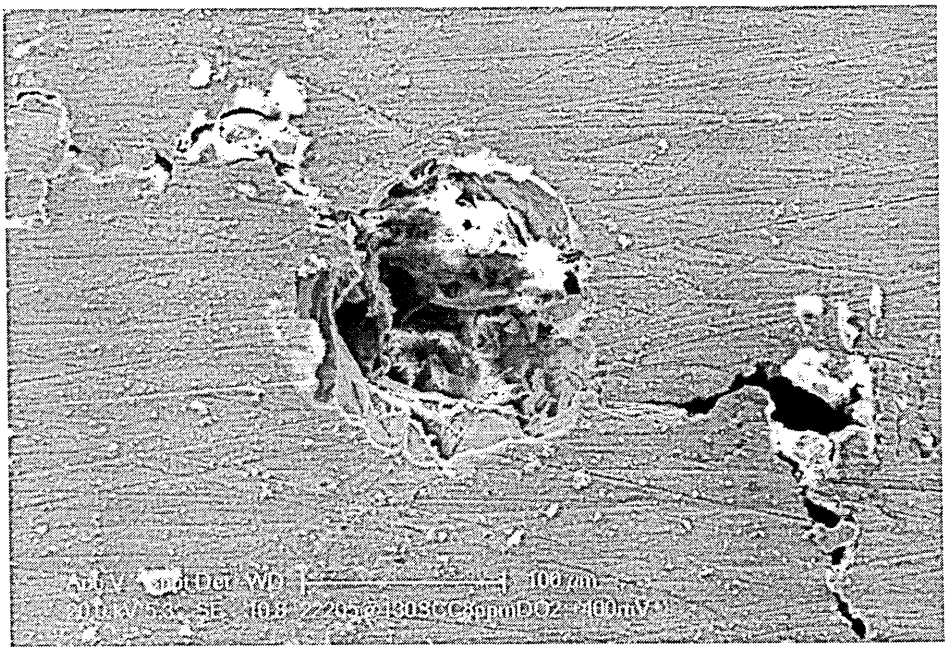

Figure: 6.27 Pits associated with cracks in 2205 duplex stainless steel at 130^0C in 1000ppm chloride solution

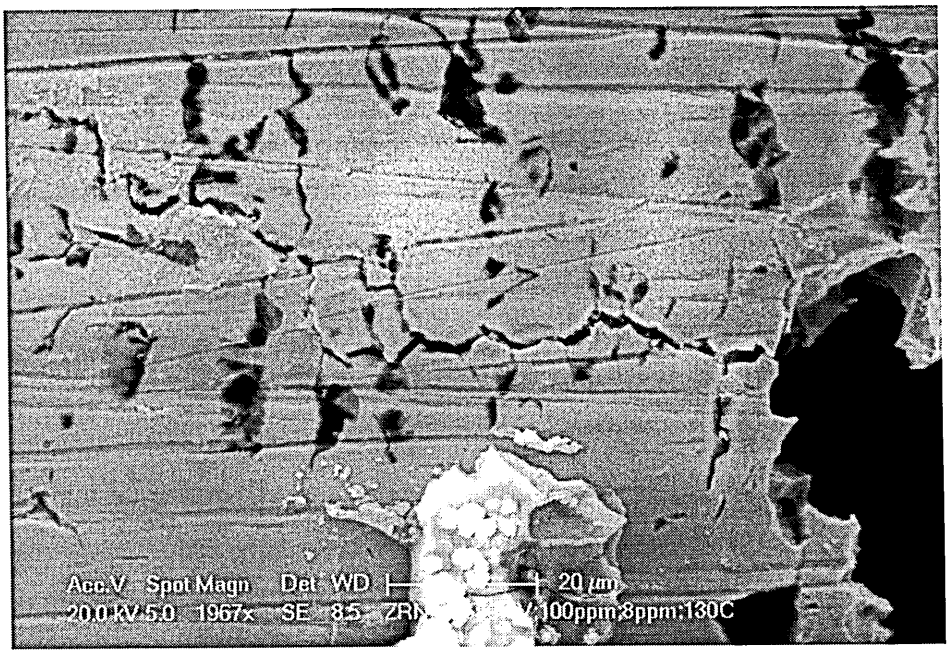

Figure: 6.28 Cracks nucleating preferentially at the bottom of a pit; test conducted at 130^0C in 100ppm chloride solution at +550mV with 8ppm dissolved oxygen

When stress corrosion cracks are nucleated they tend to be very short and occur below yield stress tend to stop after they grow for while. When pits are present these tend to reactivate these short cracks and make them involve in the failure process,

which is not a favourable condition to estimate the service life of the component. It is probable that since a SSRT test is a long-term test, pits will form by breakdown of the film due to mechanical stress. Cracks that initiate from pits may cease to propagate or eventually they coalesce with others reducing the strength of the material (Parkins, 1988).

This kind of observation is not only restricted to one type of material it was seen in 2205, 255 and Zeron100 duplex stainless steels.

From these kinds of observations it suggests that although a material is susceptible to stress corrosion it is important to know whether it involved in any localised corrosion process.

Crack coalescence:

The observation of the surfaces of the failed specimens after the SSRT test was examined using scanning electron microscopy and found crack coalescence played a major part in the failure process. It is evident that two crack tips initially travelling in different directions for short distance suddenly turns in opposite direction such that the crack tips are merged and travel as a single crack that results in final fracture. This kind of phenomenon was first noticed in pipeline steels in the studies conducted by Parkins and Singh (1990). The identical process even occurs in the coalescence of short cracks. Once the short cracks coalesce they tend to merge with longer cracks to form a path, although they both travel with different rates on the same surface as shown in Fig 6.29.The chance of coalescence increase with increase in the crack density. However it is well known that crack tip strain rate for short cracks is lesser compared to the bigger cracks as crack tip strain rate is a function of number of

cracks. It is a less severe condition if the number of cracks is more to that of less number of cracks.

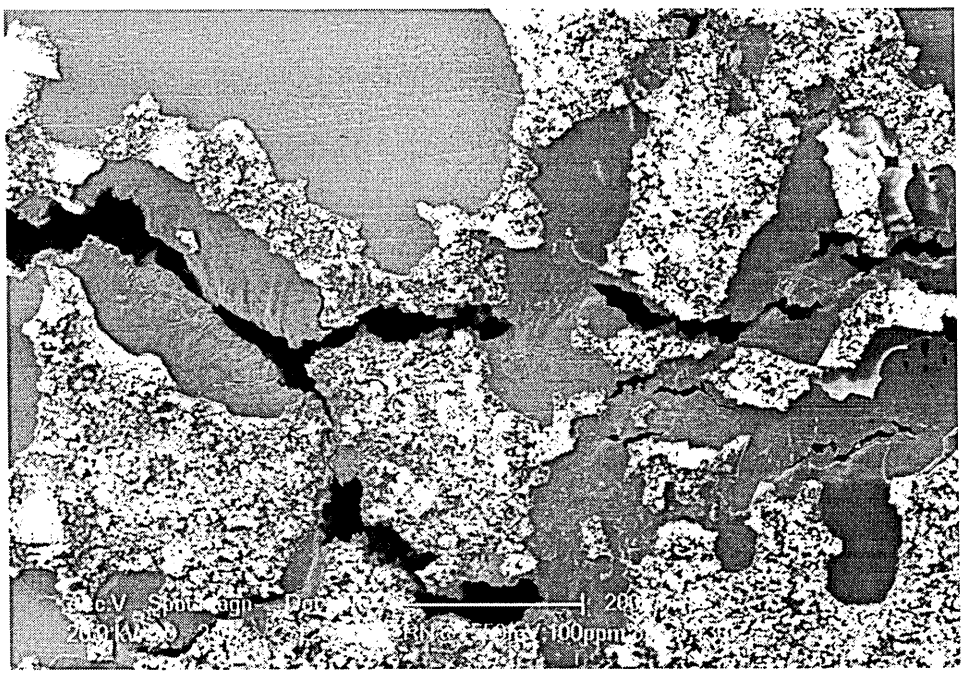

Figure: 6.29 Showing the coalescence at (+550mV; 100ppm Cl^-;) of the closest crack tips and the change in the direction before coalescence occur both for large and small cracks.

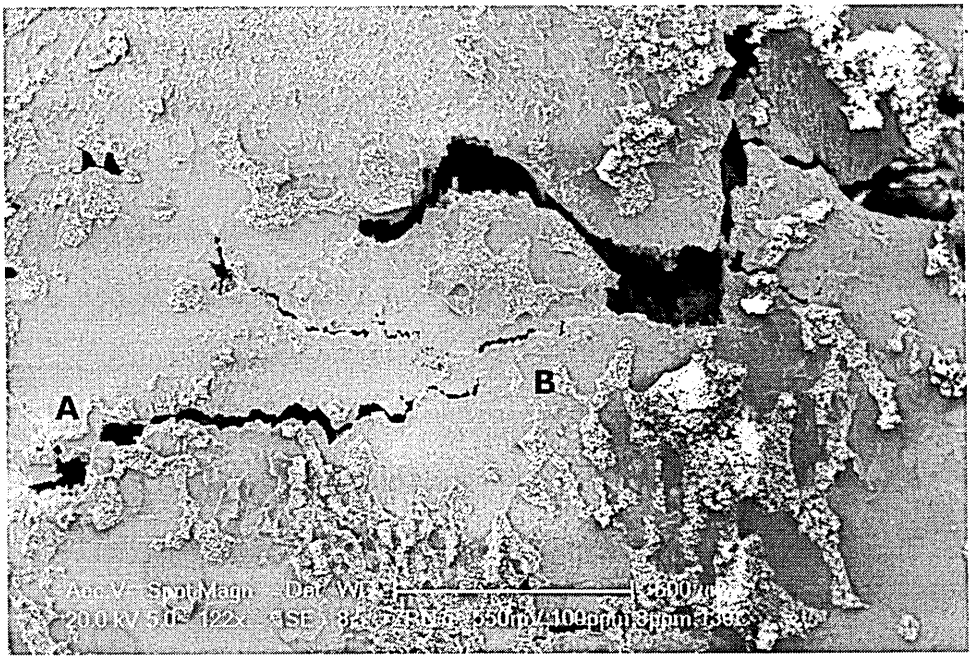

Figure: 6.30 Showing the tendency for short cracks that grow and coalesce about a line AB and merging into the longest cracks (Pot: 550mV; 8ppm O_2; 130^0c)

6.8 Mechanism of SCC damage in Zeron100 SDSS in DSS:

The mechanism of SCC damage in Zeron100 SDSS was found to be very complex from these preliminary investigations in dilute chloride environments

The fracture appearance in SDSS is found to be complex, but this study shows that it might involve two processes, as it was found to be

a) Pitting assisted anodic dissolution of both austenite and ferrite phases close to the pitting potentials (Zone 2)

b) Selective phase attack involving ferrite is evident below the pitting potentials.

The phenomenon of pitting assisted anodic dissolution is in general agreement with the other studies (Wenta-sai et al, 2000; Guenter, 1980) for duplex stainless steels conducted in concentrated chloride solutions. The possible reason for the selective corrosion in the passive potential range of Zeron100 might be due to the effect of local PREN. As is can be seen from the Fig 6.33 the loss of cross section is due to repeated blunting/ re-initiation of the pit perhaps due to local acidification near the pit bottom that allows the pits to grow after certain time intervals again.

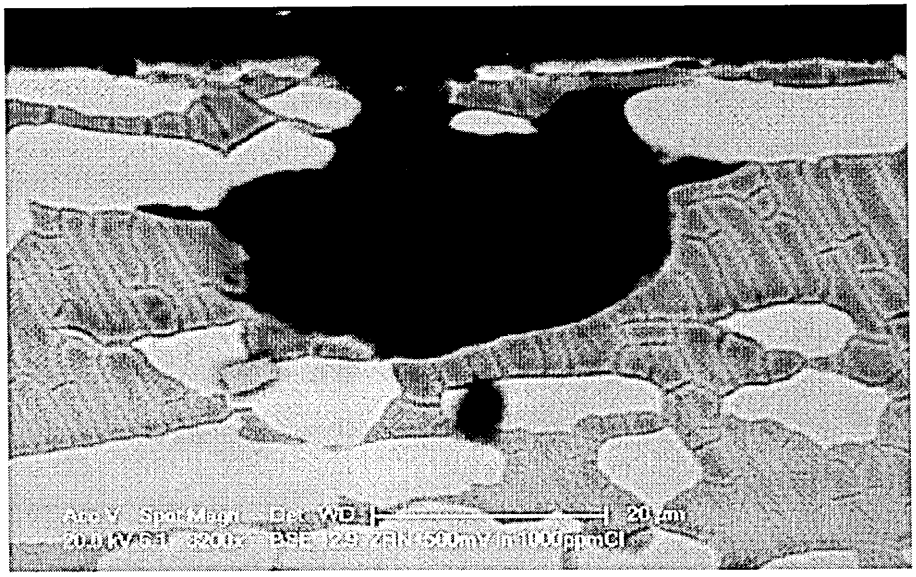

Figure: 6.31 Showing the micrograph of the preferential attack of ferrite on the cross section of the gauge length observed after SSRT test at +500mV in 1000ppm Cl^-

The process of accumulation of chloride ions in the potential gradient decreases the pH near the pit bottom and then allows it to propagate.

Whereas the selective phase attack as shown in Fig 6.32 is due to the difference in the chemical composition of the two grains, and the chemical breakdown of the passive film which controls, when the ferrite grain is preferentially dissolved, might be due to a weak passive film.

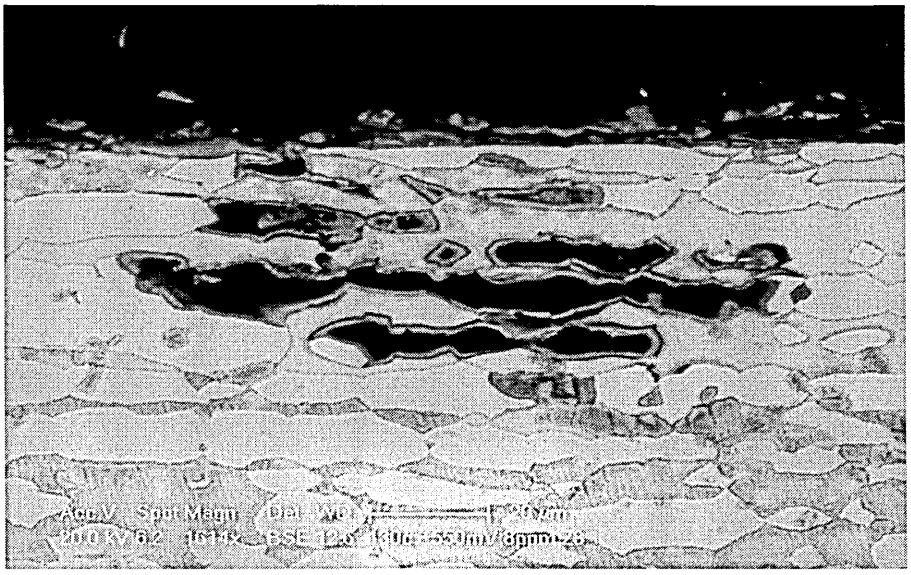

Figure: 6.32 Selective ferrite phase attack was noticed at 130^0C in Zone 2

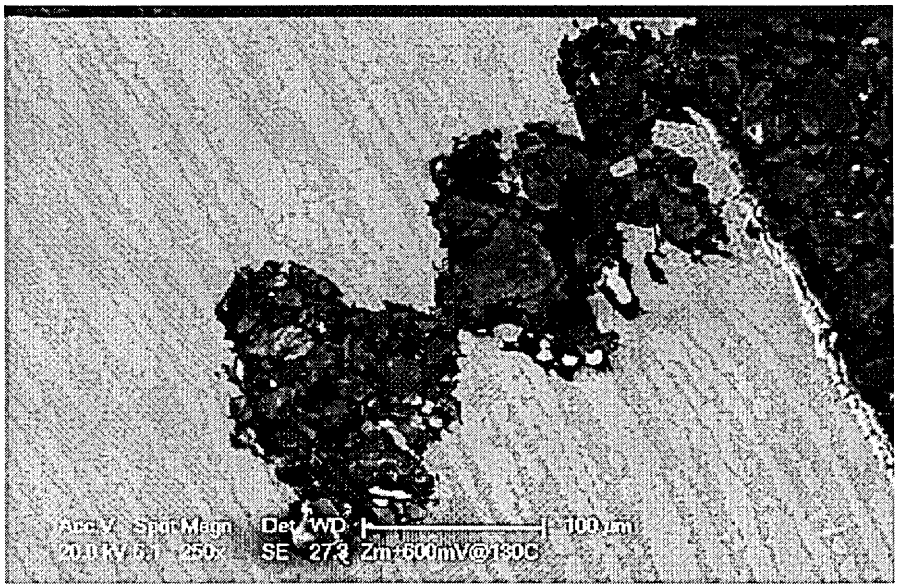

Figure: 6.33 Propagation of blunted crack through both austenite and ferrite phases observed in SSRT test conducted at 130^0C in 15ppm at +600mV.

During this process the austenite is cathodically protected and acts as a crack arrester, which increases the failure time. However more fundamental understanding on the passive film formed on the individual phases of duplex stainless is required in order to understand selective phase attack of these SDSS. The crack path observed equally in both the phases seems to be in agreement with the point made by Cottis and Newman (1993), that it can be achieved through the addition of nickel and molybdenum as they both settle in different phases (Ni in austenite and Mo in ferrite). Equalisation achieved through segregation of compositional elements resulted to crack both phases equally.

An effective measure to prevent SCC in SDSS is to maintain lower potentials $<E_P$ in the plant environment, which can also prevent localised corrosion. It is evident from this study that the electrochemical potential plays such an important role that it completely dominates the EAC behaviour. It is also apparent that SDSS can be degraded by chloride levels much lower than found in seawater or dry out zones.

Reported studies Vs Present study on SCC of Duplex steels:

The hazard of SCC under the combined influence of chloride, temperature, oxygen, and potential could be elevated by increasing either of these parameters or decreasing the severity of these parameters. Loss of control of these parameters would mean more damage to the plant. A diagrammatic representation or a map plotted in this study will be useful to safeguard the duplex and super duplex stainless steels to foresee the damage zone.

a) O_2 level Vs $[Cl]^n$ diagram:

One way to represent the current understanding of the SCC studies and to establish the importance and add the value of the current study is through the demonstration of O_2 Vs $[Cl]^n$ diagram.

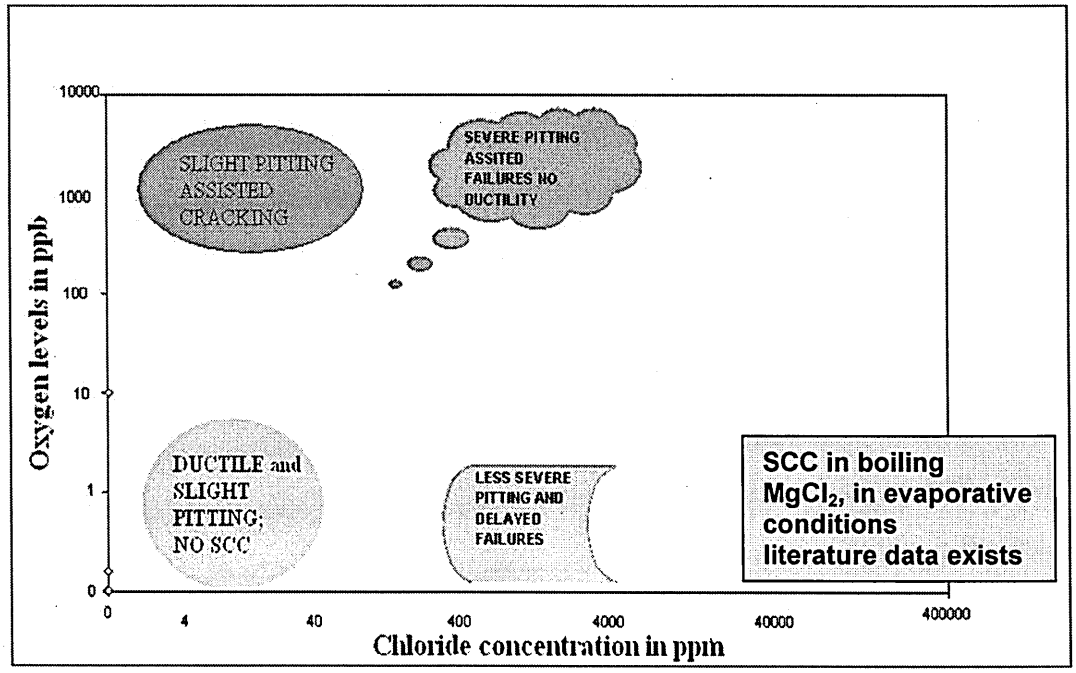

Figure: 6.34 Schematic diagram showing different failure modes for O_2 Vs $[Cl^-]$

b) E_{scc} Vs $[Cl]^n$ diagram:

Critical SCC potential (E_{SCC}) values from experimental SSRT test results and published literature was used in the construction of more general diagram. The values taken from different studies to plot the graph were converted to Ag/AgCl reference electrode scale for convenience.

The diagram defines practical conditions for prevention and control of SCC in chloride solutions for wide range of conditions. The diagram also gives information about temperature and oxygen levels and their influence on the SCC of duplex stainless steels. The validity and the consistency of the present diagram has been checked by input of several data collected from various studies in the literature and found to be in good agreement. The significance of these diagrams has been

extended to pitting corrosion produced using potentiodynamic polarisation curves. One of the critical information that can be understood is that in solution containing more chloride ions the SCC potentials tend to shift towards more negative values, and at this condition they depend very little on temperature and oxygen as enough damage to SCC to occur is already been induced.

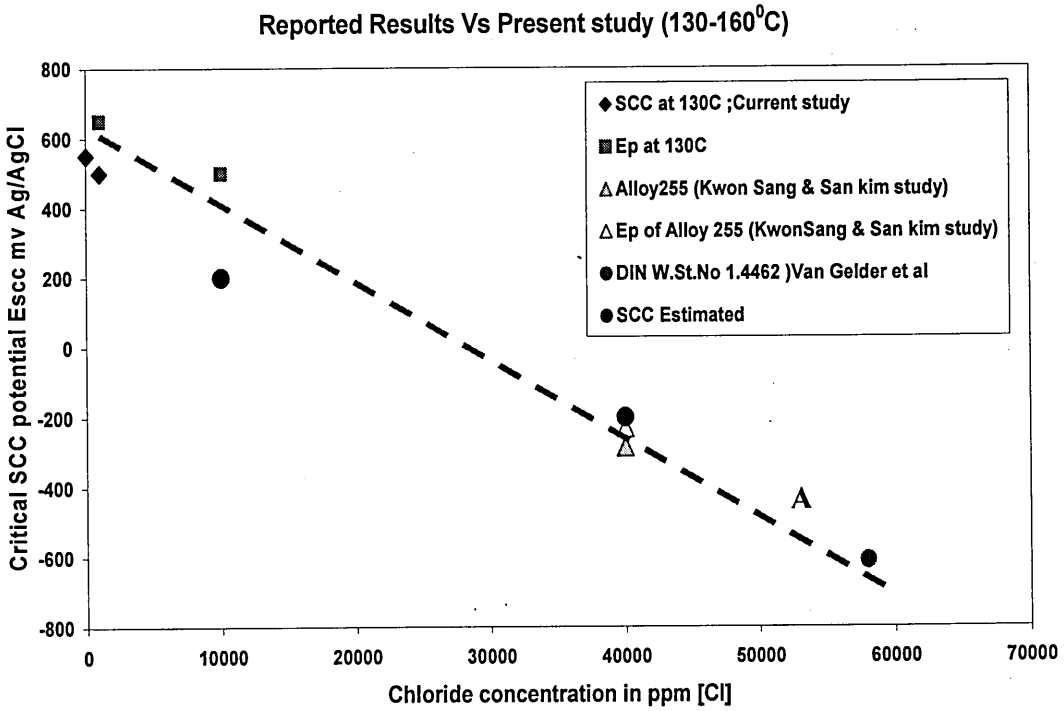

Figure: 6.35 E_{SCC} Vs [Cl^-] relation, E_{SCC} decreases with increase in [Cl^-]

1. The map clearly shows the decrease in critical SCC potential (E_{SCC}) for crack propagation and the region below line A is clearly the upper limit of the critical potential values for SCC to occur.

2. The map can also link different fracture modes for different critical SCC potentials which was shown for Zeron100 in page 156.

3. This map can be used in considering the design limits for the offshore applications to prevent hydrocarbon incidents.

4. This map would allow to guide and predict the region of SCC approximately.

5. The map indicates that there is threshold level (line A) below which cracking will not propagate/occur.

6. Fig 6.34 indicates that there are two extremes possible in a plant both in oxygenated and deoxygenated environments.

This kind of collective maps might serve as the guidance for purposes of future design and equipment. The most dangerous situation arises when all these parameters cannot be controlled and are at their peak which can be determined by the individual operations of the plant. Thus decreasing any of these parameters temperature, chloride concentration, applied potential & dissolved oxygen for one single condition would allow to benefit in order to increase the failure time.

c) Limitations of E_{scc} Vs $[Cl]^n$ diagram:

a) The data collected to check the validity, ignore the type of experimental technique used in various studies to find out the SCC susceptibility.

b) The diagram was restricted for the conditions below 200^0C.

c) The diagram indicates the initiation zone but does not predict the type of failure mechanisms.

CHAPTER 7

7.1 CONCLUSIONS

The overview of pitting and stress corrosion potentials of stainless steels presented in this study indicates the complexity of the phenomenon. Some of the significant conclusions of the current study are

1) The mathematical model equation proposed in chapter 6, p179 for all PREN values will allow prediction of pitting potentials (E_P) in 15ppm chloride at 130^0C.

$$\mathbf{E_P = 86\ [PREN] - 0.99\ [PREN]^2 - 1020}$$

2) The mathematical model equation proposed in chapter 5 for a fixed chloride concentration of 1000ppm for wide range of steels (PREN 13.6 - PREN 43) and temperature range of (65 - 170^0C)

$$\mathbf{E_P = C - D\ [Temp^0C]}$$

the values of C, and D were given in Table 5.3 on page 146.

3) A mathematical model equation was proposed for a fixed temperature (130^0C) for wide range of PREN and different chloride conditions (15 -10000) ppm is given as

$$\mathbf{E_P = (PREN)^2 - B\ ln\ [Cl^-]}$$

The values of B for various PREN values were given in Table 5.2 on page 144.

4) The beneficial effect gained by addition of nitrogen and molybdenum to achieve the maximum levels of localized corrosion resistance at 25^0C, is observed to

disappear when these steels are tested at high temperature above 130^0C. The pitting potential decrease with increase in temperature for wide range of stainless steels tested under different chloride solutions in 8ppm dissolved oxygen. Increase in chloride concentration increase the critical pitting current density, and decreases the E_P values, for various temperatures. The repassivation or breakdown potentials varied within a range (200mV) with increase in temperature for all the steels measured.

5) The stress corrosion resistance of Zeron100 was found to be superior compared to the 2205 and Ferralium alloy 255 duplex steel grades under the conditions tested. Crack initiation from pits and crack coalescence, play an important in the failure of Zeron100 SDSS.

6) Three potential zones were identified to define the SCC degradation of Zeron100 SDSS, in chapter 6 on page 158 they are

Zone a) Corrosion damage, fully ductile,

Zone b) Isolated pits/cracks, ductile and

Zone c) Large coalesced blunted cracks with severe loss of ductility

7) The SCC mechanism operating on Zeron100 in the dilute chloride solutions is potential dependent and involves two kinds of processes a) pitting assisted anodic dissolution of both austenite and ferrite phases occurring above critical corrosion potentials (Zone 3) and b) preferential ferrite attack occurring in the passive region (Zone 2). The critical EAC potential (E_{EAC}) was observed to increase with increase in PREN. This study show that even 15 ppm chloride is enough to cause EAC damage

to these expensive steels at high applied potentials > +550mV (Ag/AgCl) in 8ppm oxygen at 130^0C.

8) Anodic metal dissolution is more severe in the high oxygen environments than in low oxygen at constant applied potential of +600mV (Ag/AgCl), indicating that failure times can be altered with change in oxygen content, and a severe galvanic attack (on the ferrite) mode of failure can take place without cracking above 100^0C.

9) Finally the available results through this study can be often used to compare different alternative alloys when materials selection is made and the trends of this study will be applicable to other alloys systems in terms of localised corrosion. The reduced performance of SDSS observed above 65^0C should be noted by users and attempts make to raise the temperature ceiling by further alloy modification.

7.2 Suggestions for Future work

1) The present work can be extended to study the behaviour of Zeron100 under cyclic loading conditions under potential control in order to determine the Critical corrosion fatigue potential (E_{CF}) to establish a relationship among E_p, E_{SCC} and E_{CF}.

2) Determination of the properties of surface films a formed on DSS and SDSS at elevated temperatures might give better understanding of the improved behaviour these materials under certain conditions.

3) Extending the slow strain rate technique to study the performance of DSS and SDSS in seawater solutions at elevated temperatures at very slow strain rate will

definitely give an insight of the mechanism and can predict the failure time. This will require a more corrosion resistant experimental facility.

4) A Three dimensional mathematical model should be developed from the data collected in the present study in order to determine the pitting potential values.

REFERENCES

Abd El Meguid E.A, Abd El Latif A.A(2007) "Critical pitting temperature for type 254SMO stainless steel in chloride solution" Corrosion science,Vol 49, p263-275.

Alfonsson.E and Qvarfort.R, (1991) AvestaAB, conf proc, Electro chemical methods in corrosion research. EMCR, July 1-4, 1991, Helsiniki, Finland.

Andresen.P.A and Duquette. D.J (1980) "Slow strain rate stress corrosion testing at Elevated temperatures and High pressure" Corrosion Science, Vol 20, p211 - 213.

Andresen.P.A and Ford.P (1980) "Counter measures of pipe cracking in BWRs" EPRI – WS – 79 – 174, Vol 1, paper 7.

Angelini.E, B.De.Benedetti, Rosalbino.F, (2004) "Microstructural evolution and localized corrosion resistance of an aged super duplex stainless steel" Corrosion Science, Vol 46, p1351-1367.

ASTM E8, "Standard test methods of tension testing of metallic materials,"E8, Annual book of ASTM standards, Vol 03.01, ASTM

ASTM G 48, 1995 Annual book of standards, section 3.02, American society for testing and materials, Phildelphia (1985)

Atkinson. J.D and Clive Brashaw (1999), unpublished work; BNFL, Sellafield, 2005.

Bandy.R, Van Rooyen.D (1983) "Pitting resistant alloys in highly concentrated chloride media" Corrosion; Vol 39, No6, p 227-236.

Bandy.R, Y.C.Lu, Newman.R.C, Clayton.C.R, Surface enrichment of nitrogen during passivation of a highly resistant stainless steel" Proc.Electrochemical Society 86 (7), (1986) p 323 -339.

Bayoumi.M.Fathy and Ghanem.A.Wafaa (2005)"Effect of nitrogen on the corrosion behaviour of austenitic steel in chloride solution" Materials Letters, 59, p 3311 - 3314

Bela leffler "Stainless steels and their properties"2nd revised edition, Avesta Sheffield AB

Brigham R.J and E.W.Tozer (1973),"Temperature as pitting criterion" Corrosion, Vol29, No 33, p33-55.

Brookes H.C and Graham F.J (1989) "Influence of the electrolyte and alloy composition on the pitting behaviour of stainless steel alloys" Corrosion ,Vol 45, No 4, p 287-293.

Burstein.G.T, Pictorius.P.C, and Mattin.S.P (1993) "The Nucleation and growth of corrosion pits on stainless steel" Corrosion science, Vol35, No 1- 4, p57-62.

Burstein G.T and Ilevbare G.O (1996) "The effect of specimen size on the measured pitting potential of stainless steel" Corrosion Science, Vol 38, Issue 12, December 1996, p2257-2265.

Charles.J (2007) "Past, present, and future of the duplex stainless steels" Duplex 2007, Grado, Italy.

Chen Jia and Kuo Wu Jiann (1990) "The improved passivation of iron induced by additions oftungsten" Corrosion Science, Vol 30, Issue1, p53-58.

Cleland.J.H (1996)"What does the pitting resistance equivalent really tell us", Engineering Failure analysis, Vol 3, No 1, p 65 - 69.

Clarke.W.L and Gordon .G.M (1973) "Investigation of stress corrosion cracking susceptibility of Fe – Ni – Cr alloys in nuclear reactor water environments" Corrosion,Vol29, No 1, p 1- 12.

Combarde.P, Audouard J.P (1991), "Pitting resistance of duplex stainless steels" Editor J. Charles (Ed), Duplex Stainless steel Proceedings, Vol 1, Beaune, France, p257.

Cottis R.A, and R.C Newman, (1993) "Stress corrosion cracking resistance of duplex stainless steels" Report OTH 94 440, HSE.

Coussement.C. and Fruytier.D.J (1991) "An industrial application of duplex stainless steel in the petrochemical industry: a case study, failure analysis and subsequent investigations" Proc Conf Duplex Stainless steels, 28-30 Oct, Beaune, France, p 510 – 521.

Congleton .J, Shoji.T, Parkins.R.N (1985) "The stress corrosion cracking of reactor pressure vessel steel in high temperature water", Corrosion Science, Vol 25, p 633.

Cragnolino.G (1987)"A review of pitting corrosion in high temperature aqueous solutions" Proc International Conf on Localised corrosion , Orlando, Florida, USA, Vol 1, p 413 –431.

Cragnolino C.A and Sridhar.N "Localized corrosion of a candidate container materials for high-Level Nuclear waste disposal", Corrosion, vol 47, No.6, p 464 -471.

Cristofaro N.D.E, Piantini.M and Zacchetti.N "The influence of the passivation behaviour of a super duplex stainless steel in a Boric – buffer solution" Corrosion science, Vol.39, No 12, p 2181 – 2191.

Danielson, Mike J (1983) "A long lived external Ag/AgCl reference electrode for use in high temperature/pressure environments", Corrosion, Vol 39, No 5, p202-203.

Davis.J.R, CORROSION understanding the basics, Edited by J.R.Davis & Associates, Page no 168 ASM International, Material Park, Ohio

Davison R.M. and Redmond J.D (1991),"A guide to using duplex stainless steels", Materials and Design, Vol.12, No 4.

Desestret.A and Charles.J, (1993) Duplex stainless steels, in: Lacombe.P, Baroux.B, Beranger (Eds), stainless steels, Les editions de Physique Les Ulis, France.

El-Yazgi.A.A and Hardie.D (1998) " Stress Corrosion of duplex and super duplex stainless steels in sour environments" Corrosion science ,vol 40, No 6, p 909 – 930.

Evans .H.E, Hilton.D.A, Holm.R.A and Webster.S.J (1980) "The development of localized pits during stainless steel oxidation" Oxidation of metals, Vol 14, No 3, p 235-247.

Ergun.M and Turan.A.Y(1991) "Pitting potential and protection potential of carbon steel for chloride ion and the effectiveness of different inhibiting anions" Corrosion science, Vol. 32, No 10, p 1137 – 1142.

Ergun.M and Balbasi.M (1994) "Mathematical model for pitting potential of Fe -16%% Chromium steel" Corrosion science, vol 36, No 9, p1569 - 1574.

Ford.F.P, Andresen.P, (2002) Corrosion in nuclear systems: environmentally assisted cracking in light water reactors, in: P. Marcus (Ed.), Corrosion Mechanisms in Theory and Practice, Marcel Dekker, New York, p 605–642.

Francis R, Byrne D.G, Jones.K, (1997) Performance at reduced costs; Zeron100 Super duplex stainless steel sets the pace, Madrid, Brazil Conference proceedings; Vol 3, p 279-294.

Francis.R, Byrne.G, Warburton G.R, (1999) Experiences of Zeron100 super duplex stainless steel in the process industries, Stainless steel world 99 conferences, p 613-623.

Francis.R (2000) "The effect of tungsten on the properties of super duplex stainless steels" Confidential Report No: TN1120R1

Fruyter.D.J (1991) "Industrial experiences with duplex stainless steel related to their specific properties" Proc Conf Duplex Stainless steels 91, 28-30 Oct, Beaune, France, p 497-510.

Fontana.M. G (1987) "Corrosion Engineering" 3. ed Mc Grawhill Book company .

Garfial - Mesias.L.F, Sykes.J.M and Tuck.C.D.S (1996) "The effect of phase compositions on the pitting corrosion of 25Cr duplex stainless steel in chloride solutions" Corrosion science, Vol 38, No 8, p 1319-1330

Garfias - Mesias.L.F and Sykes.J.M (1998) "Effect of copper on active dissolution and pitting corrosion of 25%Cr duplex stainless steels" Corrosion, Vol 54, No 1, p 40-45.

Ghosal.G.H et al (1987)"The influence of potential and pH on the stress corrosion cracking of a duplex stainless steel in chloride solution" 10th International congress on metallic corrosion, Madras, India, Vol 20 – 28, p 1-4.

Ghoshal.S.K , Gadiyar.H.S and Prabhu Ganukar.G.V (1993) "Film formation and stress corrosion carcking of duplex stainless steel in boiling chloride solution" British corrosion Journal, Vol 28, No 1, p 43 –49.

Gunn.R.N(1986) Robert.N, Duplex Stainless steels (microstructure, properties and applications) Abington publishing.

Herbsleb.Guenter and Poepperling.Rolf.K (1980)"Corrosion properties of austenitic – duplex steel AF22 in chloride and sulphide containing environments" Corrosion, Vol 36, No 11, p 611-618.

Hoar.T.P, Mears.D, Rothwell.G (1965) "The Relationships between anodic passivity, brightening and pitting" Corrosion Science, Vol 5, p 279.

Horvath.J and Uhilig.H.H, (1968) "Critical Potentials for Pitting Corrosion of Ni, Cr-Ni, Cr-Fe, and Related Stainless Steels", J. Electrochem. Soc., Vol 115, Issue 8, p 791-795.

Hochmann.J, Desestret.A, R.Jolly, R.Mayoud(1977) "Stress Corrosion Cracking and hydrogen Embrittlement of Iron base alloys". NACE, p956.

Hsuang Lo.I, Yan Fu, Chang- Jian Lin, Wen Ta Tsai (2006) "Effect of electrolyte composition on the active – passive transition behaviour of 2205 duplex stainless steel in H_2SO_4 /HCl solutions" Corrosion science, Vol 48, p 696-708.

Hyuk-Sang Kwon and Hee-San Kim (1993), Investigation of stress corrosion susceptibility of duplex ($\alpha + \gamma$) stainless steel in hot chloride solution Material science engineering, A172 (1993), p159 – 166.

Issacs H.S, (1989) "Localised breakdown and repair of passive surfaces during pitting" Corrosion science, vol 29, No 2/3, p313-323.

Janik-Czachor.M, Lunarska.E, Z.Szklarska-Smialowska(1975) "Effects of Nitrogen content in a 18Cr-5Ni-10Mn steel on the pitting susceptibility in chloride solutions" corrosion 31:11 (1975), p349 – 398.

Jargelius.R.F.A, and Wallin.T (1986) "The effect of Nitrogen alloying on the pitting and crevice corrosion resistance of CrNi and CrNiMo Austenitic stainless steels" 10th Scandinavian Corrosion Congress, Stockholm, No: 31, p161-164.

Jargelius R.F.A, Blom.R, Hertzman.R, Linder.L(1991) Duplex stainless steels 91, Conf proc eds. J.Charles and S.Bernhardsson, p 211 -220, 1991.

Jargelius.R.F.A and Linder.J (1992)"Use of slow strain rate technique to assess the stress corrosion resistance of duplex and austenitic stainless steel" Application of stainless steel, Stockholm, Sweden, June, p477-484.

Jargelius.R.F.A and Linder.J (1999)" Influence of Mo and N on the stress corrosion cracking of austenitic stainless steels" Third European Materials Congress, Sardinia, Italy, 6-9 June.

Joanna Michalska, Maria Aozanska, (2006) Qualitative and quantitative analysis of sigma and chi phases in 2205 duplex stainless steel", Materials Characterization 56 (2006), p 355-362.

Kaneko.M and Issacs H.S, (2000) "Pitting of stainless steel in bromide, chloride and bromide/Chloride solutions, Corrosion Science Vol 42, p67- 68.

Kangas.P and Nichlos.J.M (1995) "Chloride –induced stress corrosion cracking of duplex stainless steels, Models, test methods and experience" Materials and Corrosion, Vol 46, p 354 – 365.

Katsumi Yamammoto and Keizo Hosoya (1995) "Corrosivity of Br^- and Cl^- on duplex stainless steel" Materials and Engineering A198, p 239-243.

Kudo K, Shibata.T, Okamoto.G and N. Sato (1968) "Ellipsometric and radiotracer measurements of the passive oxide film on Fe in neutral solution" Corrosion Science, Vol 8, Issue11, p 809-814.

Kwon -Sang Hyuk and Kin-san Hee (1993) "Investigation of stress corrosion susceptibility of duplex (α + γ) stainless steel in a hot chloride solution" Material science and Engineering, A172, pp 159-166.

Lemaitre.C, Abdel Moneim. A, R. Djoudjou, B. Baroux and G. Beranger (1993) "A statistical study of the role of molybdenum in the pitting resistance of stainless steels CorrosionScience, Vol34, Issue11, pp1913-1922.

Leonard.A (2003) "Review of external stress corrosion cracking of 22%Cr duplex stainless steel" Phase I operation data acquisition HSE report ISBN 0717627187.

Lin.L.F, Cragnolino.G, Szklarska – Smialowska.Z, Macdonlad D.D,(1981) Stress Corrosion Cracking of Sensitized Type 304 Stainless Steel in High-Temperature Chloride Solutions, Corrosion, Vol 37, p616.

Lorenz.K and Medawar.P (1969), Thysenforschung, Vol 115, p 97.

Lothongum.G. Wongpanya.P, Morito.S, Furuhara.T, Maki.T (2006); Effect of nitrogen on corrosion behaviour of 28Cr-7Ni duplex and microduplex stainless steels in air-saturated 3.5 wt% NaCl solution, Corrosion science, Vol 48, Issue 1, pp137 - 153.

Macdonald.Digby.D, (1978) "Reference electrodes for high temperature aqueous systems-A review and assessment", Corrosion, Vol 34, No 3, p75 – 84.

Macdonald Digby. D, Arthur C.Scott, and Paul Wentrcek, (1979) "External Reference electrodes for use in high temperature aqueous systems", J.Electrochem.Soc. Vol 126, No: 6, p908- 911.

Maeng W.Y, Lee J.H, and Kim U.C (2005) "Environmental effects on the stress corrosion cracking susceptibility of 3.5NiCrMoV steels in high temperature water", Corrosion science, Vol 47, p1876 - 1895.

Malik.A.U, Siddiqi.N.A, Ahmad.S and Andijani.I.N,(1995) "The effect of dominant alloy additions on the corrosion behaviour of some conventional and high alloy steels in seawater" Corrosion science, Vol 37, No 10, p1521-1535.

Mankowski.J and Szklarska-Smialowska.Z (1975)"Studies on accumulation of chloride ions in pits growing during anodic polarization" Corrosion Science, Volume 15, Issues 6-12, p493-501

Manning P.E (1980) "Effect of Scan Rate on Pitting Potentials of High-Performance Alloys in Acidic Chloride Solution", Corrosion, Vol36, No 9, p 469-474

Manning P.E and Duquette.D.J (1980), "The effect of temperature (25-289)^{0}C on pit initiation in single phase and duplex 304L stainless steels in 100ppm Cl^- solution" Corrosion Science, Vol 20, p 597 -610.

Matsch.St and Bohni.H (2000)"Influence of temperature on the localised corrosion of stainless steels" Russian Journal of Electrochemistry, Vol 36, No 10, p1122 - 1128.

Maximovitch. S, Barral.G, Cras F.Le and Claudet.F (1995) "The electrochemical incorporation of molybdenum in the passive layer of a 17% Cr ferritic stainless steel. Its influence on film stability in sulphuric acid and on pitting corrosion in chloride media CorrosionScience, Vol37,Issue2, p271-291.

McBEE.C and Kruger.J, (1971) Int. Congr. On Localized Corrosion, Williamsburg, U.S.A.

Merello.R, Botana F.J, Botella.J, Matres.M.V and Marcos.M(2003) "Influence of chemical composition on the pitting corrosion resistance of non-standard low-Ni high-Mn–N duplex stainless steels", Corrosion Science, Vol 45, issue 5, p 909-921.

Miyuki.H , Murayama.J , Kudo.T and Moroishi.T, (1984) " Localised corrosion of duplex stainless steels in $CO_2 - H_2S - Cl^-$ environments at elevated temperatures", Corrosion 84, April 2- 6, New Orleans/Louisiana, paper no :293.

Montemor M.F, Simões.A.M.P, M. G. S. Ferreira and M. Da Cunha Belo (1999)"The role of Mo in the chemical composition and semi conductive behaviour of oxide films formed on stainless steels" Corrosion Science, Vol 41, Issue 1, p17-34

Moragan. J, (1987)"Cathodic protection", p 53.

Mori.G (2004) "Users view of pitting corrosion" Proc Corrosion 2004, New Orleans, Louisiana, USA. Paper No 04304.

Nagano.H, Kudo.T, Inaba .Y and Harada.M (1981)"Highly corrosion resistant duplex stainless steel" Metaux Corrosion Industre, Vol 56, No 667, p81-88.

Newman R.C and M. A. A. Ajjawi (1986)"A micro-electrode study of the nitrate effect on pitting of stainless steels" Corrosion science, Vol 26, No 12, p1057-1063.

Newman R.C and Shahrabi.T (1987) "The effect of alloyed nitrogen or dissolved nitrate ions on the anodic behaviour of austenitic stainless steel in hydrochloric acid" Corrosion science, Vol: 27, No 8, p827 – 838.

Olefjord.I and Wegrelius.L "The influence of Nitrogen on the passivation of stainless steels" Corrosion science, Vol 38, No 7, p1203 – 1220, 1996.

Otieno-Alego.V, Hope G.A, Flitt H.J and Schweinsberg D.P (1995) "The Corrosion of Low alloy steel in a steam turbine environment: The effect of oxygen concentration and

potential scan rate of input parameters used to computer match the experimental polarization curves", Corrosion Science, Vol 37, No 3, p 509-525.

Osozawa .K and Okato.N (1976) "Passivity and its breakdown on iron and iron based alloys, eds R.W.Staehle, H.Okada (Houston, Texas, Nace) p135-143

ParkinsR.N, (1980), "Predictive approaches to stress corrosion cracking failure", Corrosion Science, Vol 20, p147-166.

Parkins R.N (1987) "Factors influencing stress corrosion crack growth kinetics" Corrosion, Vol 43, No 3, p 130 - 139.

Parkins R.N (1988) "Localised Corrosion and Crack initiation", Materials science and Engineering A103, p143- 156.

Parkins R.N and Singh.P.M, (1990) "Stress Corrosion Crack Coalescence", Corrosion, Vol 46, No 6, p 485 - 499.

Park.J.O, Matsch.S, and Bohni.H (2002) "Effects of temperature and chloride concentration on pit initiation and early pit growth of stainless steel" Journal of Electrochemical society, 149, (2) B34-B39.

Payer.J.H and Staehle.R.W (1972) "Localized attack on metal surfaces" Corrosion Ftaigue:Chemistry, mechanics and microstructure ", p 211 -269.

Perren R.A, Suter T.A, Uggowitzer P.J, L. Weber, R. Magdowski, H. Böhni and M. O. Speidel (2001)"Corrosion resistance of super duplex stainless steels in chloride ion containing environments: investigations by means of a new microelectrochemical method: I. Precipitation-free states, Corrosion Science, Vol 43, Issue 4, p 707-726.

Postlethwaite.J, Brierley.R.A, Walmesley.M.J and Goh.S.C (1974) "Pitting at elevated temperatures" Localized corrosion, Houston, Texas, p 415 - 426.

Pourbaix Antoni (1971) "Characteristics of localized Corrosion of steel in chloride solutions", Corrosion Vol 27, No 11.

Pourbaix.Marcel (1972) "Significance of protection potential in pitting, intergranular corrosion and stress corrosion cracking" Journal of less common metals, Vol 28, p51 – 65.

Qvarfort.R (1998) "Some observations regarding the influence of molybdenum on the pitting corrosion resistance of stainless steels" Corrosion Science, Vol 40, No 2/3, p215 - 223.

Raja.K.S and Jones.D.A (2006) "Effects of dissolved oxygen on passive behaviour of stainless alloys" Corrosion Science, Volume 48, Issue 7, July 2006, p1623-1638

Roscoe C.V and Gradwell K.J (1986), The history and development of duplex stainless steels "All that glistens is not gold". *Proc* conf duplex stainless steels 86, The Hague Nederland's institute voor lastechniek, paper 34, p126-135.

Rosenfeld I.L and Danilov.I.S (1967) "Electrochemical aspects of Pitting corrosion" Corrosion Science, Vol 7, p129 to 142.

Roy.A.K, Fleming.D.L and Lum.B.Y (1997)"Effect of environmental variables on localised corrosion of high performance container materials" Fifth international conference on nuclear engineering" May 26 -30, Nice, France.

Rujini .G, Srivastava.S.C. and Ives. M.B (1989) "Pitting Corrosion behaviour of UNS NO8904 Stainless steel in a chloride /sulphate solution" Corrosion -Vol 45, No 11, p 874 - 882.

Sakai et al.J, TMS-AIME fall meeting, Paper Reprint o: 8201-010, October 1982.

Scott, P.M and Bamford.W.H. (1985) "The development and use of electrochemical potential monitoring in environment assisted cracking tests in high temperature, high pressure, aqueous environments". AERE –R11741, p653

Scully.J.C (1971) "The theory of stress corrosion cracking in alloys" Nato science committee research evaluation conference, Brussels

Sedricks.J (1976) "Corrosion of stainless steels" Eds Electrochemical society.

Sedricks.A.J. (1990) " Corrosion Testing made easy: stress corrosion cracking test methods

Semino.C.J, Pedeferri .P, Burstein. G.T and Hoar.T.P (1979)"The localised corrosion of resistant alloys in chloride solutions", Corrosion Science, Vol.19, p1069 -1078.

Shibata.T (2007) "Passivity breakdown and stress corrosion cracking of stainless steel" Corrosion Science, Vol 49, p 20-30.

Sieradzki.K and Newman.R.C (1987) "Stress corrosion crackinmg" Journal of physics and chemistry of solids,Vol 48, No11, p1100 – 1113.

Symniotis.E –Barrdahl (1998) "Selective corrosion of duplex stainless steels" Proceeding Stainless steel 87, Institute of metals, London.

Symniotis, E. (1995) "Dissolution mechanism of duplex stainless steel in the active-passive transition range and the role of microstructure", Corrosion science, Vol 51, No 8, p571-580.

Shang Huang- Chi and Chang Shih Chai (2005) " Effects of nitrogen and high temperature aging on σ phase precipitation of duplex stainless steel" Material science and engineering A 402, p 66 - 75.

Siow.K.S, Song.T.Y and Qiu.J.H (2001) "Pitting corrosion of duplex stainless steels"Anti corrosion methods and materials, Vol 48, No 1, p 31-36

Sourisseau.T, Chauveau.E and Baroux.B (2005) "Mechanism of copper action on pitting phenomena observed on stainless steels in chloride media" Corrosion Science, Vol 47, Issue5, p1097-1117

Spence M.A, and Warburton.G, "An Investigation into the effects of reeling and straightening on the mechanical properties and corrosion resistance of Zeron100 super duplex stainless steel for use in Sub Sea flow line applications".

Sprowls,O.Donald, Chapter17, "Evaluation of stress corrosion cracking".

Stewart's and williams.D.E (1987)"Studies of the initiation of pitting corrosion on stainless steels" Proc "Second International conference on localised corrosion" Orlando, Florida, June1-5, p131 - 136.

Sriram .R and Tromans.D (1989) "Pitting corrosion of duplex stainless steels" Corrosion, Vol 45, No10, p 804-810.

Smialowska .S .and Czachor.M (1971) "The analysis of electrochemical methods for the determination of characteristic potentials of pitting corrosion" Corrosion science, Vol.11, no. 12, p901-914.

Strehblow.H.H and Titze.B (1977) "Pitting potentials and inhibition potentials of iron and nickel for different aggressive and inhibiting anions", Corrosion Science, Vol 17, Issue 6, p 461-472.

Swann.P.R (1965) "Stress corrosion failure" Scientific american, p73- 81.

Symniotis.E –Barrdahl (1988) "Selective corrosion of duplex stainless steels" Proceeding Stainless steel 87, Institute of metals, London, 1998.

Szklarska-Smialowska.Z and Mankowski .J (1972), Effect of temperature on the kinetics of development of pits in stainless steel in 0·5N NaCl + 0·1N in H_2SO_4 solution Corrosion Science, Vol: 12, Issue12, 1972, p925-934.

Szklarska- Smialowska.Z, (1986) Pitting Corrosion of Metals, NACE, Houston. p 3

Szklarska- Smialowska.Z, Grimes.D, and Park.J (1987)"the kinetics of pit growth on alloy 600 in chloride solutions at high temperatures" Corrosion science, Vol 27, No 8, p 859 - 867.

Szklarska-Smialowska.Z (1990) "Pit Initiation" Advances in Localized Corrosion, Orlando, Florida; USA, 1-5 June 1987, p 41-46.

Szklarska-Smialowska.Z, (2002) "Mechanism of pit nucleation by electrical breakdown of the passive film", corrosion science, Vol 44, p1143 –1149.

Truman.J.E., Coleman M.J, Prit.K.R (1977) " Note on the influence of nitrogen content on the resistance of austenitic stainless steels to pitting corrosion", British Corrosion Journal 12:4 (1977), p236-238.

Truman.J.E (1987)"Effect of composition on the resistance to pitting corrosion of stainless steels", UK Corrosion 87, Brighton, 26-28Oct, p112 -129.

Truman.J.E (1988) "Effects of alloying on corrosion behaviour of high alloy steels" Proc of High Nitrogen Steels, London, Vol 453, p225-239

Townsend.H.E, Cleary H.J, and Allegra.L (1981) "Breakdown of oxide films on steel exposed to chloride solutions" corrosion, Vol 37, No: 7, July1981.

Van Gelder.K, Erlings J.G, Damen J.W.M and Visser.A, " The stress Corrosion cracking of duplex stainless steel in H2S /CO2 / Cl- environments", Corrosion science, Vol 27, No 10/11 , p1271 -1279

Vermilyea .D.A (1977), A film rupture model for stress corrosion cracking, in: R.W. Staehle, Hochmann.J, McCright.R.D, J.E. Slater (Eds.), Stress-Corrosion Cracking and Hydrogen Embrittlement of Iron-Base Alloys, NACE, Houston, 1977, p208–217.

Wang.J.H, Su C.C, and Szklarska- Smialowska.Z, (1988) "Effects of Cl^- Concentration and temperature on pitting of AISI 304 Stainless steel", Corrosion, Vol44, No 10, October 1988.

Warburton G.R, Francis.R, Byrne.G and S.Bukovinsky, (1995) "Experiences with Zeron100 Super Duplex Stainless steels in Industrial Applications", Australian Materials Conference, Perth, Australia, p 50-61.

Weber. L and Uggowitzer.P.J (1998) "Partitioning of chromium and molybdenum in super duplex stainless steels with respect to nitrogen and nickel content" Materials Science and Engineering A 242, p 222 - 229.

Weeks.John.R, Brijesh Vyas and Issacs.Hugh (1985) "Enviornmental factors influencing stress corrosion cracking in boiling water reactors" Corrosion science, Vol 25, No 8/9, p 757 – 768.

Wen-Ta -Sai, Brigitte Reynders, Martin Stratmann and Grabke.H.J (1993) "The effect of applied potential on the stress corrosion cracking behaviour of high nitrogen steels" Corrosion science, Vol 34, No 10, p1647 - 1656.

Wen- Ta Sai, Ming -Shan Chen (2000) "Stress corrosion cracking behaviour of 2205 duplex stainless steel in concentrated NaCl solution" Corrosion science, Vol 42, p 545-559.

Wen-Ta Sai, Shyan-Liang Chou (2000) "Environmentally assisted cracking behaviour of duplex stainless steel in concentrated sodium chloride solution" Corrosion Science 42, p 1741-1762.